APPLICATION OF GEOINFORMATICS ON SOIL DEGRADATION ASSESSMENT IN UPPER LAMCHIENGKRAI WATERSHED, NAKHON RATCHASIMA PROVINCE, THAILAND

Sasikarn Plaiklang

A Thesis Submitted in Partial Fulfillment of the Requirements for the

Degree of Doctor of Philosophy in Geoinformatics

Suranaree University of Technology

Academic Year 2017

การประยุกต์ภูมิสารสนเทศสำหรับการประเมินความเสื่อมโทรมดิน ในลุ่มน้ำลำเชียงไกรตอนบน จังหวัดนครราชสีมา ประเทศไทย

นางสาวศศิกานต์ ไพลกลาง

วิทยานิพนธ์นี้เป็นส่วนหนึ่งของการศึกษาตามหลักสูตรปริญญาวิทยาศาสตรดุษฎีบัณฑิต

สาขาวิชาภูมิสารสนเทศ

มหาวิทยาลัยเทคโนโลยีสุรนารี

ปีการศึกษา 2560

APPLICATION OF GEOINFORMATICS ON SOIL DEGRADATION ASSESSMENT IN UPPER LAMCHIENGKRAI WATERSHED, NAKHON RATCHASIMA PROVINCE, THAILAND

Suranaree University of Technology has approved this thesis submitted in partial fulfillment of the requirements for the Degree of Doctor of Philosophy.

Thesis Examining Committee

Charlie Navanugraha

(Assoc. Prof. Dr. Charlie Navanugraha)

Chairperson

Suwit Ong.

(Assoc. Prof. Dr. Suwit Ongsomwang)

Member (Thesis Advisor)

S. Dasananda

(Assoc. Prof. Dr. Songkot Dasananda)

Member

S. Sarapirome

(Asst. Prof. Dr. Sunya Sarapirome)

Member

(Dr. Pantip Piyatadsananon)

Member

(Prof. Dr. Santi Maensiri)

Vice Rector for Academic Affairs and Internationalisation

(Asst. Prof. Dr. Worawat Meevasana)

Dean of Institute of Science

ศศิกานต์ ไพลกลาง : การประยุกต์ภูมิสารสนเทศสำหรับการประเมินความเสื่อมโทรมดินในลุ่มน้ำลำเชียงไกรตอนบน จังหวัดนครราชสีมา ประเทศไทย (APPLICATION OF GEOINFORMATICS ON SOIL DEGRADATION ASSESSMENT IN UPPER LAMCHIENGKRAI WATERSHED, NAKHON RATCHASIMA PROVINCE, THAILAND) อาจารย์ที่ปรึกษา : รองศาสตราจารย์ ดร.สุวิทย์ อ๋องสมหวัง, 234 หน้า.

การกร่อนของดินและดินเค็ม เป็นปัญหาด้านสิ่งแวดล้อมที่สำคัญของประเทศไทยและเป็นตัวชี้วัดที่สำคัญต่อความเสื่อมโทรมดิน วัตถุประสงค์หลักของการศึกษาคือ (1) เพื่อจำแนกการใช้ประโยชน์ที่ดินและสิ่งปกคลุมดินโดยตัวจำแนกแบบต้นไม้การตัดสินใจ (2) เพื่อประเมินการสูญเสียดินและระดับความรุนแรงโดยใช้แบบจำลอง Revised Morgan Morgan and Finney (RMMF) (3) เพื่อประเมินดินเค็ม และระดับความรุนแรงด้วยการวิเคราะห์การถดถอยเชิงเส้นตรงและมิใช่เชิงเส้นตรง (4) เพื่อประเมินอินทรียวัตถุและการสูญเสียอินทรียวัตถุในดินด้วยการวิเคราะห์การถดถอยเชิงเส้นตรงและมิใช่เชิงเส้นตรง (5) เพื่อประเมินความเสื่อมโทรมของดินและระดับความรุนแรงด้วยวิธีการคูณ ในการศึกษาเริ่มต้นด้วยการวิเคราะห์การกัดกร่อนของดิน ดินเค็ม และการสูญเสียปริมาณอินทรียวัตถุในดิน จากนั้นนำผลลัพธ์ที่ได้มารวมเข้าด้วยกันเพื่อประเมินความเสื่อมโทรมดิน

จากผลการศึกษา พบว่า แบบจำลอง CART ที่เหมาะสมที่ใช้แบนด์สีน้ำเงิน สีเขียว สีแดง อินฟราเรดใกล้ อินฟราเรดคลื่นสั้น 1 อินฟราเรดคลื่นสั้น 2 ของข้อมูลภาพจากดาวเทียมแลนด์แซท 8 ความเปียกและระดับความสูง เพื่อใช้สร้างต้นไม้การตัดสินใจสำหรับการประเมินการใช้ประโยชน์ที่ดินและสิ่งปกคลุมดิน โดยให้ค่าความถูกต้องโดยรวม ร้อยละ 87.50 และค่าสัมประสิทธิ์แคปปาร้อยละ 80.10 ในขณะที่ ค่าเฉลี่ยของการสูญเสียดินในพื้นที่ศึกษาเท่ากับ 3.37 ตันต่อเฮกแตร์ต่อปี ระดับความรุนแรงของการสูญเสียดินส่วนใหญ่เป็นระดับการกัดกร่อนน้อยมาก (≤ 6.25 ตันต่อเฮกแตร์ต่อปี) และครอบคลุมพื้นที่ 437.70 ตารางกิโลเมตร หรือคิดเป็นร้อยละ 94.14 ของพื้นที่ศึกษาทั้งหมด ในขณะเดียวกัน ระดับความรุนแรงของดินเค็มส่วนใหญ่เป็นระดับต่ำมาก และครอบคลุมพื้นที่ 415.55 ตารางกิโลเมตร หรือคิดเป็นร้อยละ 89.37 ของพื้นที่ศึกษาทั้งหมด ในขณะที่ ระดับความเสื่อมโทรมทางชีวภาพส่วนใหญ่เป็นระดับปานกลาง และครอบคลุมพื้นที่ 296.05 ตารางกิโลเมตร หรือคิดเป็นร้อยละ 63.67 ของพื้นที่ศึกษาทั้งหมด จากการประเมินความเสื่อมโทรมดินด้วยวิธีการคูณที่ไม่มีการจำแนกและมีการจำแนกระดับความรุนแรง พบว่า ระดับความเสื่อมโทรมดินส่วนใหญ่เป็นระดับต่ำมาก และครอบคลุมพื้นที่ 443.00 ตารางกิโลเมตร หรือคิดเป็นร้อยละ 95.28 และ 462.53 ตารางกิโลเมตร หรือคิดเป็นร้อยละ 99.48 ของพื้นที่ศึกษาทั้งหมด ตามลำดับ การจำแนกระดับความเสื่อมโทรมดินทั้งสองวิธีให้ผลลัพธ์ที่คล้ายคลึงกัน โดยมีพื้นที่ของระดับความ

รุนแรงที่เหมือนกันเท่ากับ 442.82 ตารางกิโลเมตร หรือร้อยละ 95.24 ของพื้นที่ศึกษาทั้งหมด ผลลัพธ์ที่ได้รับเหล่านี้สามารถบ่งชี้ได้ว่าไม่มีปัญหาความเสื่อมโทรมดินในพื้นที่ศึกษา

จากผลการศึกษาสามารถสรุปได้ว่า เทคโนโลยีภูมิสารสนเทศสามารถนำมาใช้เป็นเครื่องมือเพื่อประเมินการสูญเสียดิน ดินเค็ม การลดลงของปริมาณอินทรียวัตถุในดินและระดับความรุนแรงสำหรับการประเมินความเสื่อมโทรมดินได้อย่างมีประสิทธิภาพ

สาขาวิชาการรับรู้จากระยะไกล ลายมือชื่อนักศึกษา ศศิกานต์ ไพลกลาง

ปีการศึกษา 2560 ลายมือชื่ออาจารย์ที่ปรึกษา

SASIKARN PLAIKLANG : APPLICATION OF GEOINFORMATICS ON SOIL DEGRADATION ASSESSMENT IN UPPER LAMCHIENGKRAI WATERSHED, NAKHON RATCHASIMA PROVINCE, THAILAND. THESIS ADVISOR : ASSOC. PROF. SUWIT ONGSOMWANG, Dr. rer. Nat. 234 PP.

SOIL DEGRADATION / RMMF MODEL / SOIL SALINITY INDEX/ SOIL COLOR INDICES / UPPER LAMCHIENGKRAI WATERSHED

Soil erosion and soil salinity are major environmental problems in Thailand and they are significant indicators of soil degradation. The main objectives were (1) to classify land use and land cover (LULC) using decision tree classifier, (2) to assess soil loss and its severity using Revised Morgan Morgan and Finney (RMMF) model, (3) to assess soil salinity and its severity with linear and non-linear regression analysis, (4) to assess soil organic matter and its depletion with linear and non-linear regression analysis, and (5) to evaluate soil degradation and its severity using multiplicative method. In this study, soil erosion, soil salinity, and depletion of organic matter content are separately analyzed first and then combined to evaluation processes soil degradation.

As results, an optimum Classification and Regression Trees (CART) model that applied blue, green, red, NIR, SWIR-1, SWIR-2 bands of Landsat 8 data, wetness and elevation to construct a decision tree for LULC classification, provided overall accuracy at 87.50% and Kappa hat coefficient at 80.10%. Meanwhile, an average soil loss in the study area was 3.37 ton/ha/year. The most dominant soil loss

severity class was very slightly eroded (≤ 6.25 ton/ha/year) and covered area of 437.70 sq. km or about 94.14% of the total study area. In the meantime, the most dominant soil salinity severity class was very low and covered area of 415.55 sq. km or about 89.37% of the total study area. At the same time, the dominant biological degradation classes was moderate and covered area of 296.05 sq. km or 63.67% of the total study area. According soil degradation assessment using multiplicative method without and with severity classification, the most dominant soil degradation class were very low and they covered area with 443.00 sq. km or 95.28% and 462.53 sq. km or 99.48% of the total study area, respectively. Both soil degradation severity classification provided similar result with common severities classes about 442.82 sq. km or 95.24% of the total study area. These findings implied that serious problem of soil degradation was not existed in the study area.

In conclusion, it appeared that geoinformatics technology can be efficiently used as tools to assess soil loss, soil salinity, and soil organic matter depletion and their severities for soil degradation evaluation.

School of Remote Sensing Student's Signature SASIKARN PLAIKLANG

Academic Year 2017 Advisor's Signature Suwit Ong

ACKNOWLEDGEMENTS

I prefer express profound gratitude to my advisor, Assoc. Prof. Dr. Suwit Ongsomwang, for his support with precious advice and guidance to complete this thesis, as well as being a great teacher to me.

I really appreciate to express gratitude to the chairman and members of this thesis defense committee: Assoc. Prof. Dr. Charlie Navanugraha, Assoc. Prof. Dr. Songkot Dasananda, Asst. Prof. Dr. Sunya Sarapirome, Asst. Prof. Dr. Sodchol Wonprasaid, and Dr. Pantip Piyatadsananon for all valuable suggestions and critical comments during the proposal and thesis defense.

I would also like to show gratitude to the Land Development Department, Office of Agricultural Economics, and Thai Meteorological Department for supporting the data needed for the research.

I am especially thankful to Suranaree University of Technology for the opportunity to continue my education and for providing an outstanding results scholarship, and The National Research Council of Thailand for providing Thesis Grant for Doctoral Degree Student.

I would also like to express my sincere gratitude to Mr. Satira Udomsri from Land Development Department, Mrs. Pitchanun Raksasarp from Nakhon Ratchasima Land Development Station for their great support in providing data and knowledge about soil degradation. Mr. Monton Suriyaprasit and Mr. Yuthasart Anuluxtipun, for nowledge of RMMF model. Asst. Prof. Dr. Sanchai Prayoonpokarach, Dr. Sirilak

Tanang, Mr. Vinai Yaowaret, Ms. Nuanprang Utaida, Mr. Ketthai Panyakom, and Ms. Kanlayanee Kajsanthia from Suranaree University of Technology, Ms. Muchalin Yatan from Khon Kaen University and Ms. Jongrak Nukhunthodfor knowledge and support about soil chemical analysis.

I really appreciate that Assoc. Prof. Dr. Kanit Khaimook for kindness in providing extra job as research assistant and teacher assistant at and Dr. Supattra Puttinaovarat, Ms. Priwan Hamai, Mr. Pumet Pornjutipat, Mr. Phakorn Thianthipkarun, Mr. Tinn Thirakultomorn, and Ms. Kirada Hattakam for being a great guide for me. Assoc. Prof. Dr. Pannathon Sangarun, Dr. Intareeya Sutthivanich, Dr. Yaowaret Jantakat and Ms. Tanawan Viriyachaisirikul for helping me in English skills improvement.

Asst. Prof. Dr. Kwanjai Deejring, Dr. Tharapong Phetprayoon, and Dr. Wichan Phandee for providing me an opportunity to teach at Nakhon Ratchasima Rajabhat University.

Mrs. Napaporn Klinchan and my beloved colleagues at Plookpanya School for being my good partners and lots of help.

In addition, I would like to thank all my friends from the School of Remote Sensing for their helpful advice and well interaction. I would like to express my deepest gratitude to my beloved parents and younger brother for being my inspiration and raised me up with love.

Sasikarn Plaiklang

CONTENTS

CONTENTS (Continued)

CONTENTS (Continued)

CONTENTS (Continued)

CONTENTS (Continued)

LIST OF TABLES

LIST OF TABLES (Continued)

LIST OF TABLES (Continued)

Table **Page**

LIST OF TABLES (Continued)

Table **Page**

LIST OF TABLES (Continued)

LIST OF FIGURES

LIST OF FIGURES (Continued)

Figure **Page**

LIST OF FIGURES (Continued)

Figure **Page**

LIST OF FIGURES (Continued)

Figure **Page**

LIST OF FIGURES (Continued)

LIST OF FIGURES (Continued)

LIST OF ABBREVIATIONS

BDI	=	Biological Degradation Index
CART	=	Classification and Regression Tree
DEM	=	Digital Elevation Model
EC	=	Electrical Conductivity
IDW	=	Inverse Distance Weighting
LDD	=	Land Development Department
LULC	=	Land Use and Land Cover
ME	=	Mean Error
MLR	=	Multiple Linear Regression
MNLR	=	Multiple Non-Linear Regression
NRMSE	=	Normalized Root Mean Square Error
OK	=	Ordinary Kriging
OM	=	Organic Matter
R^2	=	Coefficient of determination
RMMF	=	Revised Morgan, Morgan and Finney
RMSE	=	Root Mean Square Error
SK	=	Simple Kriging
SLR	=	Simple Linear Regression
SNLR	=	Simple Non-Linear Regression
TPS	=	Thin Plate Spline

LIST OF ABBREVIATIONS (Continued)

UK	=	Universal Kriging

CHAPTER I

INTRODUCTION

1.1 Background problem and significance of the study

Land degradation is a world serious environmental problem (UNEP, 2006). It has harmful impacts on agricultural productivity and on ecological function that ultimately affects human sustenance and quality of life (Mhangara, 2011). The most critical component of land degradation is soil degradation (Mainguet, 1994, quoted in Denti, 2004). Soil degradation is a decline in soil quality encompassing the deterioration in physical, chemical, and biological attributes of the soil (Eaton, 1996). Indicators of soil degradation are soil erosion, soil salinity, decline of soil structure, and nutrient depletion (Lal, 1998). Soil erosion and soil salinity are major problems in Thailand because they create seriously negative impacts on agricultural and environmental sustainability (LDD and ITC, 2002; Katawatin and Sukchan, 2012) and they are also harmful to people and environment (Jumpa, 2012). In addition soil erosion leads to depletion of organic matter in soil (FAO, 2005).

Huete (2004) mentioned that general information and data regarding the spatial extent and severity of soil degradation are poorly understood and the available data are limited. Actually, the traditional approach based on field data collection is expensive, takes a long time (Abbas and Khan, 1999), and hardly reproducible (Bai, Dent, Olsson, and Schaepman, 2008). Bai et al. (2008) proposed that to solve the problem of soil degradation for field data collection in local scale, proper approaches for soil degradation assessment are required.

According to the global report of land degradation by Bai et al. (2008) it was found that area of degraded land in Thailand was 0.895% of the global degrading area. In addition, statistical report on soil degradation assessment by LDD (2015) revealed that 56.8% of the total area or about 182 million Rai in Thailand was degraded. The report showed an increasing trend of soil degradation and the major causes that include increasing population, deforestation, unsuitable land use and a lack of and improvement of soil quality. These factors cause soil erosion and loss of nutrient. Soil erosion decreases soil fertility and increases risk of desertification (Sethabut, 2008; Lohachart, 2015). Sethabut (2008) suggested that Thai government should realize soil degradation problem for mitigation and prevention the mentioned problem in short term and long term. Soil degradation assessment is mostly based on in situ soil survey (Kapalanga, 2008) and can provide the most accurate data (Jessica, 2002). However, it is costly and time consuming (Harmsen, 1996, quoted in Yazidhi, 2003). It is also difficult to detect wide and inaccessible area (Bai et al., 2008).

Geoinformatics technology is very important tool for decision-making across a wide range of disciplines. It is also a basal and essential technical core of the system for assessing geospatial information and monitoring the environment (Fadhil, 2009). Geoinformatics technology is also used to assess and monitor soil degradation (Kiekebusch, 2009), to measure variables linked to soil degradation (Prince, 2002, quoted in Mambo and Archer, 2006), to provide time series data for monitoring land cover change (Lillesand, Kiefer, and Chipman, 2004), and to detect wide and inaccessible area (Torahi, 2012).

This study aims to develop a new approach based on geoinformatics technology for assessing the extent and its severity of soil degradation. Herein soil erosion, soil salinity, and depletion of organic matter content, are separately analyzed first and then combined to assess soil degradation. This new approach is more effective than traditional approach because it can save labor, cost, time, and effort. In addition, it can quickly assess and provide up-to-date data. It is expected that the approach will greatly benefit to other area which face similar soil degradation problems.

1.2 Research objectives

In this study, the integration of soil erosion, soil salinity, and depletion of organic matter content analysis are applied for soil degradation assessment. The study seeks to fulfill the following objectives:

(1) To classify land use and land cover in 2015 using decision tree classifier;

(2) To assess soil loss and its severity in 2015 using RMMF model;

(3) To assess soil salinity and its severity in 2015 with optimum spectral salinity indices using linear and non-linear regression analysis;

(4) To assess soil organic matter and its depletion in 2015 using linear and non-linear regression analysis, and

(5) To evaluate soil degradation and its severity in 2015 using multiplicative method.

1.3 Scope and limitations of the study

Scope of this study can be summarized as follows.

(1) Land use and land cover (LULC) data in 2015 are extracted from Landsat data, spectral indices, and bio-physical factors based on an optimum decision tree with CRT algorithm under SPSS statistical software and Expert System of ERDAS Imagine software.

(2) Soil erosion, soil salinity and depletion of organic matter content, which represents physical, chemical and biological indicator of soil degradation, respectively, are firstly separately analyzed and then combined using multiplicative method to evaluate soil degradation.

(3) In situ soil sampling point collection for an optimum electrical conductivity (EC) and organic matter (OM) estimation model is conducted using stratified random sampling technique based on soil series and land use data which exclude urban and built-up land and water body as suggestion by Kheoruenromne (2005). In this study in situ data are divided into 2 sets include modeling and validation datasets.

Limitations of this study can be summarized as follows:

(1) This study utilize all available spatial and non-spatial data for soil degradation evaluation. Thus, the accuracy of soil degradation evaluation is dependent on their accuracies.

(2) Date of Landsat data 2015, which is used to classify LULC data to generate soil salinity and soil color indices, is different from ground survey date.

1.4 Study area

This study purposes to evaluate soil degradation and its severity based on three major indicators of soil degradation processes: physical, chemical, and biological degradation. Thus, the study area is represented by soil erosion, soil salinity and depletion of organic matter content analysis, which represents physical, chemical and biological indicator of soil degradation, respectively. Characteristic of the study area are briefly described in the specific aspects as follows:

1.4.1 Location and administration

The study area is a part of Upper Lamchiengkrai watershed which originated from mountainous area at Bamnet Narong district, Chaiyaphum province. It only locates in Nakhon Ratchasima province. The study area is covered by 3 districts include Theparak (Nong Prue, Nong Waeng, Samnak Takhro, and Wang Yai Thong sub-districts), Dan Khun Thot (Ban Kao, Hin Dad, and Huai Bong sub-districts), and Si Khiu (Kritsana and Wang Rong Yai sub-districts) and covered area of 464.96 sq. km (Figure 1.1). The main reason for selecting Upper Lamchiengkrai watershed is study area because it represents soil salinity exposure area which is the major problems in Northeast region of Thailand.

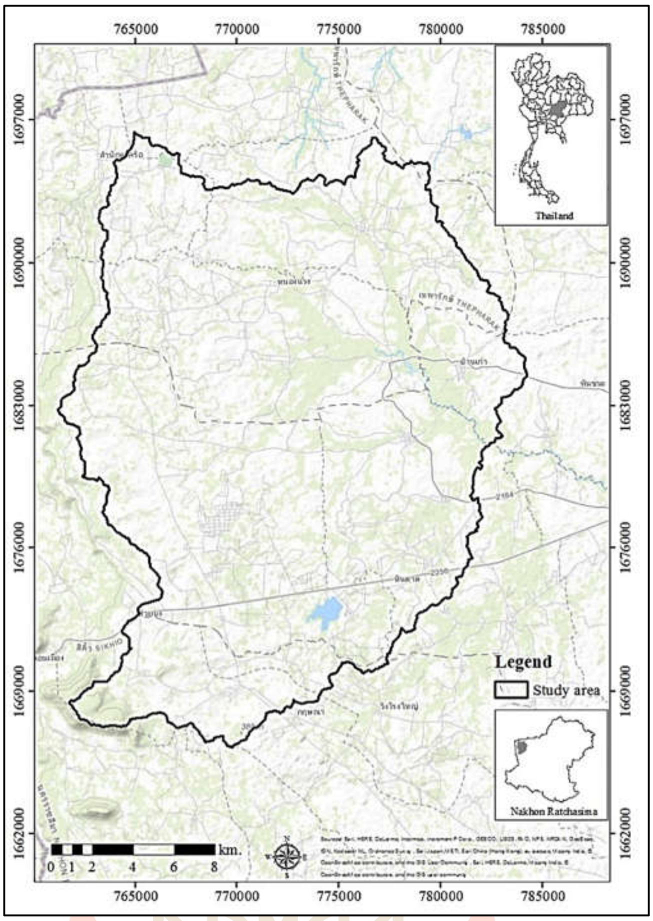

Figure 1.1 Location and administration boundaries of the study area.

1.4.2 Topography

The elevation of the study area ranges approximately from 0 m to 596 m (Figure 1.2). The eastern part of the study area, where major economic crops including paddy field, cassava, maize, and sugarcane are situated, is mostly flat. On contrary, the western part of the study area is undulate and mountainous areas and it mostly covers by cassava. The tributaries of the existing rivers in the study area flow from West to East.

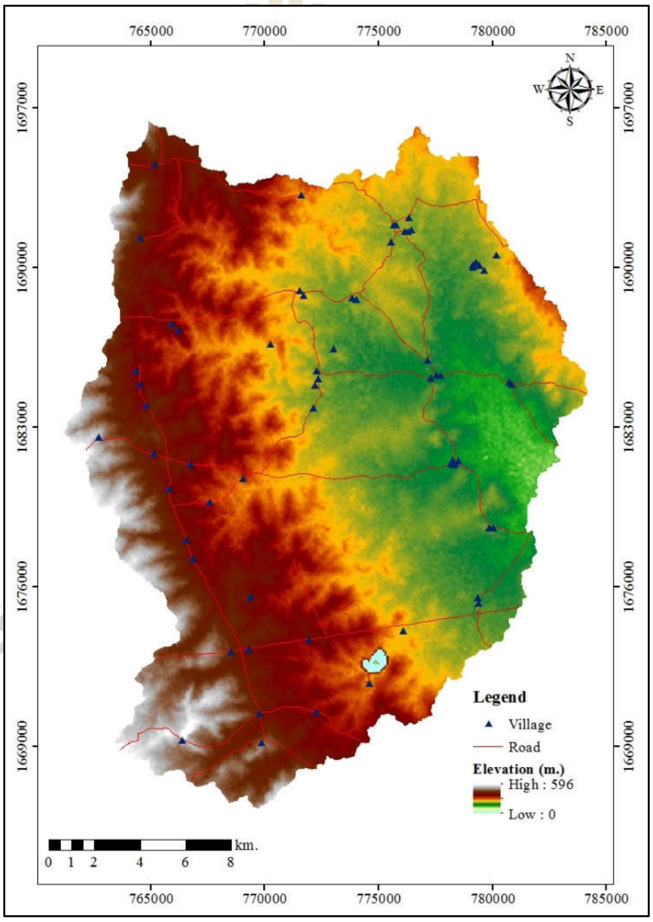

Figure 1.2 Topography of the study area.

1.4.3 Climate, temperature and rainfall

In general, there are three seasons in the Northeast region: hot season (mid February to mid May), rainy season (mid May to mid October) and cool dry season (mid October to mid February). Rainy season is under the influence of the southwest monsoons, while cool-dry season is influenced by the northeast monsoon carrying cold air from China (Saravisutra, 2010).

In 2015, the annual mean maximum temperature is 41.5 °C and annual mean minimum temperature is 13.6 °C. Temperature is highest in April and lowest in January. The annual rainfall is 1,171.1 mm, and annual mean rainy day is 104 days, and daily maximum is 104.3 mm. in 2015 (NSO, 2015).

1.4.4 Land use

According to land use data of Land Development Department (LDD) in 2015 (Figure 1.3), main land use type is agriculture land which include cassava, paddy field, and maize and covers area of 401.08 sq. km (86.27%). The second land use type is forest land include dense deciduous forest, disturbed deciduous forest, and forest plantation and covers area of 20.65 sq. km (4.44%). Other land use types are miscellaneous land, urban and built-up area, and water bodies and covers area of 4.07 sq. km (4.07%), 16.70 sq. km (3.59%) and 7.55 sq. km (1.63%), respectively (LDD, 2015).

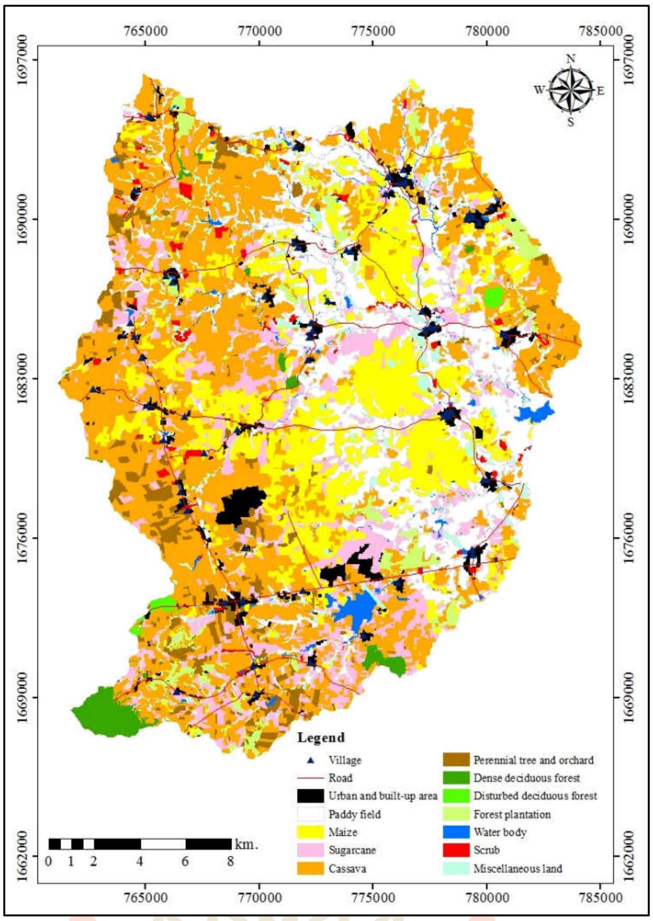

Figure 1.3 Distribution of land use in 2015 of LDD.

1.4.5 Soil

According to soil map at the scale of 1: 100,000 in 1999 of LDD, 25 soil series are found in the study area (Figure 1.4). Major characteristics of soil series are summarized in Table 1.1.

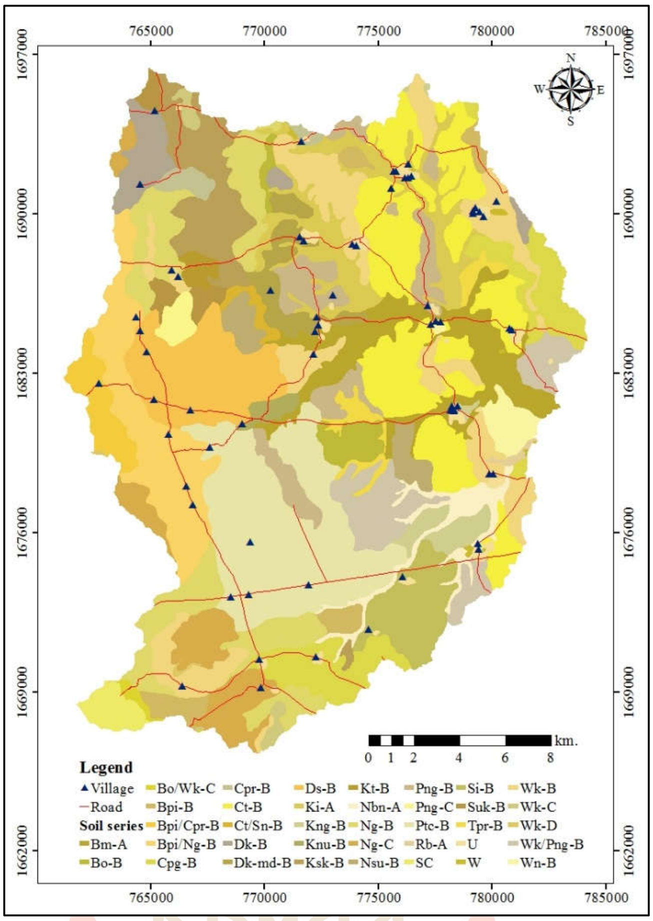

Figure 1.4 Distribution of soil series of LDD.

Table 1.1 Characteristic of soil series in the study area (LDD, 2011).

Soil series	Description
Ban Mi (Bm-A)	This group includes poorly drained, fine-textured (heavy), and dark colored soils that occupy on the Low - lying terrain mostly in karst topography and basaltic terrain. They commonly have high fertility status. Soil reaction is neutral to moderately alkaline.
Ban Phi (Bpi-B)	This group of soils is well drained or moderately well drained, deep, coarse-textured that developed from alluvial deposits of wash materials on undulating terrain. Major characteristics is thick sandy horizon which extend to 1 m. below soil surface. This is commonly underlain by medium-textured soils which has lower permeability, causing impeded drainage in the surface and sometimes water-logging. These soils are low fertility whereas the soil reaction is strong to medium acid.
Ban Phi&Chom Phra (Bpi/Cpr-B)	This group of soils is well drained or moderately well drained, deep, coarse-textured that developed from alluvial deposits of wash materials on undulating terrain. This sandy layer is commonly underlain by medium-textured soils which has lower permeability, causing impeded drainage in the surface and sometimes water-logging.

Table 1.1 (Continued).

Soil series	Description
Ban Phi&Nam Phong (Bpi/Ng-B)	This group of soils is well drained or moderately well drained, deep, coarse-textured that developed from alluvial deposits of wash materials on undulating terrain. These soils are low fertility whereas the soil reaction is strong to medium acid.
Bo Thai (Bo-B)	This group of soils is well-drained, moderately deep coarse-textured that developed from weathered rocks in dry areas. They are low fertility. Soil reaction is strong acid.
Bo Thai&Wang Nam Khieo (Bo/Wk-C)	This group of soils is low fertility. Soil reaction is strong acid.
Chatturat (Ct-B)	This group of soils is moderately deep, fine-textured and well drained that developed from elastic rocks in low precipitation areas. Weathered rock with fine-grained elastic is commonly found at depth 50 - 100 cm. They are moderate fertility and medium acid. Soil reaction is high.
Chatturat&Sung Noen (Ct/Sn-B)	This group of soils is moderately deep, fine-textured and well drained that developed from elastic rocks in low precipitation areas. Weathered rock with fine-grained elastic is commonly found at depth 50 - 100 cm. They are moderate fertility and medium acid. Soil reaction is high.
Chom Phra (Cpr-B)	This soil group is deeply, well-drained and loam-sandy that develops from alluvial terraces.
Chum Puang (Cpg-B)	This group of soils is well-drained, deep and coarse-textured that develop from alluvial deposits or wash materials on the uplands of alluvial terraces, fans or erosional surface in the areas of low precipitation. They are low fertility. Soil reaction is strong acid.
Dan Khun Thot (Dk-B)	This group of soils is deep sandy, somewhat excessively drained that occur on alluvial terraces, fans and wash surface. Soil fertility is very low.
Dan Khun Thot (Dk-md-B)	This group of soils is deep sandy, somewhat excessively drained that occur on alluvial terraces, fans and wash surface. Soil fertility is very low.
Dan Sai (Ds-B)	This group of soils is well drained, deep medium-textured (sandy loam to sandy clay loam) and occupies on uplands where precipitation is low. Fertility of these soils are relatively low. Soil reaction is very strong to strong acid.
Khao Suan Kwang (Ksk-B)	This soil group is deeply, well-drained and loam-sandy that develops from alluvial terraces.
Kong (Kng-B)	This soil group is deeply, well-drained and loam-sandy that develops from alluvial terraces.
Korat (Kt-B)	This group of soils is well drained, deep medium-textured (sandy loam to sandy clay loam) and occupies on uplands where precipitation is low. Fertility of these soils are relatively low. Soil reaction is very strong to strong acid.
Kra Nuan (Knu-B)	This soil group is deeply, well-drained and loam-sandy that develops from alluvial terraces.
Kula Ronghai (Ki-A)	This group of soils consists of somewhat poorly drained, coarse-textured soils that are salt affected and occupy on low-lying terrain of the north-east plateau and coastal plain. Most of the areas are paddy rice but yield is relatively variable due to degree of salinity.
Muak Lek (Ml-E)	This group of soils consists of well drained soils. Permeability is moderate. Surface runoff is rapid. Theses soils are from residuum and colluvium from light colored shale, slates and other equivalent rocks and occur on the undulating to hilly topography of erosion surfaces and footslopes.
Nam Phong (Ng-B)	This group of soils is deep sandy, somewhat excessively drained that occur on alluvial terraces, fans and wash surface. Its parent material is closely related to coarse grained elastic rocks and coarse grained igneous rocks in areas of low precipitation. Soil fertility is very low.

Table 1.1 (Continued).

Soil series	Description
Nam Phong (Ng-C)	This group of soils is deep sandy, somewhat excessively drained that occur on alluvial terraces, fans and wash surface. Its soil fertility is very low.
Non sung (Nsu-B)	This group of soils is well drained and deep fine-textured that occupies erosional surfaces and alluvial terraces or fans in dry areas of the country. Soil fertility is moderately low. Soil reaction ranges from strong to very strong acid.
Nong Bunnak (Nbn-A)	This soil group is next to river basin. It is flat area, is deeply, poor-drained and loam.
Phon Ngarm (Png-B)	This group of soils is moderately deep, coarser-textured and coarse and well drained that developed from elastic rocks in low precipitation areas. Weathered rock with fine-grained elastic is commonly found at depth 50 - 100 cm. They are low fertility and strong to medium acid.
Phon Ngarm (Png-C)	This group of soils is moderately deep, coarser-textured and coarse and well drained that developed from elastic rocks in low precipitation areas.
Puk Thong Chai (Ptc-B)	This group of soils is well-drained, deep and coarse-textured that develops from alluvial deposits or wash materials on the uplands of alluvial terraces, fans or erosional surface in the areas of low precipitation. They are low fertility.
Ratchaburi (Rb-A)	This soil group is in river basin. It is lowland, is deeply, poor-drained.
Satuk (Suk-B)	This group of soils is well drained, deep medium-textured (sandy loam to sandy clay loam) and occupies on uplands where precipitation is low. Fertility of these soils are relatively low. Soil reaction is very strong to strong acid.
Si Khiew (Si-B)	This group of soils is well drained, deep medium-textured (sandy loam to sandy clay loam) and occupies on uplands where precipitation is low. Fertility of these soils are relatively low. Soil reaction is medium acid or neutral and reddish color. Dry-land upland and tree crops are commonly found in the areas.
Thepharak (Tpr-B)	This soil group is develops from siltstone.
Wang Nam Khieo (Wk-C)	This group of soils is shallow to coarse-grained bed rock. They commonly occur on erosional surface, hills and mountains.
Wang Nam Khieo (Wk-D)	This group of soils is shallow to coarse-grained bed rock. They commonly occur on erosional surface, hills and mountains.
Wang Nam Khieo (Wk-E)	This group of soils is shallow to coarse-grained bed rock. They commonly occur on erosional surface, hills and mountains.
Wang Nam Khieo& Phon Ngarm (Wk/Png-B)	This group of soils is shallow to coarse-grained bed rock. They commonly occur on erosional surface, hills and mountains coarse and well drained.
Warin (Wn-B)	This group of soils is well drained, deep medium-textured (sandy loam to sandy clay loam) and occupies on uplands where precipitation is low. Fertility of these soils are relatively low. Soil reaction is very strong to strong acid.
Slope complex (SC)	Complex slope area having slope more than 35 percent, this vicinity area has not been studied, surveyed and classified because the area is high steep regarded as difficult for management and preservation for agricultural purpose.

Note: Soil series data was divided classes base on slope phase: A = 0 - 2% slope, B = 2 - 5% slope, C = 5 - 12% slope, D = 12 - 20% slope.

1.4.6 Geology

Based on geological map of Department of Mineral Resources (DMR) at the scale of 1: 250,000, there are 3 geological formations in the study area (Figure 1.5). Characteristics of geological formation is summarized in Table 1.2.

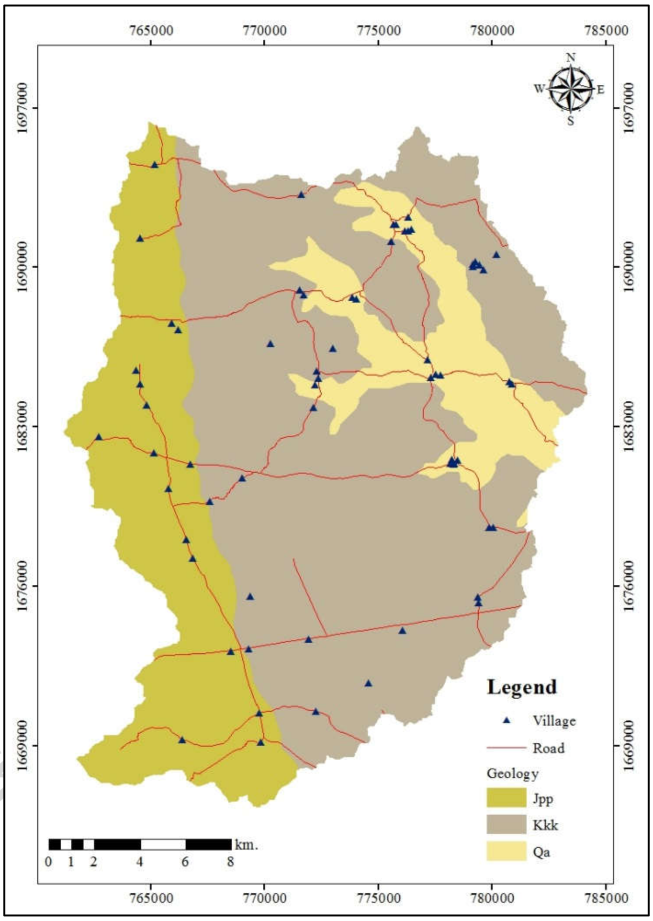

Figure 1.5 Distribution of geological information.

Table 1.2 Geological formations in the study area (Udomsri and Laorpansakul, 2013).

Symbol	Age	Formation	Description
Jpp	Jurassic	Phu Phan	Phu Phan Formation is in the south-eastern part of the Khorat Plateau. It is consisted of fine to medium-grained sandstone
Kkk	Cretaceous	Khok Kruat	The Khok Kruat Formation is a rock formation found in northeastern Thailand. It is one of the formations of the Khorat Group and is the youngest formation in the group. The group is a fluvial formation consisting primarily of red siltstones and sandstones
Qa	Quaternary	Alluvial deposit	The group is alluvial deposit, gravel, sand, silt and clay.

1.5 Benefits of the study

The specific benefits of the study are presented below:

(1) Recognizable the status of LULC of the Upper Lamchiengkrai watershed in 2015 using decision tree classifier.

(2) Understanding soil loss status and its severity using RMMF model.

(3) Understanding soil salinity status and its severity with an optimum spectral salinity index,

(4) Understanding soil organic matter status and its depletion map with an optimum soil color index,

(5) Determining soil degradation and its severity.

1.6 Outline of the thesis

The thesis is structured in two parts and follows a hierarchical organization as shown in Figure 1.6. Key information of each chapter in each part is summarized in the following section.

The first part includes Chapter I "Introduction", Chapter II "Basic Concepts and Literature Reviews" and Chapter III "Data and Methodology". Chapter I contains background problem and significance of the study, research objectives, scope and limitations of the study, study area, benefits of the study and outline of the thesis. Chapter II consists of basics of soil degradation and its assessment, soil erosion assessment by RMMF model, soil salinity assessment using spectral soil salinity index, soil organic matter assessment using spectral color index, and relevant literatures. Meanwhile, Chapter III presents data and explains details of research methodology including (1) data collection and preparation, (2) LULC classification by decision tree classifier, (3) soil degradation analysis and (4) soil degradation evaluation.

The second part consists of five chapters of the results with discussion, which separately describe according to objectives and one chapter presents conclusion and recommendation. Chapter IV "Land Use and Land Cover Classification" contains (1) an optimum CART model for land use and land cover classification and (2) land use and land use classification. Chapter V "Soil Erosion Assessment and Its Severity" consists of (1) data preparation for RMMF model, (2) RMMF model parameters extraction, (3) soil erosion analysis using RMMF model, and (4) soil erosion severity classification. Meanwhile, Chapter VI "Soil Salinity Assessment and Its Severity" contains (1) EC samples collection and analysis, (2) independent variables on EC data, (3) soil salinity model development, (4) optimum model for soil salinity assessment, and (5) soil salinity assessment and its severity. Chapter VII “Soil Organic Matter Assessment and Its Severity” contains (1) OM samples collection and analysis, (2) independent variables on OM data, (3) soil organic matter model development, (4) optimum model for soil organic matter assessment, and (5) soil organic matter assessment and its severity. Chapter VIII “Soil Degradation Evaluation” comprises the combination of soil erosion severity classification, soil salinity classification and soil biological degradation classification using multiplicative method without and with classification for data integration. Chapter IX “Conclusion and Recommendation” comprises conclusion of the study and recommendation.

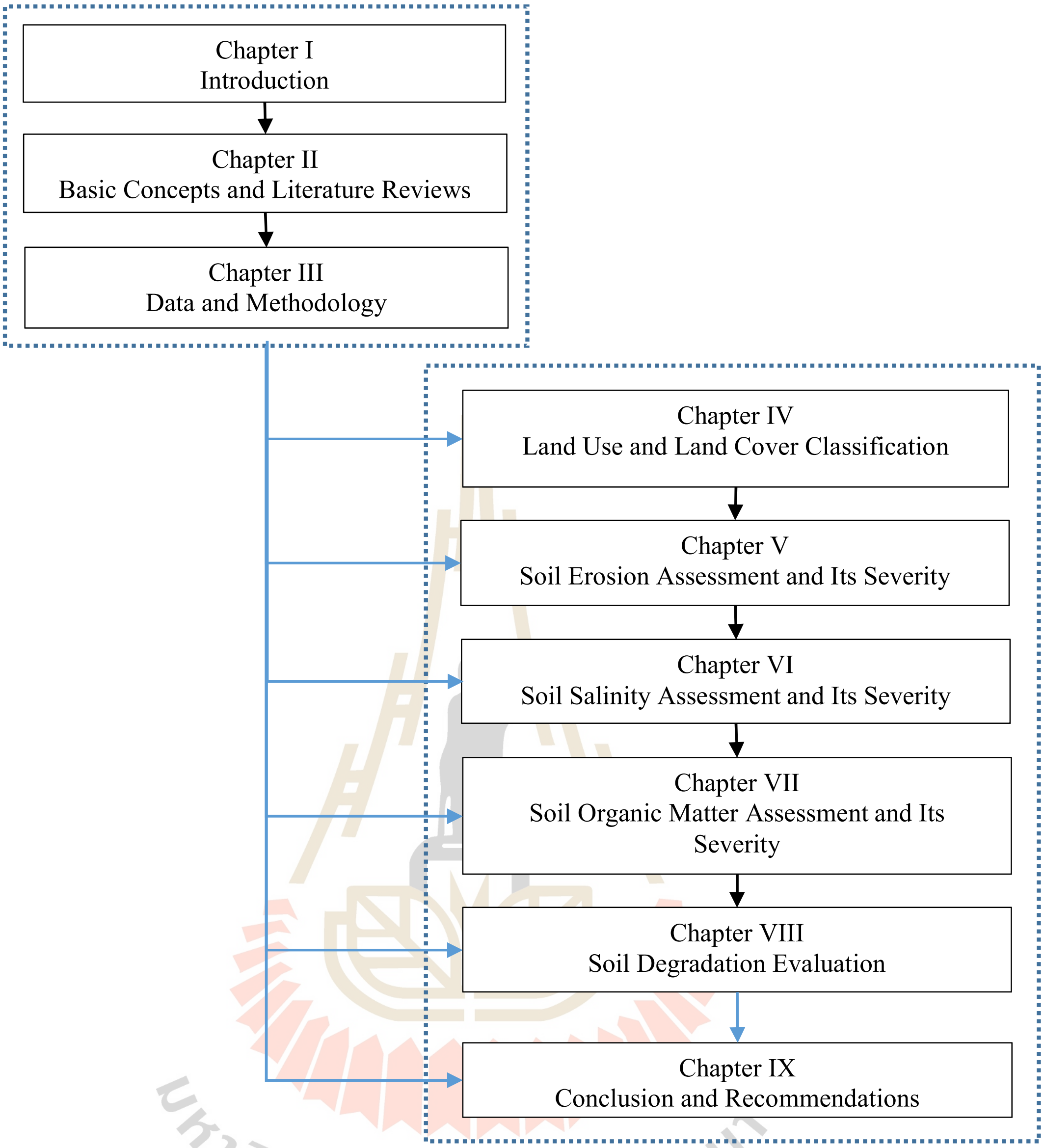

Figure 1.6 Structure of the thesis.

CHAPTER II

BASIC CONCEPTS AND LITERATURE REVIEWS

Basic concepts including (1) basics of soil degradation and its assessment, (2) soil erosion assessment by RMMF model, (3) Revised Morgan, Morgan and Finney (RMMF) model, (4) soil salinity assessment using spectral soil salinity index, (5) soil organic matter assessment using spectral color index, and (6) relevant literatures are here reviewed in this chapter.

2.1 Basics of soil degradation and its assessment

(1) Definition of soil degradation

Soil degradation is a process that causes deterioration of soil productivity and low soil utility as a result of natural or anthropogenic factors (Wim and El Hadji, 2002).

Soil degradation is the decline in quantity and quality of soil (Nagle, 2006).

(2) Causes of soil degradation

There are two groups of causes of soil degradation: natural and human causes (Greenfield geography, 2014) as follows:

- Natural causes: (a) rising temperatures, (b) falling rainfall, (c) flash floods, (d) wind, and (e) topography.

- Human causes: (a) overgrazing, (b) over cultivation, (c) deforestation, (d) overpopulation, (e) fertilizer and pesticide use, (f) industrial pollution, and (g) unsustainable water use.

In other words, causes of soil degradation are both natural and human-induced (Bhattacharyya, Ghosh, and Mishra, 2015) as follows:

a- Natural causes: (a) earthquakes, (b) tsunamis, (c) droughts, (d) avalanches, (e) landslides, (f) volcanic eruptions, (g) floods, (h) tornadoes, and (i) wildfires.

- Human-induced causes: (a) deforestation, (b) inappropriate agricultural practices, (c) urban sprawl, and (d) commercial/industrial development.

(3) Soil degradation processes

Lal (1998) mentioned that soil degradation processes are divided into three groups: physical, chemical, and biological degradation processes.

FAO (2011) stated that degradation of soil biological, chemical, physical, and hydrological properties, soil erosion and soil pollution are types of soil degradation processes.

Keller (2010) stated that soil degradation processes can be classified into four different types: water and wind erosion, chemical and physical degradation.

(4) Indicators of soil degradation processes

Lal (1998) stated that there are three major groups of indicators of soil degradation processes: physical, chemical, and biological degradation (Figure 2.1).

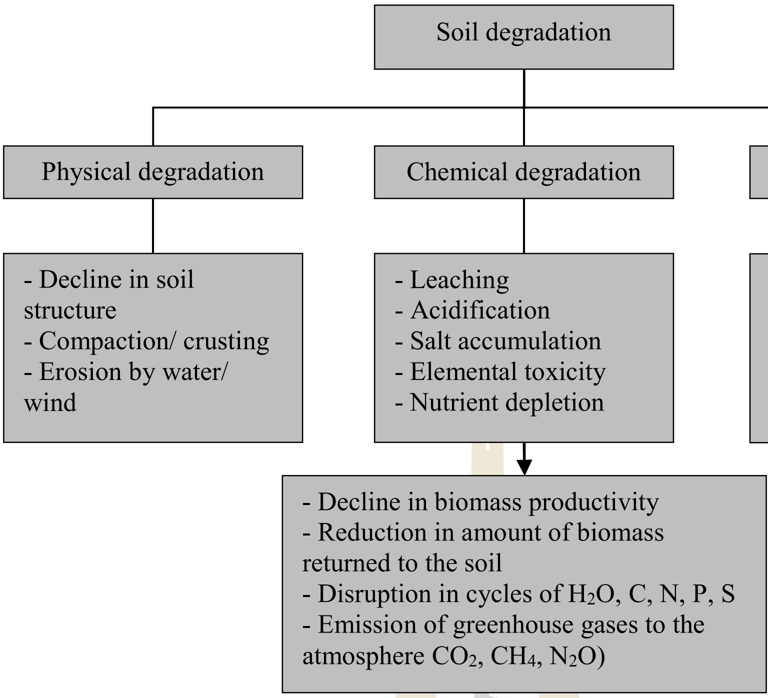

Figure 2.1 The major soil degradation processes (Lal, 1998).

The physical, chemical, and biological degradation processes causes: (a) decline in biomass productivity, (b) reduction in amount of biomass returned to the soil, (c) disruption in cycles of H_2O, C, N, P, S, and (d) emission of greenhouse gases (e.g. CO_2, CH_4, N_2O) to the atmosphere (Lal, 1998).

Likewise, Mbagwu (2003) mentioned that soil degradation processes affects the decline in soil quality and they are grouped into three types: physical, chemical, and biological processes which has different indicators base on agricultural degradation as follow:

- Physical degradation: (a) soil structural decline, (b) soil compaction, (c) soil crusting, and (d) soil erosion.

- Chemical degradation: (a) soil acidification, (b) nutrient depletion, and (c) salinization.

- Biological degradation: (a) loss of soil diversity and soil organic C decline.

(5) Soil degradation assessment

Tully, Sullivan, Weil, and Sanchez (2015) reviewed several research studies on the multiple indicators for soil degradation assessment in Sub-Saharan Africa (SSA). They found that multiple indicators can be efficiently applied for soil degradation assessment because soil degradation was a complex process, so several indicators (i.e., physical, chemical, and biological degradation) should be used to measure soil degradation (Table 2.1).

Warren (2002) suggested multiple indicators that were the best for soil degradation assessment. In his study, he used two indicators: nutrients (biological indicator) and erosion (physical indicator) to assess soil degradation in dry land Africa. He found that the two indicators could effectively identify the classes of soil degradation.

Table 2.1 Major types of soil degradation and the conditions under which they are most commonly found in SSA (Tully et al., 2015 modified from Weil and Brady, 2015).

Category	Specific degradation processes	State factors		Socioeconomic drivers
		Parent material and topography	Climate	
Physical	Soil erosion by water	Slope	Humid to semi-arid regions	Tillage agriculture, deforestation and improper grazing
	Soil erosion by wind	Less vegetation	Semi-arid to arid regions	Disturbance of soil, vegetation or bio-crust by agricultural tillage and poorly-managed grazing
	Soil erosion by tillage	Hilly landscapes		Continuous cultivation, especially with tillage
	Surface sealing	Low organic matter sandy or silty soils		Urbanization, compaction, tillage
	Soil compaction	Clayey soils	Humid regions	Heavy machinery, grazing
Chemical	Reduced capacity to store water	Low organic matter		Compaction, erosion, removal of mulch or residue
	Nutrient depletion	Low inherent fertility		Low input agriculture, grazing, excessive forest harvest
	Acidification	Old, weathered soils	Humid regions	Excessive N fertilization, leaching, sulfur and nitrogen oxidation
	Salinization	Shallow water table	Arid to semi-arid regions	Excessive irrigation
	Dispersion/ alkalization	Excessive monovalent ions, exposure and incorporation of calcareous subsoil material into surface horizon		Poor quality irrigation water, loss of perennial vegetation, tillage
	Toxic Contamination			Urbanization, mining, industrial waste spillage
Biological	Depletion of soil organic matter	Sandy texture, steep slopes, deep water table	High temperatures, limited rainfall	Degradation of vegetation, excessive tillage, lack of sufficient organic amendments and plant residues; excessive biomass removal by harvest, grazing or fire; erosion of sloping surface soil by tillage, wind and water
	Loss of soil biological diversity	Sandy texture, steep slopes, root limiting subsoil layers (fragipans, cemented layers, aluminum toxicity, calcic horizons)	High temperatures	Mono-cropping, deforestation and poorly managed grazing
	Loss of plant, animal and microbial biomass	Side slopes, shallow bedrock, root limiting subsoil layers (fragipans, cemented layers, aluminum toxicity, calcic horizons)		Reduced plant growth and subsequent addition of litter, roots and exudates limits carbon fuel for food web; exposure to extremes of dryness and temperature by removal of plant litter; destruction of macropores, aggregates and other habitat by tillage, compaction and erosion.

2.2 Soil erosion assessment by RMMF model

Huete (2004) stated that soil erosion is one of the most important processes contributing to soil degradation. Erosion degrades soil by removing topsoil, reduces levels of soil organic matter and contributes to the breakdown of soil structure. Actually, topsoil often has the highest biological activity and most soil organic matter (USDA, 2012).

(1) Definition of soil erosion

Soil erosion is the removal of soil by forces of nature more rapidly than various soil-forming processes can replace it (Roo, 1993).

Soil erosion is the deterioration of soil by the physical movement of soil particles from a given site (Tingting, Xiaoyu, Dandan, Zhenshan, and Jianminga, 2008).

Thinley (2008) mentioned that soil erosion is commonly grouped into three phases: (1) physical detachment of soil particles, (2) transportation of soil material, and (3) deposition of soil material.

(2) Critical factor of soil erosion

Soil erosion processes are generally determined by critical factors includes rainfall, soil, vegetation, management and topography.

Rainfall. Soil loss is closely related to rainfall through the combined effect of detachment by raindrops striking the soil surface and by runoff (Mkhonta, 2000, quoted in Yazidhi, 2003). The ability of rainfall to cause erosion (erosivity) depends on characteristics such as rainfall energy and rainfall intensity, particularly half-hour rainfall. These characteristics determine the ability of raindrops to detach soil particles and the possible occurrence of surface runoff, a primary means for transportation and deposition of detached soil particles (Nanna, 1996, quoted in Yazidhi, 2003). The amount of rainfall governs the overall water balance and the relative proportion that becomes runoff (Hagos, 1998, quoted in Yazidhi, 2003). Erosion is related to two types of rainfall events, the short-lived intense storm, where the infiltration capacity of the soil is exceeded, and the prolonged storm of low intensity, which saturates the soil before runoff begins. In addition to the rainfall amount, drop size distribution, kinetic energy and depth of overland flow are important characteristics affecting splash detachment. Detachment is due to the size of the raindrop and its velocity. Big raindrops have high erosive power to detach the soil particles (Yazidhi, 2003).

Soil. The effect of soil erosion is reflected through the resistance of soil to both detachment and transport, defined through the soil erodibility factor (Morgan, 1995, quoted in Yazidhi, 2003). Soils with high erodibility index are more sensitive to erosion than soils with low erodibility index. Soil erodibility (K-factor) varies with soil characteristics, e.g. texture, bulk density, shear strength, organic matter content, aggregate stability, infiltration capacity, chemical properties and transportability of loosened soil particles (Mkhonta, 2000, quoted in Yazidhi, 2003). The aggregate stability of a soil determines how easily soil particles can be detached. Transportability determines how easily these loosened soil particles can be washed away. Soil texture also influences the infiltration capacity. This is defined as the maximum sustained rate at which soil can absorb water, and depends on pore size, pore stability and the form of the soil profile (Petter, 1992, quoted in Yazidhi, 2003).

Vegetation. Vegetation covers is a very crucial factor in reducing soil loss (Petter, 1992, quoted in Yazidhi, 2003). In general, as the protective canopy of land cover increases, the erosion hazard decreases (Mkhonta, 2000, quoted in Yazidhi, 2003). It protects the soil against the action of falling raindrops, increases the degree of infiltration of water into the soil, maintains the roughness of the soil surface, reduces the speed of the surface runoff, binds the soil mechanically, diminishes micro-climatic fluctuations in the uppermost layers of the soil, and improves the physical, chemical and biological properties of the soil (Petter, 1992, quoted in Yazidhi, 2003).

Management. In circumstances where farmers cultivate in marginal and very steep slopes, soil erosion can be accelerated if there is no proper conservation techniques applied. Proper management practices such as terracing on steep slopes, mulching, and crop rotation can significantly reduce soil erosion (Yazidhi, 2003).

Topography. Slope steepness and slope length are considered to have a strong relationship to erosional process (Nanna, 1996, quoted in Yazidhi, 2003). Slope gradient and slope length are the common parameters used in erosion modeling (Petter, 1992, quoted in Yazidhi, 2003). Slope gradient has an exponential relationship with erosion. Steep slopes are more susceptible to soil erosion because the erosive forces splash, scour and transport all have a greater effect on steep slopes (Hudson, 1995, quoted in Yazidhi, 2003). On the other hand, longer slopes are more susceptible to soil loss due to greater built up of surface runoff, velocity and depth (Yazidhi, 2003).

(3) Revised Morgan, Morgan and Finney (RMMF) model

The RMMF model is a physical modeling for evaluating soil erosion (Morgan, 2001). The model is based on knowledge of: (a) the fundamental erosion processes and (b) the laws of conservation of mass and energy (Petter, 1992; Yazidhi, 2003). RMMF model was modified by Morgan (2001) was the basis for the prediction of soil loss (Ines, 2013). It was developed to cater for difficulties realized in collecting data on rooting depth and soil detachability index in MMF model which is the original version (Morgan, 2001). In the revised version, effective hydrological depth is considered instead of rooting depth as in the original version. New detachability values provide as an improvement from the soil detachability index of the original version, while the revised model also caters for leaf drainage, ability of runoff to detach as well as transport by rainfall. The model separates the soil erosion process into two phases: water and erosion phases (Yazidhi, 2003).

2.3 Soil salinity assessment using spectral soil salinity index

Soil salinity is major environmental problems worldwide, and they have serious negative impacts on various aspects of agriculture and environmental sustainability (Oldeman, 1994; El-Swaify, 1997; Toparkngarm, 2006). Soil salinity is critical indicator of soil degradation process. It also inhibits plant growth and subsequent agricultural output (Katawatin and Sukchan, 2012). Huete (2004) mentioned that salinization involves the accumulation of salts in the root zone as salts move upward in the soil and are left at the surface as the water evaporates. Presently, a salt-affected soil is most found in the northeastern part of the Thailand, where salinity affects approximately 21% of the land (Arunin, 1989, quoted in Katawatin and Sukchan, (2012). Moreover, LDD has reported a significant reduction in rice yields in lowland paddy fields affected by saline soils (LDD, 2001).

(1) Definition of soil salinity

Soil salinity is the state of accumulation of soluble salts in the soil (Al-Khaier, 2003).

Soil salinity is the state of accumulation of soluble salts in the root zone to adversely affect the growth of most crops (Iqbal and Mastorakis, 2015).

(2) Causes of soil salinity

There are two groups of causes of soil salinity: natural and human causes as follows (Japakasetr and Workman 1981; Williamson, Peck, Turner, and Arunin, 1989, quoted in Montoroi, Grünberger, Sukchan, and Kungklang, 2006):

- Natural causes: (a) climate, (b) rock salt deposit, and (c) saline groundwater.
- Human causes: (a) wood cutting, (b) water storage, and (c) groundwater pumping.

(3) Spectral soil salinity index

Remotely sensed data are effective for mapping salt-affected soils because reflected energy generally increases from the soil surface with an increasing quantity of salt crust (Singh and Sirohi, 1994). Abbas and Khan (1999) claimed that soil salinity can be mapped both directly by reflectance from bare soil, or from the salt crust, and indirectly from vegetative coverage and health. Numerous spectral salinity indices have been developed for detecting, mapping and assessing of soil salinity as summary in Table 2.2.

Table 2.2 Lists of spectral salinity indices.

Salinity indices	Equation	Note	Reference
NDSI	$NDSI = (R - NIR)/(R + NIR)$	R is red reflectance flux NIR is near infrared reflectance flux	Khan, Rastoskuev, Sato, and Shiozawa, 2005
SI1	$SI1 = \sqrt{G \times R}$	G is green reflectance flux R is red reflectance flux	Douaoui, Nicolasb, and Walter, 2006
SI2	$SI2 = \sqrt{G^2 \times R^2 \times NIR^2}$	G is green reflectance flux R is red reflectance flux NIR is near infrared reflectance flux	
SI3	$SI3 = \sqrt{G^2 \times R^2}$	G is green reflectance flux R is red reflectance flux	
S_1	$S_1 = B/R$	B is blue reflectance flux R is red reflectance flux	Abbas and Khan, 1999
S_2	$S_2 = (B - R)/(B + R)$	B is blue reflectance flux R is red reflectance flux	
S_3	$S_3 = (G \times R)/B$	G is green reflectance flux R is red reflectance flux B is blue reflectance flux	
S_4	$S_4 = \sqrt{B \times R}$	B is blue reflectance flux R is red reflectance flux	
S_5	$S_5 = (B \times R)/G$	B is blue reflectance flux R is red reflectance flux G is green reflectance flux	
S_6	$S_6 = (R \times NIR)/G$	R is red reflectance flux NIR is near infrared reflectance flux G is green reflectance flux	

2.4 Soil organic matter assessment using spectral color index

Soil organic matter is a crucial indicator of soil fertility (Ishaq, Begum, Ali, Ahmed, Ali, Ali, Baig, Ali, and Ali, 2015). The organic matter content of soils is an important parameter in assessing the quality of a soil. It promotes healthy crops, supplies resources for microbes and other soil organisms, and regulates the supply of water, air and nutrients to plants (MSU, 2011).

(1) Definition of soil organic matter

Soil organic matter is any material produced originally by living organisms (plant or animal) that is returned to the soil and goes through the decomposition process (FAO, 2005).

Soil organic matter is everything in or on the soil that is of biological origin, whether living or non-living (Bowden, 2007).

(2) Causes of depletion of soil organic matter

Depletion of organic matter contents presents a biological indicator for soil degradation (De Paz, Sa´nchez, and Visconti, 2006). It is formed by the breakdown of plant and animal in soil. SOCO (2009) mentioned that there are five groups of causes of depletion of soil organic matter as follow:

Climate. Organic matter declines more rapidly at higher temperatures, so soils in warmer climates tend to contain less organic matter than those in cooler climates.

Soil texture. Fine-textured soils tend to have more organic matter than coarse soils; they hold nutrients and water better, thus providing good conditions for plant growth.

Soil hydrology (drainage). The wetter a soil is, the less oxygen is available for organic matter to decline, so that it accumulates.

Land use (tillage). Loss of organic matter occurs because erosion washes away topsoil and humus.

Vegetation. Roots are a great contributor to soil organic matter.

(3) Spectral color index

Soil organic matter significantly affects the soil color. Mostly soil becomes darker as the percentage of increasing soil organic matter (Lickacz and Penny, 2001). Coleman and Montgomery (1987) showed that an increase in soil moisture and organic matter tends to decrease the reflectance values. The spectral response of soil is influenced by a number of soil related properties such surface condition, soil texture, soil organic matter, soil color, moisture content, iron and iron oxide content and mineralogy (Dwivedi, 2001). Mathieu and Pouget (1998) claimed that soil color indices, namely brightness, coloration, hue, redness and saturation indices, which are derived from remotely sensed data, can be used to predict soil organic matter (Table 2.3).

Table 2.3 Lists of spectral color indices.

Spectral color indices	Equation	Note	Reference
Brightness index (BI)	$BI = \sqrt{\frac{(B^2 + G^2 + R^2)}{3}}$	B is blue reflectance flux G is green reflectance flux R is red reflectance flux	Mathieu and Pouget, 1998
Coloration index (CI)	$CI = \frac{R - G}{R + G}$	R is red reflectance flux G is green reflectance flux	
Hue index (CI)	$HI = \frac{2 * R - G - B}{G - B}$	B is blue reflectance flux G is green reflectance flux R is red reflectance flux	
Redness index (RI)	$RI = \frac{R^2}{(B - G^3)}$	B is blue reflectance flux G is green reflectance flux R is red reflectance flux	
Saturation index (RI)	$SI = \frac{R - B}{R + B}$	B is blue reflectance flux R is red reflectance flux	

2.5 Literature reviews

2.5.1 Application of geoinformatics for soil degradation assessment

(1) Soil erosion assessment by RMMF model

Sapkota (2008) used RMMF model to assess soil loss in Namchun watershed, Thailand. This study divided three step research approaches included: (1) geostatistical analysis evaluated topsoil properties (e.g. topsoil clay, silt, organic matter content and crusting index) to map their distribution, (2) soil erosion modeling was assessed soil loss, and (3) relationships of soil loss with soil properties, land cover, and slopes were considered causal factors of soil erosion. The researcher found that topsoil silt and clay content had very strong spatial structure whereas organic matter and crusting index had moderate spatial structure. High mountain areas had high organic matter content and low crusting index whereas plateau landscapes had low organic matter content and high crusting index. In addition, soil loss was significantly different in land cover types and slope classes. Agriculture area had very high soil erosion followed by orchard and the soil loss was less in dense forest area. Steep to very steep slopes had high soil loss as compared to other slope classes.

Suriyaprasit (2008) applied the RMMF erosion model to predict soil loss in Nam Chun Watershed, Phetchabun, Thailand. This study was generated a new C parameter. For C-factor generation, the regression equation based on field assessment of C-factor using training values and NDVI gave the satisfy results; adjust R^2, C.E., M.E., and RMSE. The researcher found that LULC in 1988, 2000 and 2007 periods had effected on overall soil loss in this area; the highest soil loss occurred in the agriculture areas while the lowest was found in forest areas. In addition, the rate of soil loss between 1988 and 2007 was increased in the agriculture areas.

Basayigit and Dinc (2010) used Landsat ETM+, research reports, meteorological and field data for preparation parameters of RMMF model to predict soil loss in Egirdir Lake watershed of Turkey. The researchers found that the high soil loss area was observed in the high value of rainfall. Steep and very steep areas, in which soils had little vegetation density, exhibited the highest soil losses value and the steep area covered with forest is the low soil loss.

Jha and Paudel (2010) used RUSLE and RMMF model to predict the soil loss rate and spatial erosion pattern in Kalchi Khola watershed of Nepal. The researchers found that the RMMF model predictions are in close agreements with the available measured data of the region, whereas RUSLE predictions are far off, indicating that the RMMF model is a better choice to predict soil erosion rates in a steepy sloping mountainous region.

Martínez-Murillo, López-Vicente, Poesen, and Ruiz-Sinoga (2011) assessed soil erosion using RMMF model in Melgarejo and and Higuerón catchments in Southern Spain. The researchers found that vegetation cover promoted a decrease in both the average soil erosion rates and extension of the gully erosion.

Kamonrat and Jirakajohnkool (2012) used RMMF model to assess soil erosion in the Upper Lam Phra Phloeng watershed, Nakhon Ratchasima, Thailand. The researchers found that the average soil loss rate was very slight when classified according to the LDD soil loss classification, so the results can be used to plan and improve area by soil and water conservation.

(2) Soil salinity assessment

Khan, Rastoskuev, Sato, and Shiozawa (2005) studied irrigated saline soils based on IRS-1B image and GIS data of Faisalabad, Pakistan. They used several indicators for identifying salts in the area in terms of salinity indices: salinity index (SI), normalized differential salinity index (NDSI), brightness index (BI), normalized differential vegetation index (NDVI), and ratio. The researchers found that SI and NDSI were good solution for assessing salt affect area because they could be achieved for the dry season and the classification processes was to distinguish between salt affected areas, rural/village areas due to its muddy roofs producing similar reflection as of patchy saline, and dry barren distributed soils was the most difficult in this study area.

Douaoui, Nicolas, and Walter (2006) studied salinity mapping in the lower Chéliff plain of Algeria, where soil salinity appears to be a major threat to agricultural production. Eleven indices divided into three groups include: (1) intensity (Int1 and Int2), (2) soil index (SI1, SI2, SI3, and BI), (3) vegetation index (NDVI, DVI, WDVI, PVI, and TSAVI) were derived from SPOT XS data in summer 1997. They divided soil samples into two datasets: model and validation dataset to generate prediction equation and to create soil salinity distribution map for validation data. The researchers found that SI3 had the highest correlation coefficient value when compared all indices. In addition, ordinary kriging demonstrated better performance than classification and simple regression used for interpolation of EC from ground data. The regression kriging was analyzed proper for model dataset in salinity estimations.

(3) Depletion of soil organic matter assessment

De Paz et al. (2006) used physical degradation index (PDI), biological degradation index (BDI) and chemical degradation index (CDI) to evaluate the soil degradation in Valencian Community in Mediterranean coast of Spain. They found that around 29% of the area was affected by high to very high physical degradation, 36% by high to very high biological degradation, and 6% by high to very high chemical degradation of soil. This study used for planning the policy framework for actions focused on preventing soil degradation and conserving its productive potential.

Sobprasonk (2009) used soil, topography, geological, laboratory and field data to evaluate bulk density and loss of top soil, soil fertility and soil biological degradation index to assess the changes in soil degradation due to the conversion from native forests into agricultural areas in Khun Wang area, Chiang Mai province. Field investigation and soil sampling for laboratory analysis were based on standard procedures

Srisomkiew (2014) investigated the appropriate method for assessing land degradation area in Kaset Wisai district of Roi Et province, Thailand. Soil samples in 2004 and 2011 were analyzed in the laboratory for soil potential of hydrogen ion (pH), electrical conductivity (EC), organic matter (OM) content, available phosphorus

(P), available potassium (K) and extractable calcium (ECa). Soil chemical and biological assessment was conducted for soil degradation assessment. Herein, K and P were used for chemical degradation assessment and OM content was used for biological degradation assessment. Laboratory data was interpolated using the Kriging interpolation method for assessing soil degradation. It was used to generate K, P, and OM. The generated map was then reclassified for comparison of the indicator parameter with FAO (1979) guidelines. Finally, the three maps from each year of 2004 and 2011 was combined together using raster calculator to generate the overall soil degradation map. The results showed the improvement of soil quality in 2011 as compared to the soil quality in 2004. The amount of P was considerably increased in the year 2011 than year 2004 with slightly improvement of OM and K.

(4) Land use and land cover classification using CART

Xiaodong, Shuqing, Huaiqing, Xiaofeng, Huan, and Chunyue (2009) applied spectral and textural data of Landsat TM imagery and ancillary geographical data to classify land cover in wetlands of the Sanjiang Plain, Heilongjiang Province, China. Herein, the CART was applied to three different combinations for land cover classification: (1) TM imagery alone (TM-only); (2) TM imagery plus image texture (TM+TXT model); and (3) all predictors including TM imagery, image texture and additional ancillary GIS information (TM+TXT+GIS model). Compared with traditional maximum likelihood classification (MLC) supervised classification, three classification trees predictive models reduced the overall error rate significantly. Image texture measures and ancillary geographical variables depressed the speckle noise effectively and reduced classification error rate of marsh obviously. For classification trees model making use of all available predictors, omission error rate was 12.90% and commission error rate was 10.99% for marsh. The developed method was relatively easy to implement and should be applicable in other sites and over larger extents.

Matinfar and Roodposhti (2012) applied the CART to classify LULC in 1992 and 2009 in Khoram Abad, Lorestan province of Iran. In this study, multispectral data from Landsat, NDVI, tasseled cap index, and principal component, which derived from Landsat data, and elevation, slope, and aspect, which derived from DEM, were used to classify LULC. Finally, post classification analysis for change detection between 1992 and 2009 showed the classification accuracy is highly increased in all classes. The CART classifier revealed notable improvement in classification accuracy in spite of high correlation of multi-spectral data.

CHAPTER III

DATA AND METHODOLOGY

Data and equipment that are applied in the study is firstly summarized and components of research methodology including (1) data collection and preparation, (2) LULC classification by decision tree classifier, (3) soil degradation analysis and (4) soil degradation evaluation is then described in details in this chapter.

3.1 Data and equipment

Data used in this research included remotely sensed data, GIS data and field survey data while equipment for soil survey included soil core, GPS and digital camera. Equipment for data analysis consists of notebook, desktop computer and statistical, image processing and GIS software were used in this research (Table 3.1).

3.2 Research methodology

Research methodology that was designed to serve the main objectives of the research included (1) data collection and preparation, (2) LULC classification by decision tree classifier, (3) soil degradation analysis and (4) soil degradation evaluation. Workflow diagram of the research methodology is presented in Figure 3.1.

Table 3.1 List of data and equipment in this research.

Data	Data characteristic	Source	Year
Remote Sensing	Landsat data	USGS	2015
GIS Data	Administrative boundary	DEQP	2011
	DEM	USGS	2014
	Rainfall	TMD	1985-2015
	Soil	LDD	1999
	Road	RTSD	1969-1995
Field survey data	Soil salinity sampling points	In situ field survey	2015-2016
	Soil organic matter sampling points	In situ field survey	2015-2016
Equipment	**Usage**	**Source**	
Hardware			
Soil auger	Soil survey	Soil and Plant Laboratory, SUT	
GPS	Soil survey	Personnel	
Digital camera	Soil survey	Personnel	
Notebook	Soil survey/ Data analysis	Personnel	
Desktop computer	Data analysis	Remote Sensing Laboratory, SUT	
Software			
ESRI ArcGIS	Data analysis	Remote Sensing Laboratory, SUT	
ENVI	Data analysis	Remote Sensing Laboratory, SUT	
ERDAS Imagine	Data analysis	Remote Sensing Laboratory, SUT	
IDRISI Selva	Data analysis	Remote Sensing Laboratory, SUT	
SPSS	Data analysis	Personnel	

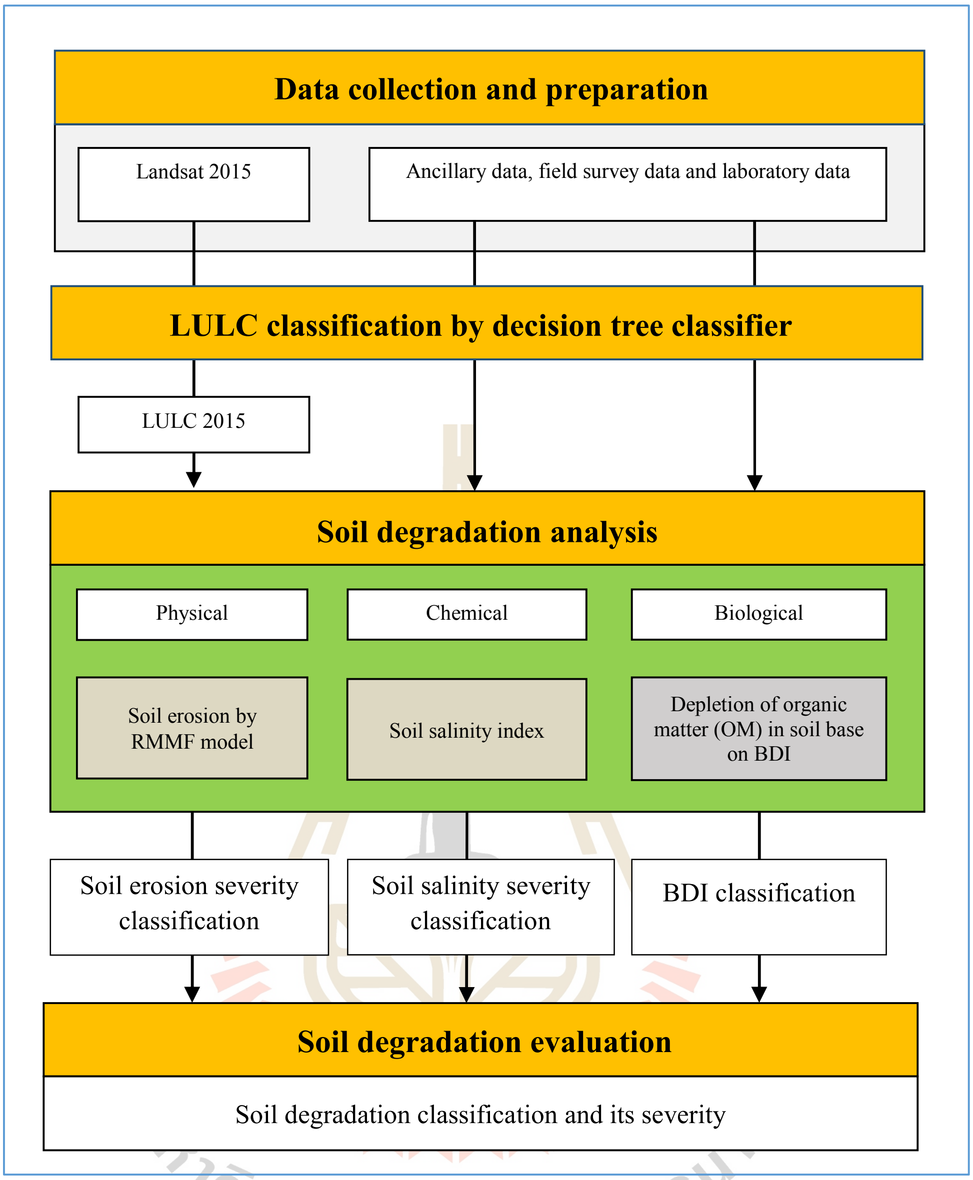

Figure 3.1 Workflow diagram of the research methodology.

3.2.1 Data collection and preparation

Basic remotely sensed data and bio-physical data were collected and prepared for analysis and modeling (Table 3.2). In this study, Landsat 8 data, Path 129 and Row 49, acquired date 9 March 2015 was downloaded from the USGS website (www.earthexplorer.usgs.gov). The false color composite of Landsat 8 data is displayed in Figure 3.2 while the characteristic of Landsat 8 data is summarized in Table 3.3.

Table 3.2 List of data collection and preparation.

Data collection	Data Preparation	Source	Year
Landsat data	Completeness checking	USGS	2015
Administrative boundary	Completeness checking	DEQP	2011
DEM	Completeness checking	USGS	2014
Slope	Extract from DEM	USGS	2014
Aspect	Extract from DEM	USGS	2014
Rainfall	Surface interpolation	TMD	1985-2015
Soil	Completeness checking	LDD	1999
Brightness	Create from Landsat data	Landsat data	2015
Greenness	Create from Landsat data	Landsat data	2015
Wetness	Create from Landsat data	Landsat data	2015
NDVI	Create from Landsat data	Landsat data	2015
NDWI	Create from Landsat data	Landsat data	2015
Spectral soil salinity indices	Create from Landsat data	Landsat data	2015
Spectral soil color indices	Create from Landsat data	Landsat data	2015
Soil salinity sampling points	Soil sample analysis	Researcher	2015-2016
Soil organic matter sampling points	Soil sample analysis	Researcher	2015-2016

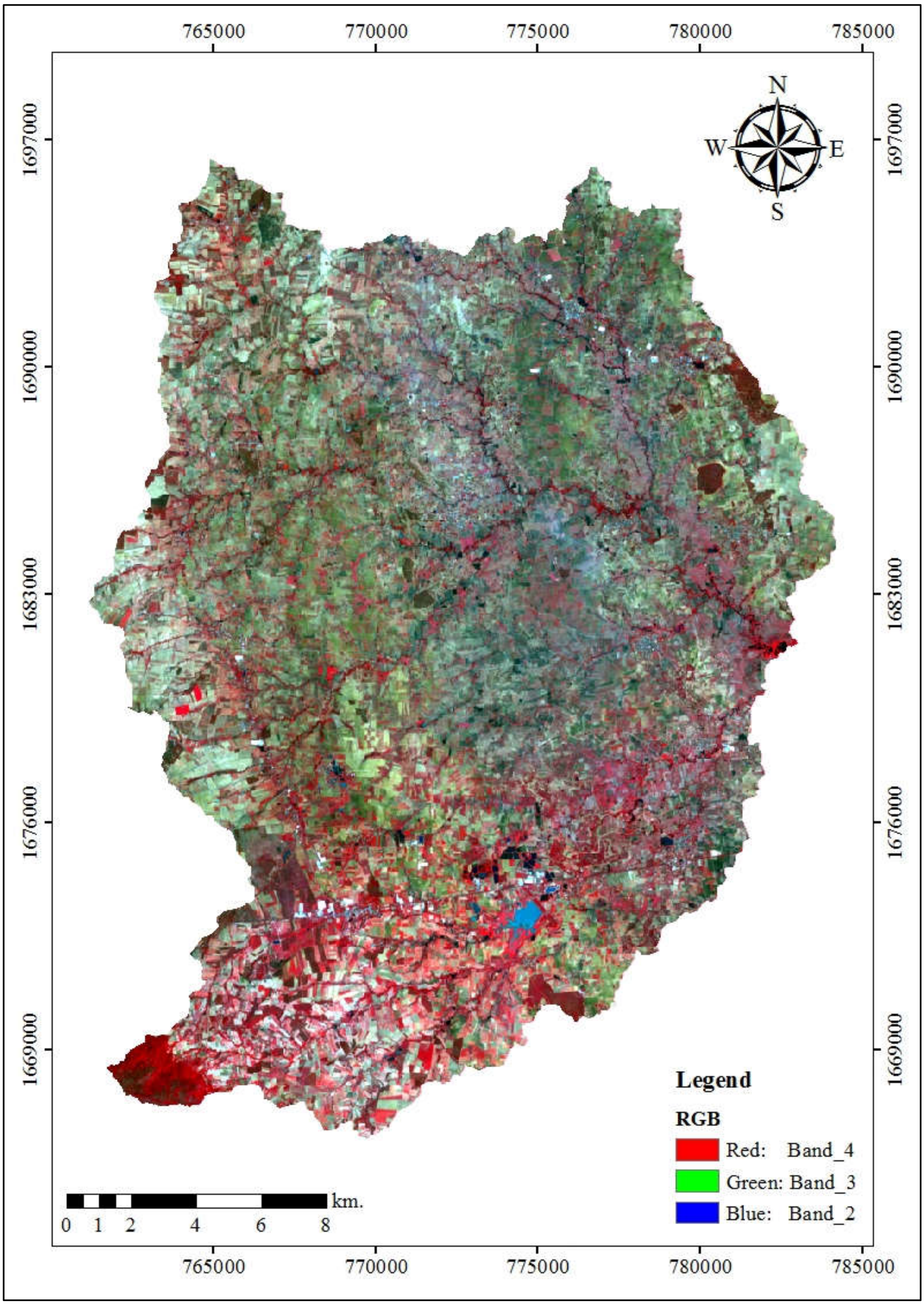

Figure 3.2 Landsat 8 data of the study area.

Table 3.3 Characteristics of Landsat 8 (USGS, 2015).

Band	Name	Wavelength	Useful for mapping	Resolution (m.)
1	Coastal aerosol	0.43 - 0.45	Coastal and aerosol studies	30
2	Blue	0.45 - 0.51	Bathymetric mapping, distinguishing soil from vegetation and deciduous from coniferous vegetation	30
3	Green	0.53 - 0.59	Emphasizes peak vegetation, which is useful for assessing plant vigor	30
4	Red	0.64 - 0.67	Discriminates vegetation slopes	30
5	Near Infrared (NIR)	0.85-0.88	Emphasizes biomass content and shorelines	30
6	Short-wave Infrared (SWIR) 1	1.57 - 1.65	Discriminates moisture content of soil and vegetation; penetrates thin clouds	30
7	Short-wave Infrared (SWIR) 2	2.11 - 2.29	Improved moisture content of soil and vegetation and thin cloud penetration	30
8	Panchromatic	0.50 - 0.68	Sharper image	15
9	Cirrus	1.36 - 1.38	Improved detection of cirrus cloud contamination	30
10	TIRS 1	10.60 – 11.19	Thermal mapping and estimated soil moisture	100 * (30)
11	TIRS 2	11.5 - 12.51	Improved thermal mapping and estimated soil moisture	100 * (30)

Note: * = TIRS bands are acquired at 100 meter resolution, but are resampled to 30 meter in delivered data product.

3.2.2 LULC classification by decision tree classifier

Supervised classification with decision tree classifier by CRT algorithm and Expert System was here applied to classify LULC types in 2015 of the study area. Herein, influential factors on LULC types and its distribution as independent variables including spectral data of Landsat-8 and its derived indices (brightness, greenness, and wetness) and biophysical factors (elevation, slope, and aspect) were selected to extract decision tree structure. The LULC classification system which was modified from land use classification scheme of LDD (2011) in level 2 consisted of:

(1) Urban and built-up land (URBAN),

(2) Paddy field (PF),

(3) Maize (MAIZE),

(4) Sugarcane (SGC),

(5) Cassava (CAS),

(6) Perennial tree and orchard (TREE),

(7) Dense deciduous forest (DDF),

(8) Disturbed deciduous forest (DIDF),

(9) Forest plantation (FP),

(10) Water body (WATER),

(11) Scrub (SCRUB), and

(12) Miscellaneous land (soil pit, sand pit, and land fill) (MISC).

In addition, accuracy assessment for the classified LULC map in 2015 was performed based on reference LULC data from field survey in 2016 using overall accuracy and Kappa hat coefficient of agreement. In practice, number of samples and sampling method scheme is firstly decided and error matrix is then constructed for accuracy assessment. In this study, number of sample size was estimated based on the binomial probability theory by Fitzpatrick-Lins (1981) and stratified random sampling scheme was applied to allocate sampling points for accuracy assessment.

3.2.3 Soil degradation analysis

Soil degradation analysis, which includes soil erosion, soil salinity and depletion of organic matter content assessment, was processed under ESRI ArcGIS environment. In practice, Model Builder module of ESRI ArcGIS was applied for semi-automatic processing of soil degradation analysis.

3.2.3.1 Soil erosion assessment

Soil erosion, which represents a physical indicator for soil degradation, was here assessed using RMMF model. Schematic diagram of soil erosion assessment is shown in Figure 3.3. It consisted of two sub-components: soil erosion analysis using RMMF model (data preparation, model parameters extraction, model operation), and soil erosion severity classification. Major tasks of this component were separately described in the following sections.

(1) RMMF data preparation

In this study, LULC data for proportion of rainfall intercepted by crop cover, percentage canopy cover, plant height, ratio of actual to potential evapotranspiration, percentage ground cover, crop cover management, effective hydrological depth of soil), rainfall data for annual rainfall total, intensity of erosive rain, number of rain days per year), soil data for soil moisture content at field capacity, bulk density of top soil, soil detachment index, and cohesion of the surface soil) and DEM data for slope steepness and streamflow were prepared to extract RMMF parameter as summarized in Table 3.4.

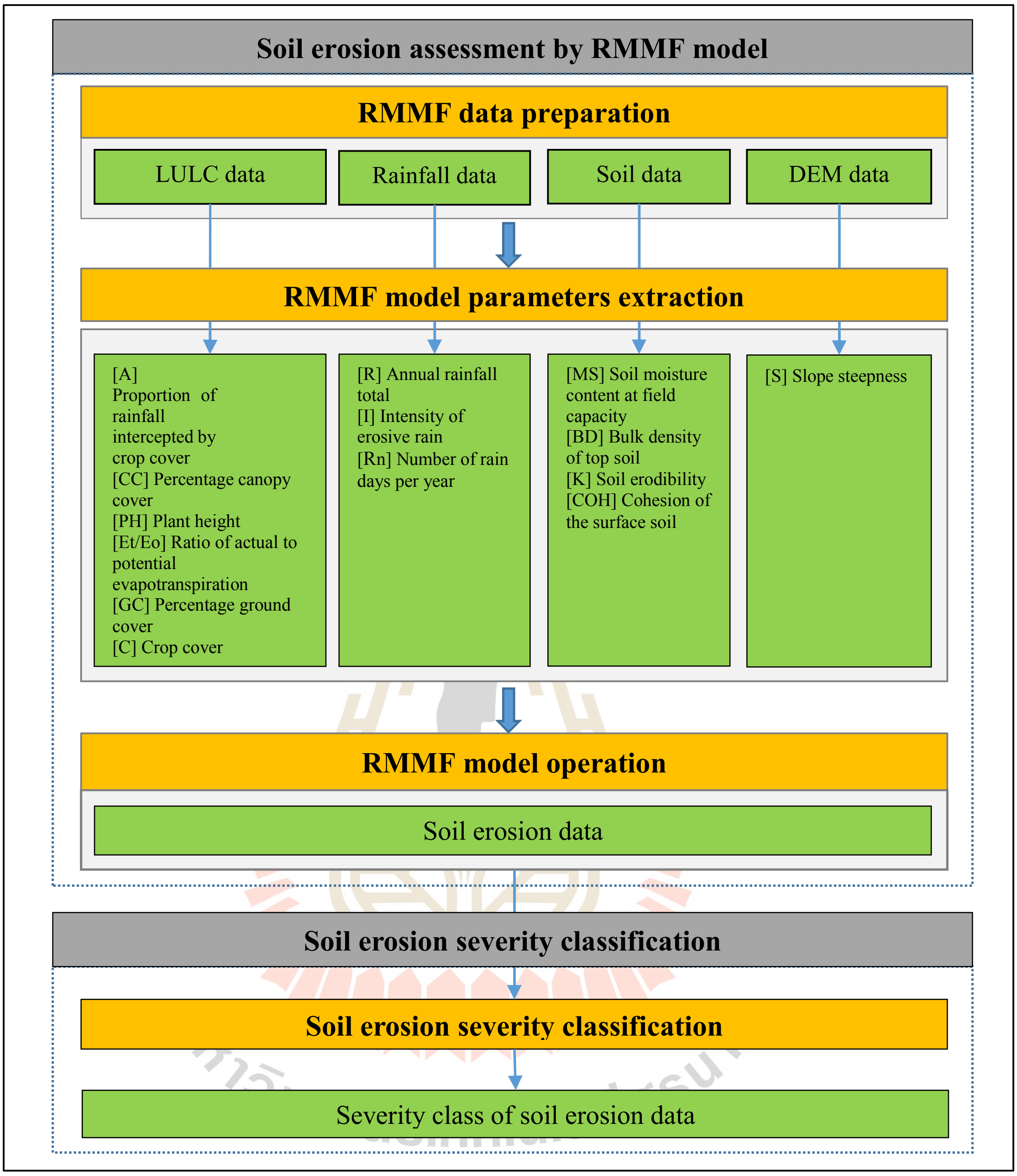

Figure 3.3 Schematic diagram of soil erosion assessment.

(2) RMMF parameters extraction

Some RMMF parameters were directly extracted based on the prepared data including annual rainfall total (R), number of rain days per year (Rn), and slope steepness (S), while others were assigned based on literature reviews from Morgan (2001); Yazidhi (2003); Morgan and Duzant (2008); Suriyaprasit (2008); and Kamonrat (2011) as summary Table 3.4.

Table 3.4 List of RMMF model parameters.

Parameter (Symbol)	Input data	Data preparation/Values	Unit	Year
Annual rainfall total (R)	Mean annual rainfall	Surface data interpolation using Kriging	mm	1985-2015
Intensity of erosive rain (I)	Intensity of erosive rain data	25 mm per hour.	mm/h	1985-2015
Number of rain days per year (R_n)	Number of rain days per year	Surface data interpolation using Kriging	mm	1985-2015
Soil moisture content at field capacity (MS)	Soil texture of soil series data	Sand = 0.08; Loamy sand = 0.15; Sandy loam = 0.28; Loam = 0.20; Silt = 0.15; Silty loam = 0.25; Sandy clay loam = 0.38; Clay loam = 0.40; Silty clay loam = 0.42; Sandy clay = 0.28; Fine sand = 0.15; Silty clay = 0.30; and Clay = 0.45.	ww %	1999
Bulk density of top soil (BD)	Soil texture of soil series data	Sand = 1.50; Loamy sand = 1.40; Sandy loam = 1.20; Loam = 1.30; Silt = 1.30; Silty loam = 1.30; Sandy clay loam = 1.40; Clay loam = 1.30; Silty clay loam = 1.30; Sandy clay = 1.40; Fine sand = 1.40; Silty clay = 1.30; and Clay = 1.10.	g/cm^3	1999
Soil detachment index (K)	Soil texture of soil series data	Sand = 1.20; Loamy sand = 0.30; Sandy loam = 0.70; Loam = 0.80; Silt = 1.00; Silty loam = 0.70; Sandy clay loam = 0.10; Clay loam = 0.70; Silty clay loam = 0.80; Sandy clay = 0.30; Fine sand = 1.00; Silty clay = 0.50; and Clay = 0.05.	g/j	1999
Cohesion of the surface soil (COH)	Soil texture of soil series data	Sand = 2.00; Loamy sand = 2.00; Sandy loam = 2.00; Loam = 3.00; Silt = 3.00; Silty loam = 3.00; Sandy clay loam = 3.00; Clay loam = 10.00; Silty clay loam = 9.00; Sandy clay = 9.00; Fine sand = 3.00; Silty clay = 10.00; and Clay = 12.00.	k Pa	1999
Proportion of rainfall intercepted by crop cover (A)	LULC data	Dense forest = 0.30; Degrade forest = 0.35; Paddy field = 0.35; Maize = 0.25; Sugarcane = 0.25; Cassava = 0.25; Scrub = 0.35; Perennial tree and orchard = 0.20; Grass land = 0.20; Miscellaneous land (soil pit, sand pit, and land fill) = 0; Urban and built-up land = 0; and Water body = 0.	unitless (0-1)	2015

Table 3.4 (Continued).

Parameter (Symbol)	Input data	Data preparation/Values	Unit	Year
Percentage canopy cover (CC)	LULC data	Dense forest = 0.81; Degrade forest = 0.35; Paddy field = 0.35; Maize = 0.26; Sugarcane = 0.30; Cassava = 0.40; Scrub = 0.80; Perennial tree and orchard = 0.31; Grass land = 0.93; Miscellaneous land (soil pit, sand pit, and land fill) = 0; Urban and built-up land = 0; and Water body = 0.	percent (0-1)	2015
Plant height (PH)	LULC data	Dense forest = 19.40; Degrade forest = 14.95; Paddy field = 1.30; Maize = 0.67; Sugarcane = 1.32; Cassava = 0.80; Scrub = 5.00; Perennial tree and orchard = 7.30; Grass land = 1.50; Miscellaneous land (soil pit, sand pit, and land fill) = 0; Urban and built-up land = 0; Water body = 0.	m	2015
Ratio of actual to potential evapotranspiration (Et/Eo)	LULC data	Dense forest = 0.90; Degrade forest = 0.90; Paddy field = 1.35; Maize = 0.78; Sugarcane = 0.90; Cassava = 0.70; Scrub = 0.80; Perennial tree and orchard = 0.70; Grass land = 0.88; Miscellaneous land (soil pit, sand pit, and land fill) = 0.05; Urban and built-up land = 0; and Water body = 0.	unitless	2015
Percentage ground cover (GC)	LULC data	Dense forest = 0.91; Degrade forest = 0.50; Paddy field = 0.50; Maize = 0.44; Sugarcane = 0.49; Cassava = 0.49; Scrub = 0.20; Perennial tree and orchard = 0.50; Grass land = 0.95; Miscellaneous land (soil pit, sand pit, and land fill) = 0.025; Urban and built-up land = 0; and Water body = 0.	percent (0-1)	2015
Crop cover management (C)	LULC data	Dense forest = 0.048; Degrade forest = 0.003; Paddy field = 0.119; Maize = 0.300; Sugarcane = 0.150; Cassava = 0.400; Scrub = 0.004; Perennial tree and orchard = 0.300; Grass land = 0.100; Miscellaneous land (soil pit, sand pit, and land fill) = 1.000; Urban and built-up land = 0; and Water body = 0.	unitless	2015
Effective hydrological depth of soil (EHD)	LULC data	Dense forest = 0.20; Degrade forest = 0.16; Paddy field = 0.12; Maize = 0.12; Sugarcane = 0.12; Cassava = 0.12; Scrub = 0.12; Perennial tree and orchard = 0.15; Grass land = 0.14; Miscellaneous land (soil pit, sand pit, and land fill) = 0.09; Urban and built-up land = 0; and Water body = 0.	m	2015
Slope steepness (S)	DEM data	Slope gradient creation	degree	2014

(3) RMMF model operation

The overview of RMMF model operation for soil erosion assessment is schematic displayed in Figure 3.4. Herewith, operating function for soil erosion assessment using by RMMF model is summarized in Table 3.5.

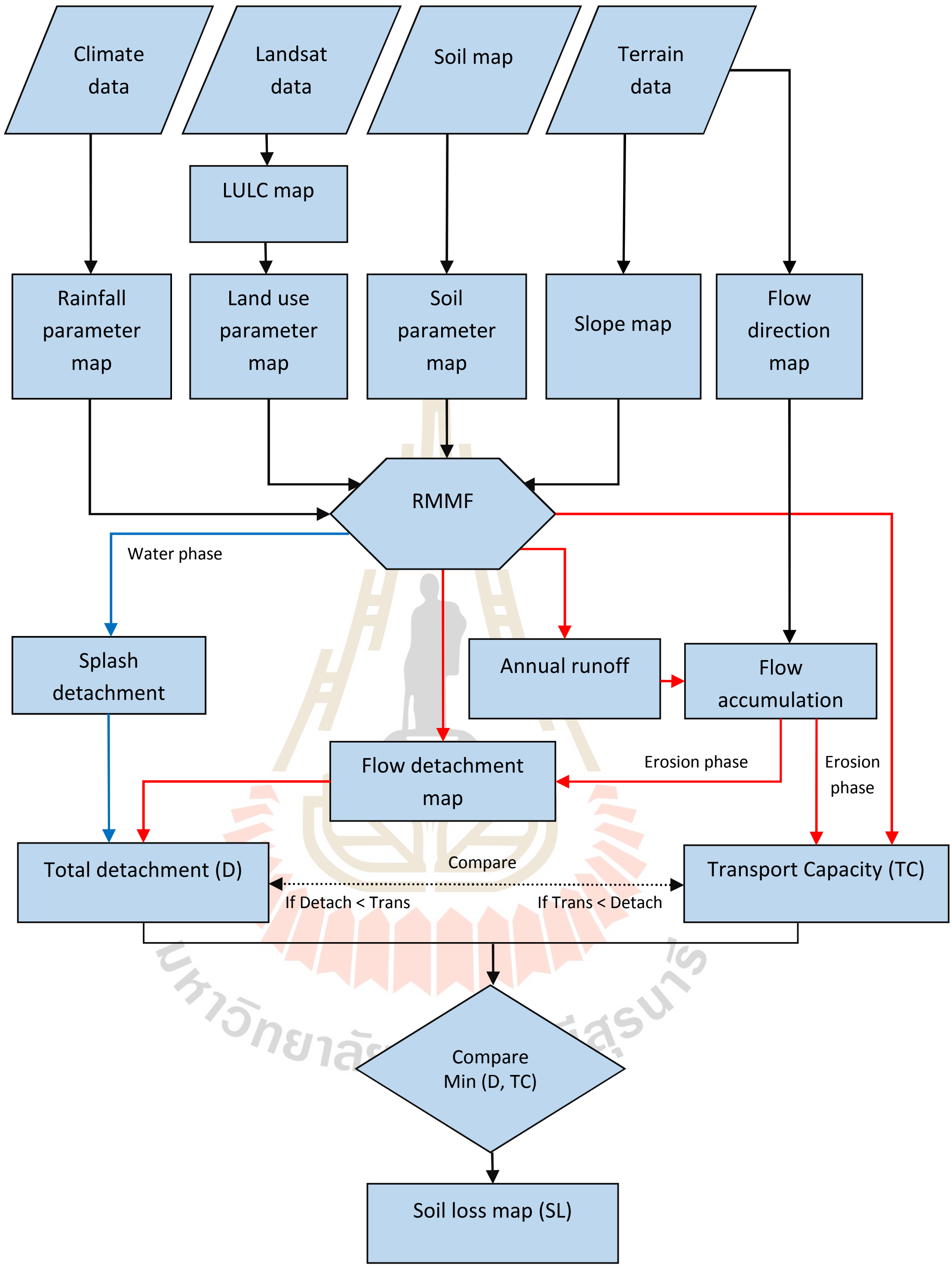

Figure 3.4 Flow diagram of RMMF model (Modified from Yazidhi, 2003).

Table 3.5 Operating function for the RMMF model (modified from Yazidhi, 2003).

Eq. No.	Function name	Symbol	Equation	Parameter
1	Effective rainfall	ER	ER = R*A	ER = Effective rainfall (mm)
2	Leaf drainage	LD	LD = ER*CC	LD = Leaf drainage (mm)
3	Direct through fall	DT	DT=ER-LD	DT = Direct through fall (mm)
4	Kinetic energy of direct through fall	KE(DT)	KE(DT) = DT*(11.9+8.7 Log_{10} I)	KE (DT) = Kinetic energy of direct through fall (J m^{-2})
5	Kinetic energy of leaf drainage	KE(LD)	KE(LD) = LD*(15.8*$PH^{0.5}$)-5.87	KE(LD) = Kinetic energy of leaf drainage (J m^{-2})
6	Kinetic energy of rainfall	KE	KE = KE(DT)+KE(LD)	KE = Kinetic energy of rainfall (J m^{-2})
7	Soil moisture storage capacity	Rc	Rc = 1000*MS*BD*EHD*$(Et/Eo)^{0.5}$	Rc = Soil moisture storage capacity (mm)
8	Mean rain per day	Ro	Ro = R/Rn	Ro = Mean rain per day (mm)
9	Annual runoff	Q	Q = R*exp (-Rc/Ro)	Q = Annual runoff (mm)
10	Soil particle detachment by raindrop impact	F	F=K*KE*10^{-3}	F = Soil particle detachment by raindrop impact (kg m^{-2})
11	Soil resistance	Z	Z = 1/ (0.5*COH)	Z = Soil resistance (unitless)
12	Runoff detachment	H	H = $ZQ^{1.5}$ sin S (1-GC)*10^{-3}	H = Runoff detachment (kg m^{-2})
13	Total particle detachment	D	D = F+H	D = Total particle detachment (kg m^{-2})
14	Transport capacity of runoff	TC	TC = CQ^2 sin S * 10^{-3}	TC = Transport capacity of runoff (kg m^{-2})
15	Annual soil loss	SL	SL = Minimum (D, TC)	SL = Annual soil loss (kg m^{-2})
				R = Annual rainfall total (mm)
				A = Proportion of rainfall intercepted by crop cover (0-1)
				Rn = Number of rain days in a year (days)
				I = Rainfall intensity (mm h^{-1})
				CC = Percentage canopy cover (%)
				PH = Plant height (m)
				MS = Soil moisture content at field capacity (ww %)
				BD = Bulk density (g cm^{-3})
				EHD = Effective hydrological depth of soil (m.)
				Et/Eo = Ratio of actual to potential evapotranspiration (unitless)
				K = Soil erodibility (g j^{-1})
				S = Slope steepness (degree)
				GC = Ground cover (%)
				COH = Cohesion of the surface soil (k Pa)
				C = Crop cover management (unitless)

(4) Soil erosion severity classification

Under this sub-component, the result of soil erosion analysis using RMMF model was further classified its severity according to standard of LDD (2000) as shown in Table 3.6.

Table 3.6 Severity class of soil erosion (LDD, 2000).

No.	Severity Class	Erosion Rate (t/ha/y)	Erosion Rate (t/rai/y)
1	Very Slightly Eroded	≤ 6.25	≤ 39.06
2	Slightly Eroded	6.26-31.25	39.13-195.31
3	Moderately Eroded	31.26-125.00	195.38-781.25
4	Highly Eroded	125.01-625.00	781.31-3,906.25
5	Very Highly Eroded	> 625.00	> 3,906.25

3.2.3.2 Soil salinity assessment

Soil salinity refers to the accumulation of water soluble salts - mostly of sodium, potassium, calcium and magnesium. Salinity levels are usually determined by measuring the electrical conductivity of soil/water suspensions. Traditionally, the electrical conductivity of saturated extracts was used (ECe) but these values are time-consuming and difficult to determine. Electrical Conductivity (EC) is commonly determined more rapidly and easily on a 1:5 soil/water suspension (EC 1:5). The conductivity of a water solution is directly related to the amount of salt dissolved in the solution. Total soluble salts (TSS) was a popular term for expressing soil salinity. The conductivity of a water solution is directly related to the amount of salt presents in solution (Richards, 1954).

Soil salinity analysis, which presents a chemical indicator for soil degradation, was here assessed using linear and non-linear regression analysis for soil salinity estimation. Schematic diagram of assessing soil salinity is shown in Figure 3.5.

It consisted of one main activity: EC samples collection and analysis, and 3 sub-components including EC estimation model development, optimum model for EC estimation, and soil salinity assessment and its severity classification.

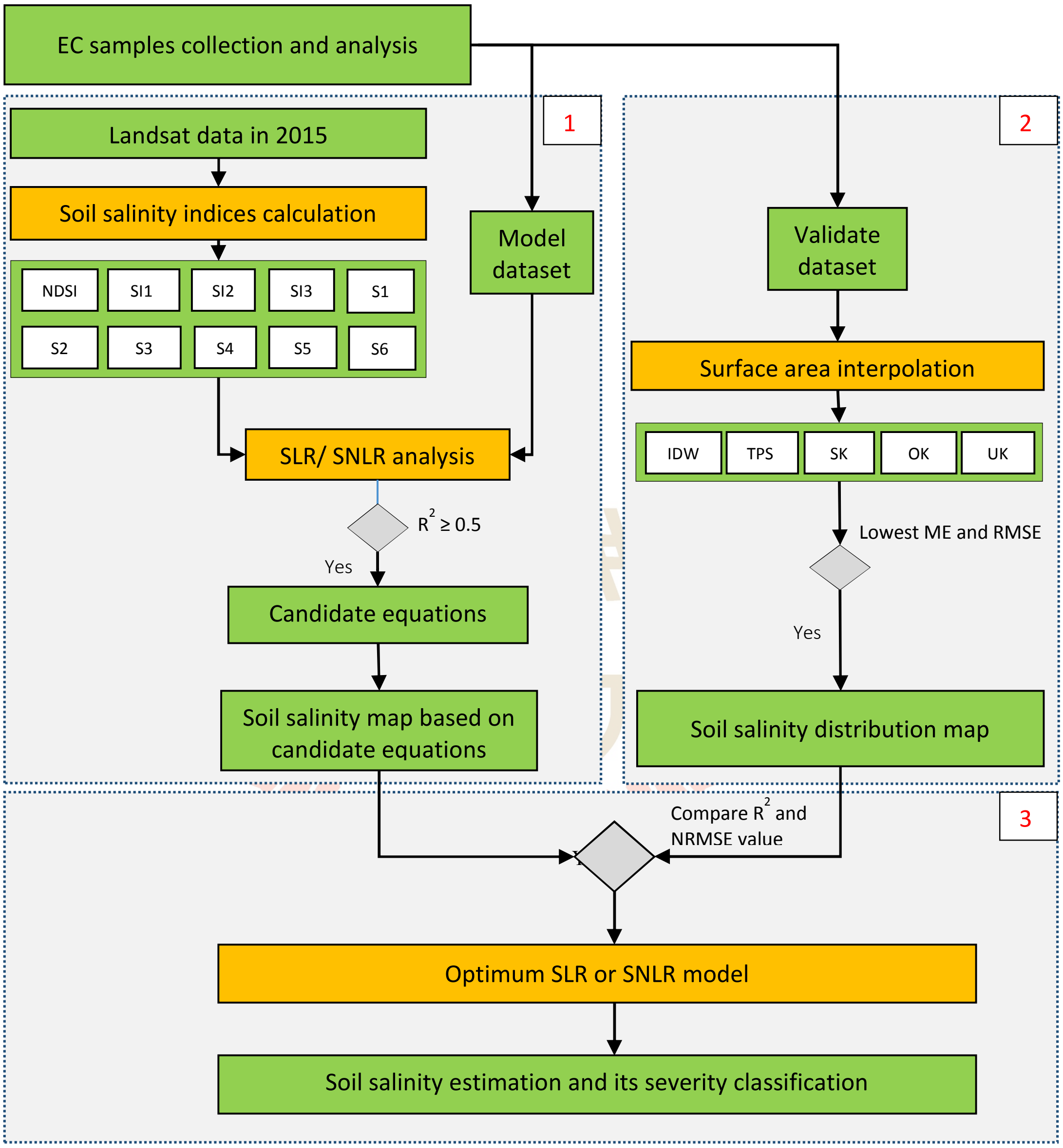

Figure 3.5 Schematic diagram of soil salinity assessment.

(1) EC samples collection and analysis

Soil survey method of LDD was here adopted for EC sample collection and analysis. Herein soil series data were firstly overlaid with land use data (excluding urban and built-up area and water body) by union operator to create combination class between soil series and land use with WGS 1984 datum of UTM coordinate zone 47 for soil sampling unit identification as result shown in Figure 3.6 (see detail in Appendix A).

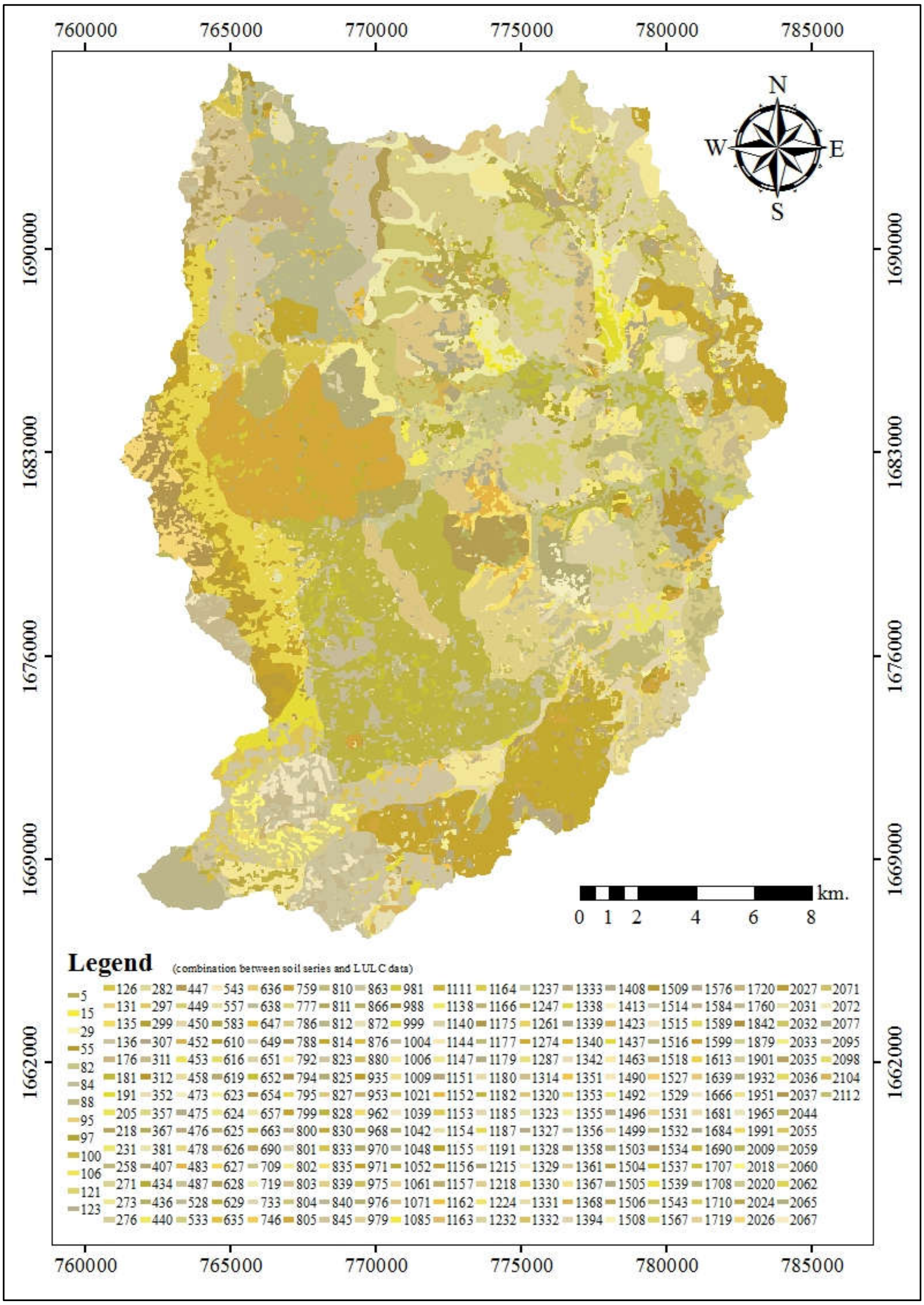

Figure 3.6 Combination between soil series and LULC data for sample point allocation.

In this study, number of soil samples was calculated according to detailed reconnaissance soil survey at the scale of 1:40,000-1:100,000 as suggested by Kheoruenromne (2005). He recommend that the intensity of soil samples per 2 sq. km should be one sample. Hence the required numbers of soil samples in the study area with area of 464.9 sq. km were 233 samples. In practice, 233 sample points were divided into two datasets: one dataset for modeling (60%) and another dataset for validating (40%).

For soil salinity survey, soil samples were collected using soil core at topsoil level (0-30 cm) and all data were further analyzed soil salinity property at Crop Production Technology Laboratory and Chemistry Laboratory of Suranaree University of Technology (SUT). In this study, EC 1:5 method with ratio of soil and water at 1:5 was applied for soil salinity extraction.

(2) EC estimation model development

Under this sub-component, soil salinity indices (NDSI, SI1, SI2, SI3, S1, S2, S3, S4, S5, and S6) as independent variable were firstly extracted according to its equation (see Table 2.2) from Landsat data in 2015. Meanwhile, the analyzed electrical conductivity (EC) data that implies soil salinity level from modelling dataset was used as dependent variable for linear or non-linear regression analysis. General equation form of simple and multiple linear and non-linear equations applied in this study were listed as follows:

Simple linear model:

$$Y = b0 + (b1 * X) \tag{3.1}$$

Multiple linear model:

$$Y = b0 + (b1 * X1) + (b2 * X2) + (b3 * X3) + \ldots (bn * Xn) \tag{3.2}$$

Logarithmic model:

$$Y = b0 + (b1 * \ln(X)) \tag{3.3}$$

Inverse model:

$$Y = b0 + (b1 / X) \tag{3.4}$$

Quadratic model:

$$Y = b0 + (b1 * X) + (b2 * X**2) \tag{3.5}$$

Cubic model:

$$Y = b0 + (b1 * X) + (b2 * X**2) + (b3 * X**3) \tag{3.6}$$

Power model:

$$Y = b0 * (X**b1) \tag{3.7}$$

Compound model:

$$Y = b0 * (b1**X) \text{ or } \ln(Y) = \ln(b0) + (\ln(b1) * X) \tag{3.8}$$

S-curve model:

$$Y = e** (b0 + (b1/X)) \text{ or } \ln(Y) = b0 + (b1/X) \tag{3.9}$$

Growth model:

$$Y = e** (b0 + (b1 * X)) \text{ or } \ln(Y) = b0 + (b1 * X) \tag{3.10}$$

Exponential model:

$$Y = b0 * (e** (b1 * X)) \text{ or } \ln(Y) = \ln(b0) + (b1 * X) \tag{3.11}$$

Where X and Y is independent variables and dependent variable, respectively.

The derived equations of linear and non-linear equations which provide the R^2 equal or more than 0.5 were used as candidate equations to identify an optimum model for EC estimation.

In addition, EC data from validation dataset was also interpolated to create EC distribution map using inverse distance weighted (IDW), thin plate splines

(TPS), simple kriging (SK), ordinary kriging (OK), and universal kriging (UK) techniques. The interpolated EC distribution map of the best interpolation technique that provides the lowest Root Mean Square Error (RMSE) and Mean Error (ME) was examined correlation analysis with the constructed EC map of candidate linear and non-linear models. This operation validated soil salinity pattern using correlation coefficient (R) and coefficient of determination (R^2) and it was also used to justify an optimum model when the NRMSE from candidate equations are equal.

(3) Optimum model for EC estimation

Under this sub-component, the derived candidate equations of linear and non-linear regression analysis were firstly applied to generate EC distribution map using Map Calculator of ESRI ArcGIS software. Then, these generated maps were assessed accuracy based on analyzed EC data from validation dataset using NRMSE with the following equations.

$$\mathrm{RMSE} = \sqrt{\frac{1}{n}\sum_{i=1}^{n}[\text{Estimated value} - \text{Observed value}]^2} \tag{3.12}$$

$$\mathrm{NRMSE} = \frac{\mathrm{RMSE}}{\text{Maximum observed value} - \text{Minimum observed value}} \tag{3.13}$$

Where n is number of observation and RMSE is root mean square error.

The linear or linear model that provides the highest accuracy with the lowest NRMSE value was chosen as optimum model for EC estimation.

Furthermore, the interpolated EC data from the best interpolation technique were examined correlation with the constructed EC map of candidate linear and non-linear models. The derived result was also used to justify an optimum model for EC estimation when the NRMSE from candidate equations are equal.

(4) Soil salinity assessment and its severity classification

The optimum EC estimation model from linear or non-linear analysis was applied to assess soil salinity data and the derived result was further classified its severity as suggestion by Lanyon, Cass and Hansen (2004); Patterson (2006) as shown in Table 3.7.

In addition, TSS was estimated to express soil salinity with EC1:5 as suggested by (Richards, 1954) with following equation:

$$\text{TSS (g/100 g or \%)} = 0.064 \times \text{EC1:5 (dS/m)} \tag{3.14}$$

Table 3.7 Severity class of soil salinity.

Level of EC	**Effect on Plant Growth**	**Soil salinity severity class**	**EC of 1:5 soil/water extract (dS m^{-1})**				
			Sand/ loamy sand	**Loam**	**Sandy clay loam**	**Light clay**	**Heavy clay**
Very low	Negligible effect	Non - saline	<0.15	<0.17	<0.25	<0.30	<0.40
Low	Very sensitive crops affected	Slightly saline	0.16-0.30	0.18-0.35	0.26-0.45	0.31-0.60	0.41-0.80
Moderate	Many crops affected	Moderately saline	0.31-0.60	0.36-0.75	0.46-0.90	0.61-1.15	0.81-1.60
High	Salt tolerant plants grow	Very saline	0.61-1.20	0.76-1.50	0.91-1.75	1.16-2.30	1.61-3.20
Very High	Few salt tolerant plants grow	Highly saline	>1.20	>1.50	>1.75	>2.30	>3.20

3.2.3.3 Soil organic matter assessment

Organic matter (OM) depletion of soil, which presents a biological indicator for soil degradation, was here assessed using Biological Degradation Index (BDI) as suggested by De Paz et al. (2006). Schematic diagram for assessing depletion organic matter of soil is shown in Figure 3.7. It consisted of one main activity: OM samples collection and analysis, and 3 sub-components including OM estimation model development, optimum model for OM estimation, and OM and BDI estimation and its severity classification.

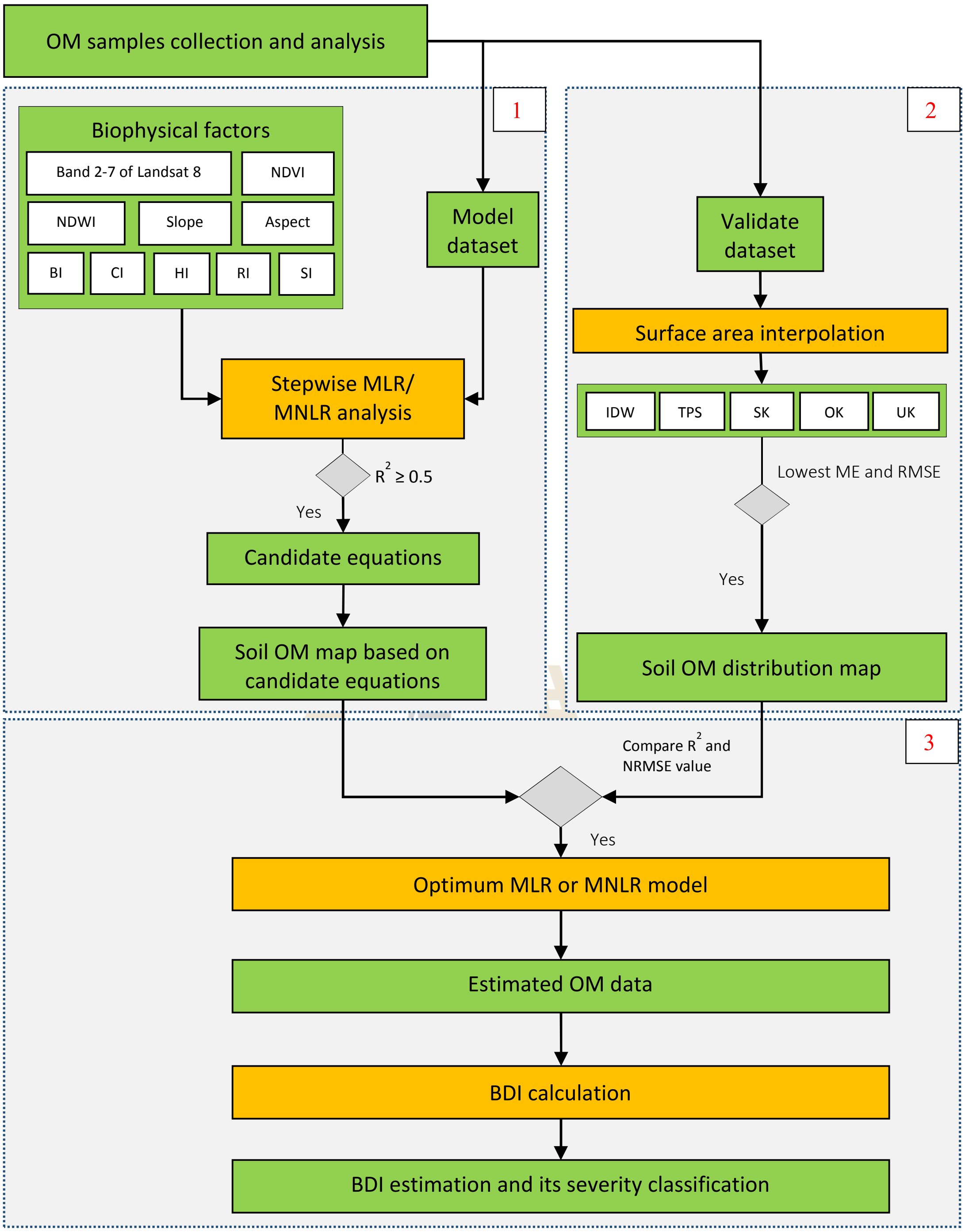

Figure 3.7 Schematic diagram of soil organic matter assessment.

(1) OM samples collection and analysis

Soil samples were collected nearby the location of soil survey for EC sampling and they were analyzed organic matter (OM) using Walkley and Black method at Crop Production Technology Laboratory of SUT. Like EC sampling points, OM sampling points was divided into two datasets: one dataset for modeling and another dataset for validation.

(2) OM estimation model development

Under this sub-component, spectral data and biophysical factors include brightness value of band 2-7 of Landsat data, soil color indices (Brightness Index (BI), Coloration Index (CI), Hue Index (HI), Redness Index (RI), and Saturation Index (SI)), NDVI, NDWI, slope and aspect as independent variables were firstly extracted according to its equation (see Table 2.3). Meanwhile, the analyzed OM data from modeling dataset was used as dependent variable for linear and non-linear regression analysis. The selected models (equations) of linear and non-linear analysis for OM analysis are similar with soil salinity analysis (Equations 3.1 to 3.11). Likewise, the derived equations of linear and non-linear analysis which provide the R^2 equal or more than 0.5 were used as candidate equations to identify an optimum model for OM estimation. In addition, candidate simple and multiple linear and non-linear equations were used to generate OM distribution maps.

Meanwhile analyzed OM data from validation dataset was also applied to create OM distribution map using IDW, TPS, SK, OK, and UK techniques. The interpolated OM distribution map of the best interpolation technique that provides the lowest RMSE and ME was examined correlation analysis with the constructed OM maps of candidate linear and non-linear models. This operation validated OM pattern using R and R^2 and it was also used to justify an optimum model when the NRMSE from candidate equations are equal.

(3) Optimum model for OM estimation

Under this sub-component, the derived candidate equations of linear and non-linear regression analysis were firstly applied to generate OM distribution map using Map Calculator of ESRI ArcGIS software. Then, these generated maps were assessed accuracy based on analyzed OM data from validation dataset using NRMSE. The linear or linear model that provides the highest accuracy with the lowest NRMSE value was chosen as optimum model for OM estimation.

Furthermore, the interpolated OM data from the best interpolation technique was also examined correlation with the constructed OM map of candidate linear and non-linear models. The derived result was also used to justify an optimum model for OM estimation when the NRMSE from candidate equations are equal.

(4) OM and BDI estimation and its severity classification

The optimum OM estimation model from linear or non-linear analysis was firstly applied to create OM data and it was normalized using the linear scale transformation method with ranging between 0 and 1 (Singh, Verma, and Thoke, 2015) using following equation.

$$\hat{X} = \frac{X - Xmin}{Xmax - Xmin} \tag{3.15}$$

Where $\hat{X}$ = the normalized value

X = the actual value

$Xmin$ = minimum of the actual value

$Xmax$ = maximum of the actual value

Then, the normalized values of OM were converted to be percent by multiplication with 100. After that, BDI that represents the depletion of soil organic matter content was calculated as suggested by De Paz et al. (2006) with the following equation.

$$BDI = \frac{1}{OM} \tag{3.16}$$

Where

BDI = biological degradation index

OM = organic matter content (%)

The BDI was further reclassified for soil biological degradation into five classes according to equal interval percentage of OM as shown in Table 3.8.

Table 3.8 Biological degradation index and its classification with equal interval method (Modified from De Paz et al., 2006).

BDI	Level of soil biological degradation				
	Very low	Low	Moderate	High	Very high
	≤ 0.0125	0.0125-0.0167	0.0167-0.0250	0.0250-0.0500	≥0.0500

3.2.4 Soil degradation evaluation

Under this section, multiple indicators (soil erosion, soil salinity and soil biological degradation) were combined using multiplicative method for soil degradation evaluation. In this study, multiplicative method without and with severity classification of soil erosion, soil salinity and soil biological degradation were examined.

(1) Multiplicative method without severity classification

Under this method, the derived soil loss, the estimated soil salinity, and BDI index data as land degradation indicators were firstly separately normalized using the linear scale transformation method (Eq. 3.15). Then, the normalized data of three indicators were multiplied together and reclassified into five soil degradation severity classes (very low, low, moderate, high and very high) using Natural break method.

(2) Multiplicative method with severity classification

Under this method, severity classification of soil erosion, soil salinity and biological degradation were combined using multiplicative method for soil degradation evaluation (see detail in Appendix B). In this study, an integer values (1, 2, 3, 4, and 5) were firstly ordinal assigned to each severity class (very low, low, moderate, high, and very high) of three soil severity classifications (soil erosion, soil salinity and biological degradation) according to its class. Then, all indicators were multiplied together and reclassified into five soil degradation severity classes (very low, low, moderate, high and very high using Equal Interval method as summary in Table 3.9.

Table 3.9 Severity class of land degradation under multiplicative method with severity classification.

No.	Severity class of soil degradation	Range value of multiplicative products
1	Very low	1 - 25
2	Low	26 -50
3	Moderate	51 - 75
4	High	76 -100
5	Very High	101 - 125

CHAPTER IV

LAND USE AND LAND COVER CLASSIFICATION

This chapter presents results of the first objectives focusing on LULC classification in 2015 using CRT algorithm and Expert System. It consists of an optimum CART model for LULC classification and result of LULC classification.

4.1 An optimum CART model for LULC classification

Under optimum CART model for LULC classification, the original Landsat-8 data in 2015 and its derived indices (brightness, greenness, and wetness) and physical factors (elevation, slope, and aspect) as independent variables were firstly created as result shown in Figure 4.1. They were used to extract their values from training areas of each LULC class as dependent variable and they are then exported as ASCII file with each LULC class as an example shown in Table 4.1. Figure 4.2 shows an example of Landsat image data and ground photograph of each LULC class in the study area. The prepared dependent and independent variables as ASCII file were here applied to construct decision tree with CRT growing method under SPSS statistical software.

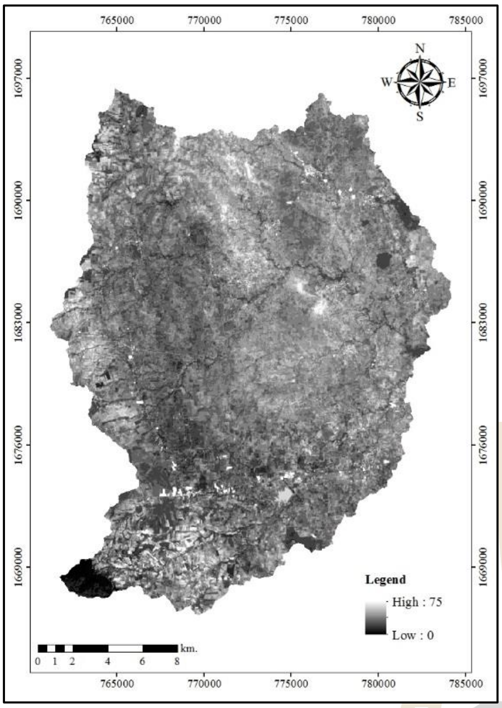

Landsat-8 Band 2 (Blue)

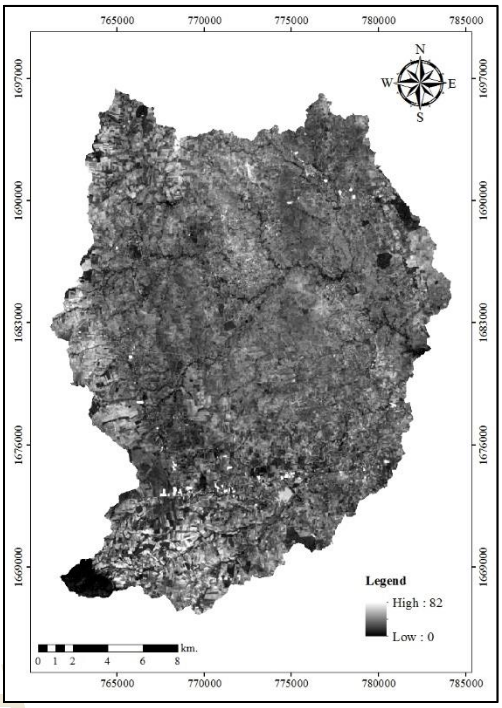

Landsat-8 Band 3 (Green)

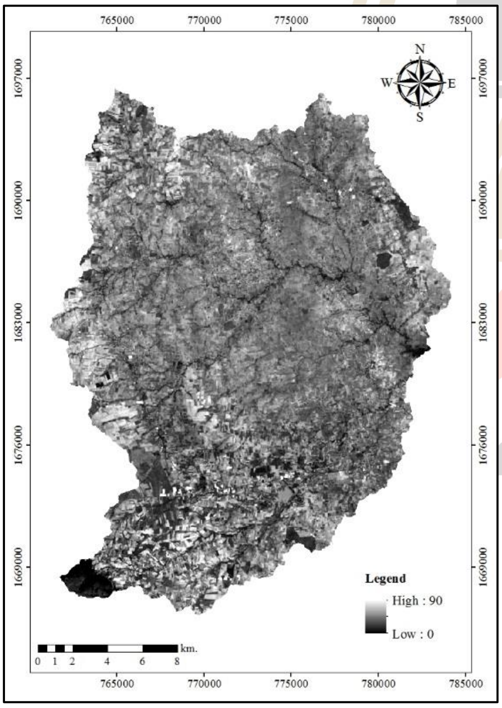

Landsat-8 Band 4 (Red)

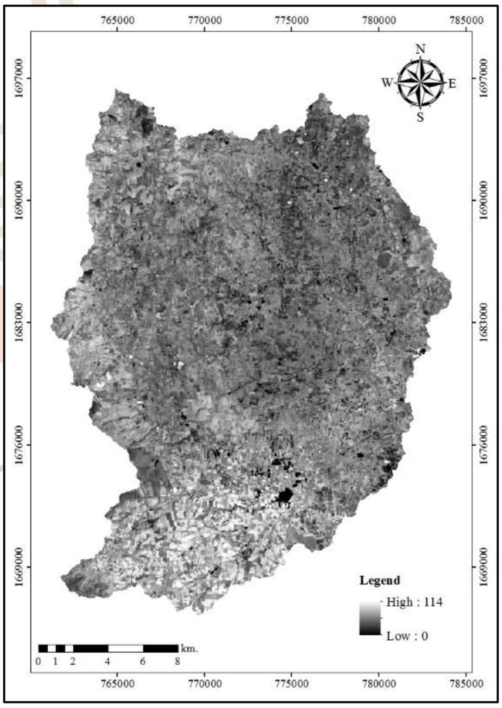

Landsat-8 Band 5 (NIR)

Figure 4.1 Independent variables.

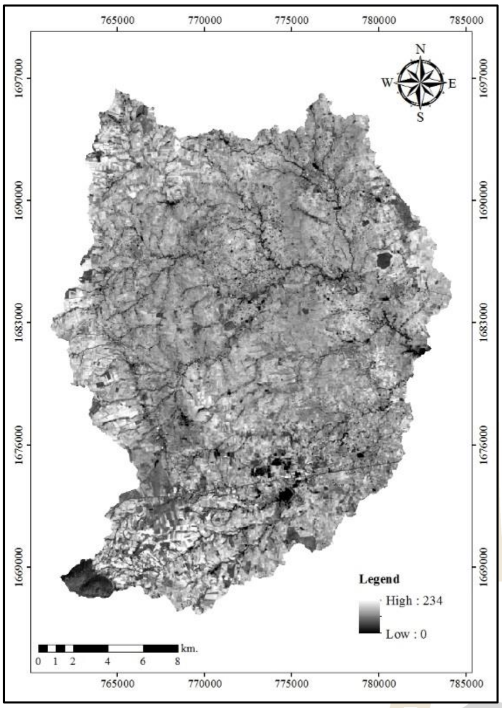

Landsat-8 Band 6 (SWIR-1)

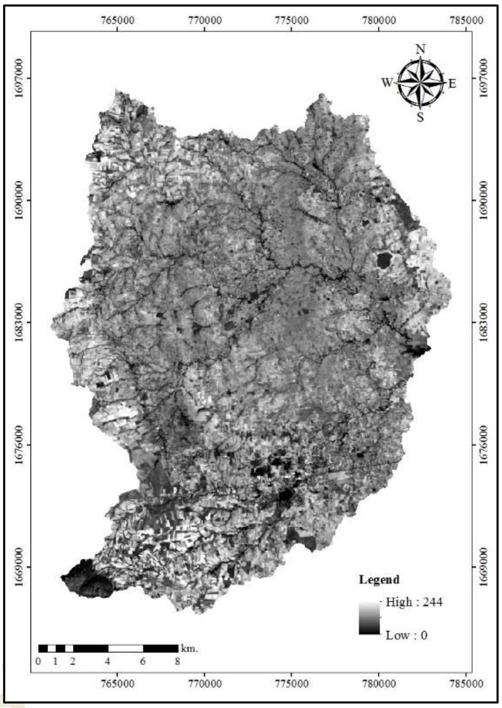

Landsat-8 Band 7 (SWIR-2)

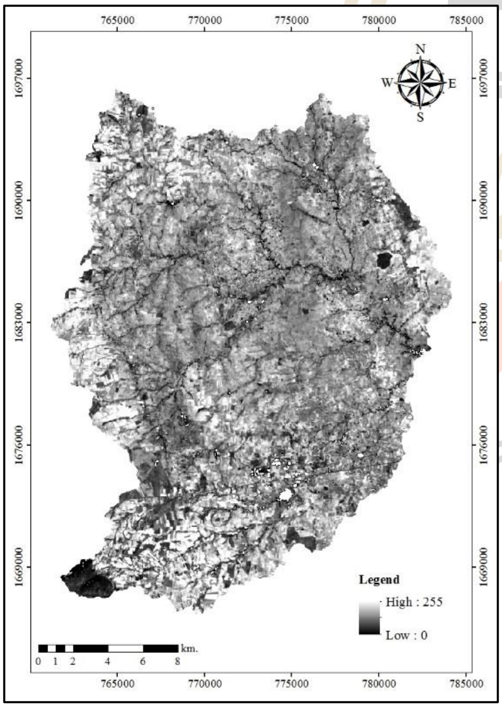

Brightness

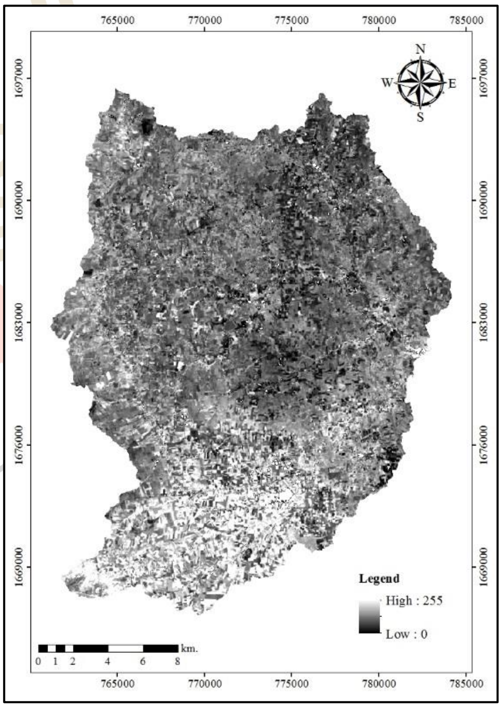

Greenness

Figure 4.1 (Continued).

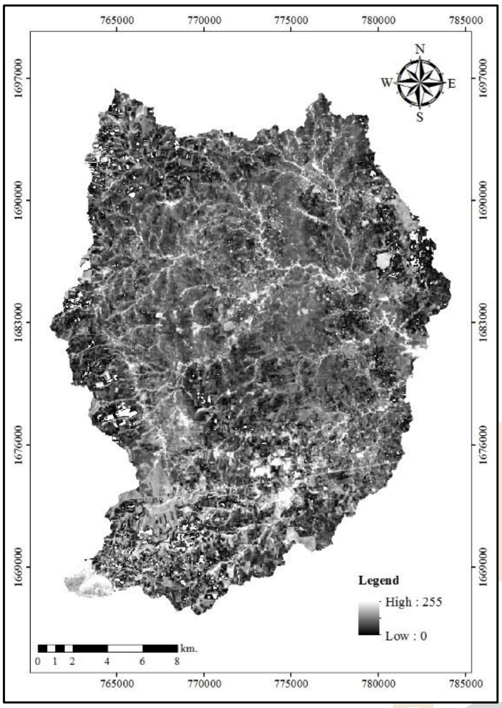

Wetness

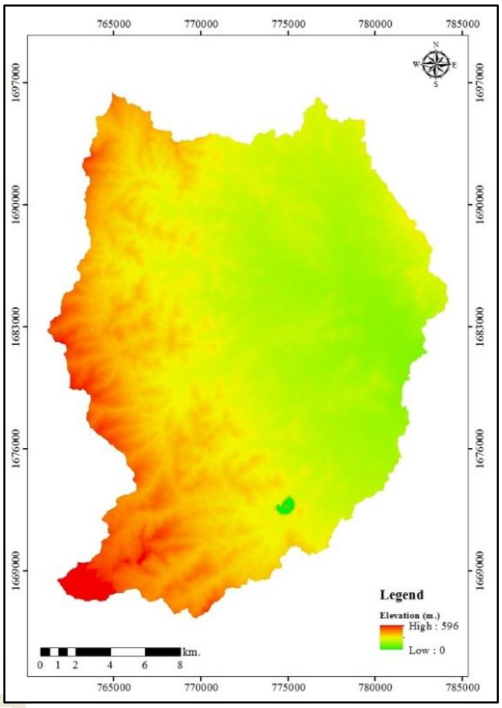

Elevation

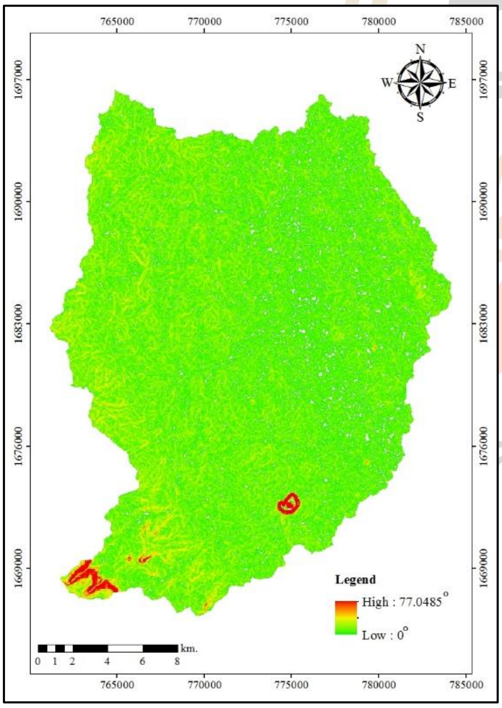

Slope

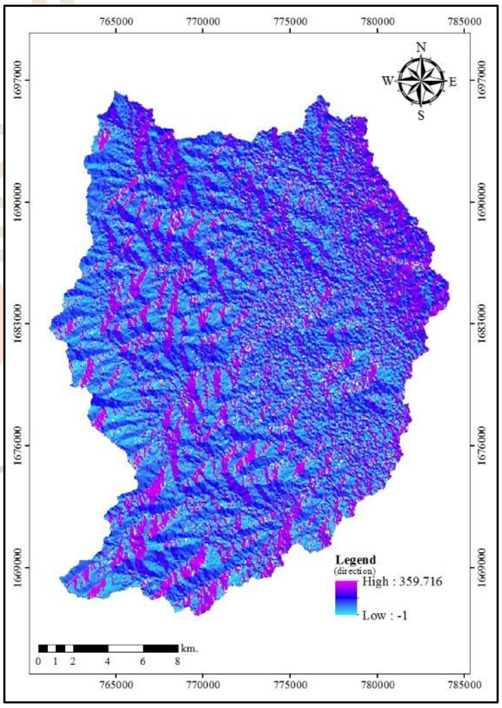

Aspect

Figure 4.1 (Continued).

Table 4.1 Example of ASCII file format from training area for decision tree construction.

LULC	Blue	Green	Red	NIR	SWIR1	SWIR2	Brightness	Greenness	Wetness	Elevation	Slope	Aspect
Paddy field	46	44	43	62	92	66	171	137	94	246	2.16	6.34
Paddy field	46	43	42	64	91	62	165	168	105	253	1.69	8.13
Paddy field	46	43	42	63	89	61	158	158	113	251	1.22	11.31
Paddy field	46	44	45	60	96	72	185	103	68	244	1.22	11.31
Paddy field	46	43	41	64	89	61	158	173	112	252	1.97	14.04
Paddy field	46	44	44	63	94	66	178	143	90	244	0.75	18.43
Paddy field	46	43	43	63	93	64	171	152	95	254	0.75	18.43
Paddy field	46	44	43	67	93	63	178	191	103	253	0.75	18.43
Paddy field	46	43	42	64	89	61	160	168	114	254	1.07	26.57
Paddy field	46	43	42	63	90	63	162	156	105	253	1.72	33.69
Paddy field	46	44	42	65	93	63	172	176	99	252	2.05	35.54
Paddy field	46	44	43	63	92	65	171	148	97	254	1.01	45.00
Paddy field	46	44	44	67	96	65	188	185	90	251	0.68	45.00
Paddy field	46	43	42	63	92	64	167	156	96	253	2.02	45.00
Paddy field	46	44	43	68	95	65	185	199	93	253	0.34	45.00
Paddy field	46	44	43	66	92	63	174	180	105	253	1.01	45.00
…	…	…	…	…	…	…	…	…	…	…	…	…
…	…	…	…	…	…	…	…	…	…	…	…	…
…	…	…	…	…	…	…	…	…	…	…	…	…
Paddy field	47	44	44	63	97	68	187	140	76	246	0.75	18.43

LULC	Landsat	Ground photograph
Urban and built-up area (URBAN)	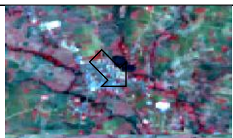	
Paddy field (PF)		
Maize (MAIZE)		
Sugarcane (SGC)		
Cassava (CAS)		
Perennial tree and orchard (TREE)		
Dense deciduous forest (DDF)		
Disturbed deciduous forest (DIDF)		
Forest plantation (FP)	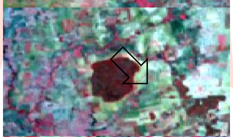	
Water body (WATER)	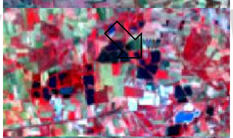	
Scrub (SCRUB)		
Miscellaneous land (MISC)		

Figure 4.2 Example of training area as color composite of Landsat 8 (SWIR-1, NIR, Red: RGB) and its photograph.

The result of the optimum CART model for LULC classification as decision tree structure is displayed in Figure 4.3. It reveals that the final criteria of the optimum CART model for LULC classification applies only 8 independent variables including Blue, Green, Red, NIR, SWIR-1, SWIR-2, Wetness, and Elevation. Meanwhile, other independent variable including Brightness, Greenness, Slope, and Aspect are dropped from the model. The decision tree consists of 59 nodes that include 30 terminal nodes of various LULC classes.

According to accuracy assessment of the model based on training data as model-based inference statistics, the derived decision tree provides overall accuracy of 87.60% (Table 4.2). Basically, model-based inference statistic is not concerned with the accuracy of the thematic map. It is concerned with estimating the error of model that generates the thematic map. Model-based inference can provide the user with a quantitative assessment of each classification decision (Stehman, 2000). The accuracy of the derived optimum model for LULC classification varies between 33.00% for sugarcane-1 and 100% for paddy field, sugarcane-3, cassava-6, and dense deciduous forest.

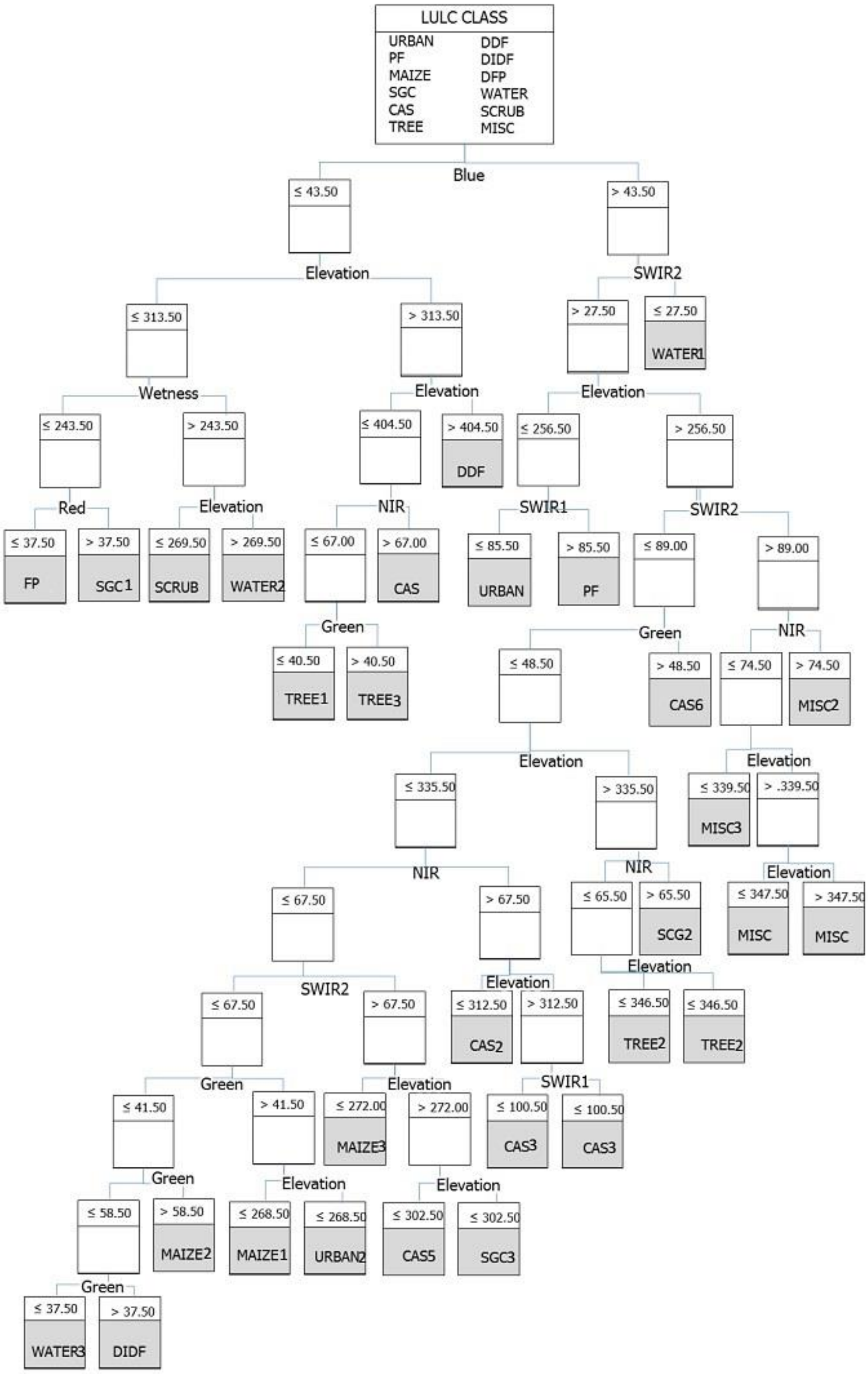

Figure 4.3 Decision tree structure for LULC classification.

Table 4.2 Accuracy assessment of decision tree classification based training dataset.

Independent variables observed	Independent variables classification																													
	MISC1	MISC2	MISC3	CAS1	CAS2	CAS3	CAS4	CAS5	CAS6	MAIZE1	MAIZE2	MAIZE3	TREE1	TREE2	TREE3	DDF	DIDF	FP	SCRUB	PF	SCG1	SCG2	SCG3	URBAN1	URBAN2	WATER1	WATER2	WATER3	Percent Correct
Miscellaneous land 1 (MISC)	145	2	71	0	0	0	0	0	1	0	0	0	0	0	0	0	0	0	0	0	0	0	0	0	0	0	0	0	66.2%
Miscellaneous land 2 (MISC2)	2	81	0	0	0	0	0	0	0	0	0	0	0	0	0	0	0	0	0	0	0	0	0	0	0	0	0	0	97.6%
Miscellaneous land 3 (MISC3)	52	0	95	0	0	0	0	0	0	0	0	0	0	0	0	0	0	0	0	0	0	0	0	0	0	0	0	0	64.6%
Cassava 1 (CAS1)	0	0	0	187	0	0	0	0	0	0	0	0	0	0	0	0	0	6	0	0	0	0	0	0	0	0	3	0	95.4%
Cassava 2 (CAS2)	0	0	0	0	99	0	0	0	0	0	0	0	0	0	0	0	0	0	0	0	7	0	0	0	0	0	0	0	93.4%
Cassava 3 (CAS3)	0	0	0	0	0	126	3	0	0	0	0	0	0	0	0	0	0	0	0	0	0	4	2	0	0	0	0	0	93.3%
Cassava 4 (CAS4)	0	1	0	0	7	14	73	0	0	0	0	0	0	0	0	0	0	0	0	0	0	0	0	0	0	0	0	0	76.8%
Cassava 5 (CAS5)	0	0	0	0	0	0	0	106	0	0	1	0	0	0	0	0	0	0	0	0	6	0	0	0	1	0	0	0	93.0%
Cassava 6 (CAS6)	0	0	0	0	0	0	0	0	128	0	0	0	0	0	0	0	0	0	0	0	0	0	0	0	0	0	0	0	100.0%
Maize 1 (MAIZE1)	0	0	0	0	0	0	0	0	0	72	0	0	0	0	0	0	2	0	0	0	0	0	0	0	0	0	0	0	97.3%
Maize 2 (MAIZE2)	0	0	0	0	0	0	0	0	0	0	87	0	0	0	0	0	1	0	0	0	0	0	0	0	0	0	0	0	98.9%
Maize 3 (MAIZE3)	0	0	0	0	0	0	0	0	0	2	0	117	0	0	0	0	0	0	0	0	0	0	0	0	0	0	0	0	98.3%
Perennial tree/orchard 1 (TREE1)	0	0	0	0	0	0	0	0	0	0	0	0	251	44	13	0	0	0	0	0	0	0	0	0	0	0	0	16	77.5%
Perennial tree/orchard 2 (TREE2)	0	0	0	0	0	0	0	0	0	0	0	0	5	186	3	0	0	0	0	0	0	0	0	0	0	0	0	3	94.4%
Perennial tree/orchard 3 (TREE3)	0	0	0	0	0	0	0	0	0	0	0	0	12	12	87	0	16	0	0	0	0	0	0	0	0	0	0	2	67.4%
Dense deciduous forest (DDF)	0	0	0	0	0	0	0	0	0	0	0	0	0	0	0	260	0	0	0	0	0	0	0	0	0	0	0	0	100.0%
Disturbed deciduous forest (DIDF)	0	0	0	0	0	0	0	0	0	0	0	0	0	0	0	0	154	0	0	0	9	0	0	0	0	0	0	1	93.9%
Forest plantation (FP)	0	0	0	0	0	0	0	0	0	0	0	0	2	0	0	0	0	691	0	0	4	0	0	3	0	0	0	1	98.6%
Scrub (SCRUB)	0	0	0	0	0	0	0	0	0	0	0	0	0	0	0	0	0	38	72	0	0	0	0	14	0	0	0	0	58.1%
Paddy field (PF)	0	0	0	0	0	0	0	0	0	0	0	0	0	0	0	0	0	0	0	269	0	0	0	0	0	0	0	0	100.0%
Sugarcane 1 (SCG1)	0	0	0	0	41	0	0	0	0	0	0	0	0	0	0	0	0	0	0	0	35	0	0	0	16	0	14	0	33.0%
Sugarcane 2 (SCG2)	0	0	0	0	0	0	0	0	0	0	0	0	0	1	0	0	0	0	0	0	0	47	0	0	0	0	0	0	97.9%
Sugarcane 3 (SCG3)	0	0	0	0	0	0	0	0	0	0	0	0	0	0	0	0	0	0	0	0	0	0	126	0	0	0	0	0	100.0%
Urban and built-up area 1 (URBAN1)	0	0	0	0	0	0	0	0	1	0	0	0	0	0	0	0	0	0	0	1	0	0	4	55	30	0	0	0	60.4%
Urban and built-up area 2 (URBAN2)	0	0	0	0	0	1	0	1	2	0	0	0	0	6	0	0	0	0	0	0	0	0	7	0	107	0	0	0	86.3%
Water body 1 (WATER1)	0	0	0	0	0	0	0	0	0	0	0	0	0	0	0	0	0	0	0	0	0	0	0	0	2	255	0	0	99.2%
Water body 2 (WATER2)	0	0	0	0	0	0	0	0	0	0	0	0	0	0	0	0	0	0	0	0	0	0	0	0	0	6	73	23	71.6%
Water body 3 (WATER3)	0	0	0	0	0	0	0	0	0	0	0	0	0	0	0	0	0	1	16	0	0	0	0	14	0	0	0	47	60.3%
Overall Percentage	4.3%	1.8%	3.6%	4.1%	3.2%	3.1%	1.7%	2.3%	2.9%	1.6%	1.9%	2.5%	5.9%	5.4%	2.2%	5.6%	3.8%	16.0%	1.9%	5.9%	1.3%	1.1%	3.0%	1.9%	3.4%	5.7%	2.0%	2.0%	87.6%

4.2 Land use and land use classification

The decision tree structure of the CART model was transferred to Expert System of ERDAS imagine software for LULC classification including hypothesis, rule, and conditions as result shown in Table 4.3. Distribution of final LULC classification in 2015 after regrouping LULC classes displays in Figure 4.4 while area and percentage of LULC classes is summarized in Table 4.4.

Table 4.3 Hypothesis, rules, and conditions of LULC classification.

Hypotheses	Rules (Variables)	Conditions
Urban and built-up area (URBAN)	Multispectral (8 bits)	Remote sensing reflectance Blue > 43.5 Blue > 45.5 SWIR1 ≤ 85.5 SWIR2 > 27.5
	Elevation	Elevation ≤ 256.5 m
Paddy field -1 (PF1)	Multispectral (8 bits)	Remote sensing reflectance Blue > 43.5 Blue > 45.5 SWIR1 ≤ 85.5 SWIR2 > 27.5
	Elevation	Elevation ≤ 250.5 m
Paddy field -2 (PF2)	Multispectral (8 bits)	Remote sensing reflectance Blue > 43.5 Blue > 45.5 SWIR1 > 85.5 SWIR2 > 27.5
	Elevation	Elevation ≤ 256.5 m Elevation ≤ 250.5 m
Maize 1 (MAIZE1)	Multispectral (8 bits)	Remote sensing reflectance Blue > 43.5 Green > 41.5 Green ≤ 42.5 Red ≤ 48.5 NIR ≤ 67.5 SWIR2 > 27.5 SWIR2 ≤ 89 SWIR2 ≤ 58.5 SWIR2 ≤ 67.5
	Elevation	Elevation > 256.5 m

Table 4.3 (Continued).

Hypotheses	**Rules (Variables)**	**Conditions**
		Elevation ≤ 268.5 m
Maize 2 (MAIZE2)	Multispectral (8 bits)	Blue > 43.5 Green > 41.5 Green > 42.5 Red ≤ 48.5 NIR ≤ 67.5 SWIR2 > 27.5 SWIR2 ≤ 89 SWIR2 ≤ 58.5 SWIR2 ≤ 67.5
	Elevation	Elevation > 256.5 m Elevation ≤ 268.5 m Elevation ≤ 335.5 m
Maize 3 (MAIZE3)	Multispectral (8 bits)	Blue > 43.5 Red ≤ 48.5 NIR ≤ 67.5 SWIR2 > 27.5 SWIR2 ≤ 89 SWIR2 > 67.5
	Elevation	Elevation > 256.5 m Elevation ≤ 335.5 m Elevation ≤ 272 m
Maize 4 (MAIZE4)	Multispectral (8 bits)	Blue > 43.5 Blue ≤ 45.5 SWIR2 > 27.5
	Elevation	Elevation ≤ 256.5 m
Maize 5 (MAIZE5)	Multispectral (8 bits)	Blue > 43.5 Green > 41.5 Red ≤ 37.5 Red ≤ 48.5 NIR ≤ 67.5 SWIR2 > 27.5 SWIR2 ≤ 89 SWIR2 > 58.5 SWIR2 ≤ 67.5
	Elevation	Elevation > 256.5 m Elevation ≤ 335.5 m

Table 4.3 (Continued).

Hypotheses	Rules (Variables)	Conditions
Sugarcane 1 (SGC1)	Multispectral (8 bits)	Blue ≤ 43.5 Red > 37.5
	Vegetation Index (8 bits)	Wetness ≤ 243.5
	Elevation	Elevation ≤ 313.5 m
Sugarcane 2 (SGC2)	Multispectral (8 bits)	Blue > 43.5 NIR ≤ 65.5 SWIR2 > 27.5 SWIR2 ≤ 89
	Elevation	Elevation > 256.5 m Elevation > 335.5 m
Sugarcane 3 (SGC3)	Multispectral (8 bits)	Blue > 43.5 Red ≤ 48.5 NIR ≤ 67.5 SWIR2 > 27.5 SWIR2 ≤ 89 SWIR2 > 67.5
	Elevation	Elevation > 256.5 m Elevation > 302.5 m Elevation ≤ 335.5 m Elevation > 272 m
Cassava 1 (CAS1)	Multispectral (8 bits)	Blue ≤ 43.5 NIR > 67
	Elevation	Elevation > 313.5 m Elevation ≤ 404.5 m
Cassava 2 (CAS2)	Multispectral (8 bits)	Blue > 43.5 Red ≤ 48.5 NIR > 67.5 SWIR2 > 27.5 SWIR2 ≤ 89
	Elevation	Elevation > 256.5 m Elevation ≤ 335.5 m Elevation ≤ 312.5 m
Cassava 3 (CAS3)	Multispectral (8 bits)	Blue > 43.5 Red ≤ 48.5 NIR > 67.5 SWIR1 ≤ 100.5 SWIR2 > 27.5 SWIR2 ≤ 89
	Elevation	Elevation > 256.5 m Elevation ≤ 335.5 m Elevation > 312.5 m

Table 4.3 (Continued).

Hypotheses	Rules (Variables)	Conditions
Cassava 4 (CAS4)	Multispectral (8 bits)	Blue > 43.5 Red ≤ 48.5 NIR > 67.5 SWIR1 > 100.5 SWIR2 > 27.5 SWIR2 ≤ 89
	Elevation	Elevation > 256.5 m Elevation ≤ 335.5 m Elevation > 312.5 m
Cassava 5 (CAS5)	Multispectral (8 bits)	Blue > 43.5 Red ≤ 48.5 NIR ≤ 67.5 SWIR2 > 27.5 SWIR2 ≤ 89 SWIR2 > 67.5
	Elevation	Elevation > 256.5 m Elevation ≤ 302.5 m Elevation ≤ 335.5 m Elevation > 272 m
Cassava 6 (CAS6)	Multispectral (8 bits)	Blue > 43.5 Red > 48.5 SWIR2 > 27.5 SWIR2 ≤ 89
	Elevation	Elevation > 256.5 m Elevation ≤ 335.5 m
Perennial trees and orchards 1 (TREE1)	Multispectral (8 bits)	Blue ≤ 43.5 Green ≤ 40.5 NIR ≤ 67
	Elevation	Elevation > 313.5 m Elevation ≤ 404.5 m
Perennial trees and orchards 2 (TREE2)	Multispectral (8 bits)	Blue ≤ 43.5 Green > 40.5 NIR ≤ 67
	Elevation	Elevation > 313.5 m Elevation ≤ 404.5 m
Perennial trees and orchards 3 (TREE3)	Multispectral (8 bits)	Blue > 43.5 NIR ≤ 65.5 SWIR2 > 27.5 SWIR2 ≤ 89
	Elevation	Elevation > 256.5 m Elevation > 335.5 m Elevation ≤ 346.5 m

Table 4.3 (Continued).

Hypotheses	Rules (Variables)	Conditions
Perennial trees and orchards 4 (TREE4)	Multispectral (8 bits)	Blue > 43.5 NIR ≤ 65.5 SWIR2 > 27.5 SWIR2 ≤ 89
	Elevation	Elevation > 256.5 m Elevation > 335.5 m Elevation > 346.5 m
Dense deciduous forest (DDF)	Multispectral (8 bits)	Blue ≤ 43.5 Red ≤ 37.5
	Vegetation Index (8 bits)	Wetness ≤ 243.5
	Elevation	Elevation ≤ 313.5 m
Disturbed deciduous forest (DIDF)	Multispectral (8 bits)	Blue > 43.5 Green ≤ 41.5 Red > 37.5 Red ≤ 48.5 NIR ≤ 67.5 SWIR2 > 27.5 SWIR2 ≤ 89 SWIR2 ≤ 58.5 SWIR2 ≤ 67.5
	Elevation	Elevation > 256.5 m Elevation ≤ 335.5 m
Forest plantation (FP)	Multispectral (8 bits)al (8	Blue ≤ 43.5 ≤ 43.5
	Elevation	Elevation > 313.5 m Elevation > 404.5 m
Water body 1 (WATER1)	Multispectral (8 bits)	Blue ≤ 43.5
	Vegetation Index (8 bits)	Wetness > 243.5
	Elevation	Elevation ≤ 313.5 m Elevation > 269.5 m
Water body 2 (WATER2)	Multispectral (8 bits)	Blue > 43.5 SWIR2 ≤ 27.5
	Elevation	Elevation > 313.5 m Elevation ≤ 404.5 m

Table 4.3 (Continued).

Hypotheses	Rules (Variables)	Conditions
Water body 3 (WATER3)	Multispectral (8 bits)	Blue > 43.5 Green > 41.5 Red ≤ 37.5 Red ≤ 48.5 NIR ≤ 67.5 SWIR2 > 27.5 SWIR2 ≤ 89 SWIR2 ≤ 58.5 SWIR2 ≤ 67.5
	Elevation	Elevation > 256.5 m Elevation ≤ 335.5 m
Scrub (SCRUB)	Multispectral (8 bits)	Blue ≤ 43.5
	Vegetation Index (8 bits)	Wetness > 243.5
	Elevation	Elevation ≤ 313.5 m Elevation ≤ 269.5 m
Miscellaneous land 1 (MISC1)	Multispectral (8 bits)	Blue > 43.5 NIR > 74.5 SWIR2 > 27.5 SWIR2 > 89
Miscellaneous land 2 (MISC2)	Multispectral (8 bits)	Blue > 43.5 NIR ≤ 74.5 SWIR2 > 27.5 SWIR2 > 89
	Elevation	Elevation ≤ 339.5 m
Miscellaneous land 3 (MISC3)	Multispectral (8 bits)	Blue > 43.5 NIR ≤ 74.5 SWIR2 > 27.5 SWIR2 > 89
	Elevation	Elevation > 339.5 m Elevation ≤ 347.5 m
Miscellaneous land 4 (MISC4)	Multispectral (8 bits)	Blue > 43.5 NIR ≤ 74.5 SWIR2 > 27.5 SWIR2 > 89
	Elevation	Elevation > 339.5 m Elevation > 347.5 m

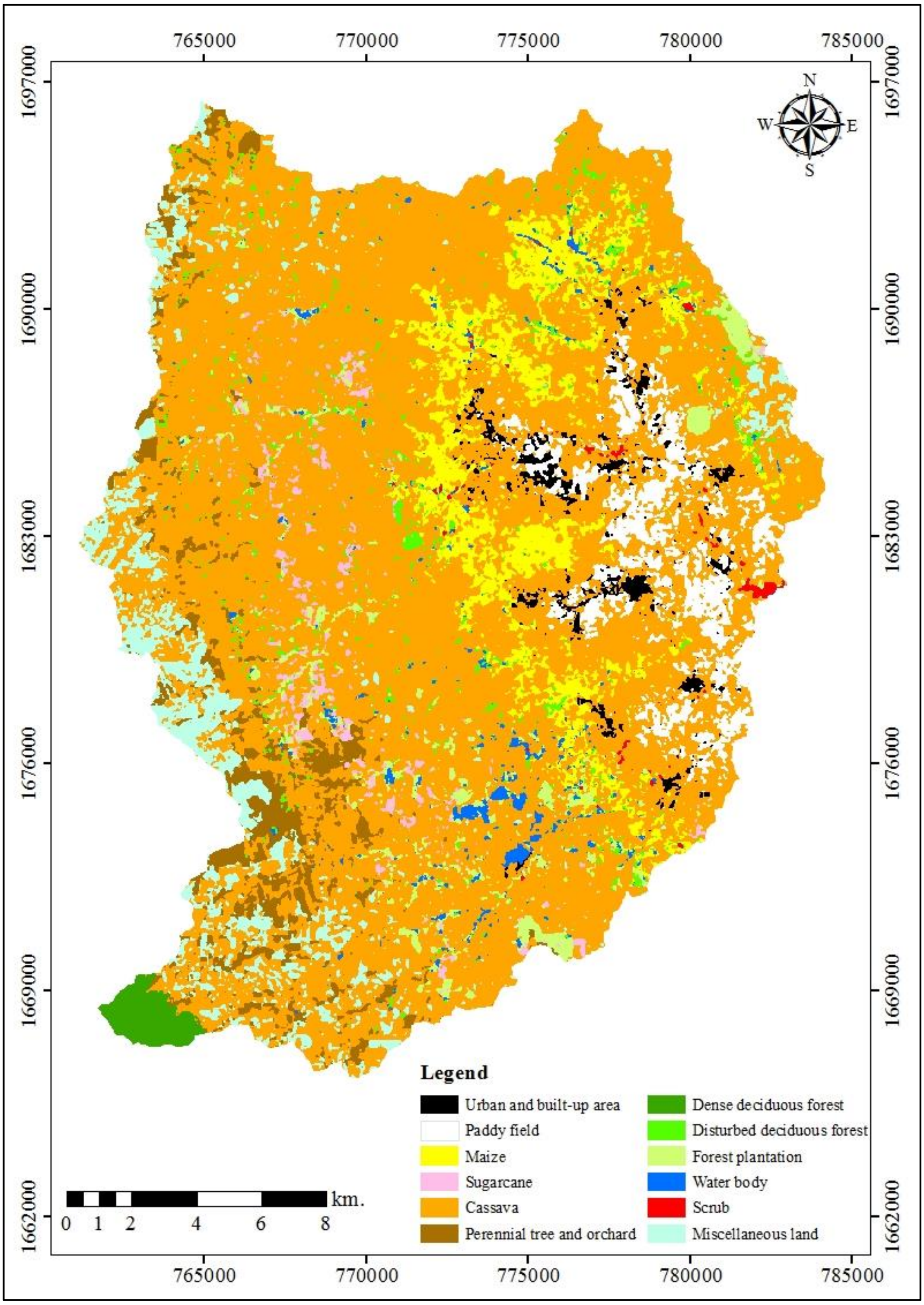

Figure 4.4 Distribution of LULC classification in 2015.

Table 4.4 Area and percentage of LULC classes in the study area.

No	LULC class	Area in sq. km	Percent
1	Urban and built-up area	6.64	1.43
2	Paddy field	21.19	4.56
3	Maize	31.54	6.78
4	Sugarcane	6.75	1.45
5	Cassava	322.21	69.30
6	Perennial tree and orchard	19.97	4.30
7	Dense deciduous forest	4.11	0.88
8	Disturbed deciduous forest	9.04	1.94
9	Forest plantation	11.92	2.56
10	Water body	5.08	1.09
11	Scrub	1.16	0.25
12	Miscellaneous land	25.35	5.45
	Total	464.96	100.00

As a result, it was found that top three dominant LULC classes are cassava, maize, and miscellaneous land and cover area of 322.21 km^2 or 69.30%, 31.54 km^2 or 6.78%, and 25.35 km^2 or 5.45% of the total study area, respectively. The pattern and area of the classified LULC data in this study, particularly agriculture land is similar with LDD data in 2015 as shown in Figure 4.5.

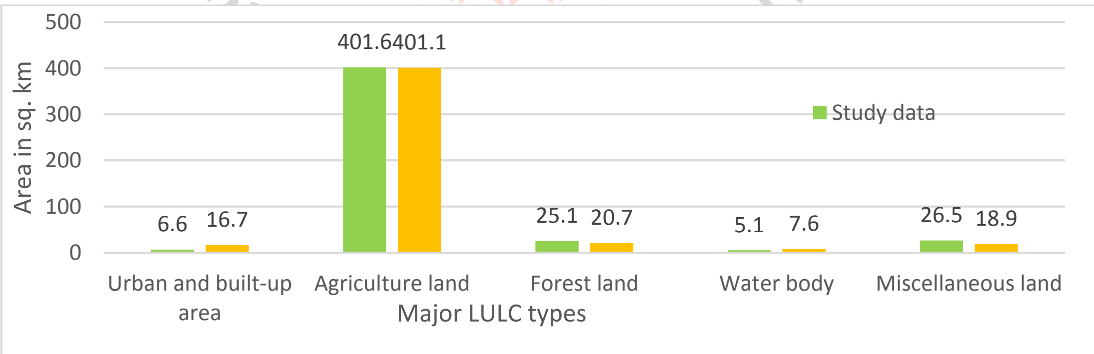

Figure 4.5 Area of main LULC type comparison between LDD data in 2015 and this study.

In addition, the classified LULC map was further performed accuracy assessment in 2016 using 152 sample points with stratified random sampling (Figure 4.6). Error matrix form for thematic LULC accuracy assessment is displayed in Table 4.5.

As results, it reveals that overall accuracy is 87.50% and Kappa hat coefficient is 80.10%. Meanwhile producer’s accuracy varies between 57.14% for sugarcane and 100.00% for urban and built-up area, water body, scrub and miscellaneous land and user’s accuracy varies between 50.00% for urban and built-up area and 100.00% for disturbed deciduous forest, water body, and scrub. Based on Fitzpatrick-Lins (1981), Kappa hat coefficient more than 80 percent represents strong agreement or accuracy between the predicted map and the reference map.

Furthermore, the derived accuracy assessment of CART model in this study is similar with the previous work of Lawrence and Wright (2001), who applied CART for LULC classification with overall accuracy of 96% and Kappa hat coefficient of 92%.

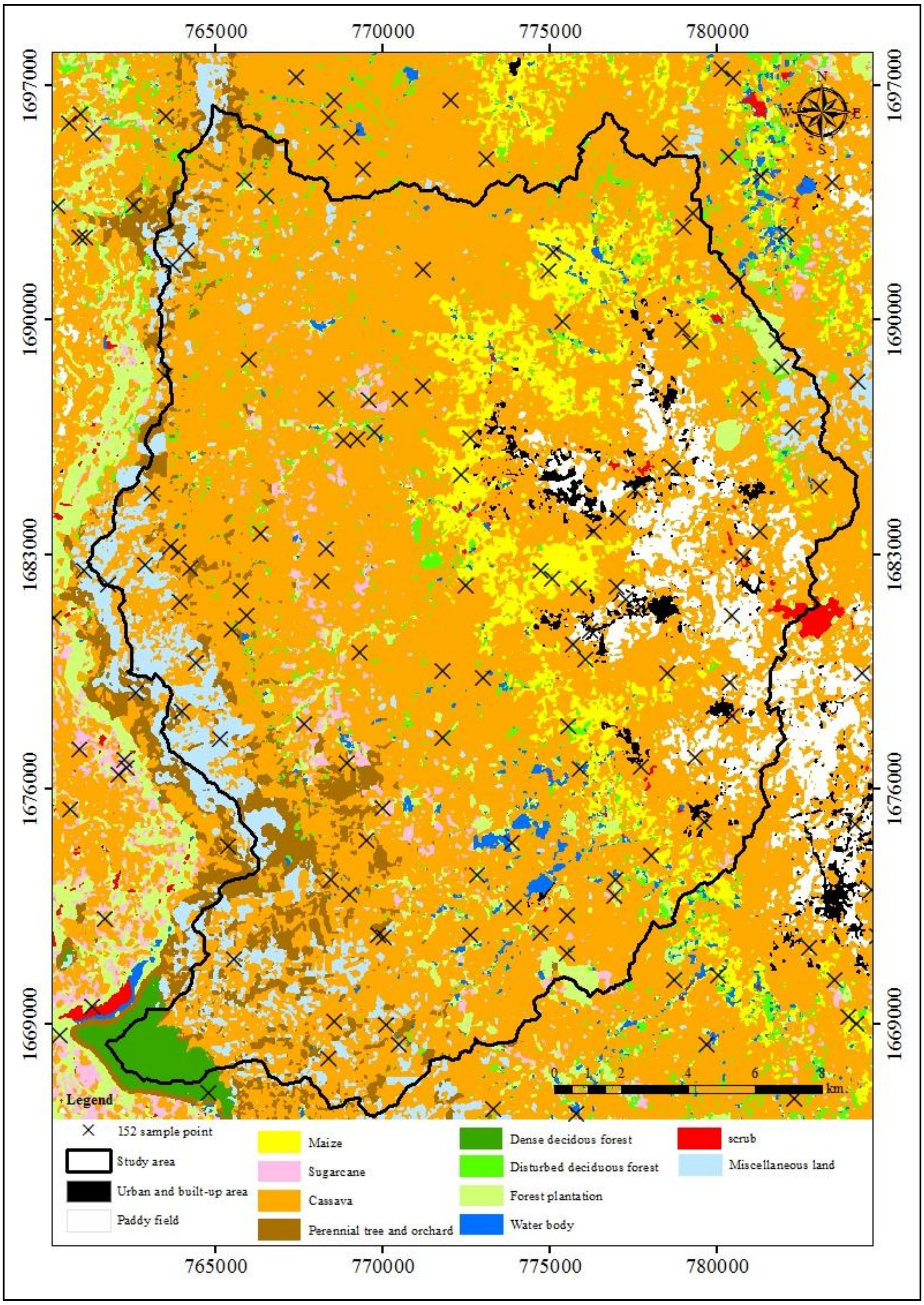

Figure 4.6 Distribution of 152 sample points with stratified random sampling**.**

Table 4.5 Error matrixes and accuracy assessment of LULC in 2015.

Classified data	Ground reference data													
	URBAN	PF	MAIZE	SGC	CAS	TREE	DDF	DIDF	FP	WATER	SCRUB	MISC	Total	UA (%)
Urban and built-up area (URBAN)	1	0	0	0	0	0	0	1	0	0	0	0	2	50.00%
Paddy field (PF)	0	9	0	2	2	0	0	0	0	0	0	0	13	69.23%
Maize (MAIZE)	0	1	8	1	1	0	0	1	0	0	0	0	12	66.67%
Sugarcane (SGC)	0	0	0	4	0	0	0	0	1	0	0	0	5	80.00%
Cassava (CAS)	0	0	2	0	85	1	0	0	0	0	0	0	88	96.59%
Perennial tree and orchard (TREE)	0	0	0	0	2	3	0	0	0	0	0	0	5	60.00%
Dense deciduous forest (DDF)	0	0	0	0	0	0	1	0	0	0	0	0	1	100.00%
Disturbed deciduous forest (DIDF)	0	1	0	0	0	0	0	4	0	0	0	0	5	80.00%
Forest plantation (FP)	0	0	0	0	1	0	0	0	7	0	0	0	8	87.50%
Water body (WATER)	0	0	0	0	0	0	0	0	0	2	0	0	2	100.00%
Scrub (SCRUB)	0	0	0	0	0	0	0	0	0	0	2	0	2	100.00%
Miscellaneous land (MISC)	0	0	0	0	1	0	0	0	1	0	0	7	9	77.78%
Total	1	11	10	7	92	4	1	6	9	2	2	7	152	
PA (%)	100.00%	81.82%	80.00%	57.14%	92.39%	75.00%	100.00%	66.67%	77.78%	1	1	1		
Overall Accuracy = 87.50%														
Overall Kappa Statistics = 80.10%														

Note: PA, producer's accuracy; UA, user's accuracy.

CHAPTER V

SOIL EROSION ASSESSMENT AND ITS SEVERITY

Main results of the second objective on assessment of soil erosion and its severity in 2015 with Revised Morgan Morgan and Finney (RMMF) model are here reported include (1) data preparation for RMMF model, (2) RMMF model parameters extraction, (3) RMMF model operation, and (4) soil erosion severity classification. Details of each result are separately described and discussed in following sections.

5.1 Data preparation for RMMF model

Four main input data included LULC, rainfall, soil and DEM data were here collected and prepared for RMMF model parameters extraction. In practice, LULC data, which was classified using CRT algorithm and Expert System as described in Chapter IV was used to extract RMMF model parameters about proportion of rainfall intercepted by crop cover, percentage canopy cover, plant height, ratio of actual to potential evapotranspiration, percentage ground cover, crop cover management, and effective hydrological depth of soil. Meanwhile, rainfall data was used to extract RMMF model parameters about annual rainfall total, intensity of erosive rain, and number of rain days per year. While, soil data was used to extract RMMF model parameters about soil moisture content at field capacity, bulk density of top soil, soil detachment index, and cohesion of the surface soil and DEM data was applied to extract slope steepness.

5.2 RMMF model parameters extraction

RMMF model parameters were here extracted based on the existing values of RMMF model parameters which were adopted from the previous works as mentioned in Table 3.4 of Chapter III.

The extracted RMMF model parameters from LULC data include proportion of rainfall intercepted by crop cover (A), percentage canopy cover (CC), plant height (PH), ratio of actual to potential evapotranspiration (Et/Eo), percentage ground cover (GC), crop cover management (C), and effective hydrological depth of soil (EHD) is present in Figure 5.1.

Meanwhile rainfall data of TMD between 1985 and 2015 from 55 rainfall stations in Nakhon Ratchasima and Chaiyaphum provinces were applied to examine the best interpolated results from five selected techniques (IDW, TPS, SK, OK, and UK) for annual rainfall total (R) and number of rain days per year (Rn) of RMMF model parameters. As results, Simple kriging (SK) provides the best interpolated result of annual rainfall total with the lowest ME of and RMSE of 9.000 and 208.636 as summary in Table 5.1. At the same time, Ordinary kriging (OK) provides the best interpolated result of number of rain days per year with the lowest ME of and RMSE of -0.094 and 18.008 as summary in Table 5.2. In addition, intensity of erosive rain (I) was prepared based on the literature reviews, the extracted RMMF model parameters from rainfall data include distribution of rainfall stations and its derived parameters is displayed in Figure 5.2.

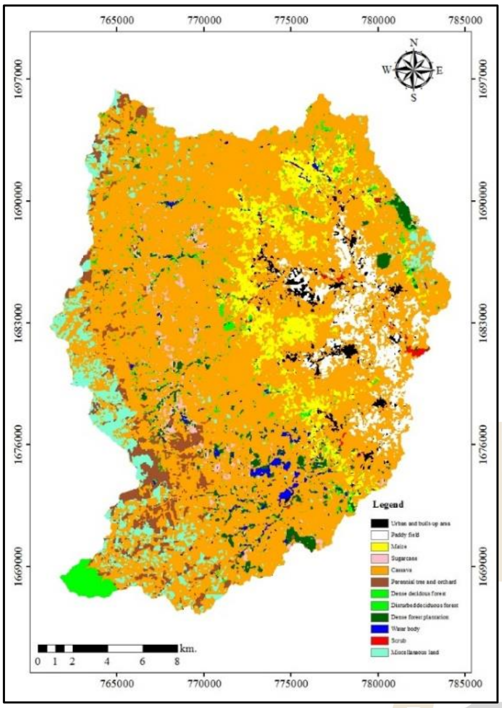

LULC data

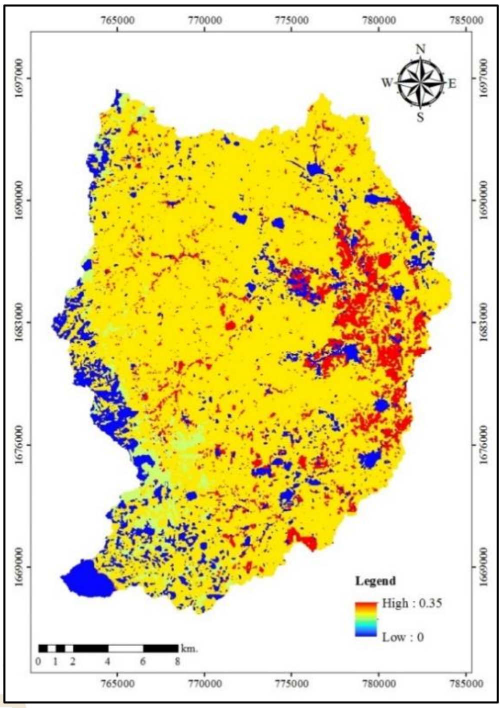

Proportion of rainfall intercepted by crop cover: A

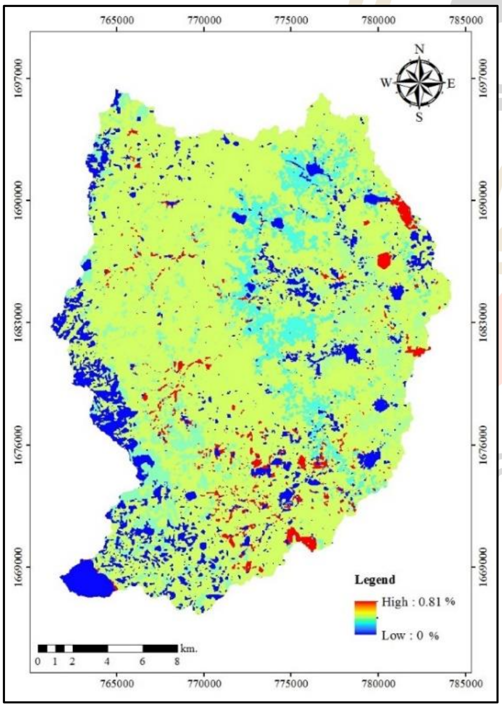

Percentage canopy cover: CC

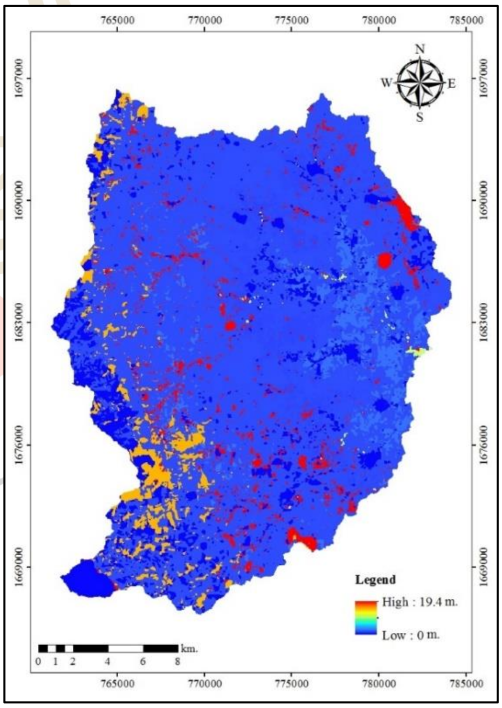

Plant height: PH

Figure 5.1 LULC data and its extracted RMMF model parameters.

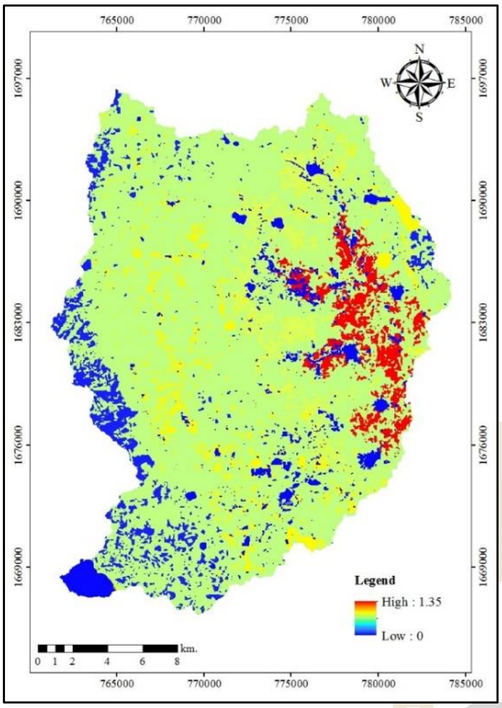

Ratio of actual to potential evapotranspiration: Et/Eo

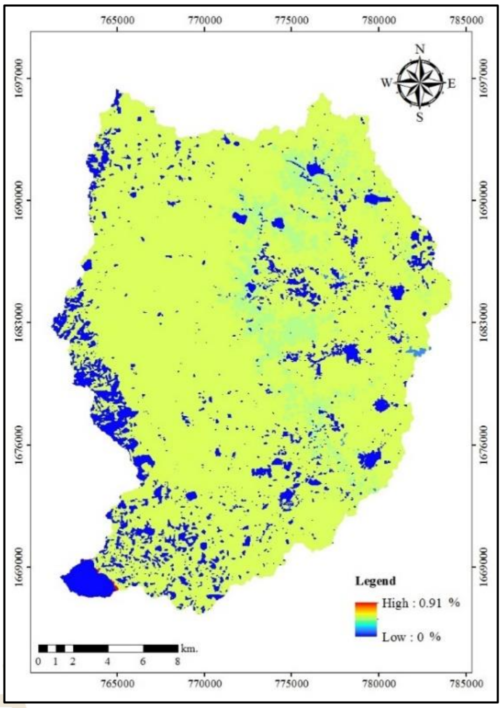

Ground cover: GC

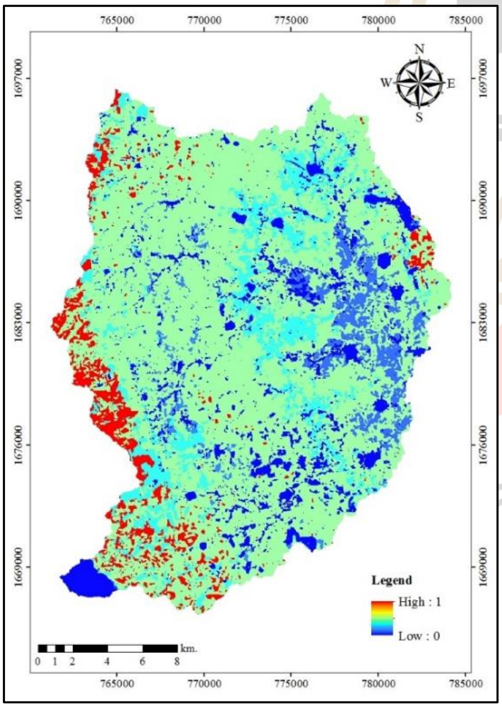

Crop cover management: C

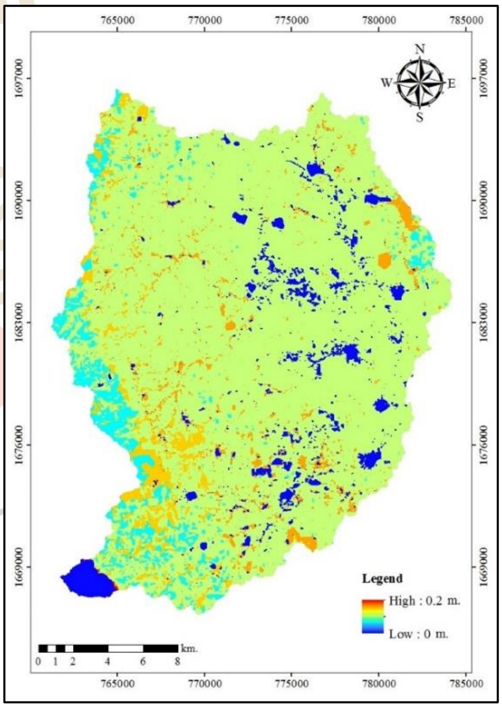

Effective hydrological depth of soil: EHD

Figure 5.1 (Continued).

Table 5.1 Accuracy assessment of five interpolation technique for annual rainfall total data estimation.

No.	Interpolation technique	ME	RMSE	Rank
1	IDW	12.520	229.271	4
2	TPS	15.126	304.596	5
3	SK	9.000	208.636	1
4	OK	-4.405	223.535	2
5	UK	-4.405	223.535	2

Table 5.2 Accuracy assessment of five interpolation technique for number of rain days per year estimation.

No.	Interpolation technique	ME	RMSE	Rank
1	IDW	-0.971	19.741	4
2	TPS	-0.280	23.119	5
3	SK	-0.170	18.175	3
4	OK	-0.094	18.008	1
5	UK	-0.094	18.008	1

In addition, soil data of LDD were applied to extract soil moisture content at field capacity (MS), bulk density of top soil (BD), soil detachment index (K), and cohesion of the surface soil (COH) as results shown in Figure 5.3. Likewise, DEM was applied to extract slope steepness (S) as shown in Figure 5.4. The basic statistics data of RMMF model parameters is summarized in Table 5.3.

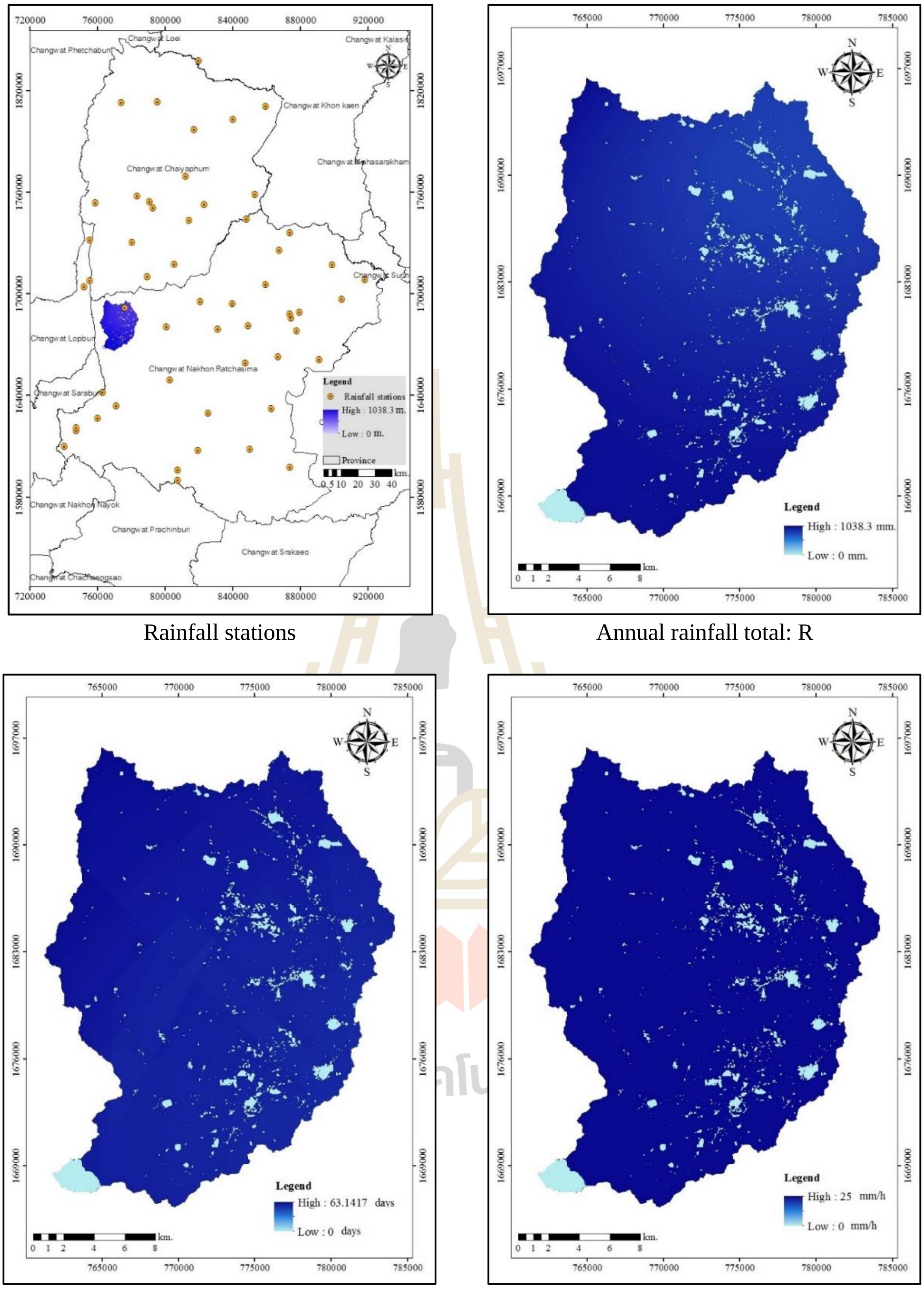

Rainfall stations | Annual rainfall total: R

Number of rain days in a year: Rn | Rainfall intensity: I

Figure 5.2 Rainfall stations data and its extracted RMMF model parameters.

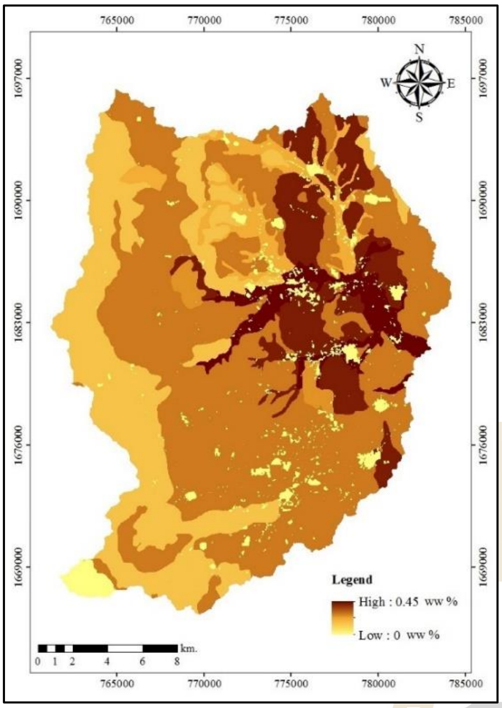

Soil moisture content at field capacity: MS

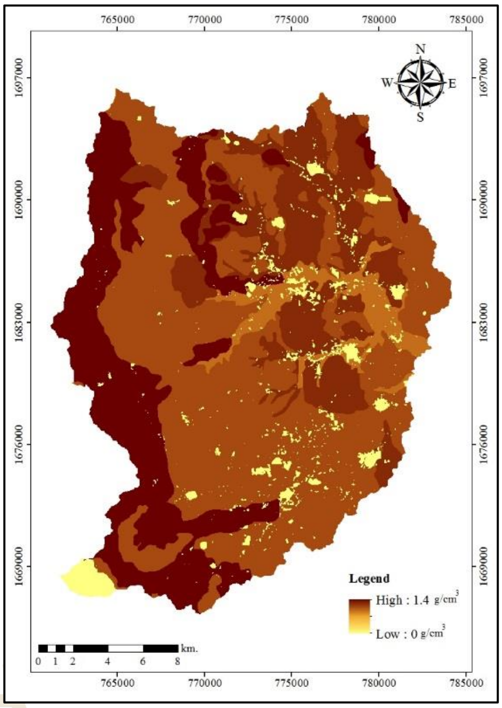

Bulk density: BD

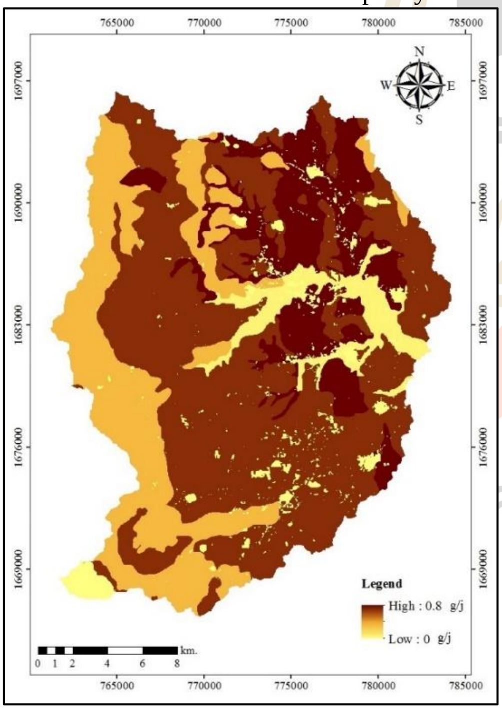

Soil erodibility: K

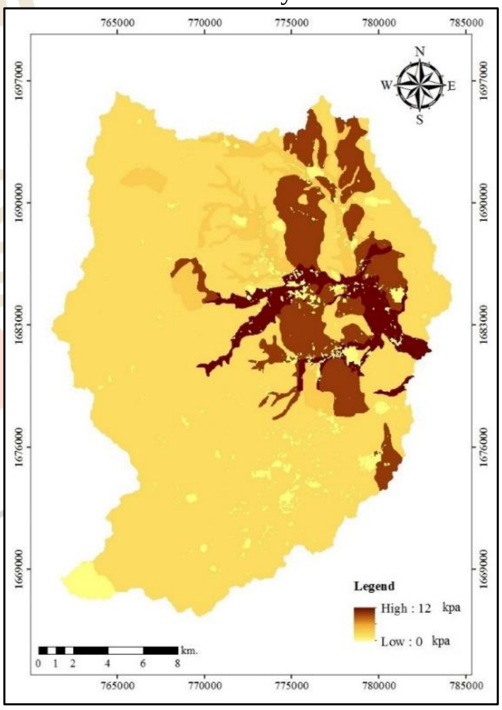

Soil resistance is in turn dependent on surface cohesion: COH

Figure 5.3 Extracted RMMF model parameters from soil data.

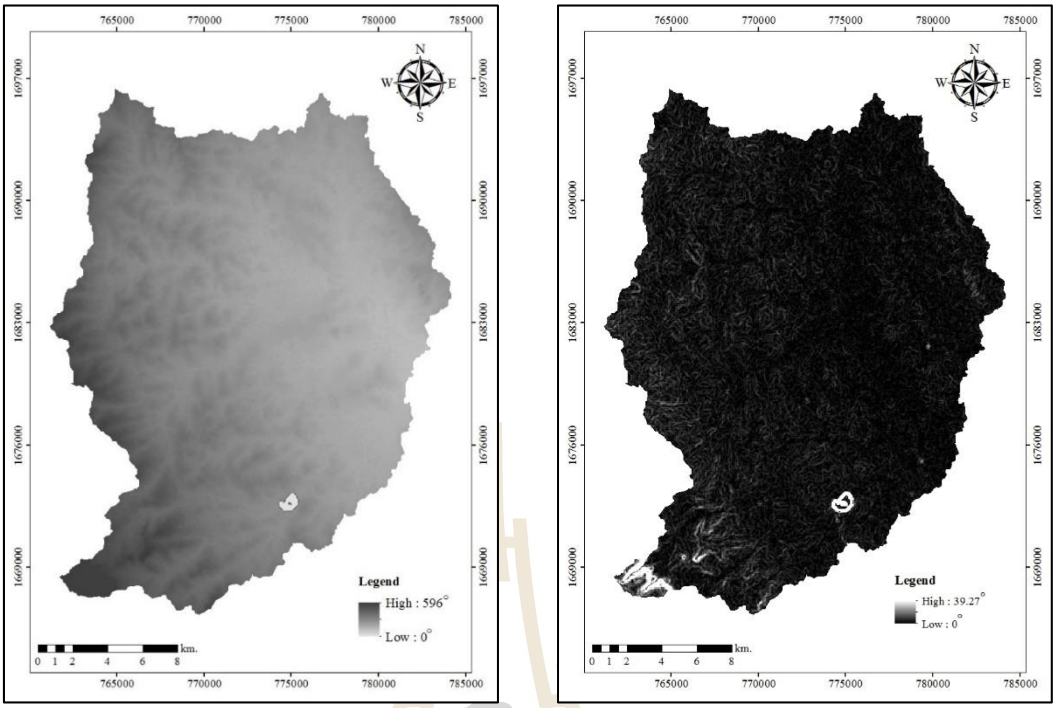

DEM Slope steepness: S

Figure 5.4 DEM and its extracted RMMF model parameters.

Table 5.3 The basic statistics data of RMMF model parameters.

RMMF data	RMMF parameters	Unit	Basic statistical value				
			Min	Max	Mean	S.D.	Variance
LULC	A	0-1	0	0.350	0.238	0.076	0.006
	CC	%	0	0.810	0.352	0.144	0.021
	PH	m	0	19.400	1.621	3.121	9.741
	Et/Eo	unitless	0	1.350	0.674	0.261	0.068
	GC	%	0	0.910	0.438	0.147	0.022
	C	unitless	0	1.000	0.368	0.197	0.039
	EHD	m	0	1.350	0.674	0.261	0.068
rainfall	R	mm	0	1038.300	922.357	204.524	41830.188
	Rn	days	0	63.142	57.533	12.536	157.157
	I	Mm/h	0	25.000	23.875	5.182	26.858
Soil	MS	ww %	0	0.450	0.257	0.105	0.011
	BD	g/cm^3	0	1.400	1.206	0.277	0.077
	K	g/j	0	0.800	0.561	0.249	0.062
	COH	kpa	0	12.000	3.283	3.033	9.199
DEM	S	degree	0	39.274	0.386	0.850	0.722

5.3 RMMF model operation

The RMMF model is applied to analyze soil erosion under ESRI ArcGIS software. The RMMF model parameters were calculated by operating function of the RMMF model as summarized in Table 3.5 under Chapter III.

Under RMMF model operation, five functions of the model is operated include (a) estimation of rainfall energy, (b) estimation of annual runoff, (c) estimation of soil particle detachment, (d) estimation of transport capacity of runoff, and (e) estimation of soil loss. Details of each group are separately described in the following sections.

5.3.1 Estimation of rainfall energy

The RMMF model parameters that were used to estimate rainfall energy included annual rainfall (R), proportion of rainfall intercepted by crop cover (A), canopy cover (CC) and plant height (PH). The annual rainfall in the study area varies between 0-1,038.300 mm. Plant rainfall interception rates range between 0 and 1. The percentage of canopy cover and plant height and their values are here reviewed from Morgan (2001). In practice, an annual rainfall layer was overlaid with the crop rainfall interception layer culminating into the effective rainfall map (ER) using Eq. 1 in Table 3.5. Since the RMMF model separates kinetic energy into 2 groups include: kinetic energy of direct through fall, KE(DT) and kinetic energy of leaf drainage, KE(LD), the effective rainfall data was split into two maps. These were leaf drainage map obtained as a function of kinetic energy and canopy cover (Eq. 2 in Table 3.5), and the direct through fall map computed as effective rainfall minus leaf drainage (Eq. 3 in Table 3.5). The rainfall intensity value (I) of 25 suggested by Morgan (2001) for tropical countries was used to calculate kinetic energy of direct through fall, KE(DT) using Eq. 4 in Table 3.5. Another map for kinetic energy of leaf drainage, KE(LD) was also generated as a function of plant height using Eq. 5 in Table 3.5. The two maps were added together to obtain the rainfall energy map of the study area using Eq. 6 in Table 3.5. The derived map of rainfall energy estimation is displayed in Figure 5.5.

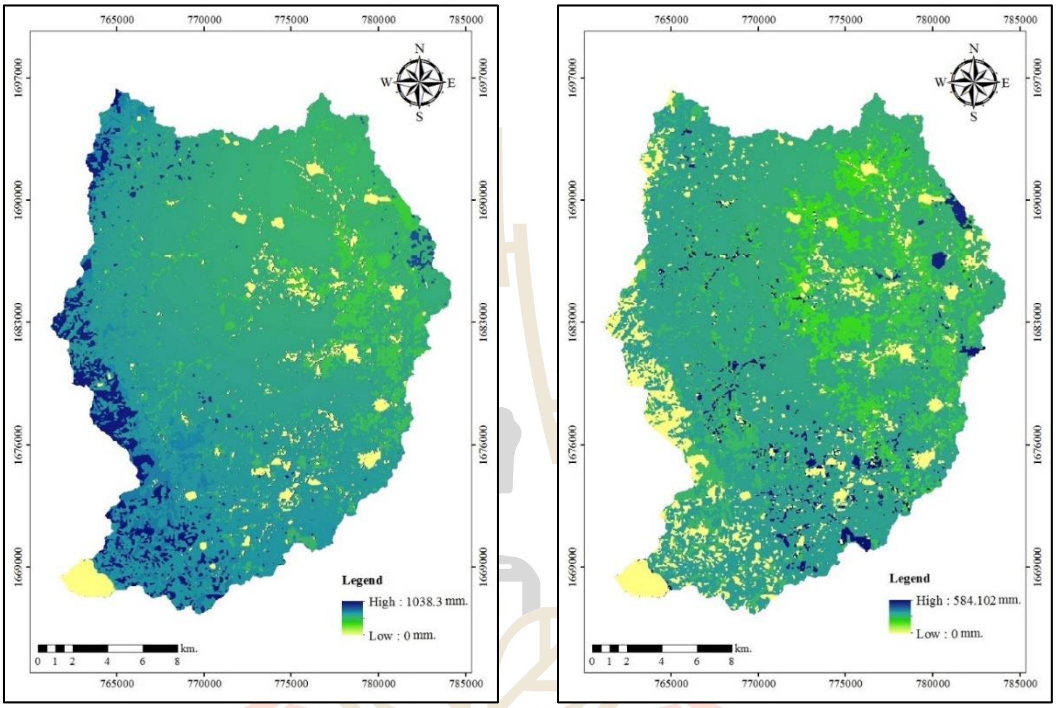

Effective rainfall: ER

Leaf drainage: LD

Figure 5.5 The derived map for rainfall energy estimation.

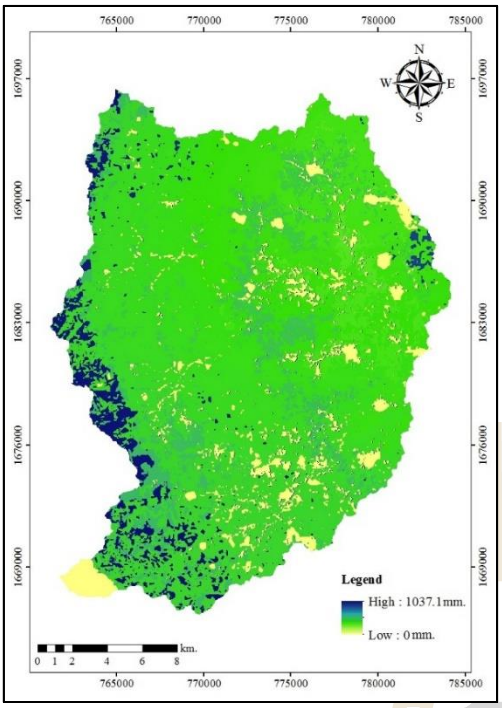

Direct through fall: DT

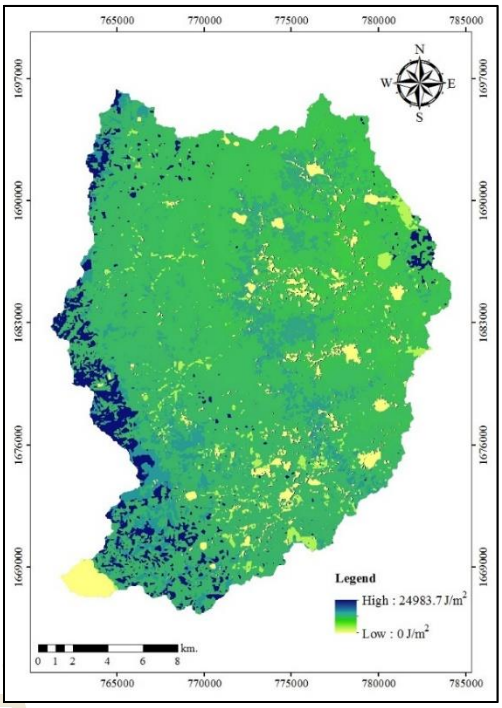

Kinetic energy of direct through fall: KE(DT)

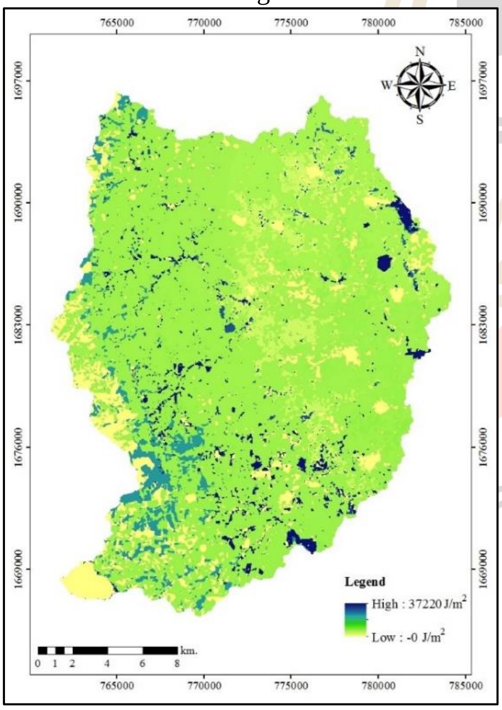

Kinetic energy of leaf drainage: KE(LD)

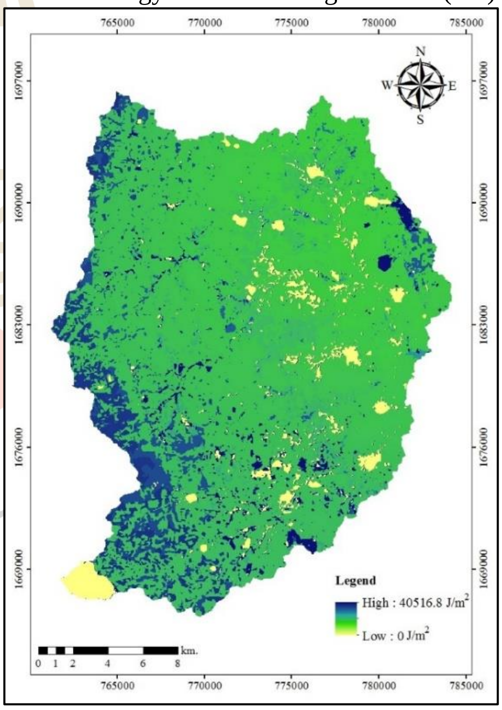

Kinetic energy of rainfall: KE

Figure 5.5 (Continued).

As results, it can be observed that effective rainfall (ER) varies between 0 and 1,038 mm, leaf drainage (LD) ranges between 0 and 584 mm and direct through fall (DT) varies between 0 and 1,037 mm. Kinetic energy of direct through fall (KE(DT)) ranges between 0 and 24,984 J m^{-2} , kinetic energy of leaf drainage (KE(LD)) ranges between 0 and 37,220 J m^{-2} , and kinetic energy of rainfall (KE) varies between 0 and 40,517 J m^{-2}.

5.3.2 Estimation of annual runoff

Annual runoff (Q) was estimated from soil moisture storage capacity of the soil (Rc) and mean rain per day (Ro). Soil moisture storage capacity (Rc) was estimated as a function of bulk density (BD), soil moisture content at field capacity (MS), effective hydrological depth (EHD), and the ratio of actual to potential evapotranspiration (Et/Eo). The specific values for these parameters were reviewed from Morgan (2001) to calculate soil moisture storage capacity. In practice, maps for these parameters were generated as attributes from the soil and LULC maps. These maps were then overlaid to obtain the soil moisture storage capacity layer using Eq. 7 in Table 3.5. Meanwhile the number of rainy days was obtained by averaging the annual rain days of the study area for a period of 30 years (1985-2015) varies between 0 and 63 days by using Eq. 8 in Table 3.5. Finally, the annual runoff layer was generated as a combination of annual rainfall map, soil moisture storage capacity and mean rain day using Eq. 9 in Table 3.5. The derived map of annual runoff estimation is displayed in Figure 5.6.

As results, it can be observed that soil moisture storage capacity (Rc) varies between 0 and 83 mm, mean rain per day (Ro) ranges between 0 and 17 mm and annual runoff varies between 0 and 1,030 mm.

5.3.3 Estimation of soil particle detachment

Soil particle detachment (D) was obtained in two phases. In the first phase, a soil particle detachment map by raindrop impact was computed by overlaying the total kinetic energy layer with the soil detachment index map using Eq. 10 in Table 3.5. In the second phase, a soil particle detachment map by runoff (H) was computed with the slope gradient layer obtained from DEM, runoff layer (Q), resistance of the soil layer (Z) and ground cover layer (GC) using Eq. 12 in Table 3.5. The soil resistance map was derived from surface cohesion values (COH) obtained from reviewed from Morgan (2001) using Eq. 11 in Table 3.5. Total soil particle detachment (D) was finally obtained by adding the soil particle detachment layer by runoff (H) to the soil particle detachment map by raindrop impact (F) using Eq. 13 in Table 3.5. The derived map of soil particle detachment estimation is displayed in Figure 5.7.

As results, it can be observed that soil particle detachment by raindrop impact (F) varies between 0 and 28 kg m^{-2}, soil resistance (Z) ranges between 0 and 1, and runoff detachment (H) varies between 0 and 20 kg m^{-2}. Total particle detachment (D) varies between 0 and 373 kg m^{-2}.

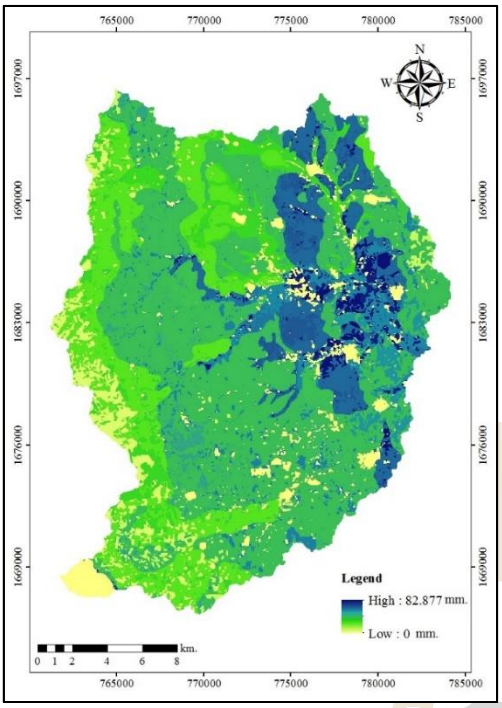

Soil moisture storage capacity: Rc

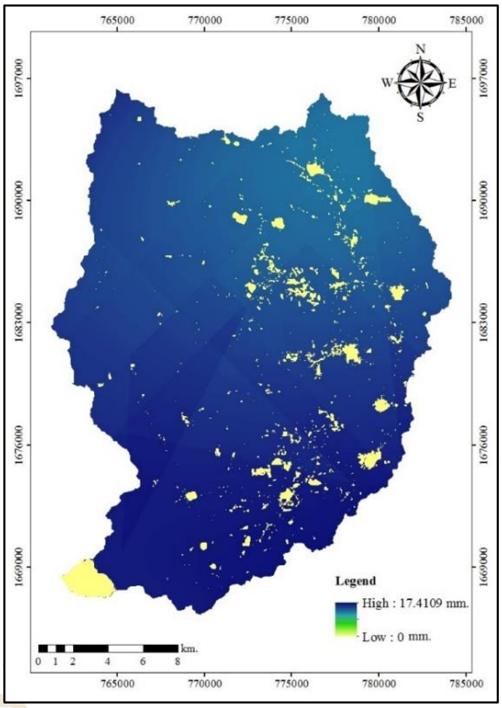

Mean rain per day: Ro

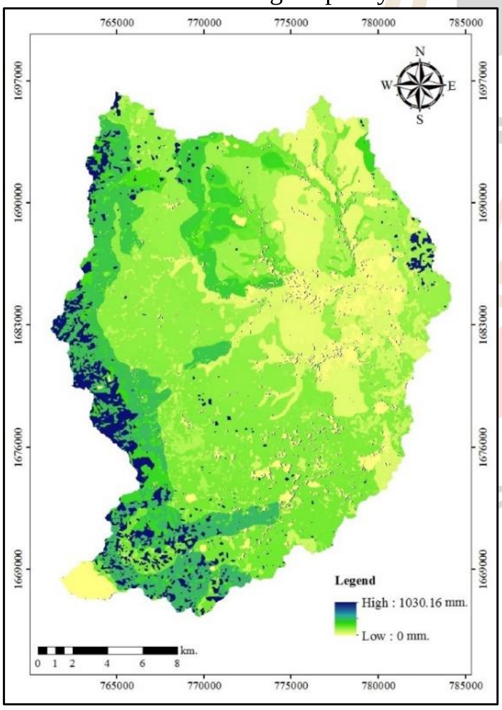

Annual runoff: Q

Figure 5.6 The derived map for annual runoff estimation.

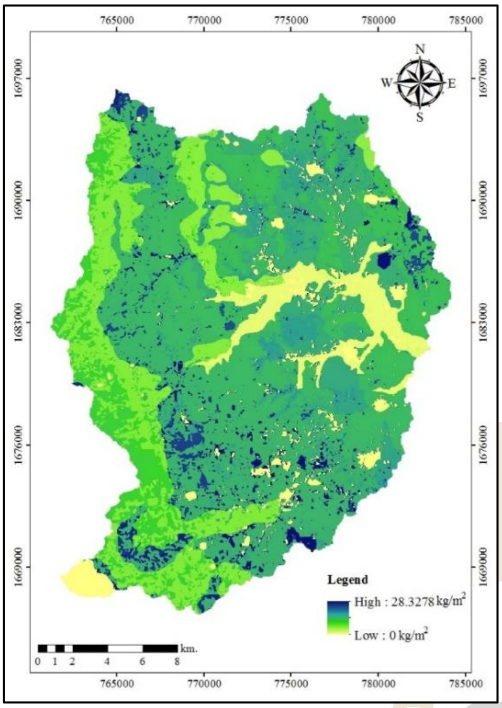

Soil particle detachment by raindrop impact: F

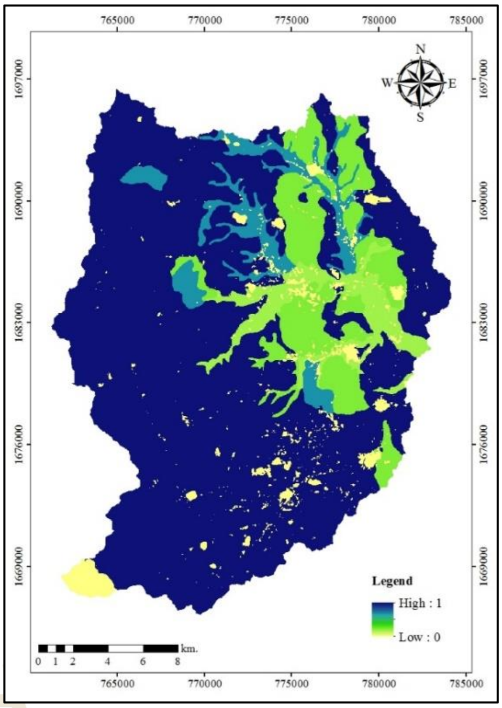

Soil resistance: Z

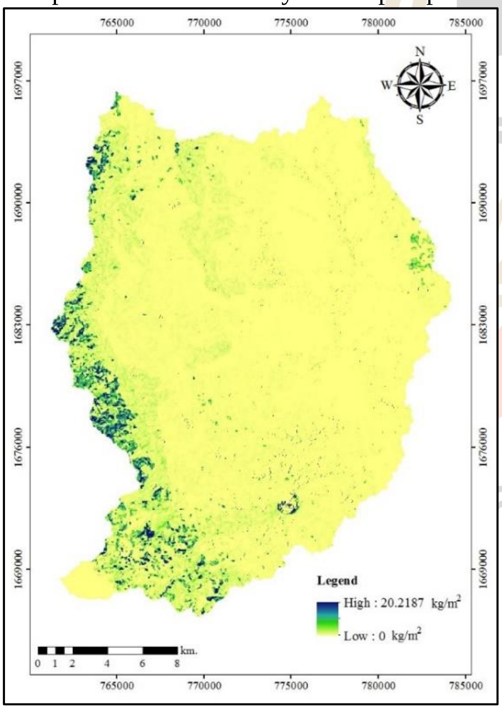

Runoff detachment: H

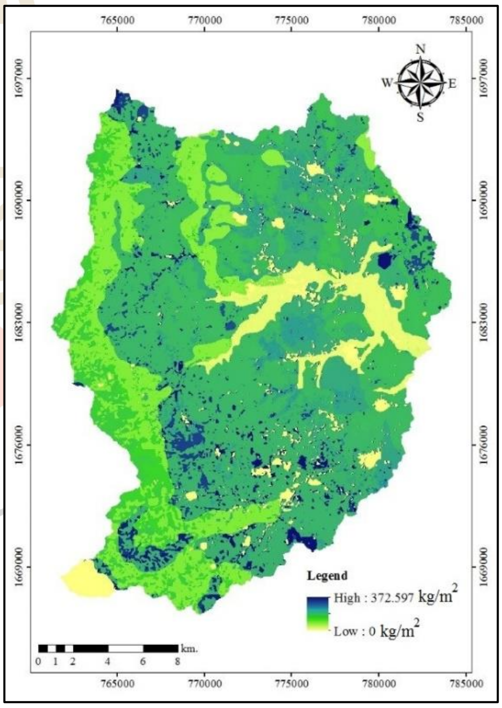

Total particle detachment: D

Figure 5.7 The derived map for soil particle detachment estimation.

5.3.4 Estimation of transport capacity of runoff

The transport capacity layer (TC) was derived as a function of surface cover (C), runoff (Q) and slope steepness (S) generated from the DEM using Eq. 14 in Table 3.5 as result shown in Figure 5.8.

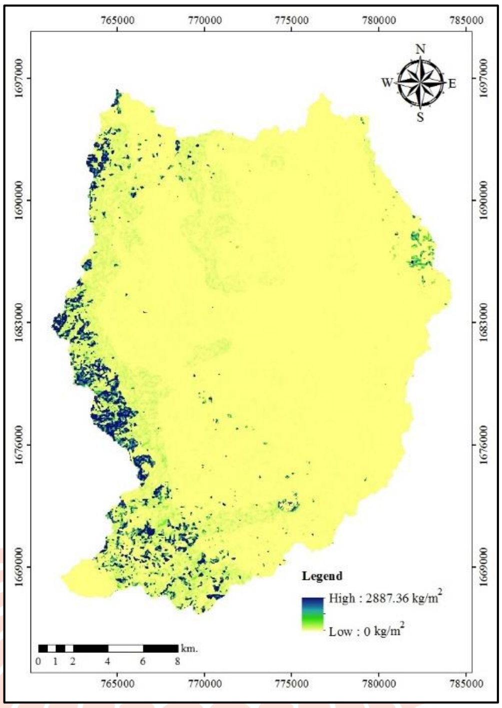

Transport capacity of runoff: TC

Figure 5.8 Transport capacity of runoff map.

As results, it reveals that transport capacity of runoff (TC) in the study area varies between 0 and 2,887 kg m^{-2}.

5.3.5 Estimation of soil loss

The estimated transport capacity map (TC) represents soil loss rates reflecting the transport potential in the study area while the total detachment map (D) represents soil loss rates showing the detachment capability by raindrop impact (F) and runoff (H). To obtain actual annual soil loss predictions of the RMMF model, these two maps (D and TC) were compared in each grid and the minimum of the two was taken as the estimated annual soil loss denoting whether soil detachment or transport capacity by runoff is the limiting factor (Figure 5.9). In this study, actual annual soil loss estimation using RMMF model was operated using the Model builder in ESRI ArcGIS software with the relevant tools (Figure 5.10).

Under RMMF model, soil loss equation (Soil loss = Minimum (D/1000*(10000), TC/1000*(10000)) gives soil loss rates in kg m^{-2}. The derived result is further converted to ton/ha/yr. The distribution of soil erosion by RMMF model is presented in Figure 5.11.

The result of soil erosion analysis using RMMF model generates an average soil loss of 3.368 ton/ha/year in the year 2015 with minimum of 0 ton/ha/year and maximum soil loss of 278.196 ton/ha/year (see Figure 5.11).

As results, it revealed that soil loss from soil particle detachment covered area of 6.61 sq. km or about 1.42% of the total study area and soil loss from transport capacity of runoff (TC) covered area of 437.43 sq. km or about 94.08% of the total study area. In addition, urban and built-up area and water body covered area of 20.92 sq. km or about 4.50% of the total study area. Both LULC types were excluded soil loss assessment and they had value of 0.

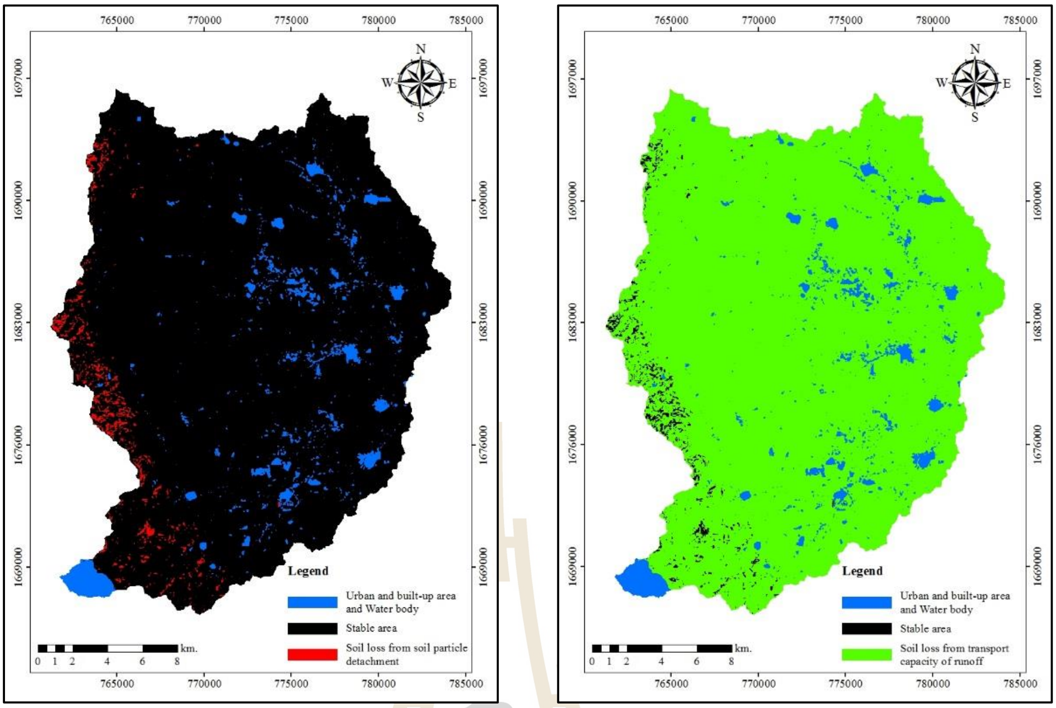

Soil loss from soil particle detachment   Soil loss from transport capacity of runoff

Figure 5.9 Annual soil loss from soil particle detachment (D) and transport capacity of runoff (TC) map which were compared in each grid and the minimum of the two was taken as the estimated annual soil loss.

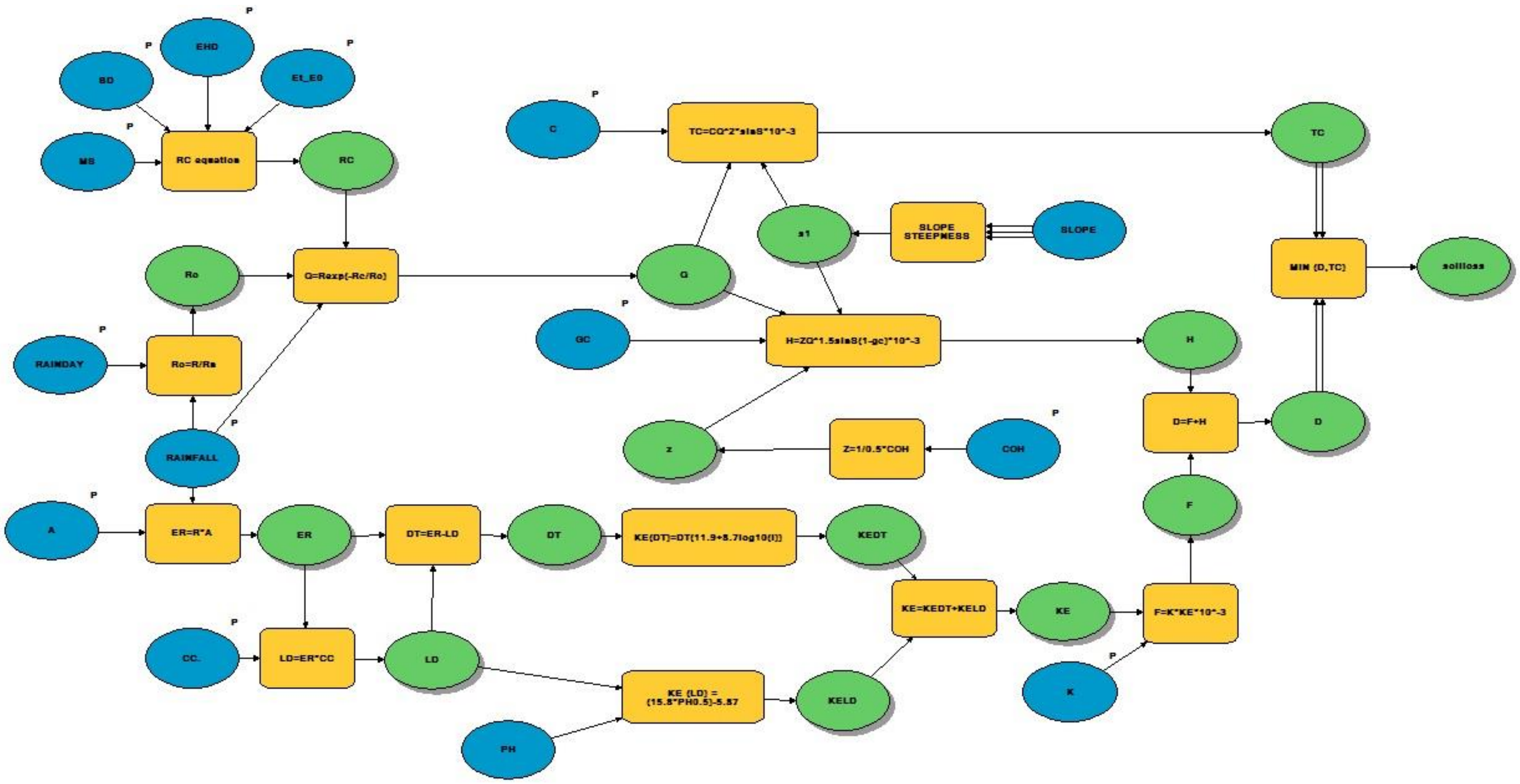

Figure 5.10 Model structure for RMMF model in ERSI ArcGIS software.

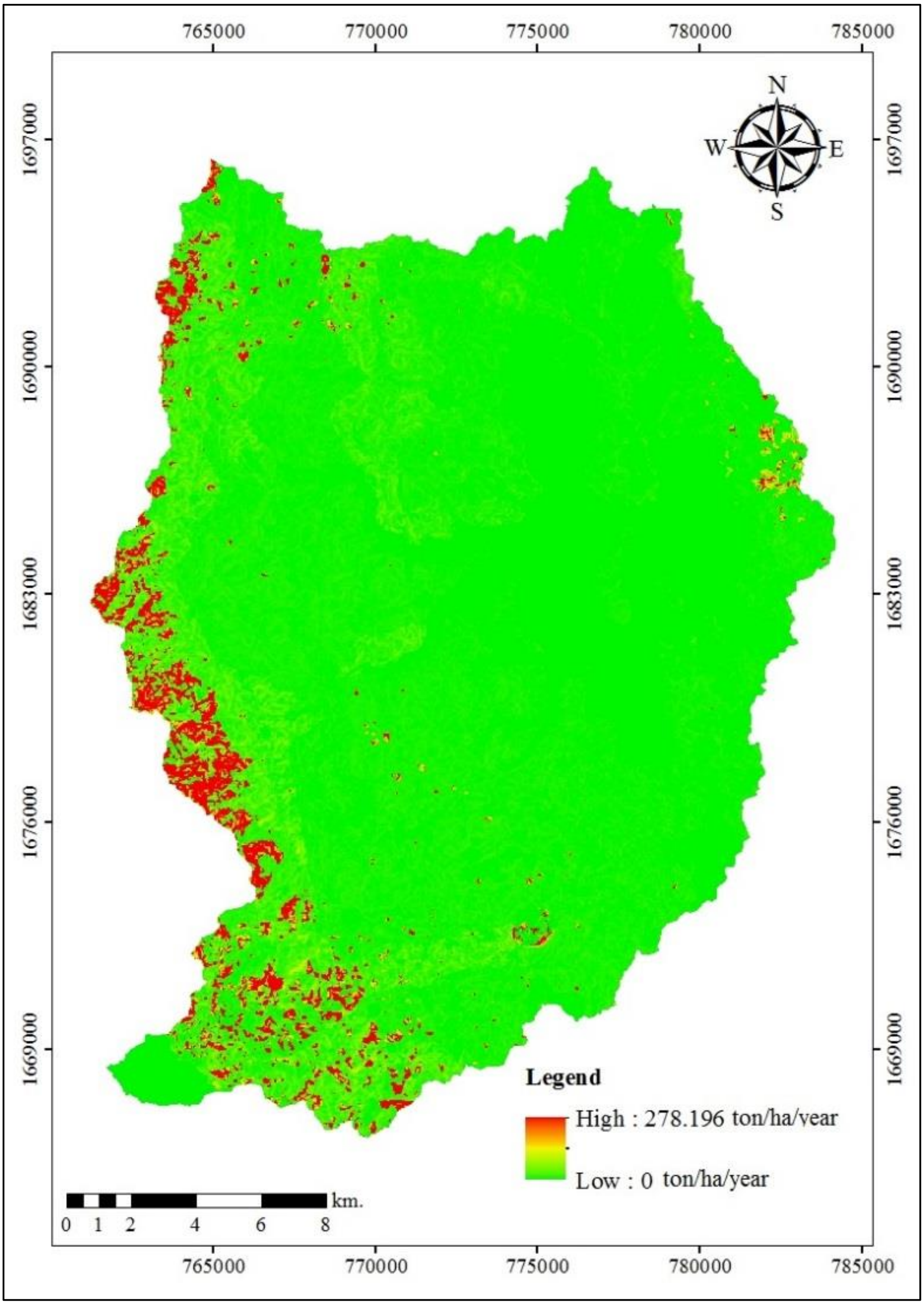

Figure 5.11 Distribution of soil erosion by RMMF model in the study area.

5.4 Soil erosion severity classification

The derived soil loss data is further classified its severity according to LDD standard (2000) as shown in Figure 5.12. Area and percentage of soil erosion severity classes is presented in Table 5.4.

Table 5.4 Severity class of soil loss (LDD, 2000).

No.	Severity Class	Erosion Rate (t/ha/y)	Area in sq. km	Percentage
1	Very Slightly Eroded	≤ 6.25	437.70	94.14
2	Slightly Eroded	6.26-31.25	8.97	1.93
3	Moderately Eroded	31.26-125.00	17.98	3.87
4	Highly Eroded	125.01-625.00	0.31	0.07
	Total		**464.96**	**100.00**

As a result it reveals that the most dominant soil loss severity class in the study area is very slightly eroded (≤ 6.25 ton/ha/year) and it covers area of 437.70 sq. km or about 94.14% of the total study area. Meanwhile, moderately and highly eroded classes cover area of 17.98 sq. km and 0.31 sq. km or 3.87% and 0.06% of the total study area, respectively.

According to overlay analysis between soil erosion severity classification and LULC data in 2015 (Table 5.5), top three dominant crops in very slightly eroded class are cassava, maize, and paddy field. Meanwhile, moderate and highly eroded classes are mostly found in miscellaneous land (soil pit, sand pit, and land fill) and they cover area of 14.96 and 0.25 sq. km or 3.22% and 0.05% of the study area, respectively. These results reflect the effect of LULC on soil erosion process. Herein, miscellaneous land generates higher soil erosion than other LULC types.

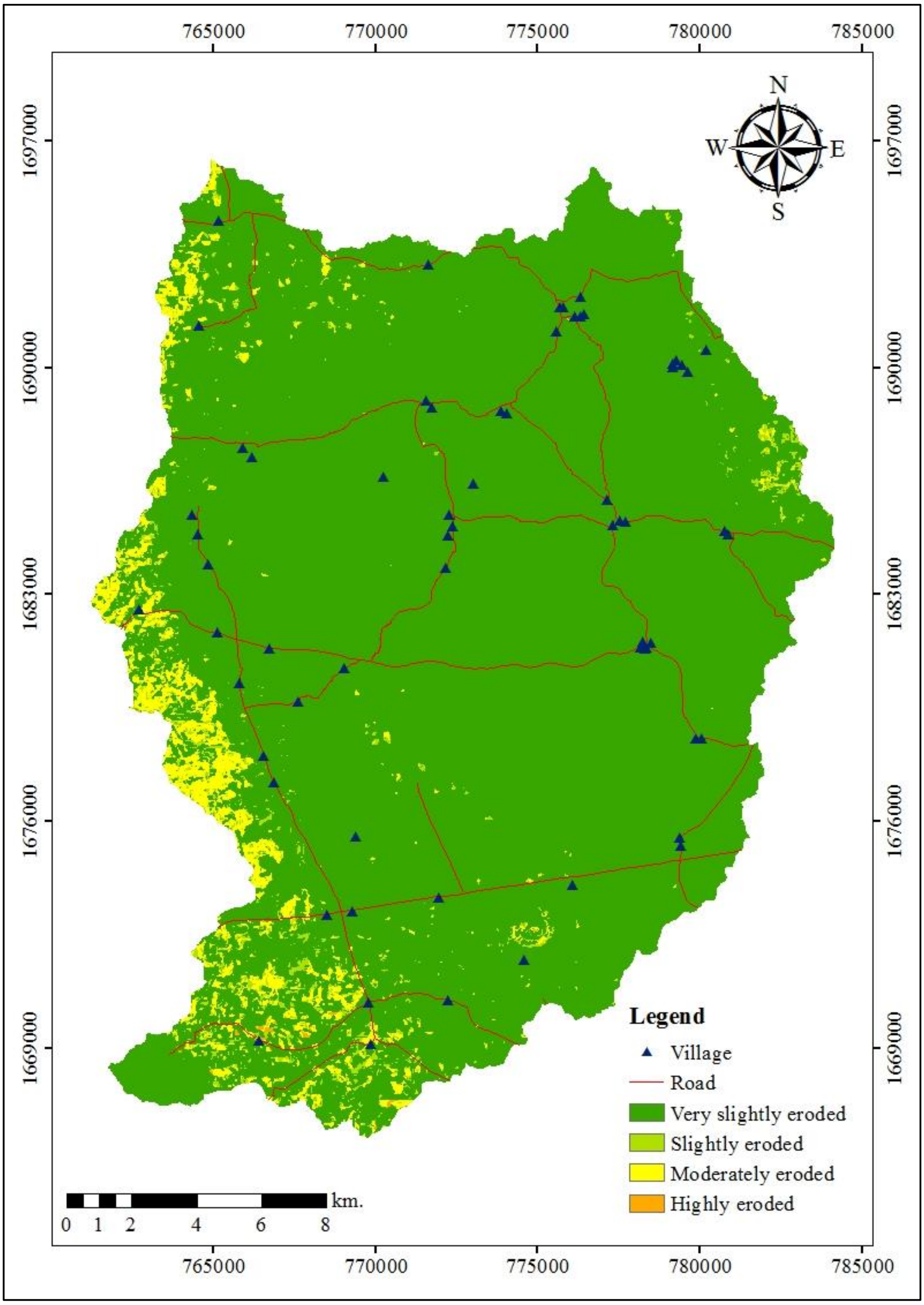

Figure 5.12 Soil erosion severity classes in the study area.

Table 5.5 Soil loss severity and LULC classes.

Land use and land cover classes	Very Slightly Eroded		Slightly Eroded		Moderately Eroded		Highly Eroded	
	Sq.km.	%	Sq.km.	%	Sq.km.	%	Sq.km.	%
Urban and built-up area	6.64	1.43	0	0	0	0	0	0
Paddy field	21.25	4.57	0	0	0	0	0	0
Maize	31.56	6.79	0	0	0	0	0	0
Sugarcane	6.76	1.45	0	0	0	0	0	0
Cassava	316.45	68.06	3.61	0.78	2.43	0.52	0.05	0.01
Perennial tree and orchard	18.98	4.08	0.30	0.06	0.56	0.12	0.01	0.00
Dense deciduous forest	4.11	0.88	0	0	0	0	0	0
Disturbed deciduous forest	9.03	1.94	0.01	0.00	0	0	0	0
Forest plantation	11.93	2.57	0.02	0.00	0.01	0	0	0
Water body	5.08	1.09	0	0	0	0	0	0
Scrub	1.17	0.25	0	0	0	0	0	0
Miscellaneous land	4.75	1.02	5.03	1.08	14.96	3.22	0.25	0.05
Total	**437.70**	**94.14**	**8.97**	**1.93**	**17.98**	**3.87**	**0.31**	**0.07**

Soil severity class spans all soil loss columns.

In addition, the prepared elevation and slope (see Figure 4.1) were here further reclassify as thematic classes based on standard classification of LDD (2009) as shown in Figure 5.13 for overlay analysis with soil loss severity classification. Area and percentage of elevation and slope in the study area is summarized in Tables 5.6 to 5.7, respectively.

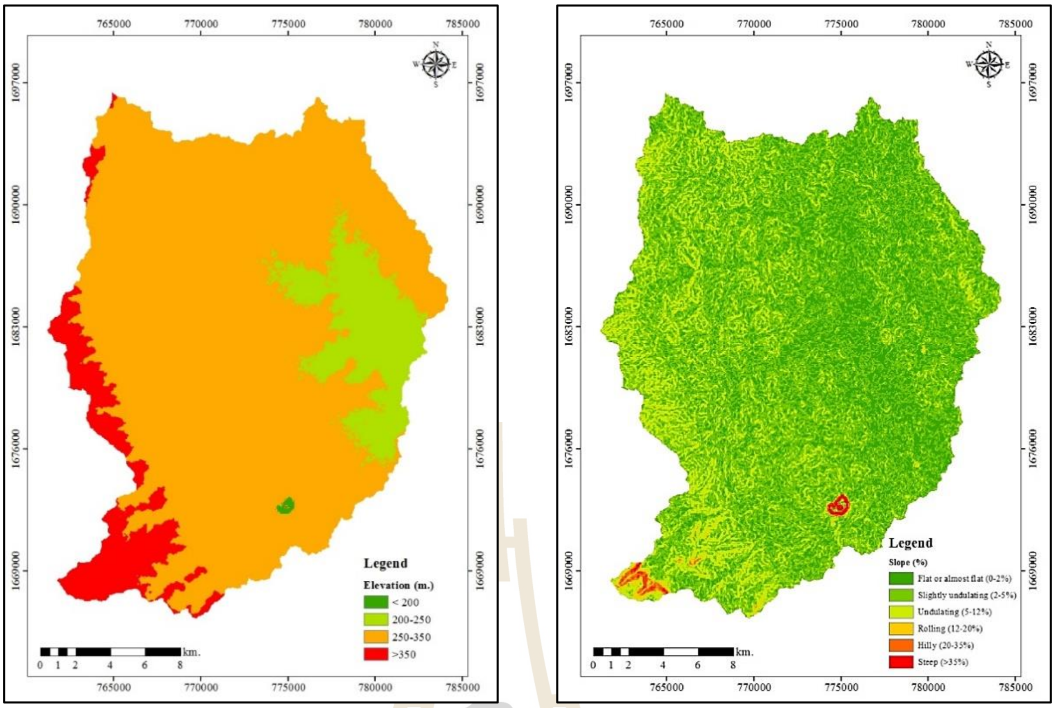

Elevation classification Slope classification

Figure 5.13 Distribution of elevation and slope classification.

Table 5.6 Area and percentage of elevation classification in the study area.

No	Elevation (m)	Area (sq. km)	Percentage
1	< 200	0.59	0.13
2	200-250	51.89	11.16
3	250-350	373.18	80.26
4	350-750	39.30	8.45
	Total	**464.96**	**100.00**

Table 5.7 Area and percentage of slope classification in the study area.

No	Slope (%)	Topography	Area (sq. km)	Percentage
1	0-2	Flat or almost flat	140.21	30.12
2	2-5	Slightly undulating	236.11	50.79
3	5-12	Undulating	84.21	18.13
4	12-20	Rolling	1.90	0.41
5	20-35	Hilly	1.46	0.31
6	>35	Steep	1.06	0.23
		Total	**464.96**	**100.00**

Table 5.8 Soil loss severity and elevation classes.

Elevation classes	Soil loss severity classes							
	Very Slightly Eroded		Slightly Eroded		Moderately Eroded		Highly Eroded	
	Sq.km.	%	Sq.km.	%	Sq.km.	%	Sq.km.	%
< 200 m.	0.48	0.10	0.05	0.01	0.06	0.01	0.00	0.00
200-250 m.	51.87	11.16	0.00	0.00	0.02	0.00	0.00	0.00
250-350 m.	362.18	77.89	4.70	1.01	6.28	1.35	0.04	0.01
350-750 m.	23.18	4.99	4.22	0.91	11.62	2.50	0.28	0.06
Total	**437.70**	**94.14**	**8.97**	**1.93**	**17.98**	**3.87**	**0.31**	**0.07**

According to overlay analysis between soil erosion severity and elevation classifications (Table 5.8), it reveals that most of very slightly eroded class situates between 250 and 350 m above mean sea level and covers area of 362.18 sq. km or 77.89% of the total study area. Meanwhile, moderately and highly eroded classes are frequently found between 350 and 750 m above mean sea level and cover area of 11.62 sq. km and 0.28 sq. km or 2.50% and 0.06% of the total study area, respectively.. Likewise, according to overlay analysis between soil erosion severity and slope classifications (Table 5.9), it shows that it reveals that most of very slightly eroded class locates at slightly undulation terrain (2-5%) and covers area of 224.91 sq. km or 48.37% of the total study area. Meanwhile, moderately and highly eroded classes are frequently found at undulating terrain (5-12%) and cover area of 9.63 sq. km and 0.16 sq. km or 2.07% and 0.03% of the total study area, respectively.

In addition, the most dominant soil loss severity class at hilly (20-35%) and steep (>35%) landforms was very slightly eroded because those areas mostly covered by dense deciduous forest.

Table 5.9 Soil loss severity and slope classes.

Slope classes	Soil loss severity classes							
	Very Slightly Eroded		Slightly Eroded		Moderately Eroded		Highly Eroded	
	Sq. km.	%	Sq. km.	%	Sq. km.	%	Sq. km.	%
Flat or almost flat (0-2%)	137.74	29.63	1.93	0.42	0.54	0.12	0	0
Slightly undulating (2-5%)	224.91	48.37	3.69	0.79	7.51	1.62	0	0
Undulating (5-12%)	71.46	15.37	2.97	0.64	9.63	2.07	0.16	0.03
Rolling (12-20%)	1.47	0.32	0.19	0.04	0.13	0.03	0.11	0.02
Hilly (20-35%)	1.35	0.29	0.07	0.02	0.01	0	0.03	0.01
Steep (>35%)	0.77	0.17	0.12	0.03	0.16	0.04	0.01	0
Total	**437.70**	**94.14**	**8.97**	**1.93**	**17.98**	**3.87**	**0.31**	**0.07**

These findings clearly imply the effect of elevation and landform on soil erosion process in the study area. Herein, soil erosion was very slightly eroded since the most dominant elevation class was rather low (250-350 m) and the most dominant landform were flat or almost flat and slightly undulating.

CHAPTER VI

SOIL SALINITY ASSESSMENT AND ITS SEVERITY

Main results of the third objective on assessment of soil salinity and its severity in 2015 with optimum spectral salinity index are here separately reported include (1) EC samples collection and analysis, (2) independent variables on EC data, (3) EC estimation model development, (4) optimum EC estimation model, and (5) soil salinity assessment and its severity. Details of each result are separately described and discussed in following sections.

6.1 EC samples collection and analysis

EC samples of modeling and validation datasets that were collected in field according to the combination between soil series and LULC data (see Figure 3.6) and analyzed at SUT laboratory in 2016 is presented in Tables 6.1 and 6.2, respectively. The distribution of EC samples of modelling and validation datasets is displayed in Figure 6.1 while the basic statistic of both EC sample datasets is summarized in Table 6.3. The analyzed EC modelling dataset was here applied as dependent dataset for linear and non-linear regression analysis while the analyzed EC validation dataset was applied for accuracy assessment.

Table 6.1 EC samples data of modeling dataset.

ID	X	Y	Class	LULC	Soil series	EC (dS m^{-1})
ID100	773218	1681331	827	5	123	0.050
ID104	770998	1673921	828	5	124	0.045
ID106	776848	1684091	801	5	97	0.138
ID108	778558	1688501	801	5	97	0.063
ID11	777898	1678721	801	5	97	0.023
ID111	772048	1687901	719	5	15	0.069
ID113	770098	1680851	811	5	107	0.066
ID114	768628	1675421	1004	6	124	0.051
ID115	774358	1684211	709	5	5	0.066
ID119	776668	1673291	830	5	126	0.090
ID12	771718	1684061	434	3	82	0.113
ID121	771028	1687781	719	5	15	0.084
ID125	780118	1686521	1329	8	97	0.174
ID126	765568	1673231	999	6	119	0.026
ID127	775888	1678391	473	3	121	0.096
ID13	769828	1668611	2095	12	159	0.014
ID130	777658	1686641	827	5	123	0.054
ID132	774988	1679171	483	3	131	0.296
ID134	764758	1681901	805	5	101	0.102
ID136	771388	1689341	452	3	100	0.025
ID137	780808	1681211	312	2	136	0.280
ID139	777028	1676561	810	5	106	0.327
ID14	768418	1691081	812	5	108	0.011
ID142	779668	1678061	205	2	29	0.178
ID147	778918	1688141	271	2	95	0.059
ID15	773938	1679231	1140	7	84	0.072
ID151	770338	1682771	1333	8	101	0.360
ID152	778738	1686011	835	5	131	0.117
ID154	763648	1691621	2035	12	99	0.023
ID158	765178	1695671	833	5	129	0.010
ID160	780898	1679171	218	2	42	0.200
ID161	766888	1692881	1164	7	108	0.058
ID162	767488	1681991	1157	7	101	0.064
ID164	774688	1692101	440	3	88	0.141
ID169	774268	1671851	1261	8	29	0.268
ID170	778438	1672361	1191	7	135	0.008
ID171	768448	1693271	2044	12	108	0.016

Table 6.1 (Continued).

ID	X	Y	Class	LULC	Soil series	EC (dS m^{-1})
ID172	764098	1685021	971	6	91	0.047
ID174	775048	1689521	1153	7	97	0.275
ID175	765808	1695701	988	6	108	0.029
ID178	767308	1685801	1185	7	129	0.052
ID181	777688	1672301	1182	7	126	0.019
ID182	766858	1684721	690	1	162	0.077
ID183	772768	1680641	436	3	84	0.078
ID189	766078	1687421	610	4	82	0.019
ID195	776968	1672781	1358	8	126	0.080
ID196	767788	1679801	1180	7	124	0.006
ID198	777568	1687871	191	2	15	0.087
ID199	779608	1676351	282	2	106	0.101
ID2	768718	1692461	823	5	119	0.049
ID20	772528	1679711	828	5	124	0.051
ID200	782008	1688351	1151	7	95	0.011
ID201	769708	1680731	1237	8	5	0.142
ID203	766558	1678901	1323	8	91	0.254
ID207	775738	1680161	297	2	121	0.100
ID209	768598	1686251	626	4	98	0.072
ID21	776938	1690931	449	3	97	0.035
ID210	768088	1689611	636	4	108	0.090
ID212	771448	1669361	975	6	95	0.272
ID213	772438	1684271	1061	7	5	0.110
ID214	771898	1676591	1355	8	123	0.264
ID215	769708	1687331	628	4	100	0.047
ID217	776008	1677791	1085	7	29	0.230
ID218	769798	1688621	543	4	15	0.044
ID219	769318	1687751	647	4	119	0.082
ID220	766288	1691981	1328	8	96	0.027
ID221	780178	1687991	447	3	95	0.034
ID222	769888	1688381	1247	8	15	0.009
ID223	765328	1695491	1009	6	129	0.059
ID224	764908	1668041	1021	6	141	0.115
ID226	766648	1684631	1042	6	162	0.052
ID229	766768	1691831	1152	7	96	0.055
ID23	771748	1681781	709	5	5	0.107
ID230	764998	1667711	1901	11	141	0.140

Table 6.1 (Continued).

ID	X	Y	Class	LULC	Soil series	EC (dS m^{-1})
ID231	767458	1685831	1361	8	129	0.086
ID233	768328	1685711	1177	7	121	0.028
ID25	774028	1680041	788	5	84	0.078
ID27	778408	1693091	801	5	97	0.045
ID28	770968	1685561	1179	7	123	0.104
ID29	781768	1686401	2031	12	95	0.041
ID31	769678	1680821	1339	8	107	0.034
ID34	775228	1678511	839	5	135	0.092
ID35	775228	1691261	449	3	97	0.126
ID36	776518	1691021	367	3	15	0.060
ID38	774148	1688021	786	5	82	0.069
ID39	770668	1671101	823	5	119	0.020
ID40	764818	1692371	803	5	99	0.033
ID41	778798	1684211	273	2	97	0.100
ID44	772108	1686101	475	3	123	0.078
ID45	779038	1680701	258	2	82	0.050
ID47	779668	1685291	181	2	5	0.169
ID5	769978	1666631	2104	12	168	0.057
ID50	778228	1690391	801	5	97	0.120
ID51	776968	1679801	801	5	97	0.035
ID52	764068	1680191	795	5	91	0.074
ID53	770158	1677551	828	5	124	0.008
ID54	768058	1670261	2018	12	82	0.009
ID56	769318	1692821	823	5	119	0.032
ID58	779428	1679861	786	5	82	0.023
ID6	775498	1679231	357	3	5	0.241
ID60	766678	1690091	812	5	108	0.013
ID61	773818	1685261	804	5	100	0.090
ID63	767848	1677101	1356	8	124	0.039
ID67	772948	1670951	799	5	95	0.038
ID68	766318	1670441	1039	6	159	0.028
ID69	776098	1678181	381	3	29	0.310
ID7	766858	1679351	795	5	91	0.068
ID72	767128	1670351	863	5	159	0.015
ID79	767248	1687031	814	5	110	0.053
ID8	770068	1693721	719	5	15	0.067
ID80	781288	1679591	746	5	42	0.368

Table 6.1 (Continued).

ID	X	Y	Class	LULC	Soil series	EC (dS m^{-1})
ID81	779518	1678511	786	5	82	0.108
ID85	782218	1684091	311	2	135	0.020
ID86	778258	1677851	801	5	97	0.094
ID9	769618	1684151	825	5	121	0.018
ID90	771568	1683371	786	5	82	0.019
ID92	780418	1688291	799	5	95	0.044
ID95	777448	1674911	830	5	126	0.080
ID96	763168	1682231	2026	12	90	0.023
ID99	777658	1688831	719	5	15	0.096

Table 6.2 EC samples data of validation dataset.

ID	X	Y	Class	LULC	Soil series	EC (dS m^{-1})
ID1	772888	1675601	828	5	124	0.070
ID101	777718	1679531	801	5	97	0.333
ID102	771898	1679831	828	5	124	0.065
ID103	774418	1673471	828	5	124	0.089
ID105	764998	1668941	823	5	119	0.068
ID107	783208	1683611	839	5	135	0.027
ID109	767188	1672601	823	5	119	0.011
ID112	780898	1680101	312	2	136	0.235
ID116	778138	1674401	478	3	126	0.041
ID120	765838	1677791	2027	12	91	0.068
ID122	774898	1692341	367	3	15	0.055
ID123	772198	1676651	827	5	123	0.080
ID129	774868	1670141	623	4	95	0.021
ID131	765178	1670471	962	6	82	0.013
ID133	774148	1670171	799	5	95	0.028
ID135	772828	1682141	827	5	123	0.206
ID138	774838	1671101	1327	8	95	0.011
ID140	772648	1682531	357	3	5	0.111
ID141	778978	1672841	487	3	135	0.337
ID143	772678	1687181	475	3	123	0.075

Table 6.2 (Continued).

ID	X	Y	Class	LULC	Soil series	EC (dS m^{-1})
ID144	769828	1675691	652	4	124	0.152
ID146	768838	1674671	1004	6	124	0.053
ID150	778918	1687001	835	5	131	0.084
ID153	763648	1690211	979	6	99	0.103
ID155	781018	1683731	181	2	5	0.029
ID156	775678	1677731	1191	7	135	0.341
ID157	776668	1670471	654	4	126	0.321
ID159	765148	1695161	2065	12	129	0.023
ID16	780538	1688711	799	5	95	0.031
ID163	767968	1686461	833	5	129	0.056
ID165	773668	1679111	1187	7	131	0.252
ID166	767008	1676561	971	6	91	0.010
ID167	767338	1688171	812	5	108	0.106
ID168	781048	1678481	271	2	95	0.002
ID17	779878	1677041	733	5	29	0.019
ID173	779098	1675571	1690	10	106	0.092
ID176	781738	1681421	1589	10	5	0.030
ID177	777988	1691861	1071	7	15	0.084
ID179	767398	1690781	800	5	96	0.014
ID18	765958	1680131	1147	7	91	0.125
ID180	766408	1691021	1175	7	119	0.259
ID184	775258	1676801	1367	8	135	0.387
ID185	781438	1688711	1155	7	99	0.015
ID186	777748	1688081	191	2	15	0.134
ID187	766648	1683551	2037	12	101	0.062
ID188	772048	1681601	476	3	124	0.381
ID190	767248	1684661	629	4	101	0.088
ID191	778528	1675631	1338	8	106	0.069
ID192	768688	1685651	649	4	121	0.081
ID193	772798	1676921	2060	12	124	0.116
ID194	763768	1669361	2077	12	141	0.095

Table 6.2 (Continued).

ID	X	Y	Class	LULC	Soil series	EC (dS m^{-1})
ID197	771508	1671911	1351	8	119	0.008
ID202	778018	1676531	1613	10	29	0.107
ID204	778978	1687481	307	2	131	0.103
ID205	779728	1673501	1719	10	135	0.044
ID206	766648	1688261	638	4	110	0.055
ID208	780838	1686851	2033	12	97	0.022
ID211	767728	1679051	619	4	91	0.125
ID216	765958	1688651	1340	8	108	0.017
ID22	781798	1681091	840	5	136	0.082
ID225	766918	1685591	657	4	129	0.031
ID227	774808	1672421	1710	10	126	0.034
ID228	767398	1690931	2032	12	96	0.306
ID232	777088	1692491	1599	10	15	0.062
ID24	776158	1671821	830	5	126	0.111
ID26	766588	1693181	812	5	108	0.021
ID30	768268	1677791	1356	8	124	0.006
ID37	774088	1690211	449	3	97	0.055
ID4	766888	1679261	795	5	91	0.089
ID42	775318	1684121	801	5	97	0.126
ID43	769978	1681271	811	5	107	0.292
ID46	780088	1690691	786	5	82	0.008
ID49	765928	1671341	1039	6	159	0.072
ID55	766708	1680701	805	5	101	0.080
ID59	767428	1684931	805	5	101	0.089
ID62	774328	1685411	804	5	100	0.127
ID64	770518	1680551	709	5	5	0.022
ID65	763858	1680251	2026	12	90	0.163
ID66	771898	1682111	709	5	5	0.059
ID70	770668	1668491	872	5	168	0.016
ID73	768868	1685921	825	5	121	0.059
ID74	773848	1680581	788	5	84	0.087

Table 6.2 (Continued).

ID	X	Y	Class	LULC	Soil series	EC (dS m^{-1})
ID75	778858	1693601	792	5	88	0.092
ID76	776938	1680251	273	2	97	0.031
ID77	762388	1682141	794	5	90	0.118
ID78	777988	1686941	719	5	15	0.029
ID83	768568	1669751	823	5	119	0.010
ID88	765418	1693631	803	5	99	0.019
ID91	766078	1682411	981	6	101	0.157
ID93	777928	1677401	839	5	135	0.026
ID94	768568	1668341	2095	12	159	0.012
ID97	769108	1692071	823	5	119	0.064
ID98	765808	1692521	1331	8	99	0.084

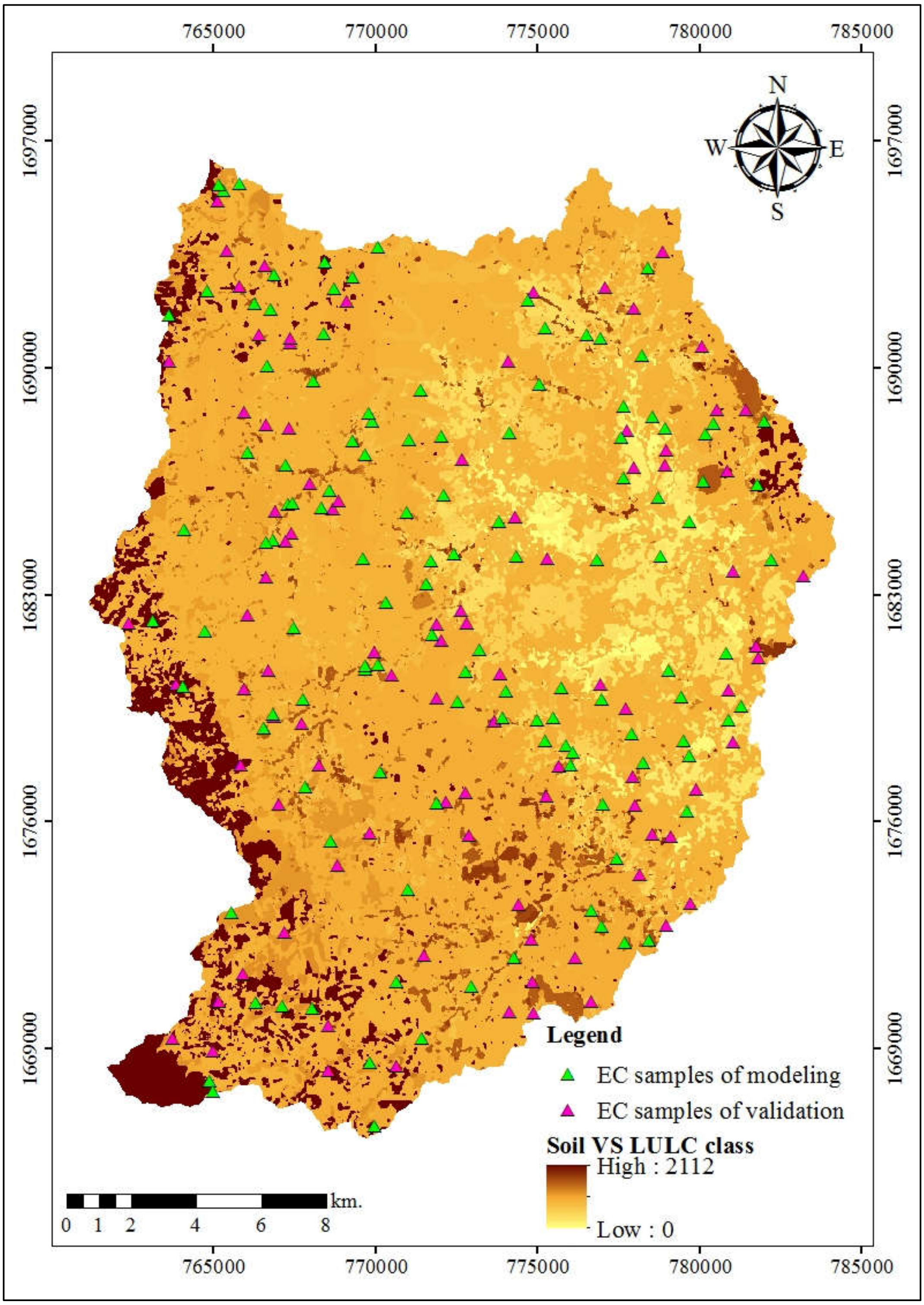

Figure 6.1 Distribution of modeling and validation datasets of EC sampling points for an optimum EC model development.

Table 6.3 Basic statistics of analyzed EC samples dataset.

EC Dataset	No of samples	Basic statistical value (dS m^{-1})				
		Minimum	Maximum	Mean	S.D.	Variance
Modelling	120	0.006	0.368	0.088	0.082	0.007
Validation	93	0.002	0.387	0.093	0.092	0.009

6.2 Independent variables on EC data

Soil salinity indices include NDSI, SI1, SI2, SI3, S1, S2, S3, S4, S5, and S6 as independent variables were firstly calculated according to its equation (see Table 2.3 in Chapter II) from Landsat data in 2015. The distribution of these indices is presented in Figure 6.2 and basic statistics data of soil salinity indices is summarized in Table 6.4. These data were further applied to identify relationship with EC data using linear and non-linear regression analysis.

Table 6.4 Basic statistics of independent variable data for EC estimation model development.

Variables	**No of pixels**	**Basic statistical value (dS m^{-1})**				
		Minimum	**Maximum**	**Mean**	**S.D.**	**Variance**
NDSI	120	-0.507	0.154	-0.176	0.050	0.002
SI-1	120	32.404	95.467	42.432	3.070	9.424
SI-2	120	34336.000	1084566.000	110433.574	24975.997	623800405.628
SI-3	120	1050.000	9114.000	1809.888	264.765	70100.503
S1	120	0.783	1.344	1.072	0.082	0.007
S2	120	-0.121	0.147	0.033	0.038	0.001
S3	120	26.250	111.146	40.084	4.864	23.656
S4	120	34.641	89.644	43.613	2.668	7.120
S5	120	37.098	77.816	45.528	2.162	4.674
S6	120	24.650	125.398	60.097	60.097	3611.701

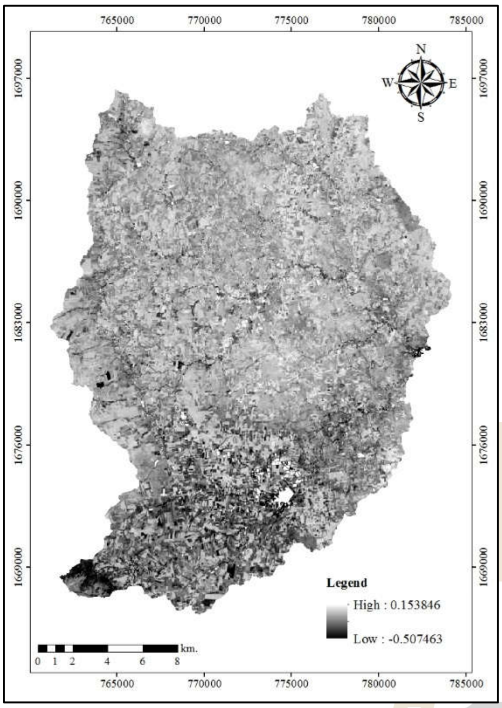

(a) NDSI

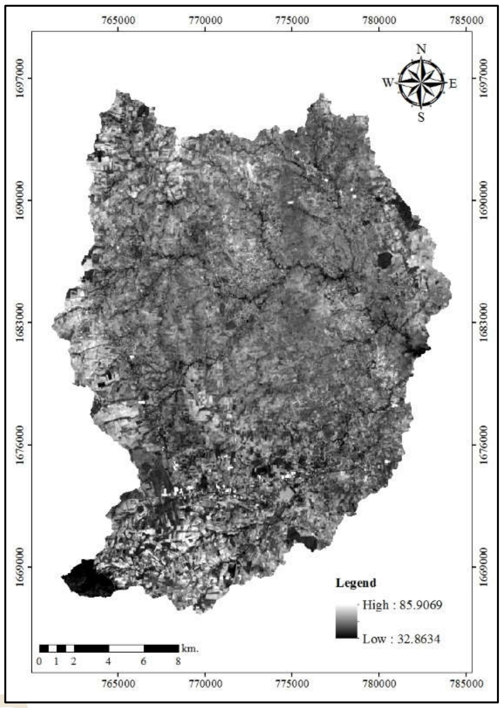

(b) SI-1

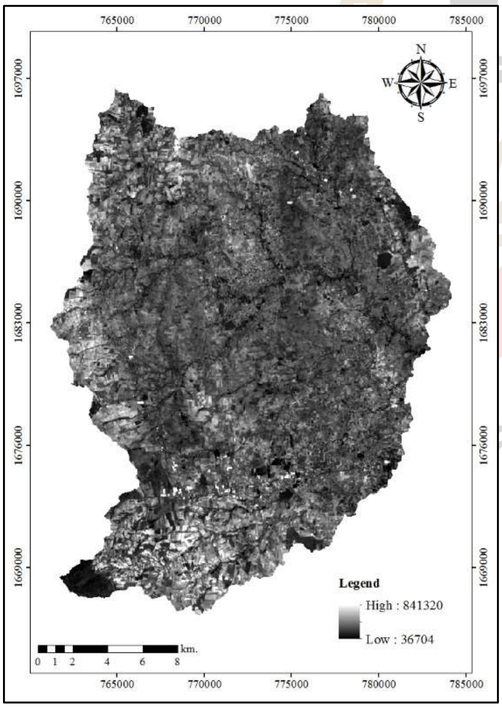

(c) SI-2

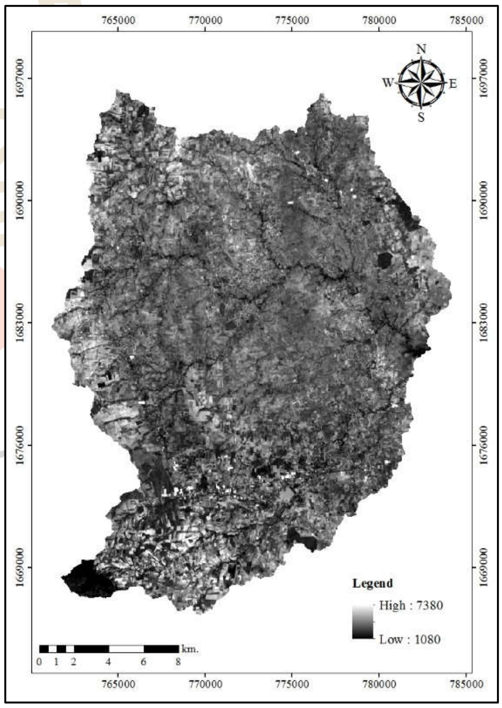

(d) SI-3

Figure 6.2 Distribution of spectral salinity indices: (a) NDSI, (b) SI1, (c) SI2, (d) SI3, (e) S1, (f) S2, (g) S3, (h) S4, (i) S5, and (j) S6.

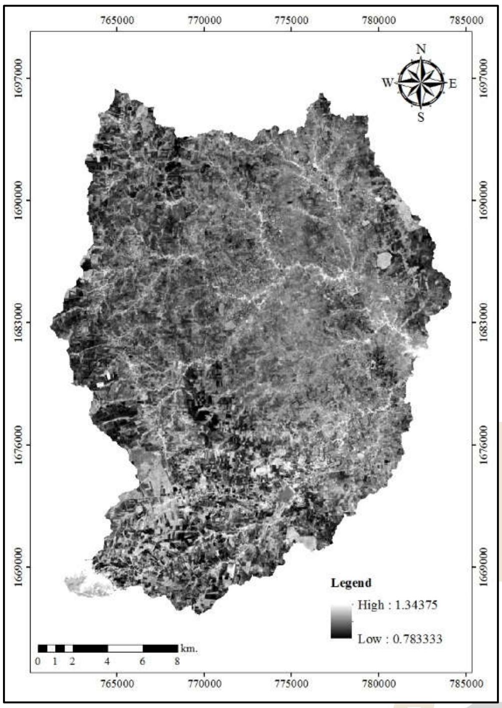

(e) S1

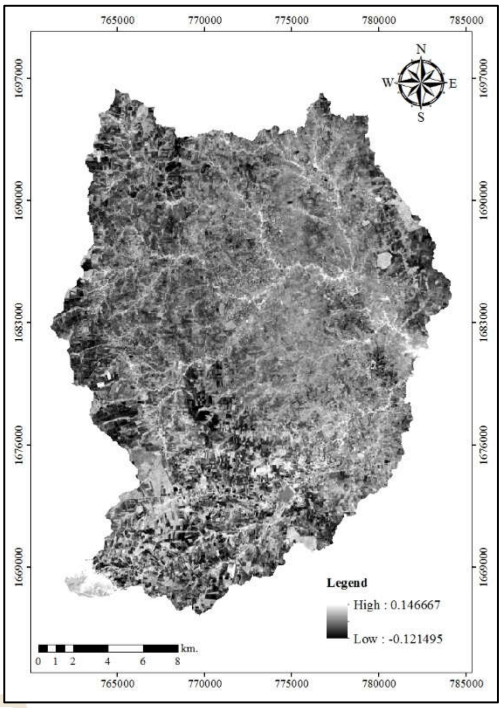

(f) S2

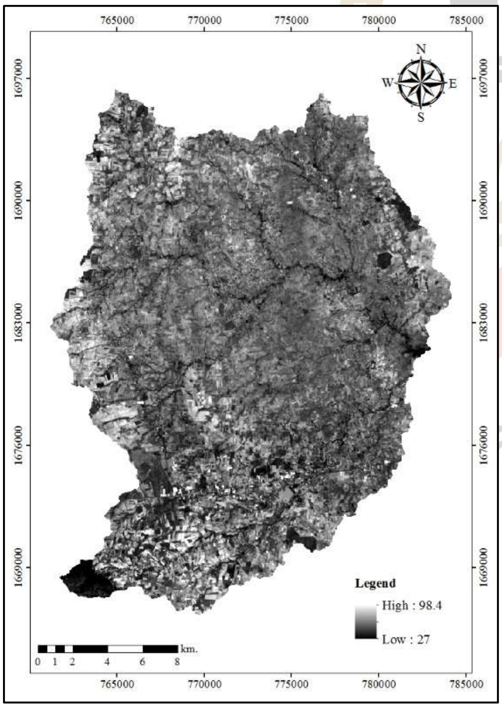

(g) S3

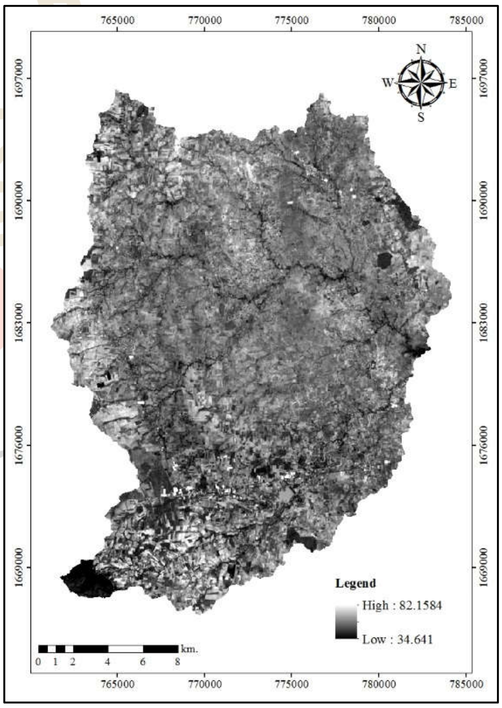

(h) S4

Figure 6.2 (Continued).

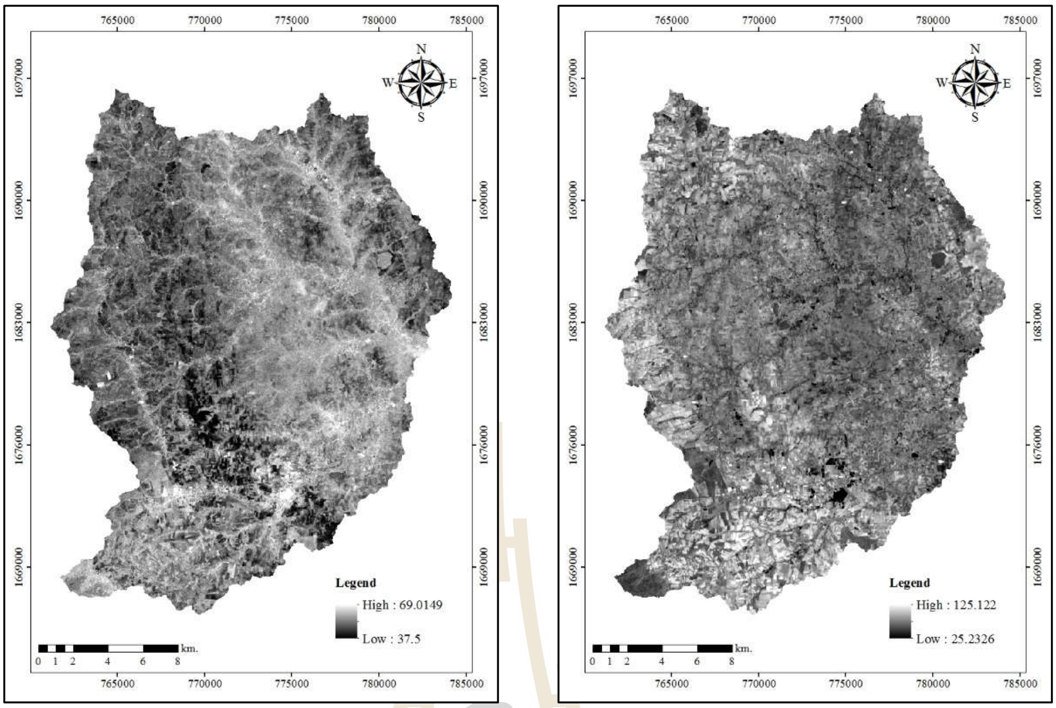

(i) S5 (j) S6

Figure 6.2 (Continued).

6.3 EC estimation model development

Data input include dependent and independent variables as mentioned in Sections 6.1 and 6.2 were here applied to develop optimum EC estimation model using linear and non-linear regression analysis under SPSS statistical software. The derived equations from both analyses which provide the R^2 equal or greater than 0.5 was then chosen as candidate equations for identifying an optimum EC estimation model using accuracy assessment with NRMSE. In addition, spatial regression analysis between the derived candidate EC maps with the best interpolated EC map from five surface interpolation techniques (IDW, TPS, SK, UK, and OK) was examined using R and R^2.

6.3.1 Linear regression analysis of EC estimation model development

Simple linear and multiple linear regression analysis were here analyzed to select candidate equations for identifying an optimum EC estimation model with non-linear regression analysis.

All equations of simple and multiple linear regression analysis between of modelling EC samples and spectral salinity indices that provide R^2 equal or greater than 0.5 is presented in Table 6.5. It was found that only one spectral salinity index, S5 provides positively correlation with EC data with R^2 of 0.502 under simple linear regression analysis. Meanwhile, combination of spectral salinity indices represents under two multiple linear equations include SI2, S1, S3, S4, S5, and S6. The first multiple linear equation provides R^2 of 0.521 and shows positively correlation among S1, S3, S5, and S6 with EC data and gives negatively correlation among SI2 and S4 with EC data. The spectral salinity index that shows the highest positive influence on soil salinity is S1 with coefficient value of 1.531523. Likewise, second multiple linear equation provides R^2 of 0.521 and shows positively correlation among S1, S3, S5, and S6 with EC data and gives negatively correlation between SI2 and EC data. The spectral salinity index that shows the highest positive influence on soil salinity is also S1 with coefficient value of 1.618453.

Distribution of EC data that derives from 3 candidate equations of linear regression analysis for an optimum EC estimation model identification is presented in Figures 6.3 to 6.5.

Table 6.5 List of candidate equations of simple and multiple linear regression analysis.

Linear regression	**Equation**	R^2
Simple	Y =-1.894 + 0.043 * S5	0.502
Multiple No. 1	Y = -5.270 - 0.000008*SI2 + 1.531523*S1 + 0.047627*S3 - 0.002451*S4 + 0.043484*S5 + 0.013310*S6	0.521
Multiple No. 2	Y = -5.412 - 0.000008*SI2 + 1.618453*S1 + 0.047424*S3 + 0.042294*S5 + 0.013517*S6	0.521

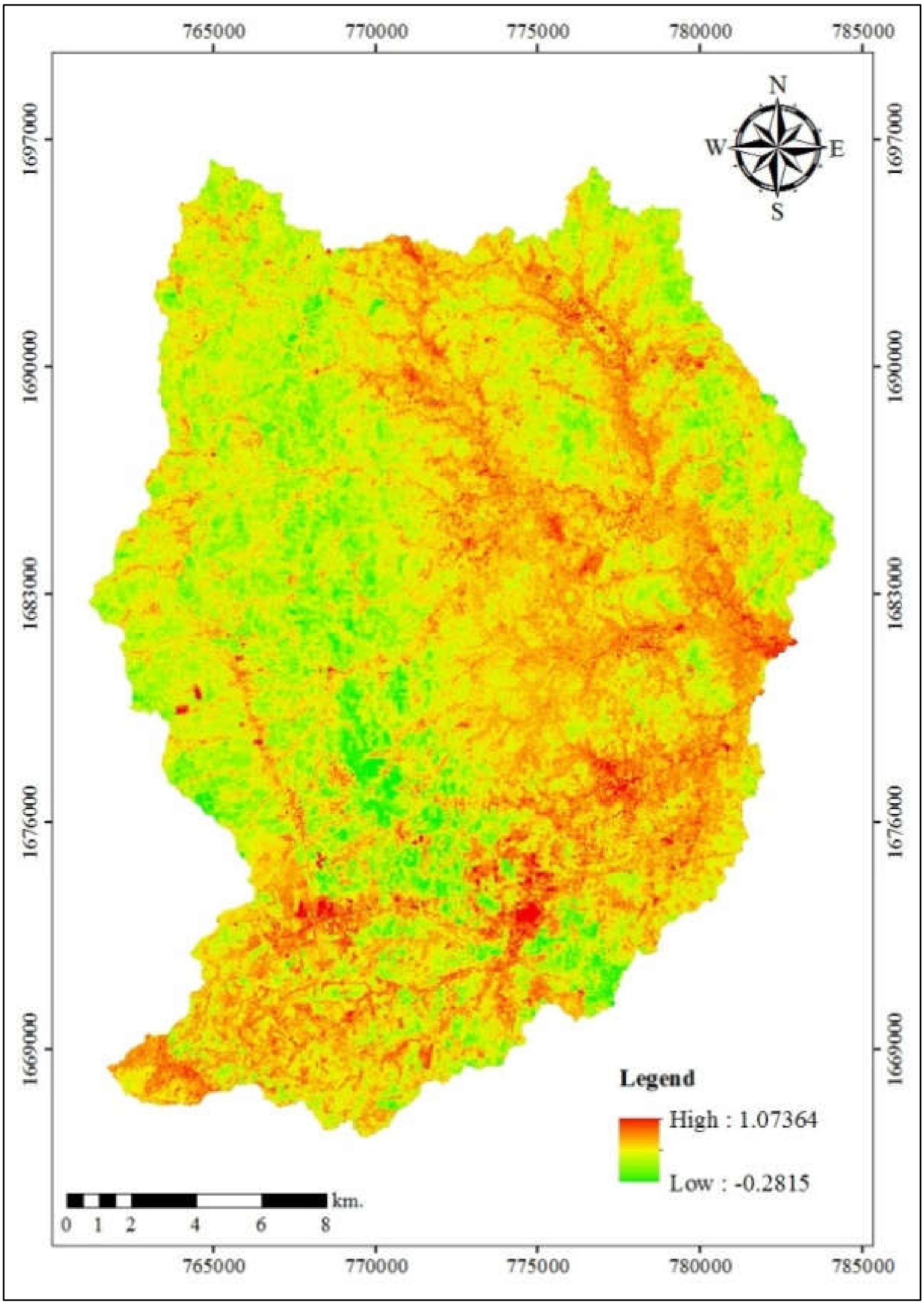

Figure 6.3 Distribution of EC data deriving from simple linear equation.

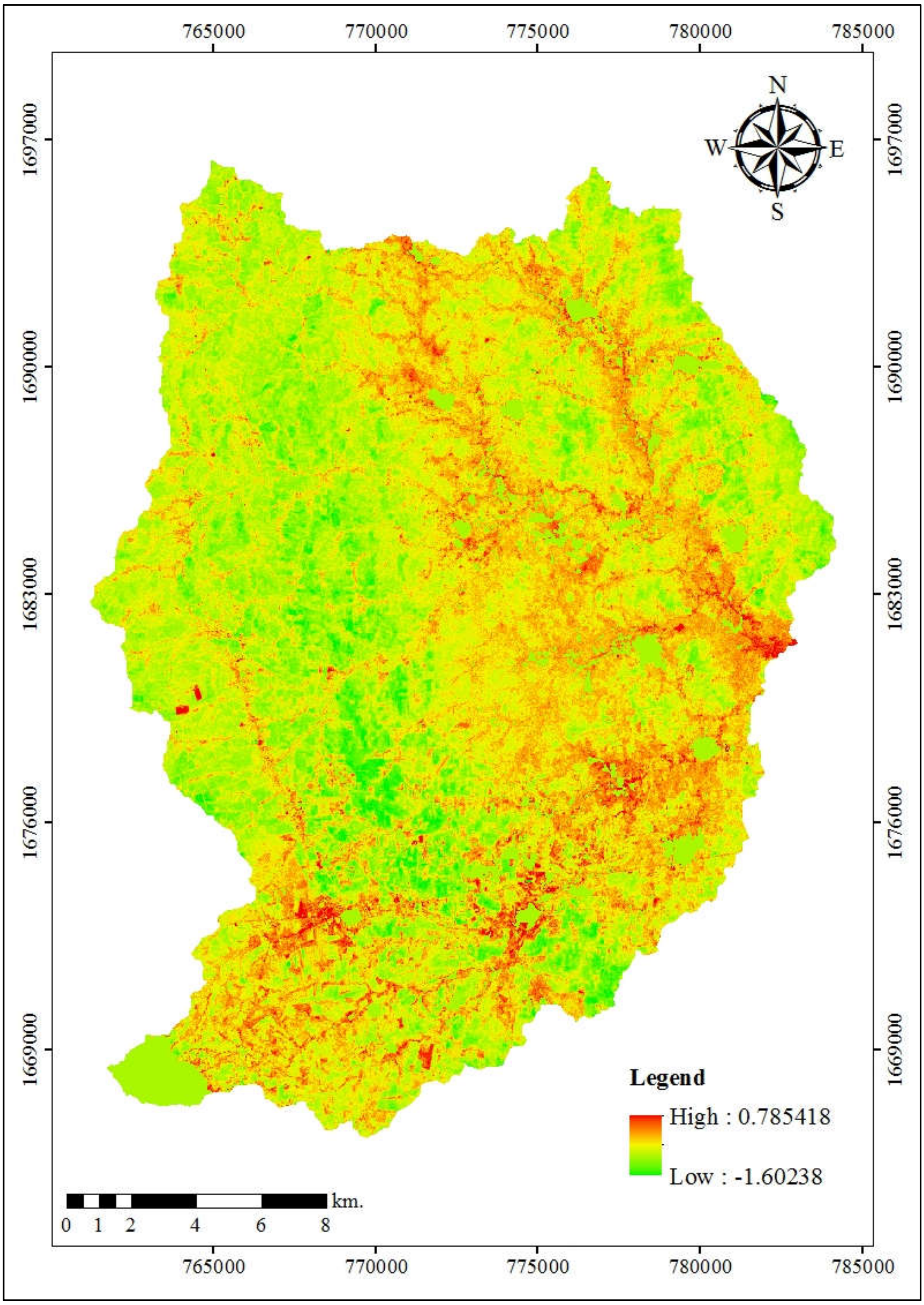

Figure 6.4 Distribution of EC data deriving from multiple linear equation Model 1.

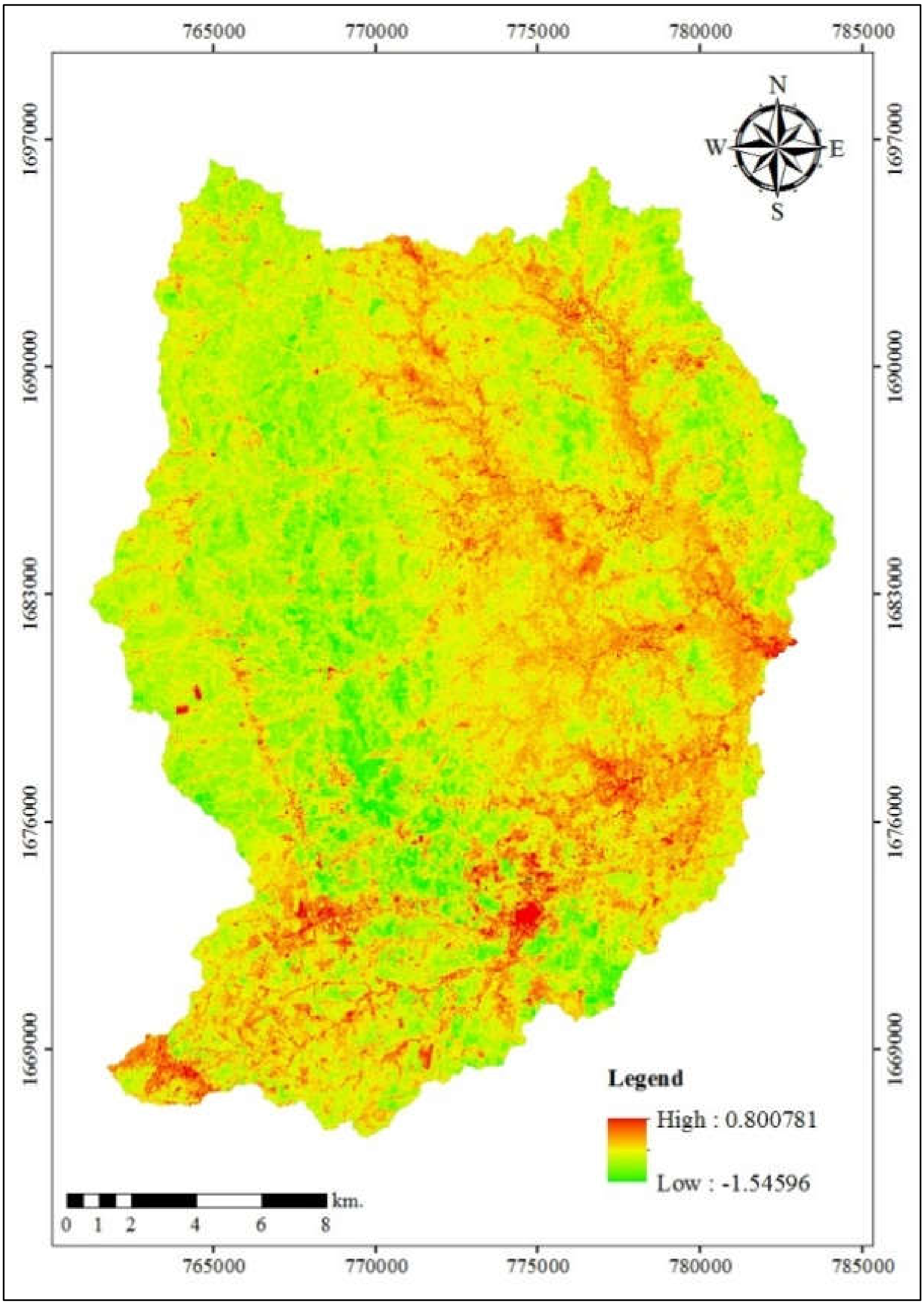

Figure 6.5 Distribution of EC data deriving from multiple linear equation Model 2.

6.3.2 Non-linear regression analysis of EC estimation model development

Similar to linear regression analysis, equations of non-linear regression analysis that provide R^2 equal or greater than 0.5 were here chosen as candidate equations for identifying an optimum EC estimation model with non-linear regression analysis.

All equations of non-linear regression analysis between of modelling EC samples and spectral salinity indices that provide R^2 equal or greater than 0.5 is presented in Table 6.6. It was found that only one spectral salinity index, S5 provides positively correlation with EC data with R^2 of 0.611 and 0.612 under non-linear regression analysis with quadratic and cubic models, respectively. Distribution of EC map that derives from 2 candidate equations of non-linear regression analysis for an optimum EC estimation model development is presented in Figures 6.6 to 6.7.

Table 6.6 List of candidate equations of non-linear regression analysis.

Non-linear regression	Equation	R^2
Quadratic model	Y = 22.576 + (-1.015 * S5) + (0.011 * S5 **2)	0.611
Cubic model	Y = 6.960 + (-0.011 * S5 **2) + (0.000 * S5 **3)	0.612

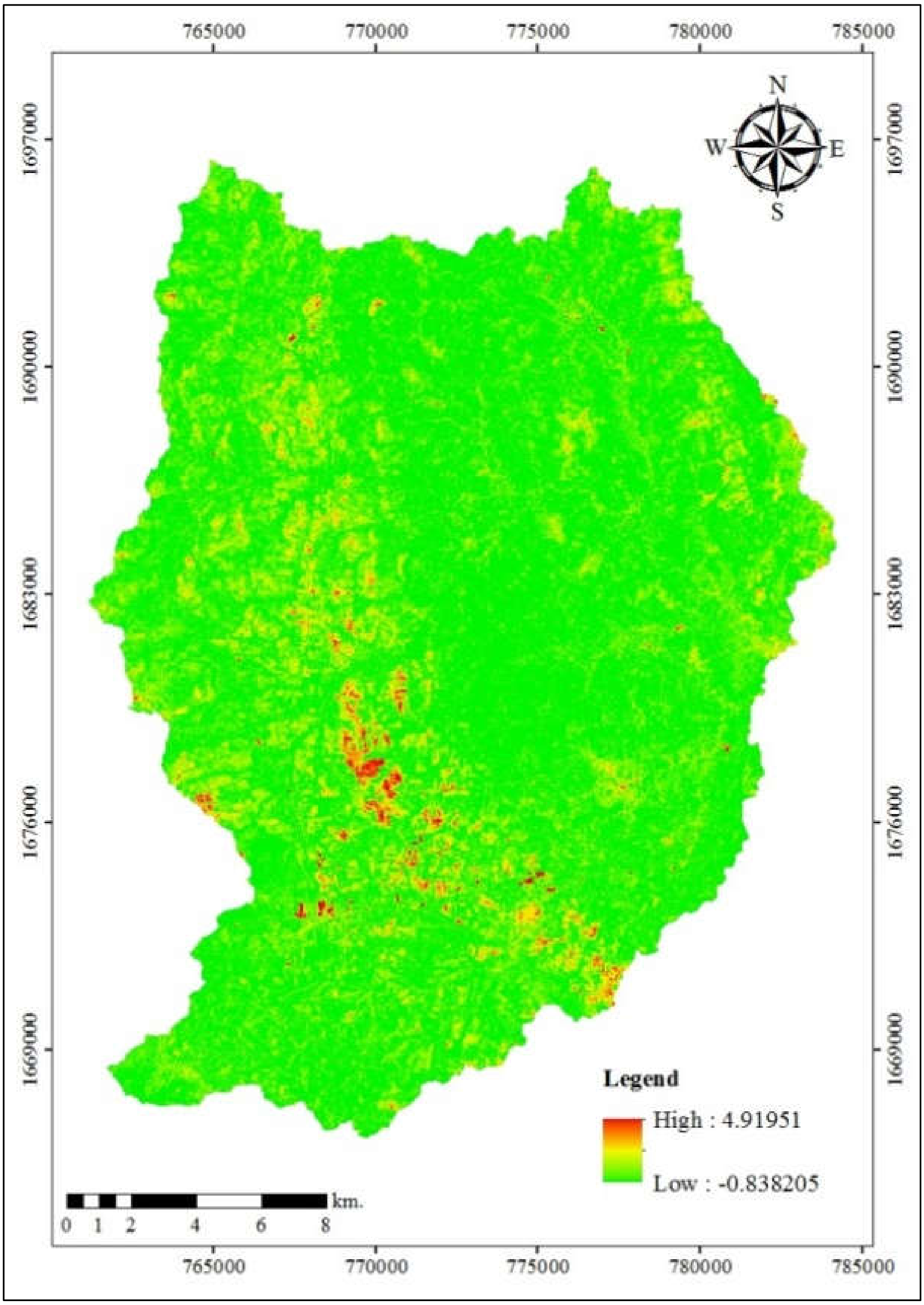

Figure 6.6 Distribution of EC data deriving from quadratic model.

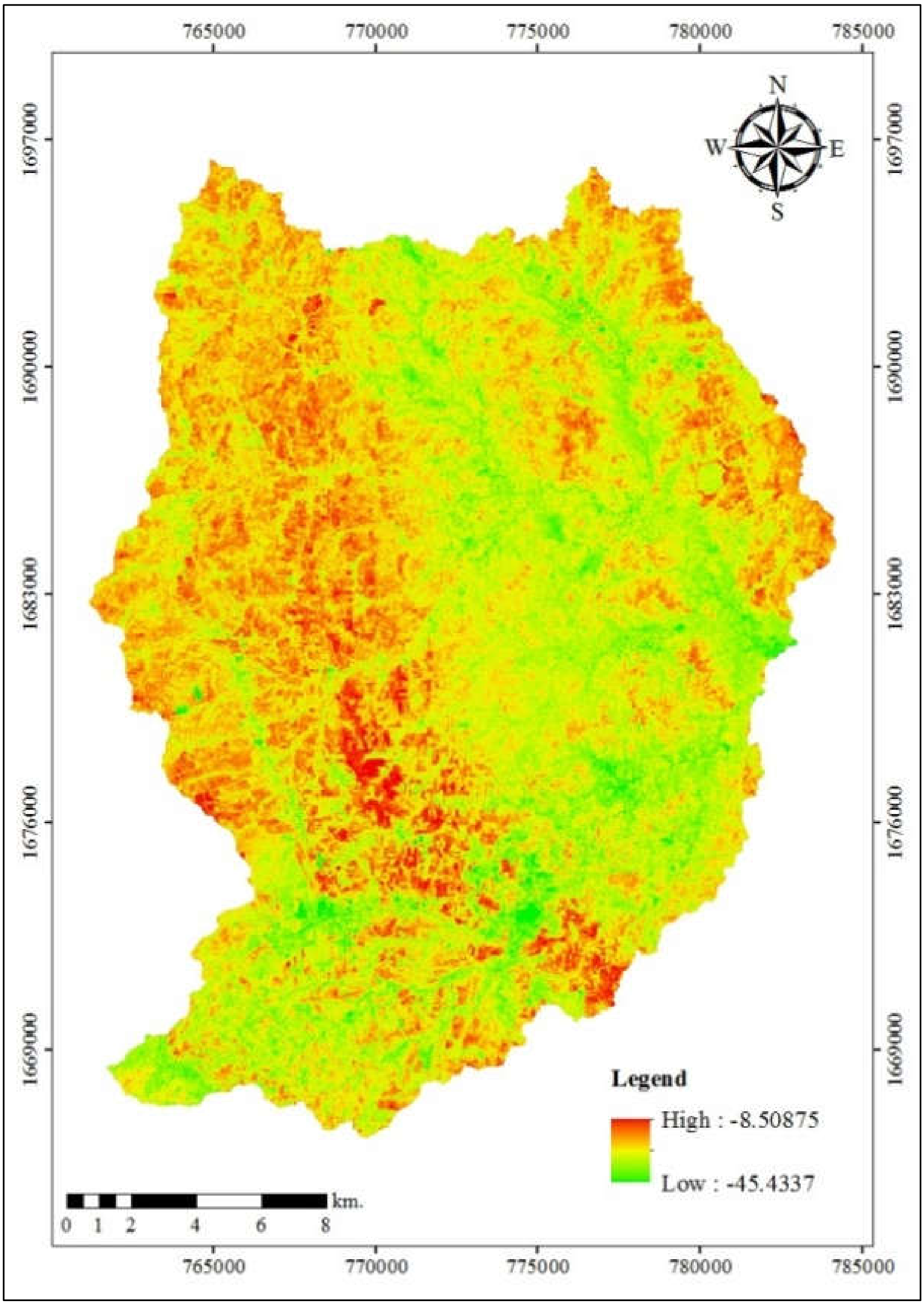

Figure 6.7 Distribution of EC data deriving from cubic model.

6.4 Optimum EC estimation model

According to accuracy assessment of EC data from candidate linear and non-linear models (see Figures 6.4 to 6.8) with the analyzed EC validation dataset using NRMSE, it was found that multiple linear equation of Model 1 provides the highest accuracy for EC estimation with NRMSE of 0.35235 as summary in Table 6.7. So, multiple linear equation of model 1 (Y = -5.270 - 0.000008*SI2 + 1.531523*S1 + 0.047627*S3 - 0.002451*S4 + 0.043484*S5 + 0.013310*S6) is here chosen as an optimum model for EC estimation in the study area as shown in Figure 6.4. The lowest EC value is -1.602 dS m^{-1} and the highest EC value is 0.785418 dS m^{-1} while an average EC value of the study area is 0.785 dS m^{-1}.

Table 6.7 Accuracy assessment of EC data from candidate equations of linear and non-linear regression analysis.

No.	Model	RMSE	NRMSE	Rank
1	Simple linear model	0.13927	0.36193	3
2	Multiple linear Model 1	0.13559	0.35235	1
3	Multiple linear Model 2	0.13802	0.35868	2
4	Quadratic model	0.86581	2.25003	4
5	Cubic model	16.35473	42.50190	5

In addition, the most suitable interpolation technique for EC estimation from EC validation dataset in the current study according to ME and RMSE is Simple kriging (SK) that provides the lowest ME and RMSE of 0.00154 and 0.0884, respectively as summary in Table 6.8. The distribution of the interpolated EC data from five selected techniques (IDW, TPS, SK, OK, and UK) is displayed in Figures 6.8 to 6.12, respectively.

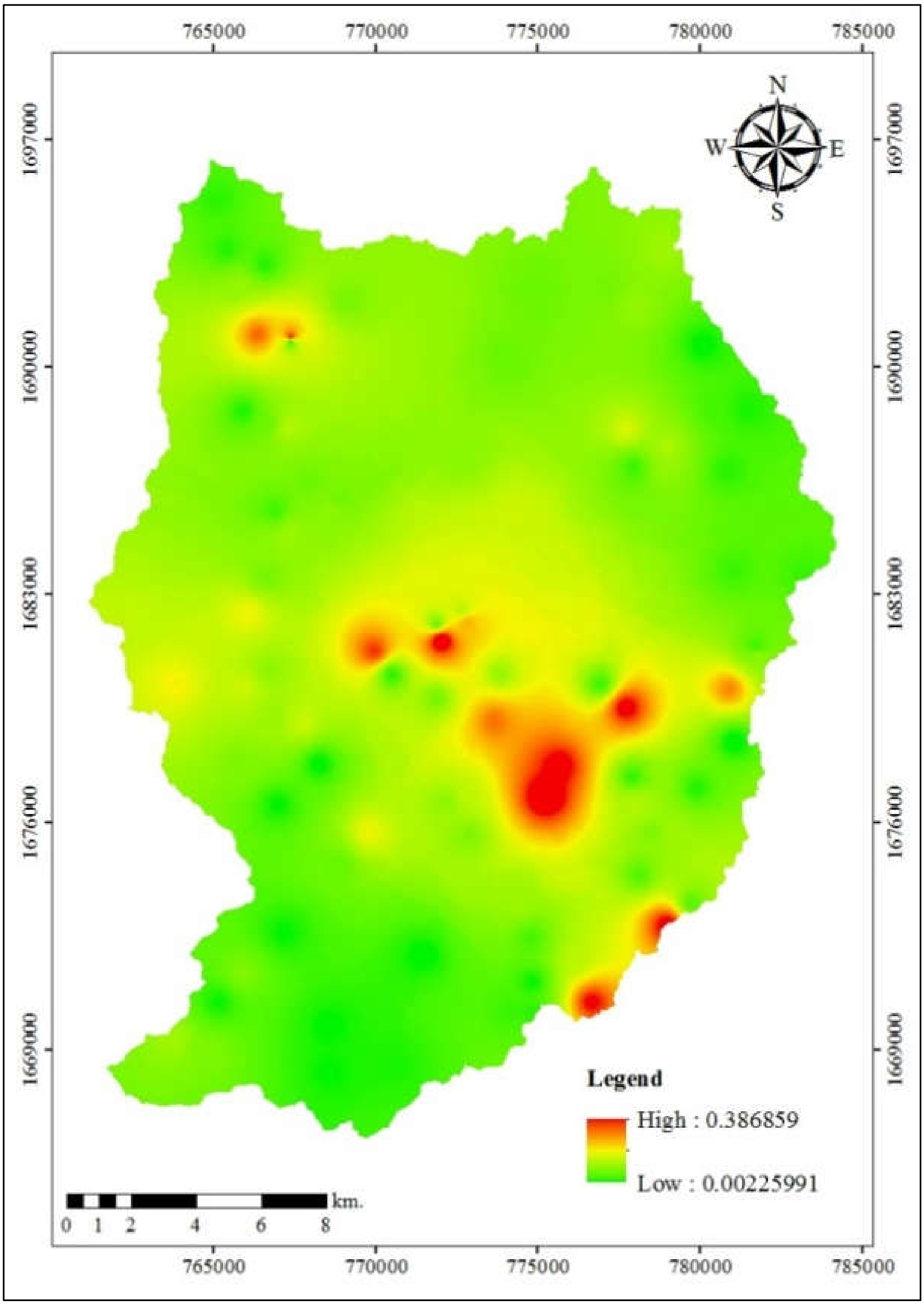

Figure 6.8 Distribution of EC data deriving from IDW technique.

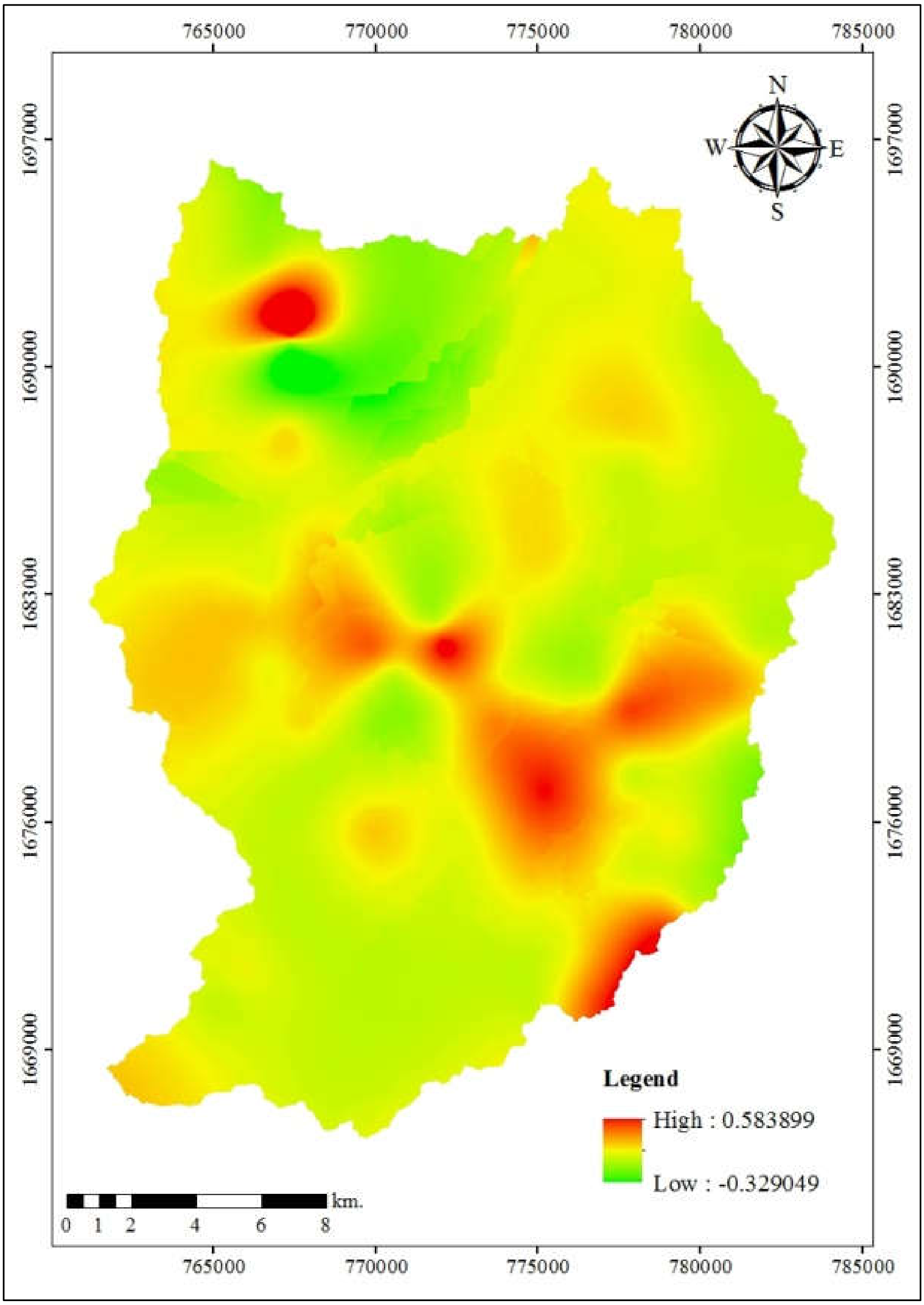

Figure 6.9 Distribution of EC data deriving from TPS technique.

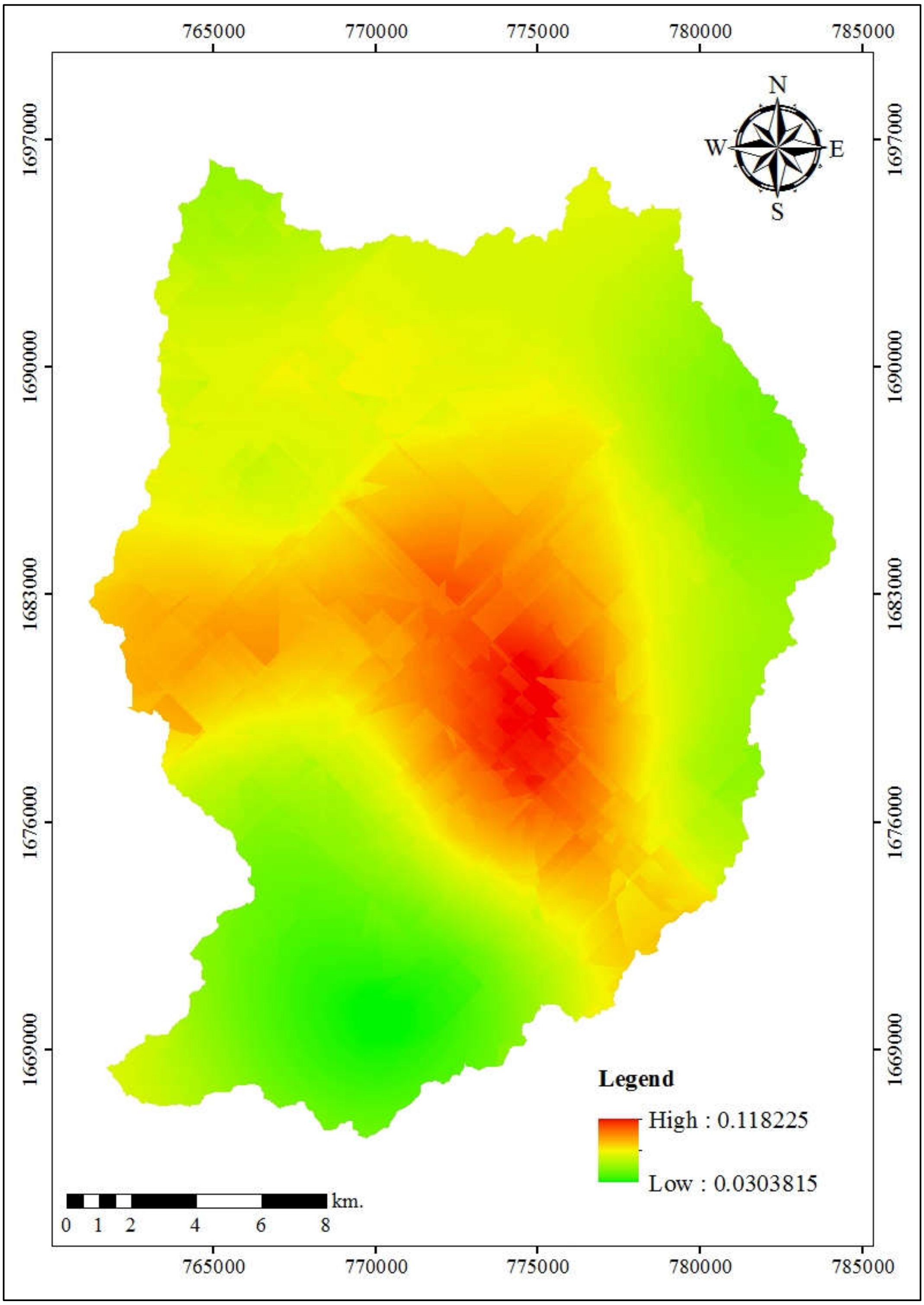

Figure 6.10 Distribution of EC data deriving from SK technique.

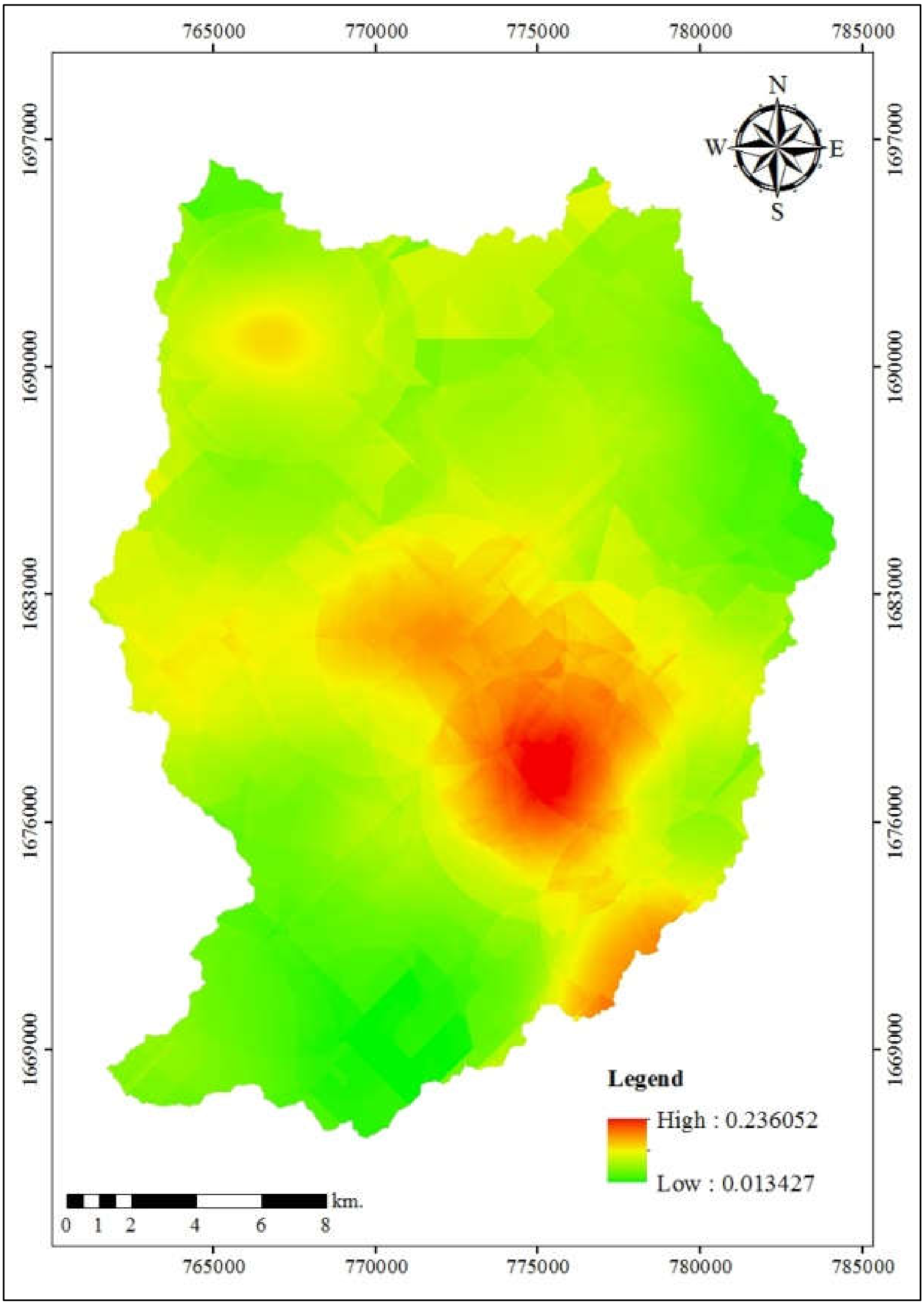

Figure 6.11 Distribution of EC data deriving from OK technique.

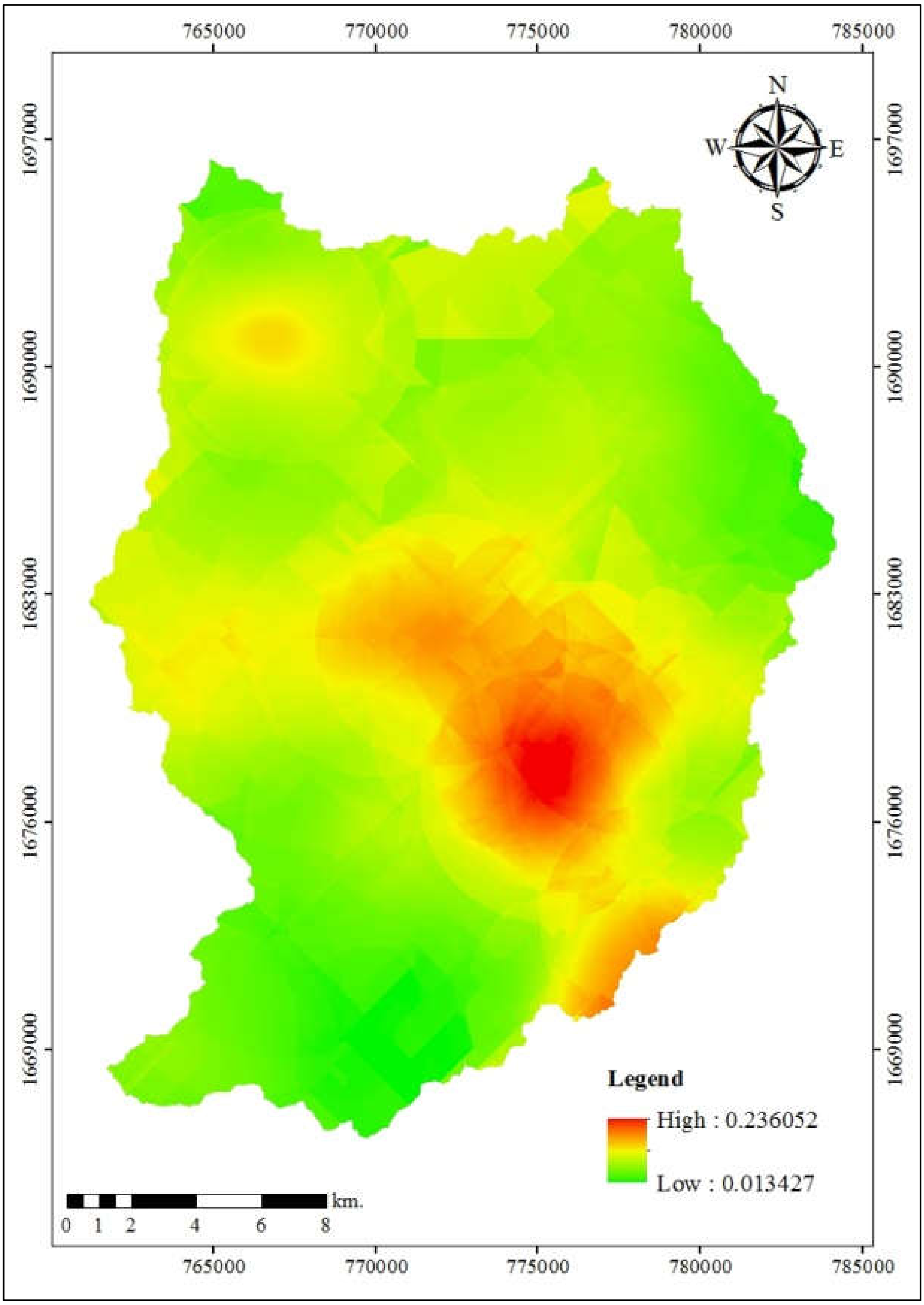

Figure 6.12 Distribution of EC data deriving from UK technique.

The interpolated EC data of SK technique is further examined correlation with the estimated EC maps of candidate linear and non-linear models (see Figures 6.3 to 6.7). It reveals that multiple linear equation of Model 1 provides the highest correlation with the interpolated EC data by SK technique with R of 0.762386 and R^2 of 0.5812324 as summary in Table 6.9. As a result, it can be confirmed that multiple linear equation of Model 1 is the optimum model for EC estimation in the study area. The ranking of correlation between the interpolated EC data with the constructed EC data of linear and non-linear equations (Table 6.9) are same as ranking of NRMSE as shown in Table 6.7.

Table 6.8 Accuracy assessment of five interpolation technique for EC estimation.

No.	Interpolation technique	ME	RMSE	Rank
1	IDW	0.00186	0.09869	4
2	TPS	0.00222	0.12007	5
3	SK	0.00154	0.08843	1
4	OK	-0.00017	0.09035	2
5	UK	-0.00017	0.09035	2

Table 6.9 Correlation coefficient and coefficient of determination between the interpolated EC data by SK technique and the estimated EC data of candidate linear and non-linear models.

No.	Model	R	R^2	Rank
1	Simple linear model	0.69528	0.48342	3
2	Multiple linear Model 1	0.76238	0.58123	1
3	Multiple linear Model 2	0.76218	0.58093	2
4	Quadratic model	0.22437	0.05034	4
5	Cubic model	0.76027	0.57801	5

6.5 Soil salinity assessment and its severity

The optimum EC estimation model from multiple linear equation of Model 1 was applied to assess soil salinity data with soil texture as shown in Figure 6.4. The derived result is further reclassified its severity as suggestion by Patterson (2006) as result shown in Figure 6.13 while area and percentage of soil salinity severity classification is summarized in Table 6.10.

As result, the dominant soil salinity severity class in the study area is very low and it covers area of 415.55 sq. km or about 89.374% of the total study area which had total soluble salts varies between 0 - 0.03%. This finding implies that effect of soil salinity in Upper Lamchiengkrai watershed is very low.

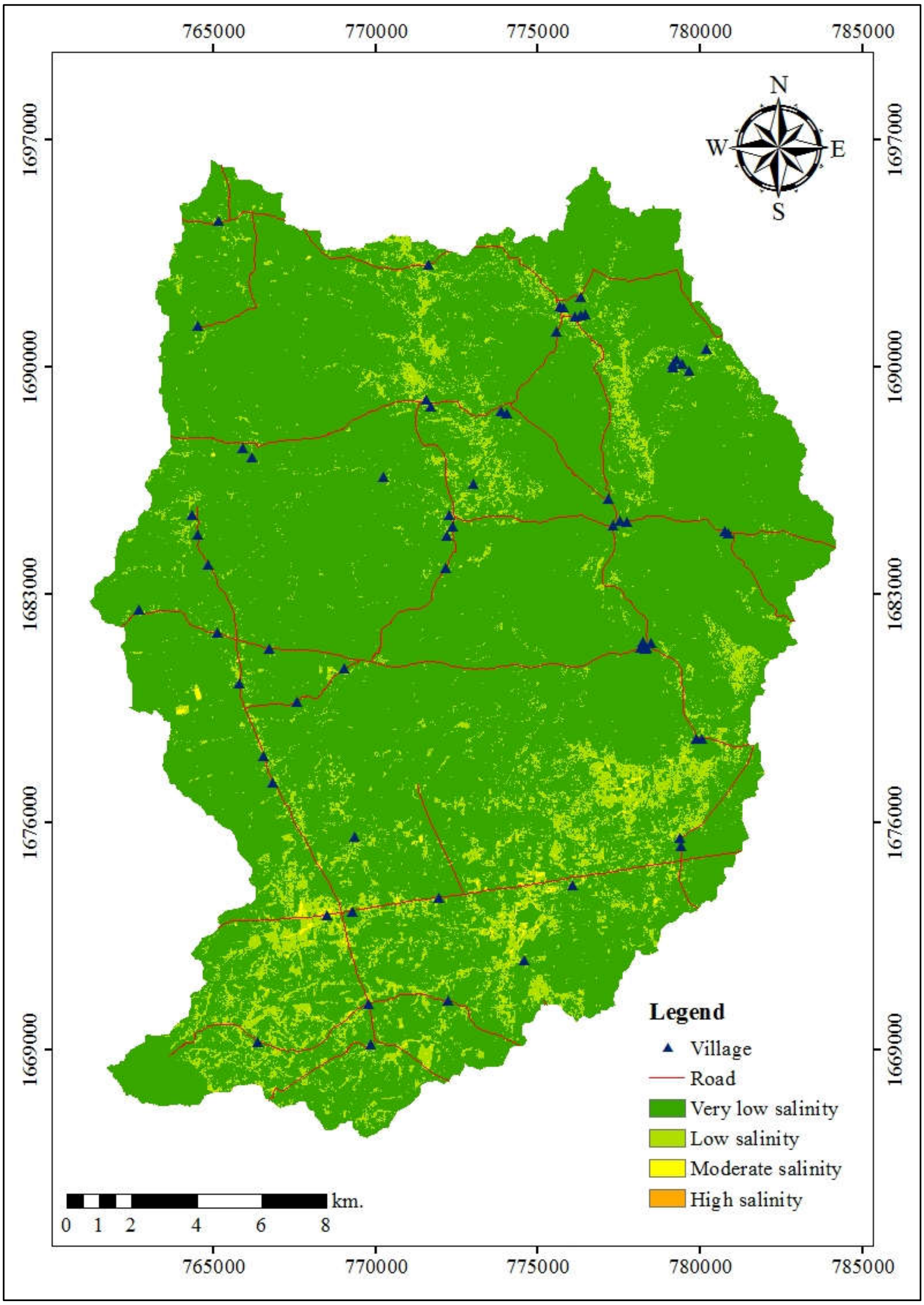

Figure 6.13 Distribution of soil salinity severity classes in the study area.

Table 6.10 Severity class of soil salinity.

No.	Level of EC	Soil salinity severity class	EC of 1:5 soil/water extract (dS m $^{-1}$)					Area in sq. km	Area in %	Total soluble salts (TSS) in g/100 g or %
			sand	loam	sandy clay loam	light clay	heavy clay			
1	Very low	Non-saline	<0.15	<0.17	<0.25	<0.30	<0.40	415.55	89.374	0 - 0.03
2	Low	Slightly saline	0.16 - 0.30	0.18-0.35	0.26-0.45	0.31-0.60	0.41-0.80	47.34	10.181	0.01 - 0.03
3	Moderate	Saline	0.31 - 0.60	0.36-0.75	0.46-0.90	0.61-1.15	0.81-1.60	2.06	0.443	0.02 - 0.04
4	High	Very saline	0.61-1.20	0.76-1.50	0.91-1.75	1.16-2.30	1.61-3.20	0.01	0.002	0.04 - 0.05
			Total					**464.96**	**100.00**	

In addition, according to overlay analysis between soil salinity severity classification and LULC data (Table 6.11), top three dominant crops in very low soil salinity class are cassava, maize, and paddy field. Meanwhile, low, moderate and high salinity classes are mostly found in cassava and they cover area of 47.34, 2.06, and 0.01 sq. km or 10.181%, 0.443%, and 0.002% of the study area, respectively.

Table 6.11 Soil salinity severity classification and LULC classes.

Land use and land cover classes	Soil salinity severity class							
	Very Low		Low		Moderate		High	
	Sq.km.	%	Sq.km.	%	Sq.km.	%	Sq.km.	%
Urban and built-up area	4.96	1.067	1.56	0.336	0.12	0.026	0.00	0.000
Paddy field	19.39	4.170	1.85	0.397	0.01	0.003	0.00	0.000
Maize	27.60	5.936	3.94	0.848	0.02	0.003	0.00	0.000
Sugarcane	6.63	1.426	0.14	0.030	0.00	0.000	0.00	0.000
Cassava	297.27	63.935	24.20	5.205	1.06	0.227	0.01	0.002
Perennial tree and orchard	14.29	3.074	5.47	1.176	0.08	0.018	0.00	0.000
Dense deciduous forest	4.05	0.870	0.06	0.013	0.00	0.001	0.00	0.000
Disturbed deciduous forest	8.29	1.784	0.75	0.161	0.00	0.000	0.00	0.000
Forest plantation	6.46	1.389	5.34	1.149	0.15	0.033	0.00	0.000
Water body	1.59	0.342	2.97	0.639	0.52	0.112	0.00	0.000
Scrub	0.89	0.191	0.25	0.053	0.03	0.007	0.00	0.000
Miscellaneous land	24.12	5.188	0.81	0.175	0.06	0.013	0.00	0.000
Total	**415.55**	**89.374**	**47.34**	**10.181**	**2.06**	**0.443**	**0.01**	**0.002**

CHAPTER VII

SOIL ORGANIC MATTER ASSESSMENT AND ITS DEPLETION

Main results of the fourth objective on assessment of soil organic matter and its depletion in 2015 with optimum spectral data and biophysical factors are here separately reported include (1) OM samples collection and analysis, (2) independent variables on OM data, (3) soil organic matter model development, (4) optimum soil organic matter estimation model, and (5) soil organic matter assessment and its depletion. Details of each result are separately described and discussed in following sections.

7.1 OM samples collection and analysis

OM samples of modeling and validation datasets that were collected in field in 2016 according of the combination between soil series and LULC data (see Figure 3.6) and analyzed in SUT laboratory is presented in Tables 7.1 and 7.2, respectively. The distribution of OM samples of modelling and validation datasets is displayed in Figure 7.1 while the basic statistic of both OM sample datasets is summarized in Table 7.3. The analyzed OM modelling dataset was here applied as dependent dataset for linear and non-linear regression analysis while the analyzed OM validation dataset was applied for accuracy assessment.

Table 7.1 OM samples data of modeling dataset.

ID	X	Y	Class	LULC	Soil series	OM (%)
ID1	772888	1675601	828	5	124	0.500
ID104	770998	1673921	828	5	124	0.930
ID105	764998	1668941	823	5	119	1.480
ID106	776848	1684091	801	5	97	0.480
ID107	783208	1683611	839	5	135	1.170
ID108	778558	1688501	801	5	97	1.660
ID109	767188	1672601	823	5	119	0.440
ID113	770098	1680851	811	5	107	1.480
ID115	774358	1684211	709	5	5	0.640
ID116	778138	1674401	478	3	126	0.800
ID119	776668	1673291	830	5	126	1.005
ID120	765838	1677791	2027	12	91	1.140
ID121	771028	1687781	719	5	15	0.050
ID125	780118	1686521	1329	8	97	2.100
ID127	775888	1678391	473	3	121	0.880
ID128	771418	1670381	799	5	95	0.908
ID13	769828	1668611	2095	12	159	0.250
ID132	774988	1679171	483	3	131	1.020
ID134	764758	1681901	805	5	101	0.583
ID135	772828	1682141	827	5	123	0.900
ID136	771388	1689341	452	3	100	0.130
ID137	780808	1681211	312	2	136	1.208
ID141	778978	1672841	487	3	135	0.220
ID143	772678	1687181	475	3	123	0.470
ID145	771928	1673531	652	4	124	1.180
ID146	768838	1674671	1004	6	124	1.260
ID147	778918	1688141	271	2	95	0.840
ID151	770338	1682771	1333	8	101	1.440
ID152	778738	1686011	835	5	131	2.100
ID153	763648	1690211	979	6	99	0.860
ID154	763648	1691621	2035	12	99	0.290

Table 7.1 (Continue).

ID	X	Y	Class	LULC	Soil series	OM (%)
ID157	776668	1670471	654	4	126	1.100
ID159	765148	1695161	2065	12	129	0.990
ID161	766888	1692881	1164	7	108	0.960
ID162	767488	1681991	1157	7	101	0.960
ID163	767968	1686461	833	5	129	1.100
ID167	767338	1688171	812	5	108	1.120
ID169	774268	1671851	1261	8	29	1.300
ID17	779878	1677041	733	5	29	0.820
ID170	778438	1672361	1191	7	135	0.490
ID171	768448	1693271	2044	12	108	2.080
ID175	765808	1695701	988	6	108	1.190
ID177	777988	1691861	1071	7	15	0.990
ID179	767398	1690781	800	5	96	0.350
ID180	766408	1691021	1175	7	119	0.570
ID181	777688	1672301	1182	7	126	0.400
ID182	766858	1684721	690	1	162	0.440
ID183	772768	1680641	436	3	84	0.500
ID184	775258	1676801	1367	8	135	0.620
ID185	781438	1688711	1155	7	99	0.810
ID187	766648	1683551	2037	12	101	1.840
ID188	772048	1681601	476	3	124	1.310
ID189	766078	1687421	610	4	82	0.900
ID19	766018	1693151	812	5	108	1.650
ID191	778528	1675631	1338	8	106	0.540
ID194	763768	1669361	2077	12	141	0.540
ID195	776968	1672781	1358	8	126	1.490
ID198	777568	1687871	191	2	15	1.180
ID199	779608	1676351	282	2	106	1.300
ID200	782008	1688351	1151	7	95	0.340
ID203	766558	1678901	1323	8	91	0.320
ID207	775738	1680161	297	2	121	0.570

Table 7.1 (Continue).

ID	X	Y	Class	LULC	Soil series	OM (%)
ID21	776938	1690931	449	3	97	0.620
ID211	767728	1679051	619	4	91	0.800
ID212	771448	1669361	975	6	95	0.250
ID215	769708	1687331	628	4	100	0.170
ID22	781798	1681091	840	5	136	1.800
ID221	780178	1687991	447	3	95	0.680
ID222	769888	1688381	1247	8	15	0.800
ID223	765328	1695491	1009	6	129	0.700
ID224	764908	1668041	1021	6	141	1.060
ID228	767398	1690931	2032	12	96	0.290
ID230	764998	1667711	1901	11	141	0.080
ID231	767458	1685831	1361	8	129	0.770
ID25	774028	1680041	788	5	84	0.450
ID26	766588	1693181	812	5	108	0.420
ID27	778408	1693091	801	5	97	0.990
ID28	770968	1685561	1179	7	123	1.004
ID29	781768	1686401	2031	12	95	0.990
ID30	768268	1677791	1356	8	124	0.710
ID32	771508	1670501	1327	8	95	1.210
ID33	767908	1680521	828	5	124	0.680
ID34	775228	1678511	839	5	135	0.550
ID36	776518	1691021	367	3	15	1.240
ID42	775318	1684121	801	5	97	0.900
ID45	779038	1680701	258	2	82	1.490
ID46	780088	1690691	786	5	82	0.840
ID47	779668	1685291	181	2	5	1.240
ID48	766168	1683131	805	5	101	1.140
ID50	778228	1690391	801	5	97	0.520
ID52	764068	1680191	795	5	91	0.740
ID54	768058	1670261	2018	12	82	0.290
ID55	766708	1680701	805	5	101	1.580

Table 7.1 (Continue).

ID	X	Y	Class	LULC	Soil series	OM (%)
ID57	764758	1676801	2095	12	159	0.480
ID58	779428	1679861	786	5	82	1.810
ID59	767428	1684931	805	5	101	1.240
ID6	775498	1679231	357	3	5	0.600
ID61	773818	1685261	804	5	100	1.002
ID64	770518	1680551	709	5	5	1.170
ID65	763858	1680251	2026	12	90	1.200
ID66	771898	1682111	709	5	5	1.180
ID67	772948	1670951	799	5	95	0.800
ID68	766318	1670441	1039	6	159	1.380
ID69	776098	1678181	381	3	29	0.600
ID70	770668	1668491	872	5	168	1.100
ID72	767128	1670351	863	5	159	0.550
ID75	778858	1693601	792	5	88	0.340
ID76	776938	1680251	273	2	97	0.720
ID79	767248	1687031	814	5	110	0.130
ID81	779518	1678511	786	5	82	1.680
ID82	778618	1674611	733	5	29	1.270
ID83	768568	1669751	823	5	119	0.320
ID84	770248	1678391	828	5	124	0.290
ID85	782218	1684091	311	2	135	0.270
ID86	778258	1677851	801	5	97	0.890
ID88	765418	1693631	803	5	99	0.130
ID9	769618	1684151	825	5	121	0.940
ID92	780418	1688291	799	5	95	0.880
ID93	777928	1677401	839	5	135	0.200
ID97	769108	1692071	823	5	119	0.710

Table 7.2 OM samples data of validation dataset.

ID	X	Y	Class	LULC	Soil series	OM (%)
ID10	766468	1690571	812	5	108	1.010
ID100	773218	1681331	827	5	123	0.920
ID101	777718	1679531	801	5	97	1.330
ID102	771898	1679831	828	5	124	1.170
ID103	774418	1673471	828	5	124	0.450
ID11	777898	1678721	801	5	97	0.960
ID110	766558	1681751	805	5	101	0.880
ID112	780898	1680101	312	2	136	1.330
ID114	768628	1675421	1004	6	124	0.690
ID117	765628	1677431	795	5	91	0.710
ID118	778048	1676351	733	5	29	2.000
ID12	771718	1684061	434	3	82	1.200
ID122	774898	1692341	367	3	15	0.240
ID123	772198	1676651	827	5	123	0.240
ID124	777838	1684841	840	5	136	2.050
ID129	774868	1670141	623	4	95	0.220
ID130	777658	1686641	827	5	123	2.080
ID131	765178	1670471	962	6	82	1.180
ID133	774148	1670171	799	5	95	1.280
ID138	774838	1671101	1327	8	95	1.500
ID14	768418	1691081	812	5	108	1.109
ID140	772648	1682531	357	3	5	1.200
ID144	769828	1675691	652	4	124	0.880
ID149	766618	1691351	800	5	96	1.100
ID15	773938	1679231	1140	7	84	0.590
ID150	778918	1687001	835	5	131	1.250
ID155	781018	1683731	181	2	5	0.490
ID156	775678	1677731	1191	7	135	1.310
ID158	765178	1695671	833	5	129	1.230
ID16	780538	1688711	799	5	95	1.210
ID165	773668	1679111	1187	7	131	0.660

Table 7.2 (Continue).

ID	X	Y	Class	LULC	Soil series	OM (%)
ID166	767008	1676561	971	6	91	0.880
ID168	781048	1678481	271	2	95	0.540
ID172	764098	1685021	971	6	91	0.540
ID173	779098	1675571	1690	10	106	0.840
ID174	775048	1689521	1153	7	97	0.520
ID176	781738	1681421	1589	10	5	0.610
ID178	767308	1685801	1185	7	129	1.100
ID18	765958	1680131	1147	7	91	1.400
ID186	777748	1688081	191	2	15	1.100
ID193	772798	1676921	2060	12	124	0.650
ID196	767788	1679801	1180	7	124	0.490
ID197	771508	1671911	1351	8	119	1.120
ID2	768718	1692461	823	5	119	1.650
ID20	772528	1679711	828	5	124	0.870
ID201	769708	1680731	1237	8	5	1.220
ID202	778018	1676531	1613	10	29	0.680
ID205	779728	1673501	1719	10	135	0.670
ID208	780838	1686851	2033	12	97	1.120
ID213	772438	1684271	1061	7	5	0.670
ID214	771898	1676591	1355	8	123	0.540
ID216	765958	1688651	1340	8	108	0.860
ID217	776008	1677791	1085	7	29	1.190
ID220	766288	1691981	1328	8	96	2.100
ID226	766648	1684631	1042	6	162	1.120
ID227	774808	1672421	1710	10	126	1.330
ID229	766768	1691831	1152	7	96	0.570
ID23	771748	1681781	709	5	5	0.820
ID232	777088	1692491	1599	10	15	0.960
ID233	768328	1685711	1177	7	121	1.510
ID24	776158	1671821	830	5	126	1.260
ID3	783328	1683521	839	5	135	0.800

Table 7.2 (Continue).

ID	X	Y	Class	LULC	Soil series	OM (%)
ID31	769678	1680821	1339	8	107	1.100
ID37	774088	1690211	449	3	97	0.620
ID38	774148	1688021	786	5	82	0.840
ID39	770668	1671101	823	5	119	0.340
ID4	766888	1679261	795	5	91	0.490
ID40	764818	1692371	803	5	99	0.540
ID41	778798	1684211	273	2	97	0.840
ID43	769978	1681271	811	5	107	1.330
ID44	772108	1686101	475	3	123	1.330
ID49	765928	1671341	1039	6	159	0.750
ID5	769978	1666631	2104	12	168	1.340
ID51	776968	1679801	801	5	97	0.900
ID53	770158	1677551	828	5	124	0.860
ID56	769318	1692821	823	5	119	1.500
ID60	766678	1690091	812	5	108	2.200
ID62	774328	1685411	804	5	100	1.250
ID63	767848	1677101	1356	8	124	0.520
ID7	766858	1679351	795	5	91	0.920
ID71	769708	1692641	823	5	119	1.160
ID73	768868	1685921	825	5	121	0.500
ID74	773848	1680581	788	5	84	0.420
ID78	777988	1686941	719	5	15	0.100
ID8	770068	1693721	719	5	15	1.580
ID87	767188	1682981	805	5	101	0.240
ID89	770488	1672481	828	5	124	0.220
ID90	771568	1683371	786	5	82	0.690
ID94	768568	1668341	2095	12	159	0.700
ID95	777448	1674911	830	5	126	0.400
ID96	763168	1682231	2026	12	90	0.890
ID98	765808	1692521	1331	8	99	1.310
ID99	777658	1688831	719	5	15	0.170

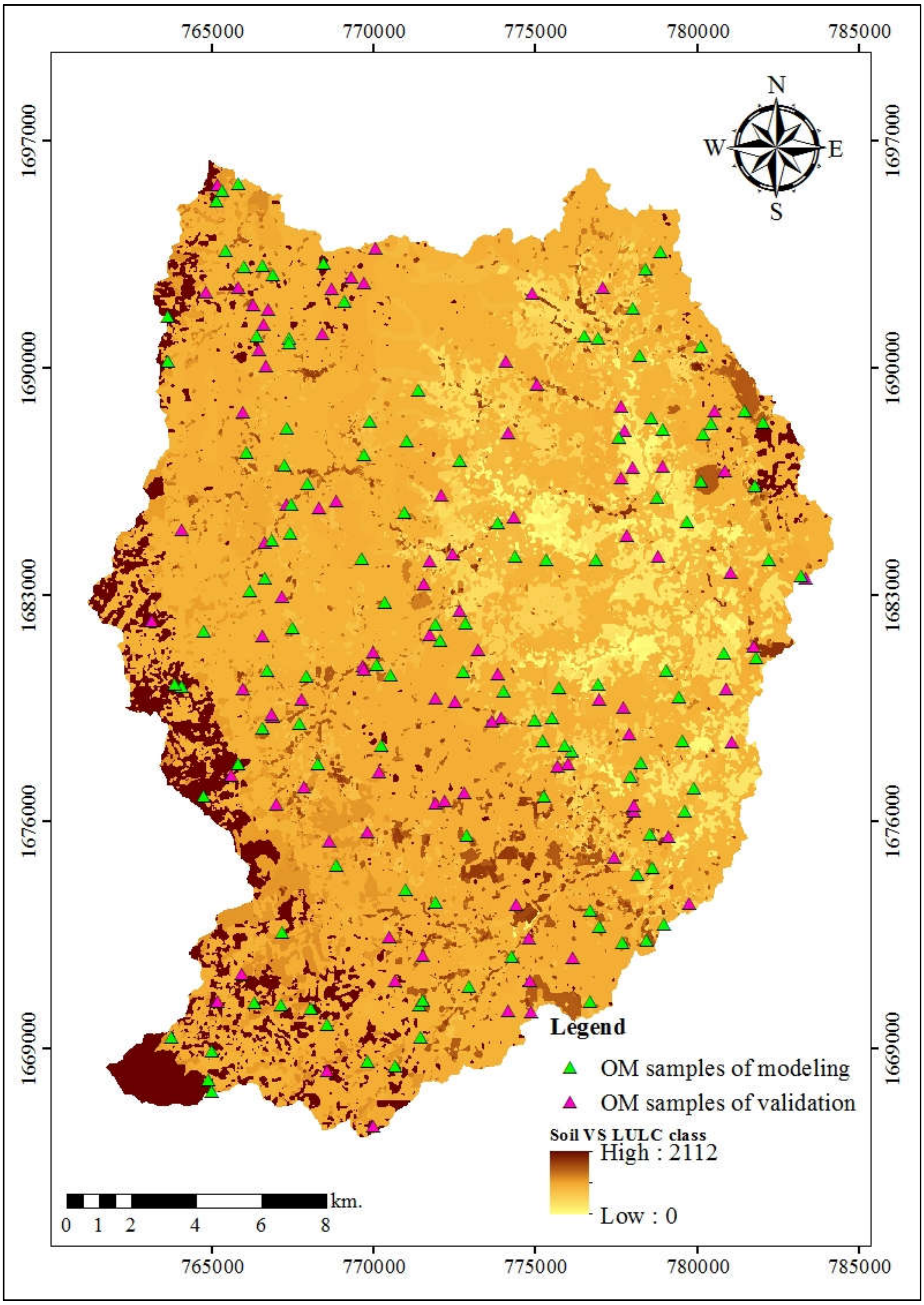

Figure 7.1 Distribution of modeling and validation datasets of OM sampling points for an optimum soil organic matter estimation model development.

Table 7.3 Basic statistics of OM samples dataset

OM Dataset	No of samples	Basic statistical value (%)				
		Minimum	Maximum	Mean	S.D.	Variance
Modelling	120	0.050	2.100	0.867	0.466	0.217
Validation	93	0.100	2.200	0.949	0.455	0.207

7.2 Independent variables on OM data

Spectral data and biophysical factors include brightness value of band 2-7 of Landsat data, soil color indices (Brightness Index (BI), Coloration Index (CI), Hue Index (HI), Redness Index (RI), and Saturation Index (SI)), NDVI, NDWI, slope and aspect as independent variables of soil organic matter were firstly extracted and calculated from Landsat data in 2015 and DEM. Herein soil color indices were extracted according equations in Table 2.4 under Chapter II. The distribution of these independent variables is presented in Figure 7.2 and basic statistics data of independent variables is summarized as shown in Table 7.4. These data were further applied to identify relationship with OM data using linear and non-linear regression analysis.

Table 7.4 Basic statistics of independent variable data for soil organic matter estimation model development.

Variable	No of pixels	Basic statistical value (%)				
		Minimum	Maximum	Mean	S.D.	Variance
Band 2	120	0	75.000	30.278	21.191	449.071
Band 3	120	0	82.000	28.842	20.230	409.246
Band 4	120	0	90.000	28.619	20.276	411.129
Band 5	120	0	114.000	41.756	29.616	877.082
Band 6	120	0	234.000	58.720	42.323	1791.276
Band 7	120	0	244.000	44.307	32.579	1061.396
BI	120	0	82.561	29.270	20.550	422.287
CI	120	-0.111	0.093	-0.004	0.023	0.001
HI	120	-15.000	19.000	0.728	2.213	4.898
RI	120	0	0.001	0	0	0
SI	120	-0.147	0.121	-0.020	0.033	0.001
NDVI	120	-0.154	0.507	0.186	0.054	0.003
NDWI	120	-0.443	0.190	-0.181	0.044	0.002
Slope	120	0	77.048	1.372	2.378	5.653
Aspect	120	-1.000	359.716	101.060	112.048	12554.686

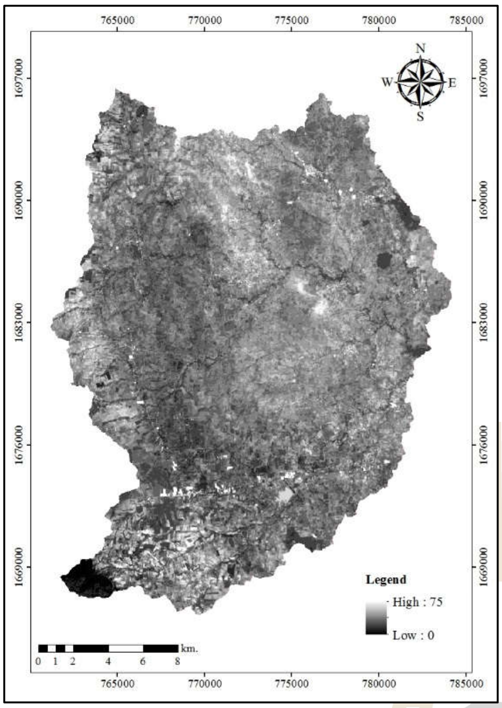

(a) Band 2

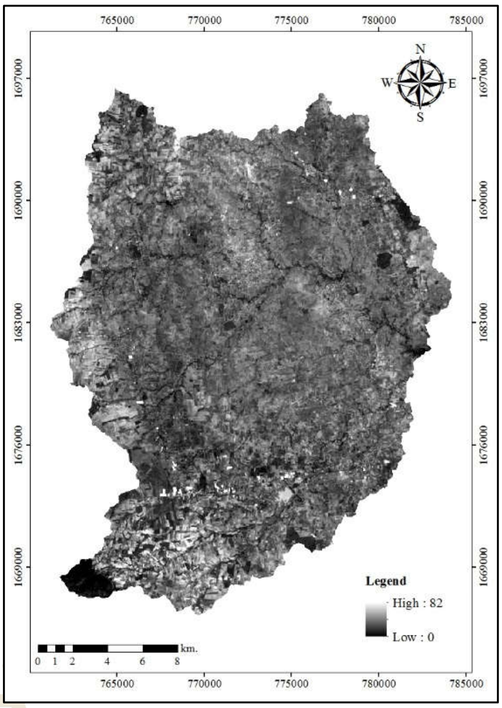

(b) Band 3

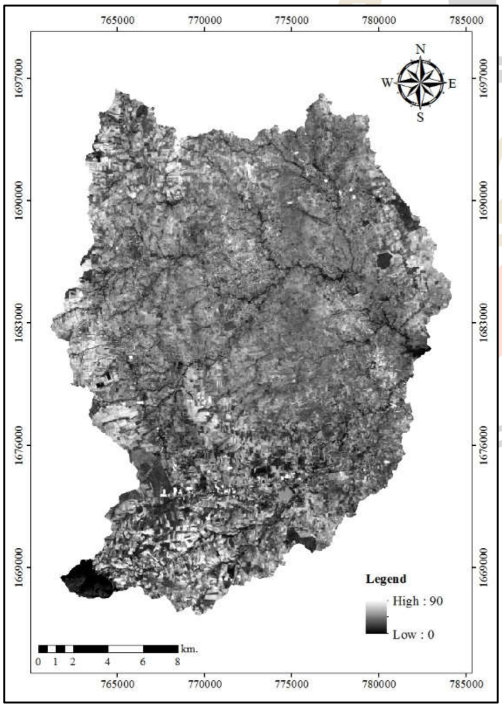

(c) Band 4

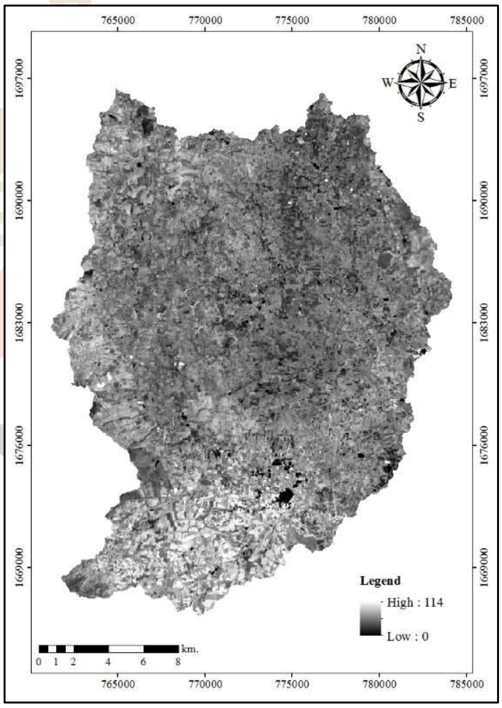

(d) Band 5

Figure 7.2 Distribution of these independent variables: (a) Band 2, (b) Band 3, (c) Band 4, (d) Band 5, (e) Band 6, (f) Band 7, (g) BI, (h) CI, (i) HI, (j) RI, (k) SI, (l) NDVI, (m) NDWI, (n) Slope, and (o) Aspect.

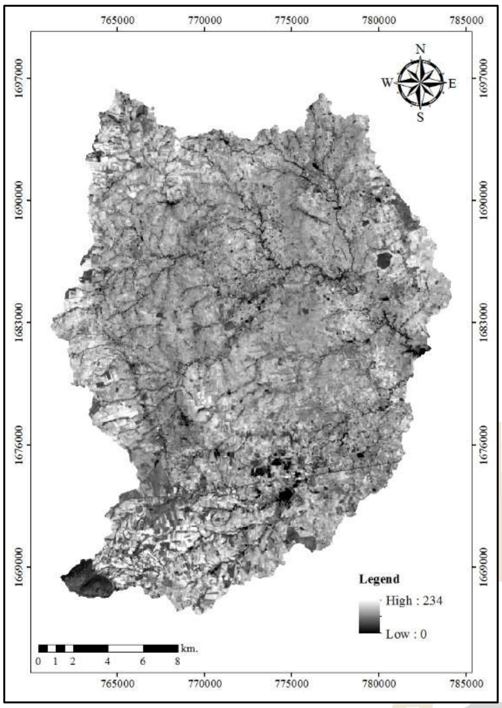

(e) Band 6

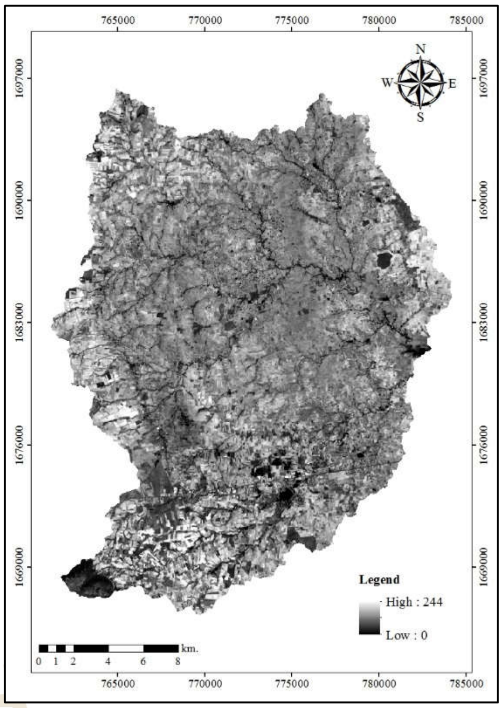

(f) Band 7

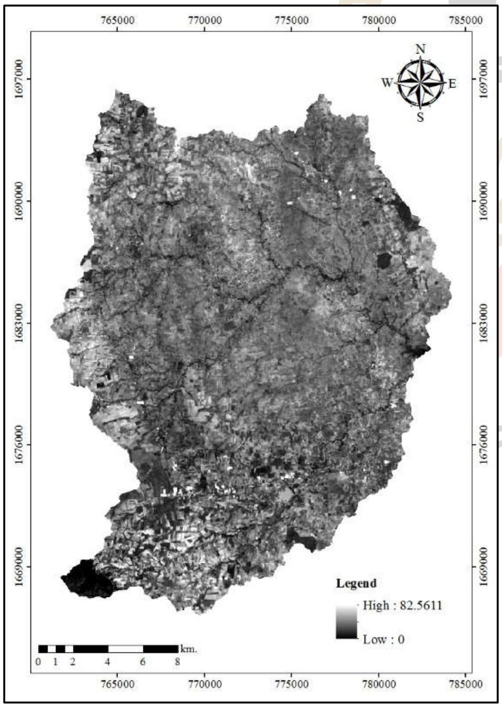

(g) BI

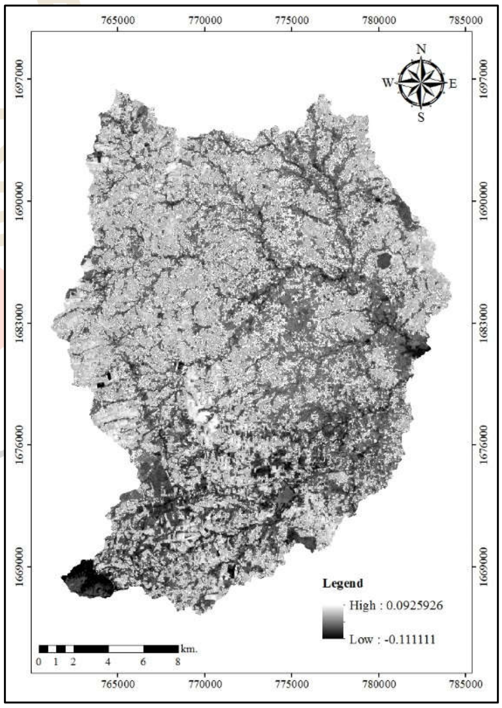

(h) CI

Figure 7.2 (Continued).

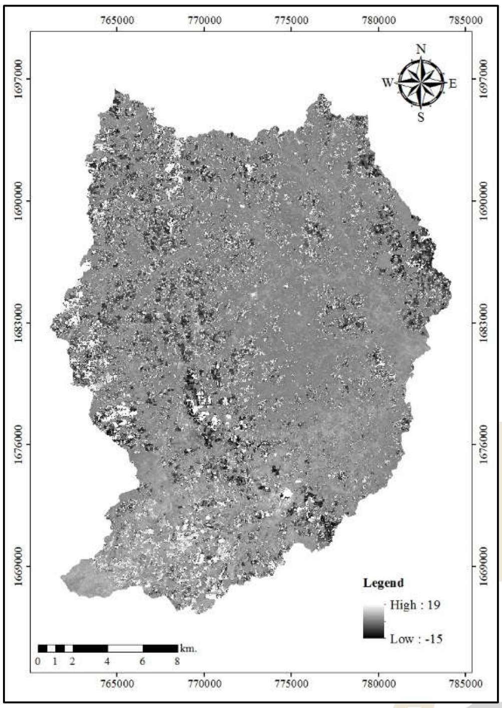

(i) HI

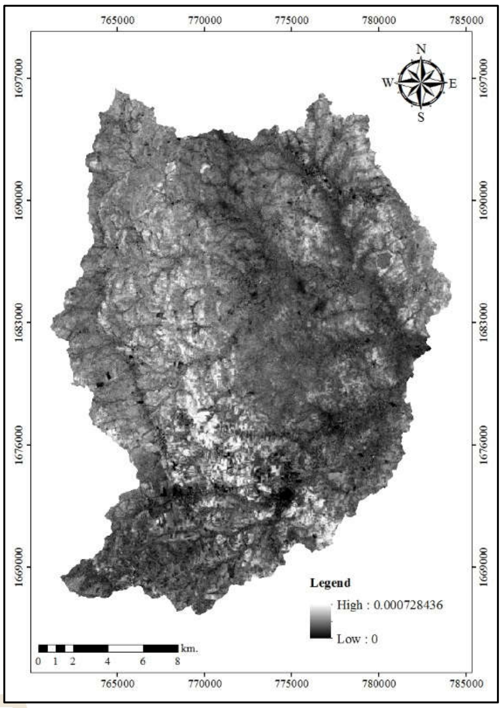

(j) RI

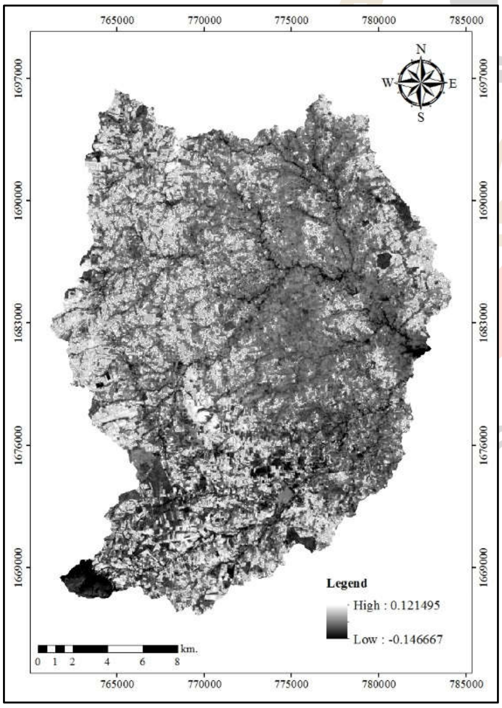

(k) SI

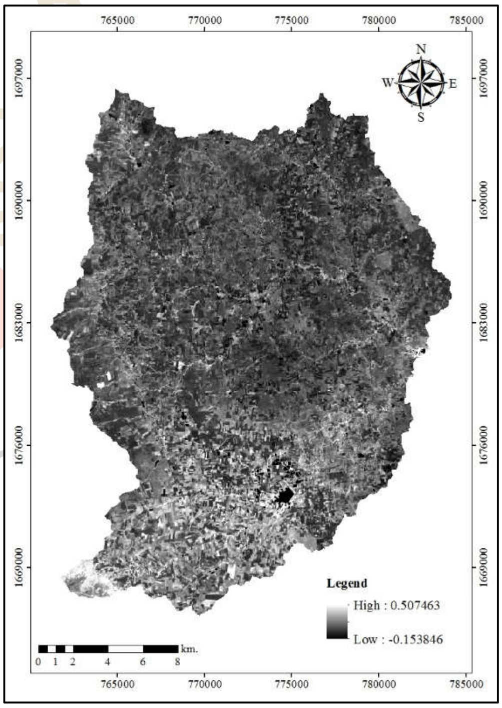

(l) NDVI

Figure 7.2 (Continued).

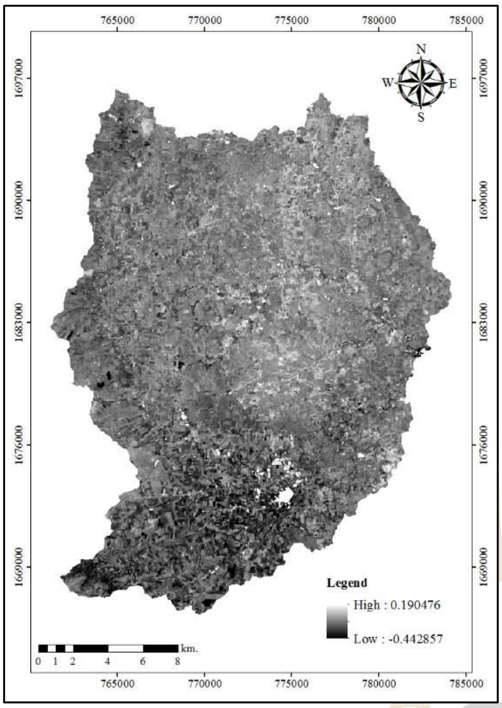

(m) NDWI

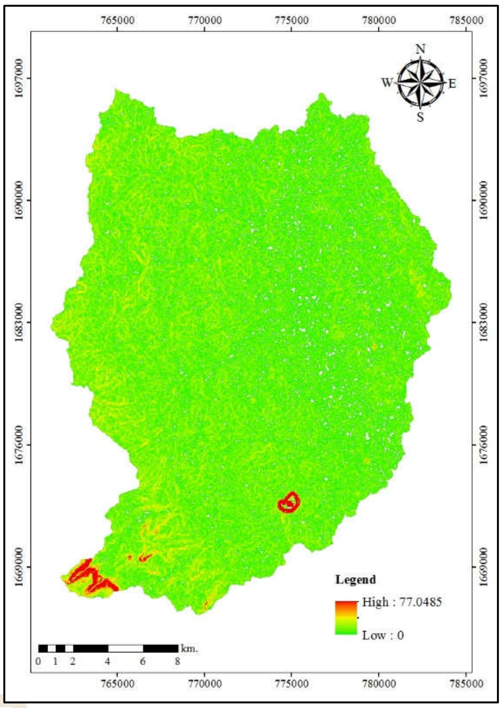

(n) Slope

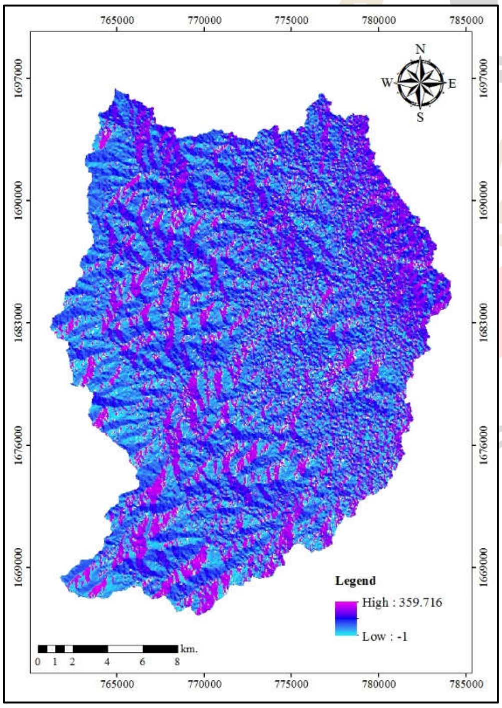

(o) Aspect

Figure 7.2 (Continued).

7.3 Soil organic matter estimation model development

Data input for linear regression analysis include dependent and independent variables as mentioned in Sections 7.1 and 7.2 were here applied to develop optimum soil organic matter estimation model using linear and non-linear regression analysis under SPSS statistical software. The derived equations from both analyses which provide the R^2 equal or greater than 0.5 was then chosen as candidate equations for identifying an optimum soil organic matter estimation model using accuracy assessment with NRMSE. In addition, spatial regression analysis between the derived candidate organic matter maps with the best interpolated soil salinity data from five surface interpolation techniques (IDW, TPS, SK, UK, and OK) was examined using R and R^2.

7.3.1 Linear regression analysis of soil organic matter estimation model development

Simple linear and multiple linear regression analysis were here analyzed to select candidate equations for identifying an optimum soil organic matter estimation model with non-linear regression analysis.

All equations of simple and multiple linear regression analysis between of modelling OM samples and spectral data and biophysical factors including brightness value of band 2-7 of Landsat data, soil color indices (Brightness Index: BI Coloration Index: CI, Hue Index: HI, Redness Index: RI, and Saturation Index: SI), NDVI, NDWI, slope that provide R^2 equal or greater than 0.5 is presented in Table 7.5. It was found that only one spectral data, brightness value of band 5 provides negatively correlation with OM data with R^2 of 0.553 under simple linear regression analysis. Meanwhile, combination of spectral data and biophysical factors under eight multiple linear equations include Band2, Band3, Band4, Band5, Band6, Band7, Slope, CI, RI, and SI.

The first multiple linear equation provides R^2 of 0.618 and shows positively correlation among Band3, Band6, CI, and RI with OM data and gives negatively correlation among Band2, Band4, Band5, Band7, Slope, and SI with OM data. The spectral data or biophysical factor that show the highest positive influence on soil organic matter is RI with coefficient value of 3,941.633. Likewise, second multiple linear equation provides R^2 of 0.617 and shows positively correlation among Band3, Band6, and CI with OM data and gives negatively correlation among Band2, Band4, Band5, Band7, Slope, and SI with OM data. The spectral data or biophysical factor that show the highest positive influence on soil organic matter is CI with coefficient value of 76.431.

The third multiple linear equation provides R^2 of 0.615 and shows positively correlation among Band3, Band6, and CI with OM data and gives negatively correlation among Band2, Band4, Band5, Slope, and SI with OM data. The spectral data or biophysical factor that show the highest positive influence on soil organic matter is CI with coefficient value of 73.963.

The fourth multiple linear equation provides R^2 of 0.611 and shows positively correlation among Band3, Band6, and CI with OM data and gives negatively correlation among Band2, Band4, Band5, and SI with OM data. The spectral data or biophysical factor that show the highest positive influence on soil organic matter is CI with coefficient value of 77.066.

The fifth multiple linear equation provides R^2 of 0.604 and shows positively correlation among Band3 and CI with OM data and gives negatively correlation among Band2, Band4, Band5, and SI with OM data. The spectral data or biophysical factor that show the highest positive influence on soil organic matter is CI with coefficient value of 81.990.

The sixth multiple linear equation provides R^2 of 0.595 and shows positively correlation among Band3 and CI with OM data and gives negatively correlation among Band4, Band5, and SI with OM data. The spectral data or biophysical factor that show the highest positive influence on soil organic matter is CI with coefficient value of 17.632.

The seventh multiple linear equation provides R^2 of 0.591 and shows positively correlation among Band3 and CI with OM data and gives negatively correlation among Band5 and SI with OM data. The spectral data or biophysical factor that show the highest positive influence on soil organic matter is CI with coefficient value of 10.614.

Finally, the eighth multiple linear equation provides R^2 of 0.571 and shows positively correlation between Band2 and OM data and brightness value of band 5 provides negatively correlation with OM data. The spectral data or biophysical factor that show the highest positive influence on soil organic matter is Band5 with coefficient value of 0.032.

Distribution of estimated soil organic matter data that derives from 9 candidate equations of linear regression analysis for an optimum soil organic matter estimation model identification is presented in Figures 7.3 to 7.11.

Table 7.5 List of candidate equations of simple and multiple linear regression analysis.

Linear regression	**Equation**	**R^2**
Simple	Y = 3.262 - 0.038 * Band5	0.553
Multiple No. 1	Y = -5.298 - 0.618 * Band2 + 0.890 * Band3 - 0.149 * Band4 -0.034 * Band5 + 0.014 * Band6 - 0.007 * Band7 - 0.010 * Slope + 71.046 * CI + 3941.633 * RI - 66.852 * SI	0.618
Multiple No. 2	Y = 0.933 - 0.655 * Band2 + 0.810 * Band3 - 0.127 * Band4 - 0.034 * Band5 + 0.013 * Band6 - 0.008 * Band7+ - 0.010 * Slope + 76.431 * CI - 65.738* SI	0.617
Multiple No. 3	Y = 1.058 - 0.607 * Band2 + 0.777 * Band3 - 0.147 * Band4 - 0.032 * Band5 + 0.008 * Band6 - 0.011 * Slope + 73.963 * CI - 61.988 * SI	0.615
Multiple No. 4	Y = 0.905 - 0.613 * Band2 + 0.814 * Band3 - 0.174 * Band4 -0.033 * Band5 + 0.007 * Band6 + 77.066 * CI - 62.835 * SI	0.611
Multiple No. 5	Y = 0.367 - 0.609* Band2 + 0.859 * Band3 - 0.201 * Band4 - 0.029 * Band5 + 81.990 * CI - 63.638 * SI	0.604
Multiple No. 6	Y = 1.279 + 0.123 * Band3 - 0.091 * Band4 - 0.032 * Band5 + 17.632 * CI - 8.779 * SI	0.595
Multiple No. 7	Y = 1.173+0.036 * Band3+ -0.033 * Band5+ 10.614 * CI + -9.463* SI	0.591
Multiple No. 8	Y = 2.026 - 0.041 * Band5 + 0.032 * Band2	0.571

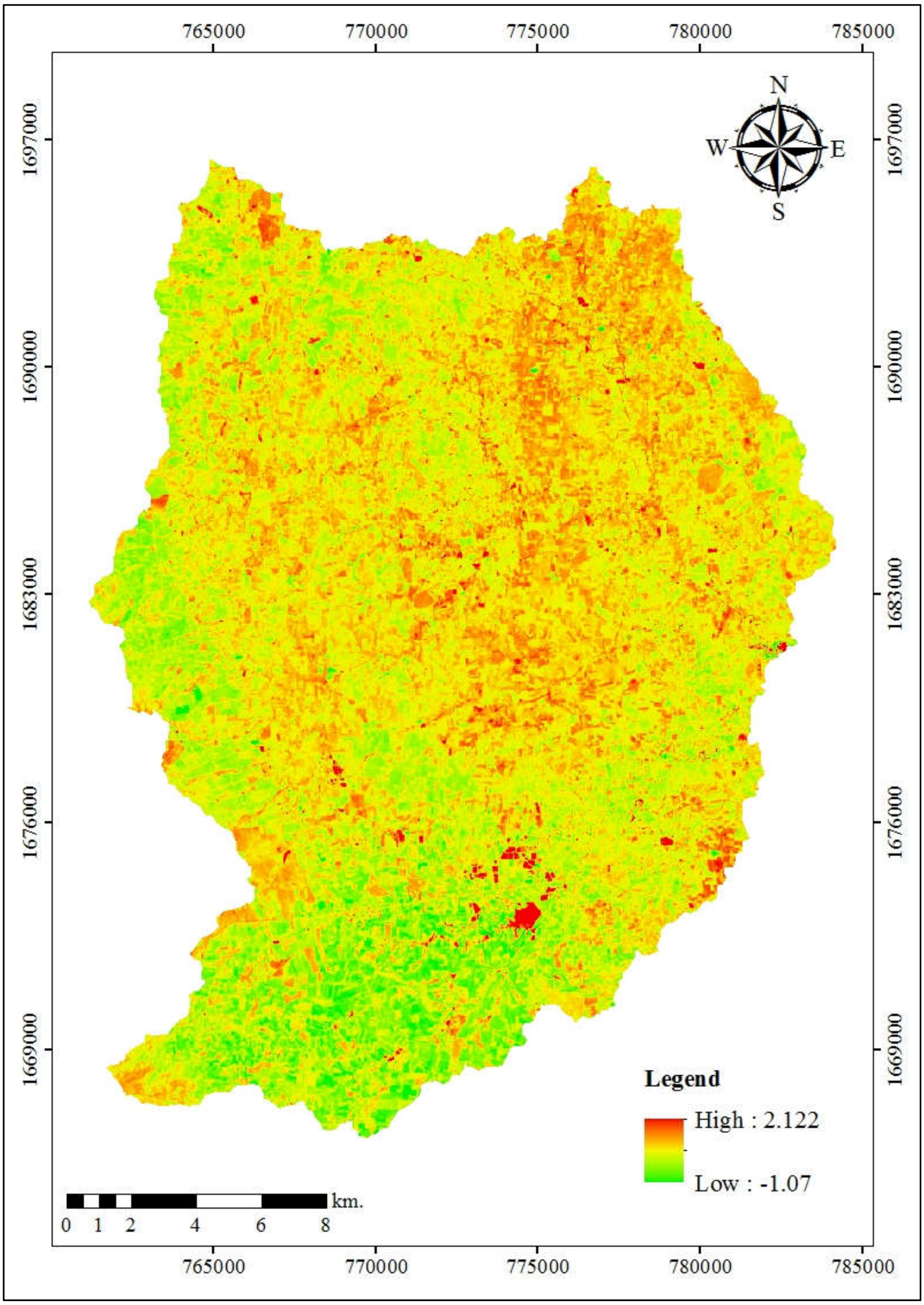

Figure 7.3 Distribution of estimated soil organic matter data deriving from simple linear equation.

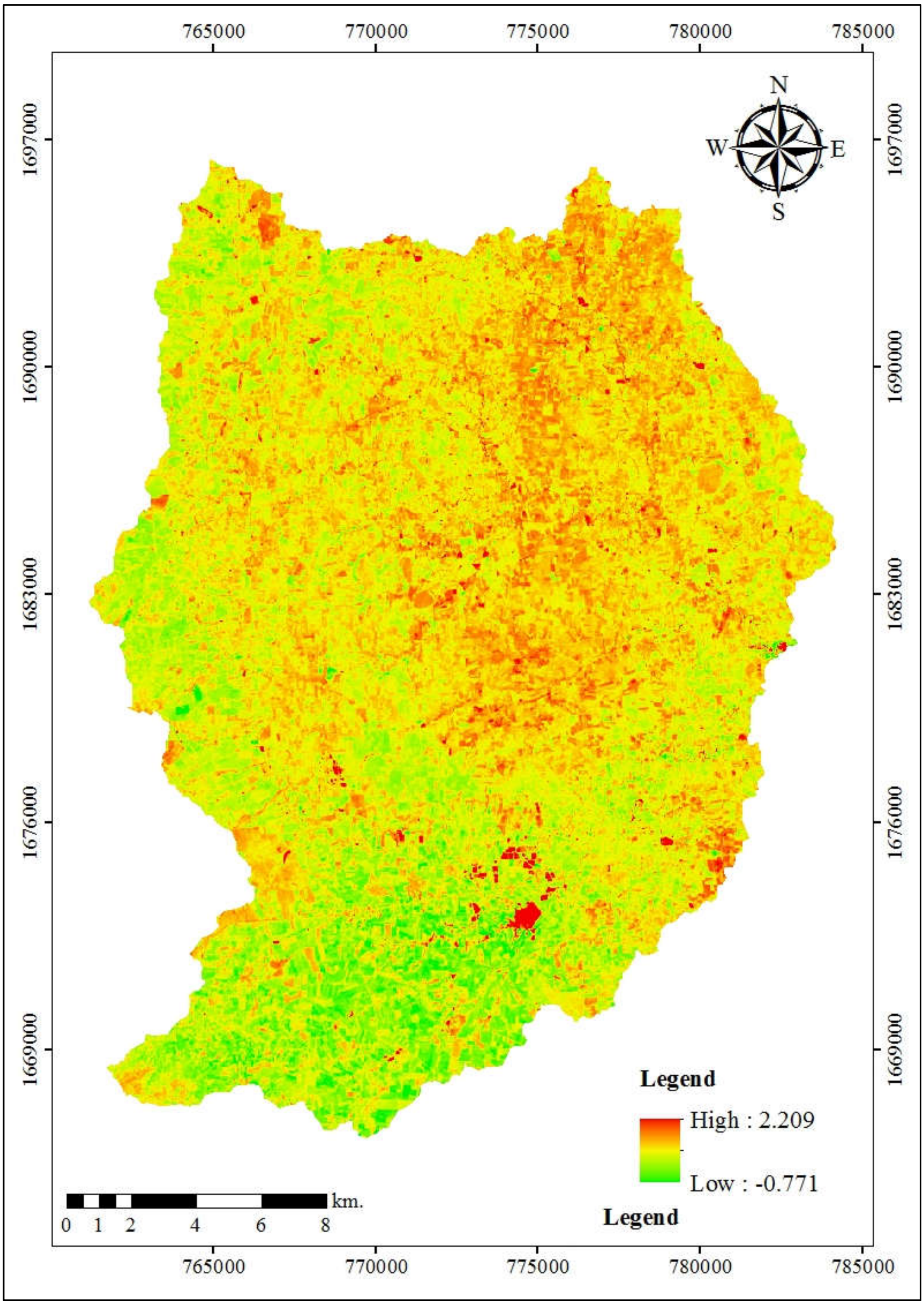

Figure 7.4 Distribution of estimated soil organic matter data deriving from multiple linear equation Model 1.

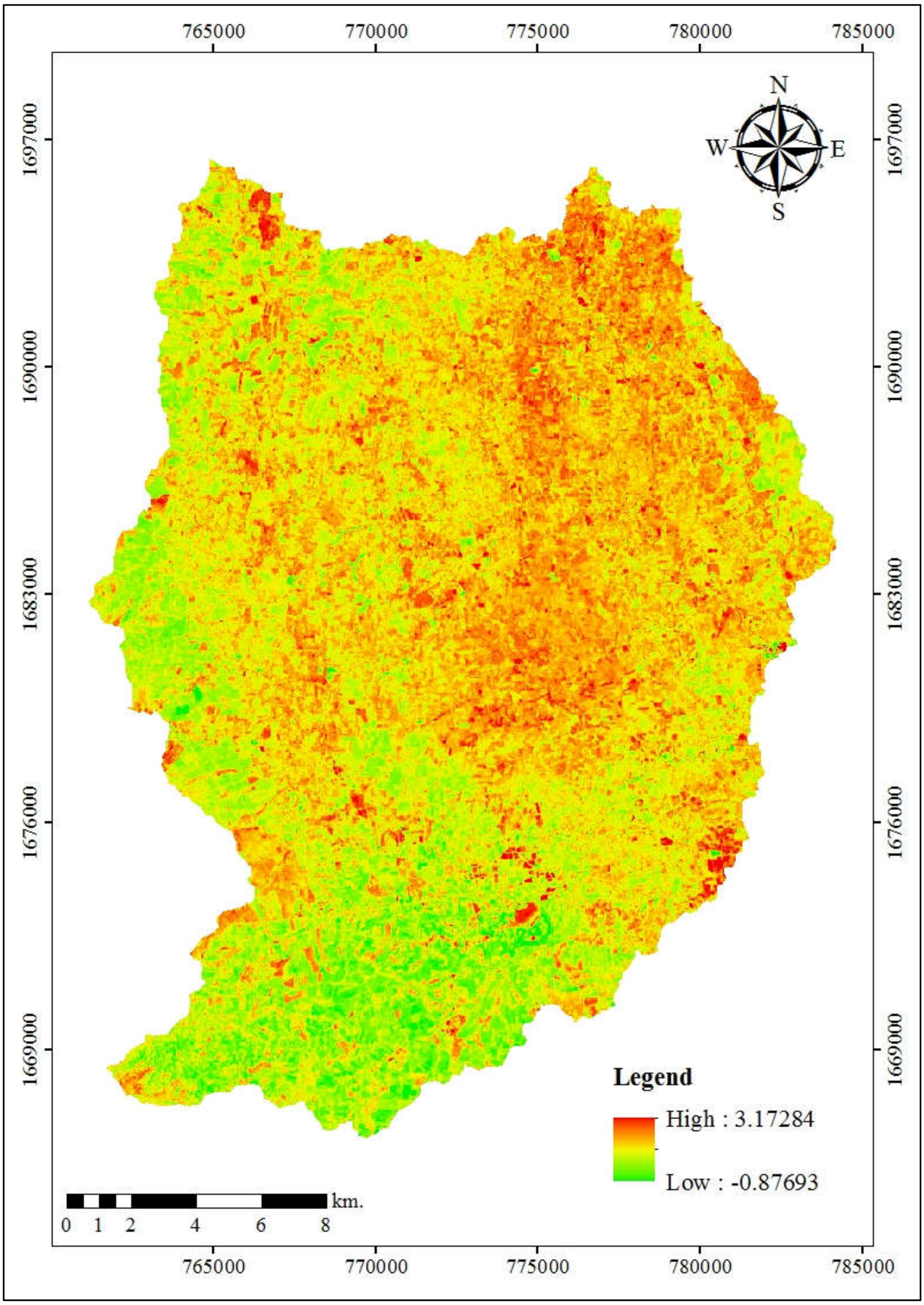

Figure 7.5 Distribution of estimated soil organic matter data deriving from multiple linear equation Model 2.

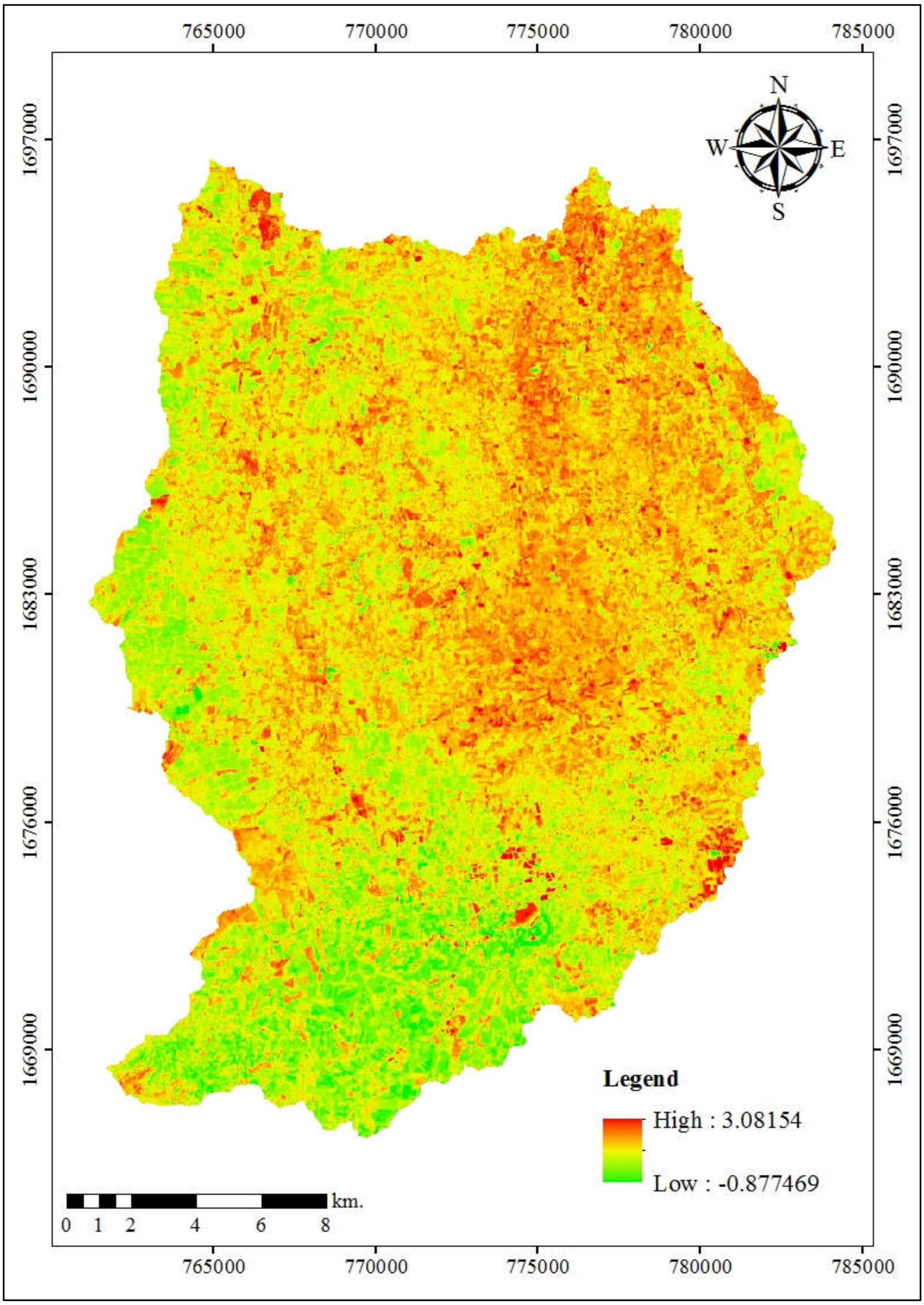

Figure 7.6 Distribution of estimated soil organic matter data deriving from multiple linear equation Model 3.

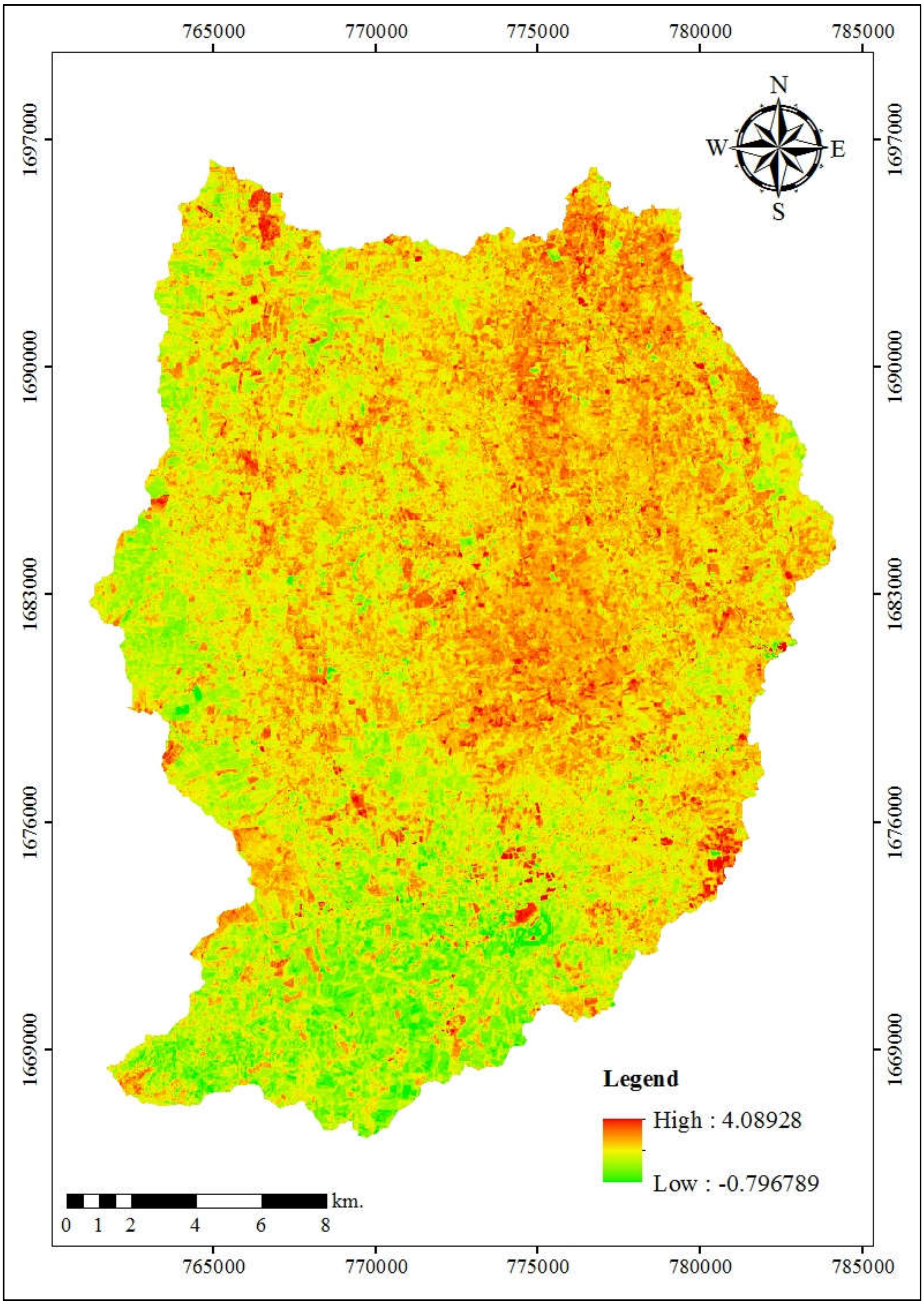

Figure 7.7 Distribution of estimated soil organic matter data deriving from multiple linear equation Model 4.

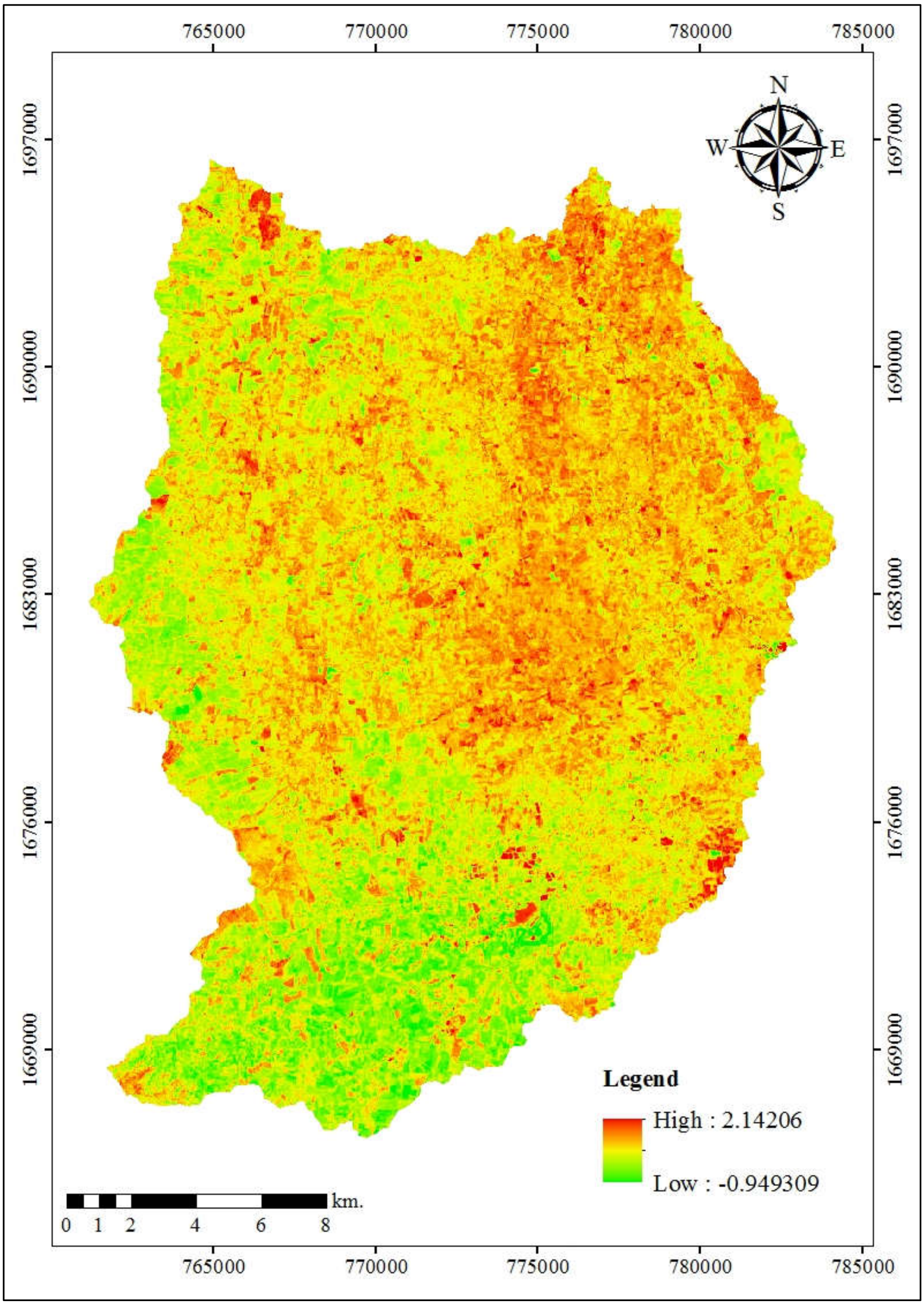

Figure 7.8 Distribution of estimated soil organic matter data deriving from multiple linear equation Model 5.

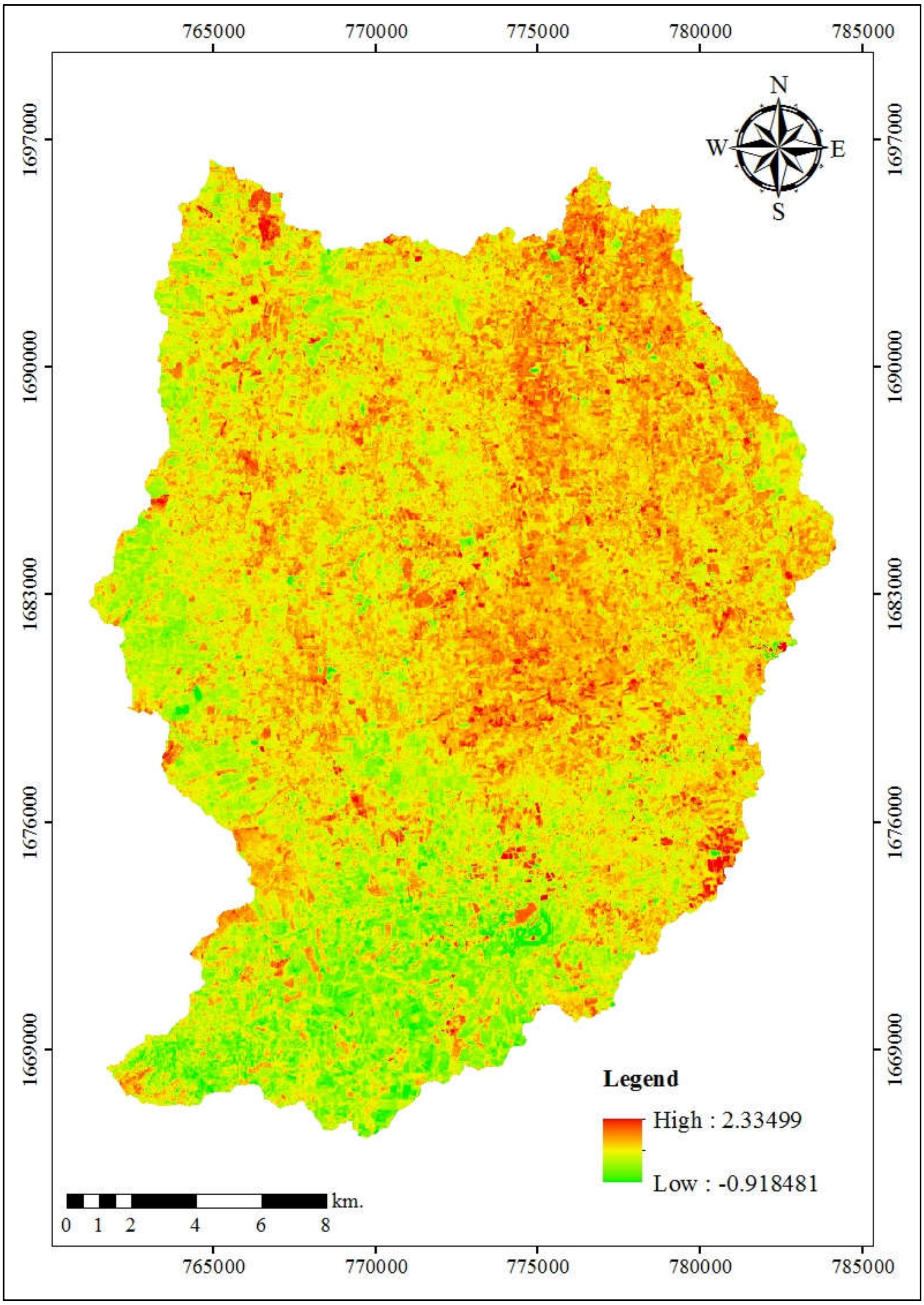

Figure 7.9 Distribution of estimated soil organic matter data deriving from multiple linear equation Model 6.

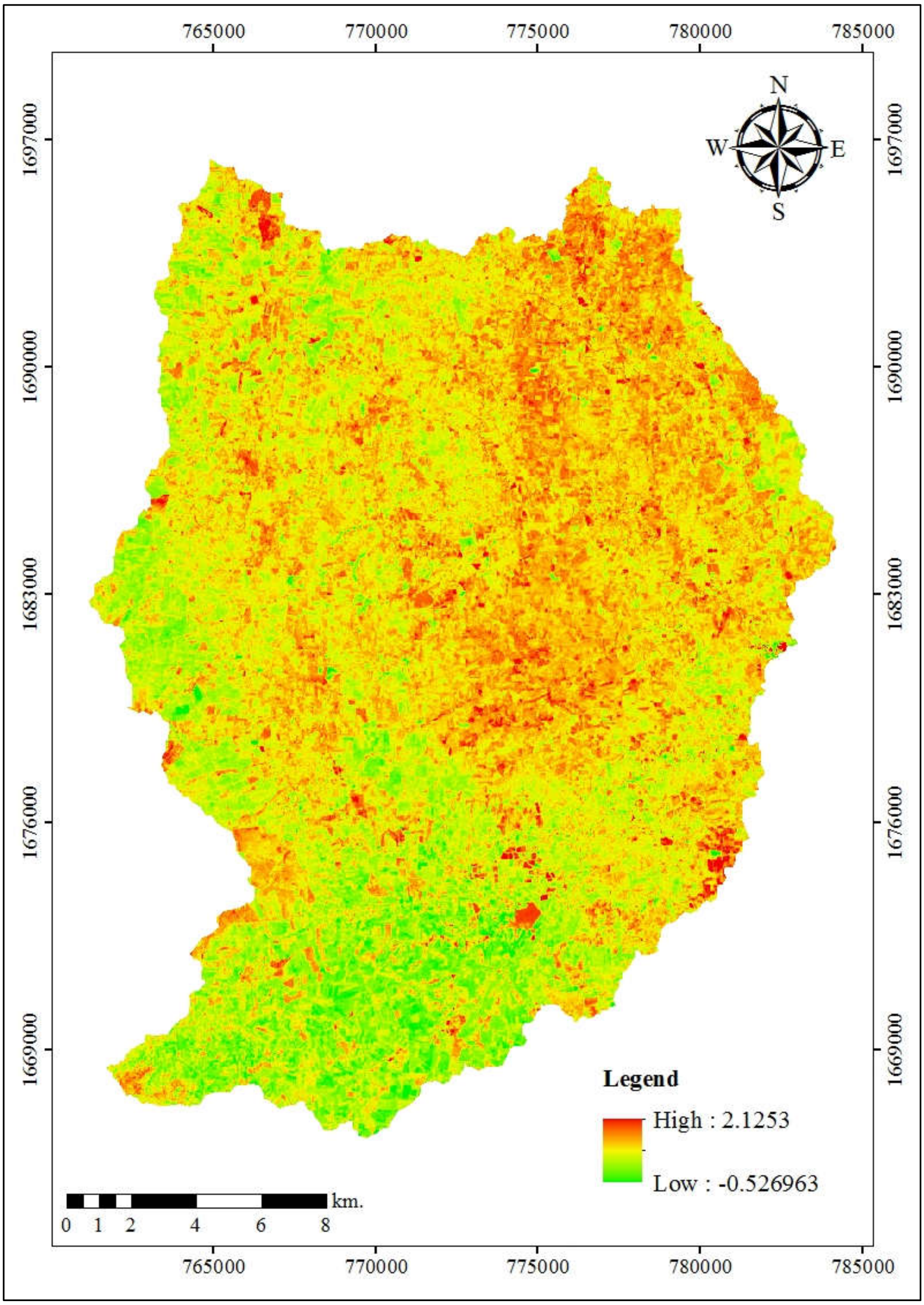

Figure 7.10 Distribution of estimated soil organic matter data deriving from multiple linear equation Model 7.

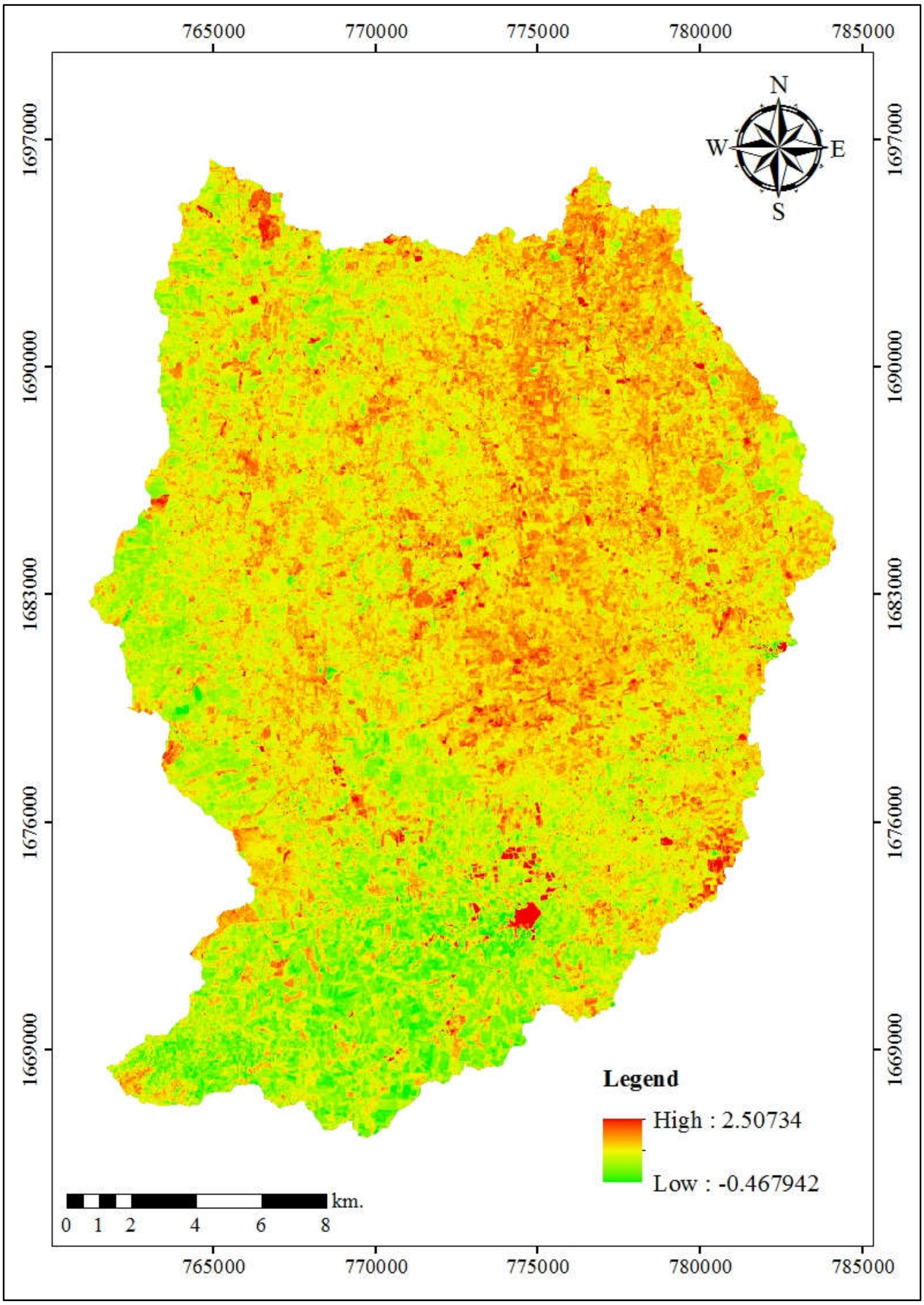

Figure 7.11 Distribution of estimated soil organic matter data deriving from multiple linear equation Model 8.

7.3.2 Non-linear regression analysis of soil organic matter estimation model development

Similar to linear regression analysis, equations of non-linear regression analysis that provide R^2 equal or greater than 0.5 were chosen as candidate equations for identifying an optimum soil organic matter estimation model with linear regression analysis.

All equations of non-linear regression analysis between of modelling OM samples and spectral data and biophysical factors that provides R^2 equal or greater than 0.5 is presented in Table 7.6. It was found that only one spectral data, Band5 provides positively correlation with OM data with R^2 of 0.557, 0.556, 0.516, and 0.516 under non-linear regression analysis with cubic, quadratic, growth, and exponential models, respectively. Distribution of soil organic matter map that derives from 4 candidate equations of non-linear regression analysis for an optimum soil organic matter model development is presented in Figures 7.12 to 7.15.

Table 7.6 List of candidate equations of non-linear regression analysis.

Non-linear regression	**Equation**	**R^2**
Cubic model	Y = 4.251 - 0.062 * Band5 + 0.000002 * Band5**3	0.557
Quadratic model	Y = 4.597 - 0.081 * Band5 + 0.000 * Band5**2	0.556
Growth model	Y = e** 3.313 - 0.057 * Band5	0.516
Exponential model	Y = 27.457 * e** - 0.057 * Band5	0.516

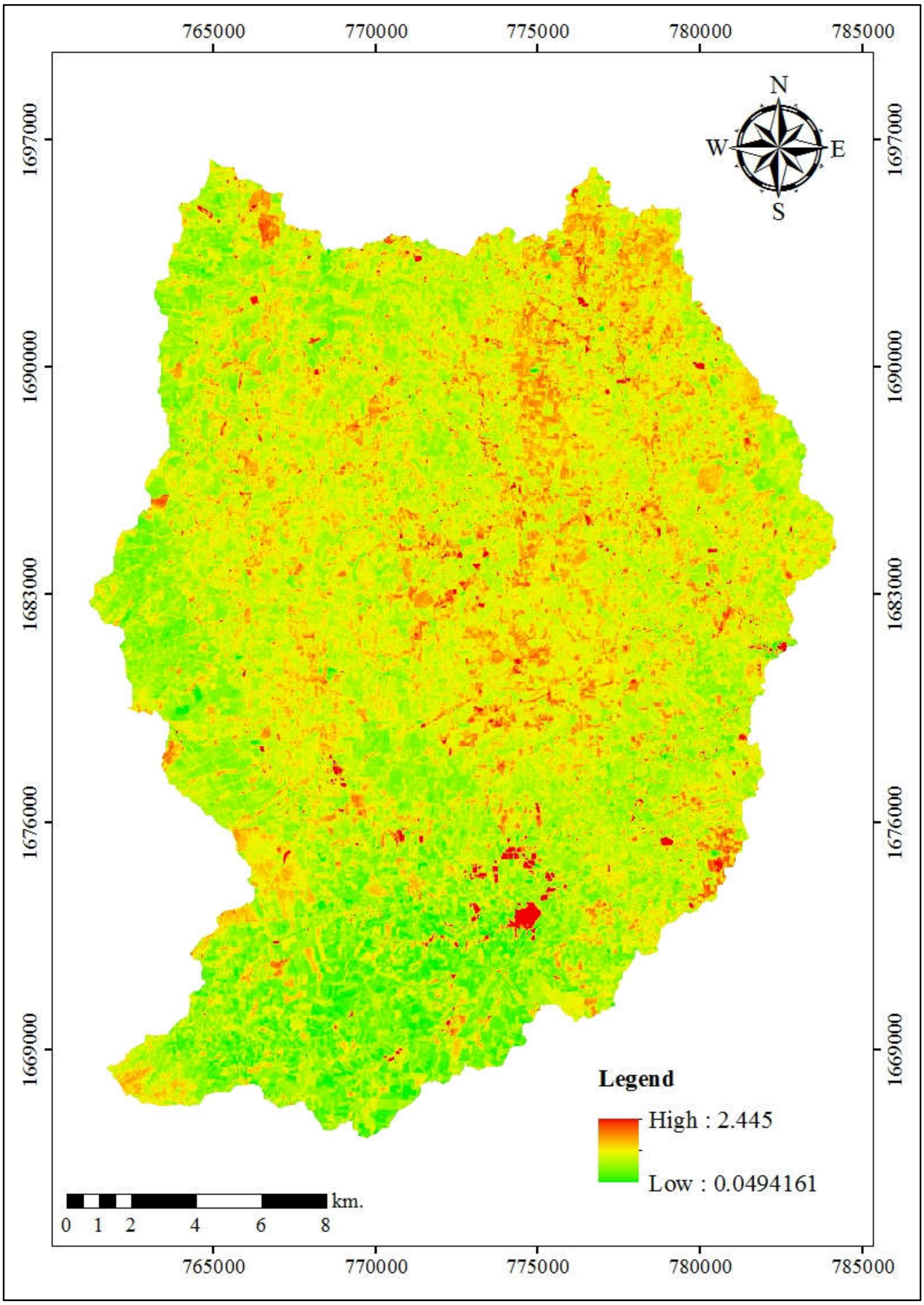

Figure 7.12 Distribution of estimated soil organic matter data deriving from cubic model.

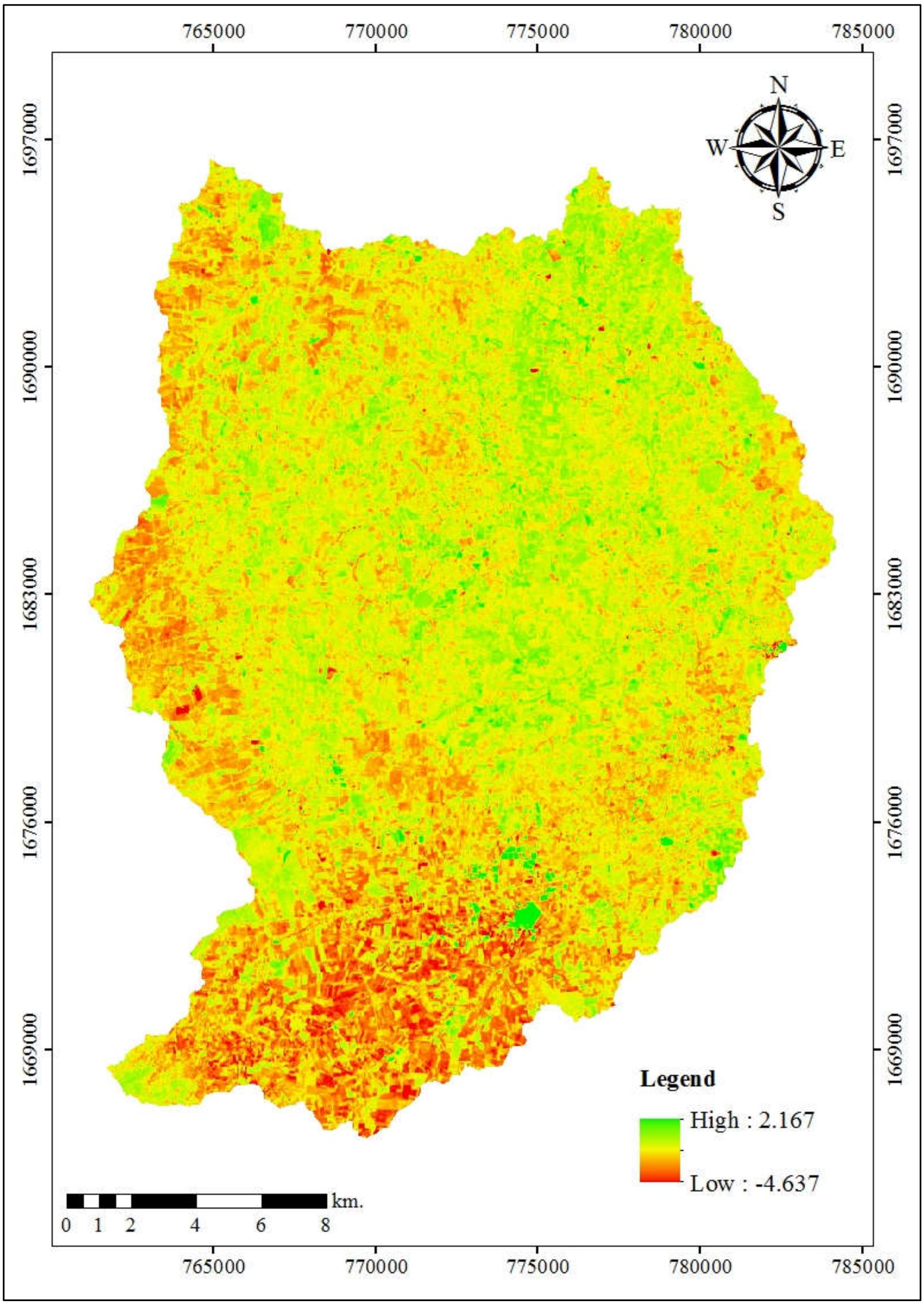

Figure 7.13 Distribution of estimated soil organic matter data deriving from quadratic model.

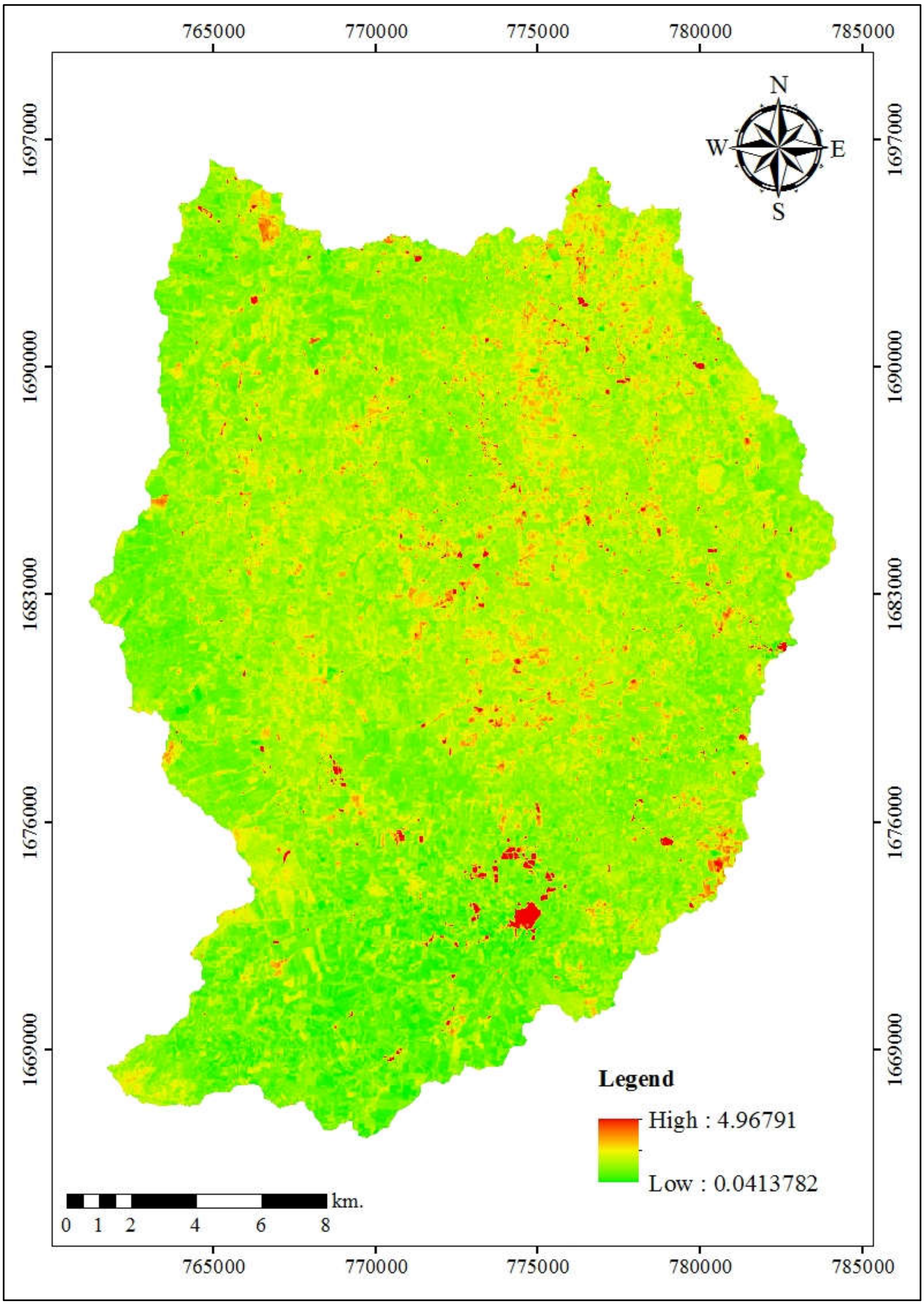

Figure 7.14 Distribution of estimated soil organic matter data deriving from growth model.

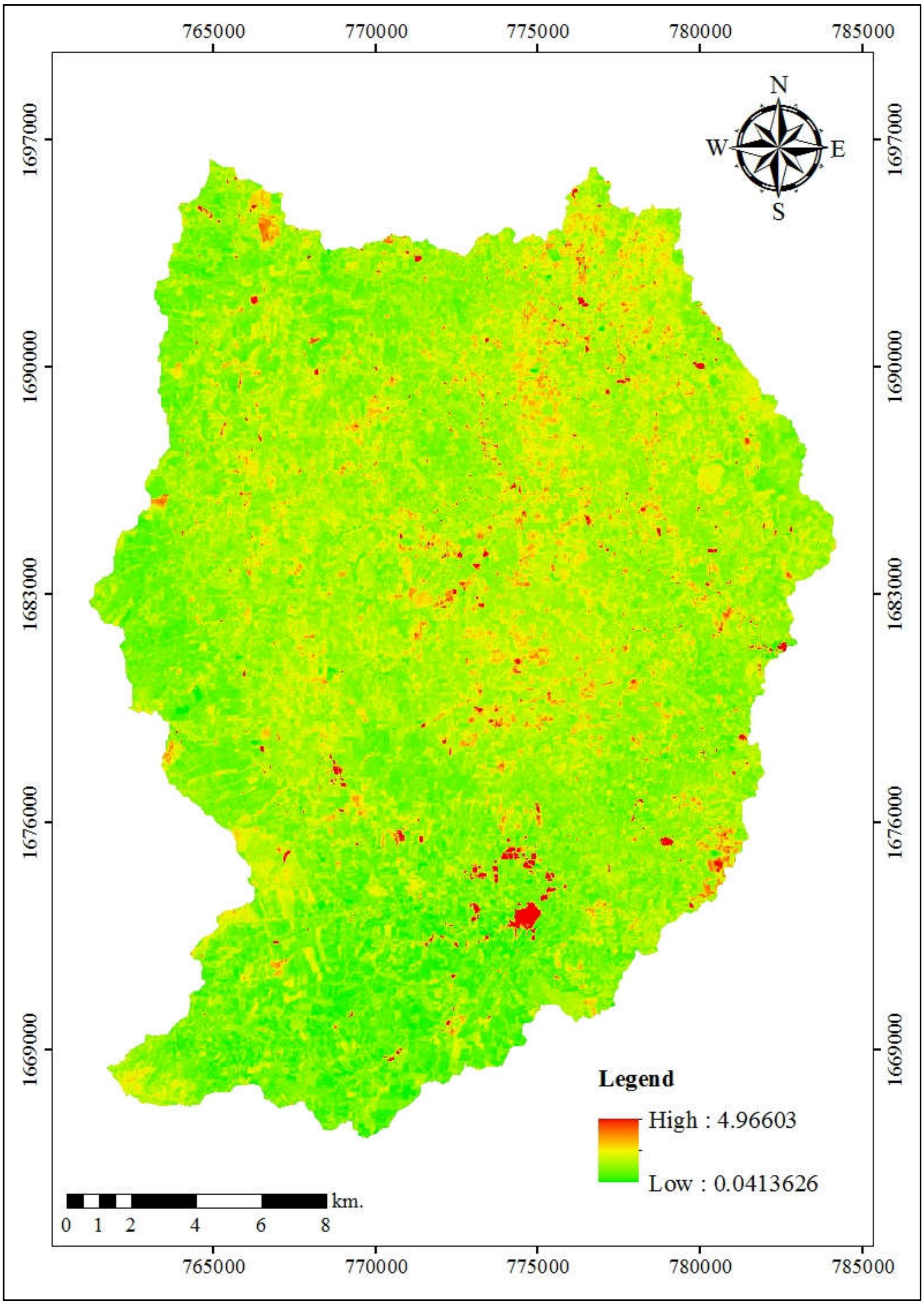

Figure 7.15 Distribution of estimated soil organic matter data deriving from exponential model.

7.4 Optimum soil organic matter estimation model

According to accuracy assessment of soil organic matter data from candidate linear and non-linear models (see Figures 7.3 to 7.15) with the analyzed OM validation dataset using NRMSE, it was found that multiple linear equation of Model 3 provides the highest accuracy for soil organic matter estimation with NRMSE of 0.29744 as summary in Table 7.7. So, multiple linear equation of Model 3 (Y = 1.058 - 0.607 * Band2 + 0.777 * Band3 - 0.147 * Band4 - 0.032 * Band5 + 0.008 * Band6 - 0.011 * Slope + 73.963 * CI - 61.988 * SI) is here chosen as an optimum model for soil organic matter estimation in the study area as shown in Figure 7.6. The lowest OM value is -0.91848 and the highest OM value is 2.33499 while an average OM value of the study area is 0.94295.

Table 7.7 Accuracy assessment of soil organic matter data from candidate equations of linear and non-linear regression analysis.

No.	Model	RMSE	NRMSE	Rank
1	Simple linear model	0.65023	0.29964	6
2	Multiple linear Model 1	0.64630	0.29783	2
3	Multiple linear Model 2	0.64438	0.34904	10
4	Multiple linear Model 3	0.64544	0.29744	1
5	Multiple linear Model 4	0.64752	0.29840	5
6	Multiple linear Model 5	0.64673	0.29803	3
7	Multiple linear Model 6	0.64695	0.29813	4
8	Multiple linear Model 7	0.65049	0.29976	7
9	Multiple linear Model 8	0.66060	0.30442	9
10	Cubic model	0.65929	0.30382	8
11	Quadratic model	1.47980	0.68194	13
12	Growth model	0.75756	0.34910	12
13	Exponential model	0.75741	0.34904	11

In addition, the most suitable interpolation technique for soil organic matter estimation from OM validation dataset in the current study according to ME and RMSE is Simple kriging (SK) that provides the lowest ME and RMSE of -0.01277 and 0.53760, respectively as summary in Table 7.8. The distribution of the interpolated soil organic matter data from five selected techniques (IDW, TPS, SK, OK, and UK) is displayed in Figures 7.16 to 7.20, respectively.

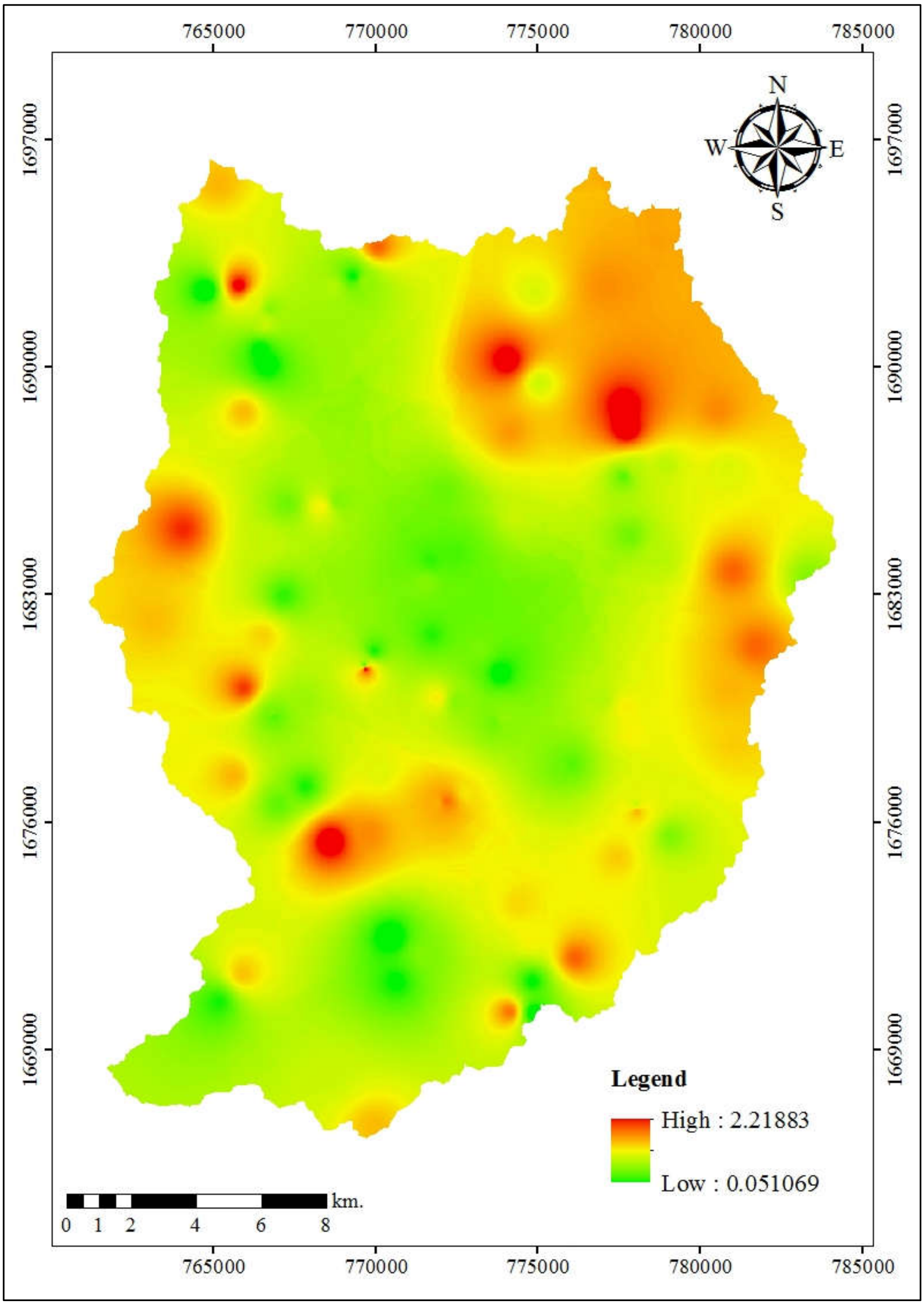

Figure 7.16 Distribution of soil organic matter data deriving from IDW technique.

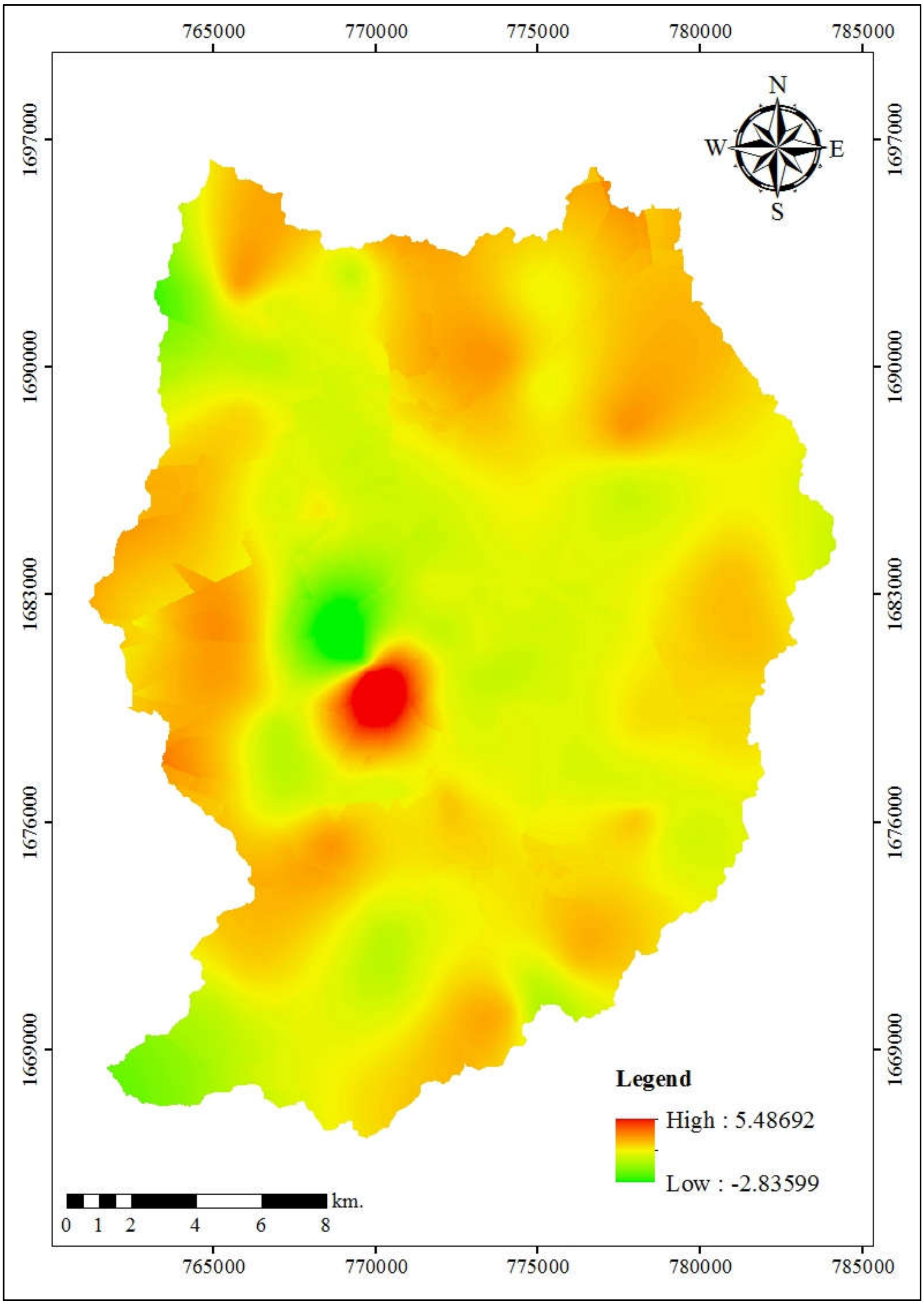

Figure 7.17 Distribution of soil organic matter data deriving from TPS technique.

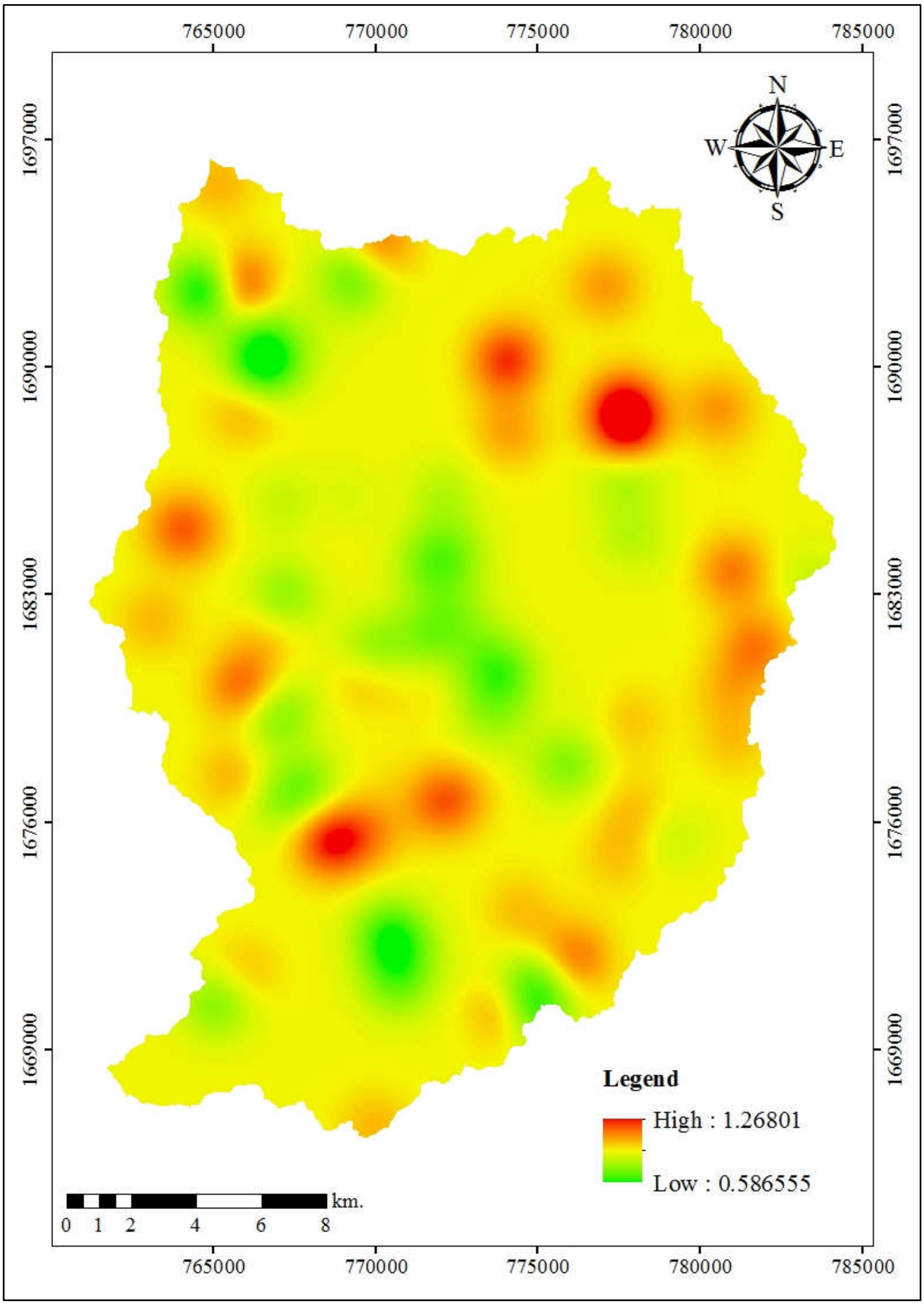

Figure 7.18 Distribution of soil organic matter data deriving from SK technique.

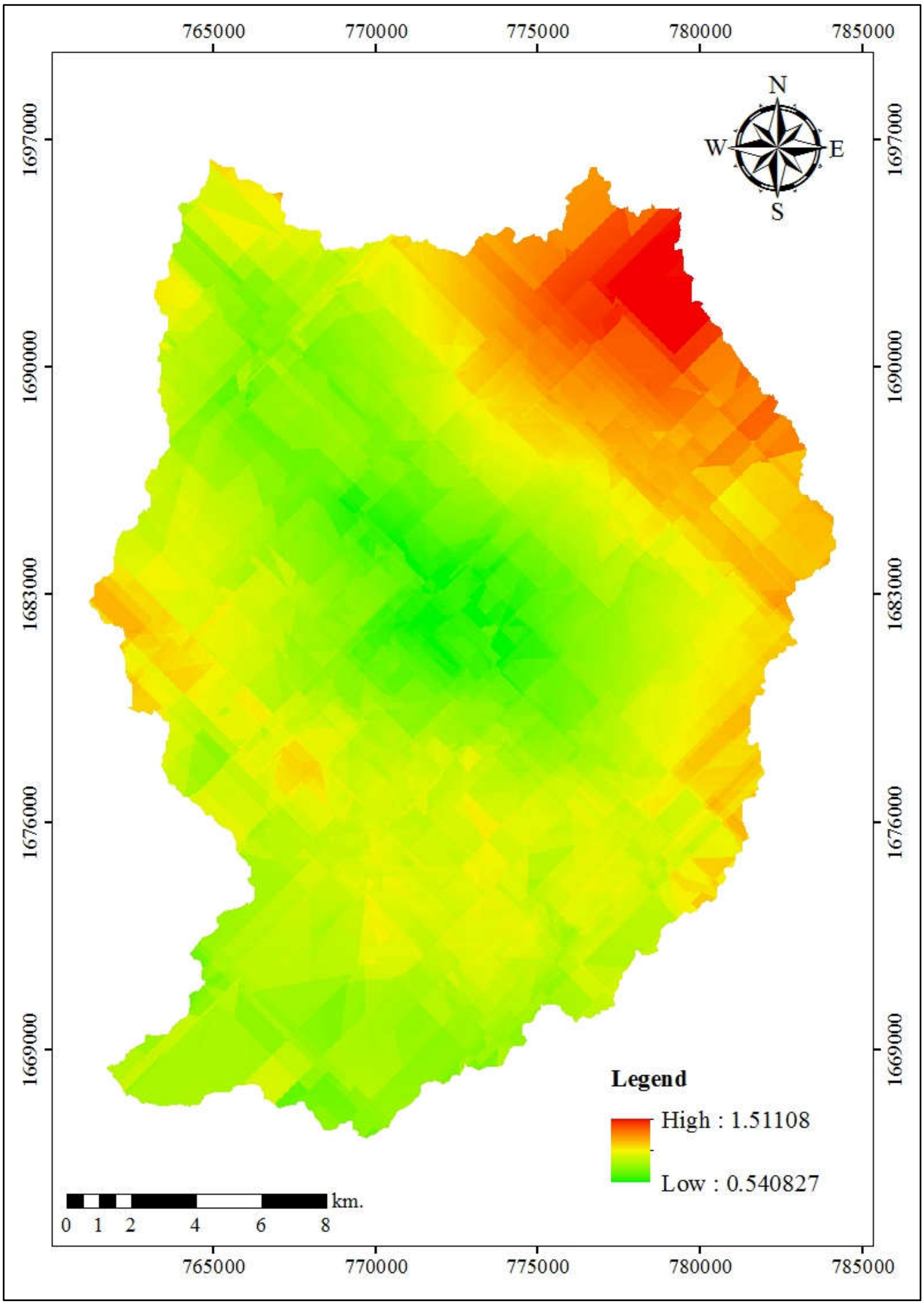

Figure 7.19 Distribution of soil organic matter data deriving from OK technique.

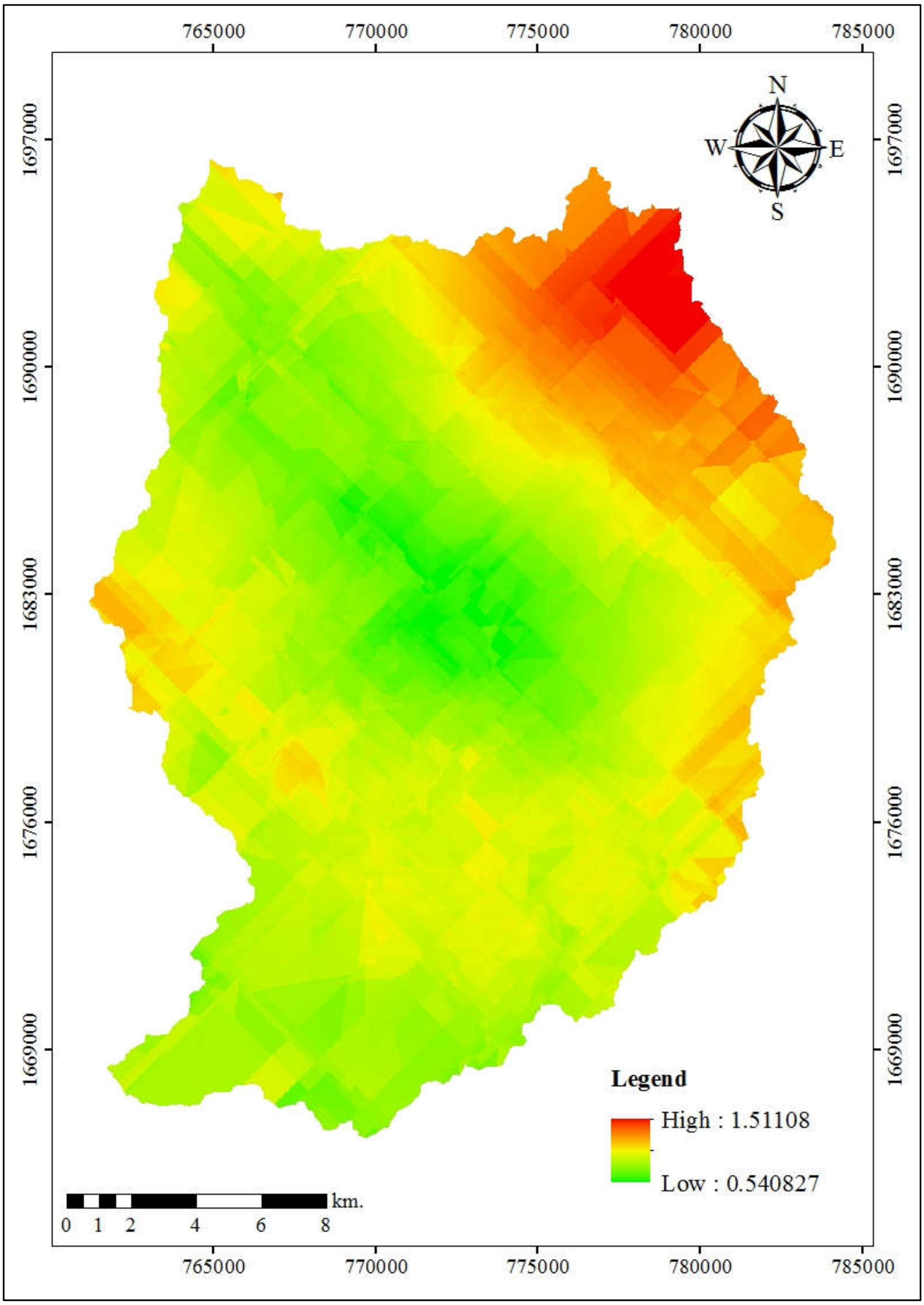

Figure 7.20 Distribution of soil organic matter data deriving from UK technique.

The interpolated soil organic matter data of SK technique is further examined correlation with the estimated soil organic matter maps of candidate linear and non-linear models (see Figures 7.3 to 7.11) as a result shown in Table 7.9. It reveals that simple linear equation and simple non-linear equation of quadratic model provide the highest correlation with the interpolated soil organic matter by SK technique with R of 0.912161 and R^2 of 0.83204. Meanwhile multiple linear equation of model 3 that was chosen as an optimum model for soil organic matter estimation provides R of 0.911045 and R^2 of 0.83000. It shows very slightly different form the highest value. In addition, according to accuracy assessment using NRMSE both simple linear and non-linear equations provide accuracy lower than multiple linear equation of Model 3 as shown in Table 7.7.

Table 7.8 Accuracy assessment of five interpolation technique for soil organic matter estimation.

No.	Interpolation technique	ME	RMSE	Rank
1	IDW	-0.04287	0.57689	4
2	TPS	-0.01468	0.76437	5
3	SK	-0.01277	0.53760	1
4	OK	-0.01033	0.55510	2
5	UK	-0.01033	0.55510	2

Table 7.9 Correlation coefficient and coefficient of determination between the interpolated soil organic matter data by SK technique and the estimated soil organic matter data of candidate linear and non-linear models.

No.	Model	R	R^2	Rank
1	Simple linear model	0.912161	0.83204	1
2	Multiple linear Model 1	0.909656	0.82747	4
3	Multiple linear Model 2	0.908304	0.82502	5
4	Multiple linear Model 3	0.911045	0.83000	3
5	Multiple linear Model 4	0.893818	0.79891	10
6	Multiple linear Model 5	0.895003	0.80103	8
7	Multiple linear Model 6	0.898397	0.80712	7
8	Multiple linear Model 7	0.894119	0.79945	9
9	Multiple linear Model 8	0.903442	0.81621	6
10	Cubic model	0.838734	0.70347	11
11	Quadratic model	0.912161	0.83204	1
12	Growth model	0.765402	0.58584	12
13	Exponential model	0.765402	0.58584	12

7.5 Soil organic matter assessment and its depletion

The optimum soil organic matter estimation model from multiple linear equation of Model 3 was here applied to create soil organic matter data as shown in Figure 7.6. Then, the derived soil OM data was normalized with ranging between 0 and 1, and it was converted in percent as result shown in Figure 7.21. The converted soil OM data in percent was further applied to calculate BDI data using Equation 3.15 for depletion of soil organic matter content evaluation as result shown in Figure 7.22. The derived BDI was then applied to extract soil biological degradation classes according to BDI value (see Table 3.8). Distribution of soil biological degradation classification is displayed in Figure 7.23 while area and percentage of soil biological degradation classification is summarized Table 7.10.

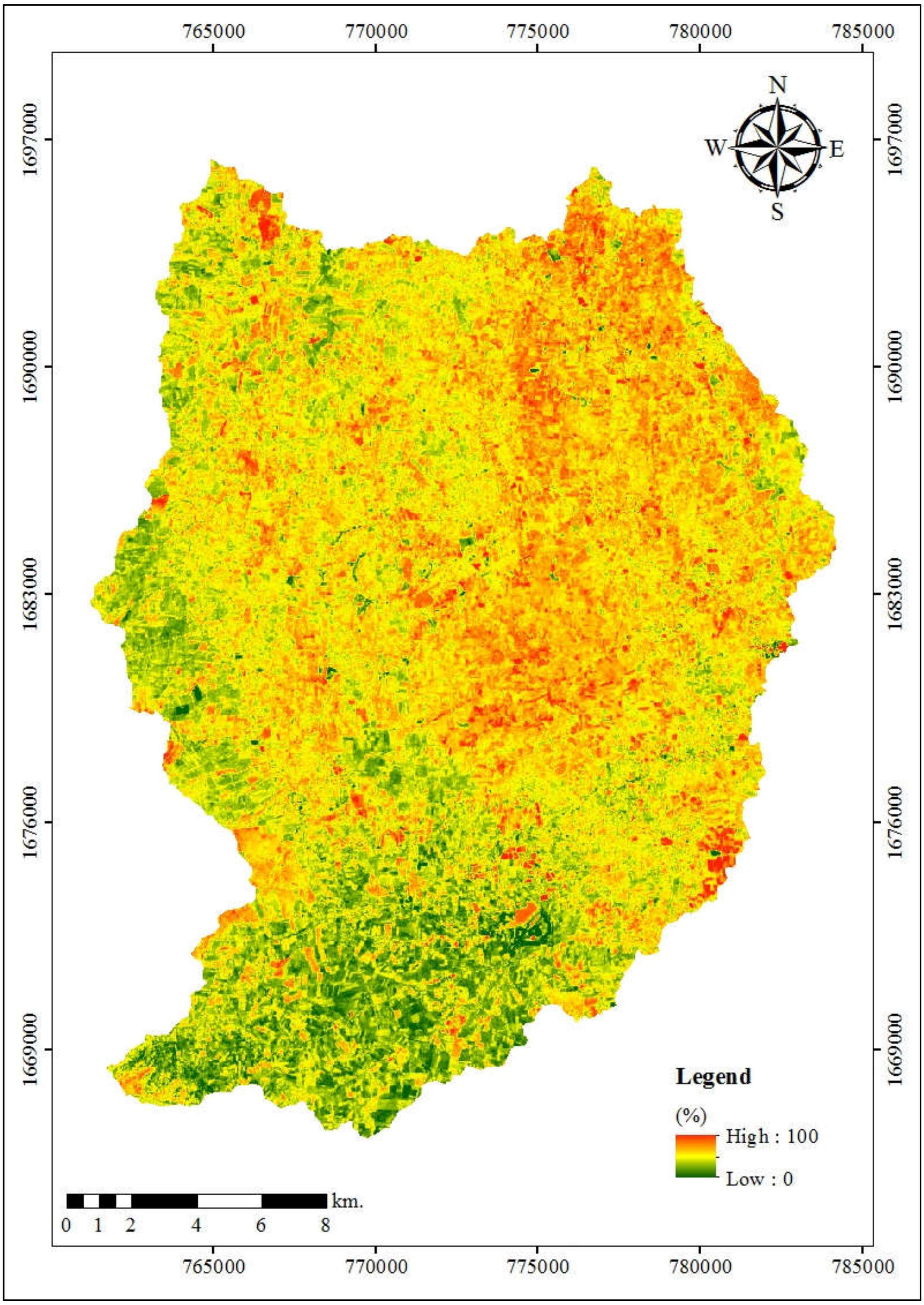

Figure 7.21 Distribution of soil organic matter in the study area.

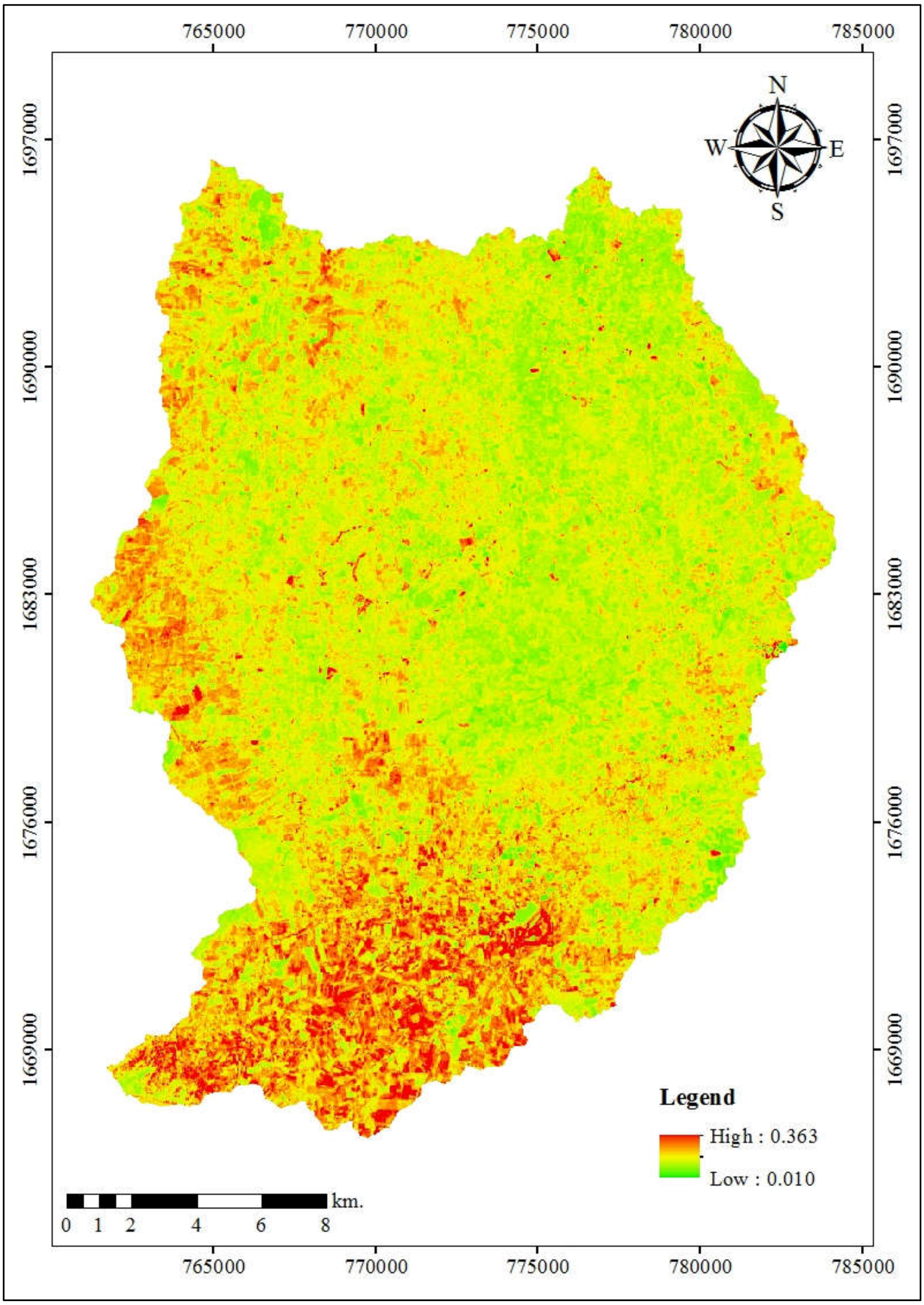

Figure 7.22 Distribution of soil biological degradation index (BDI) in the study area.

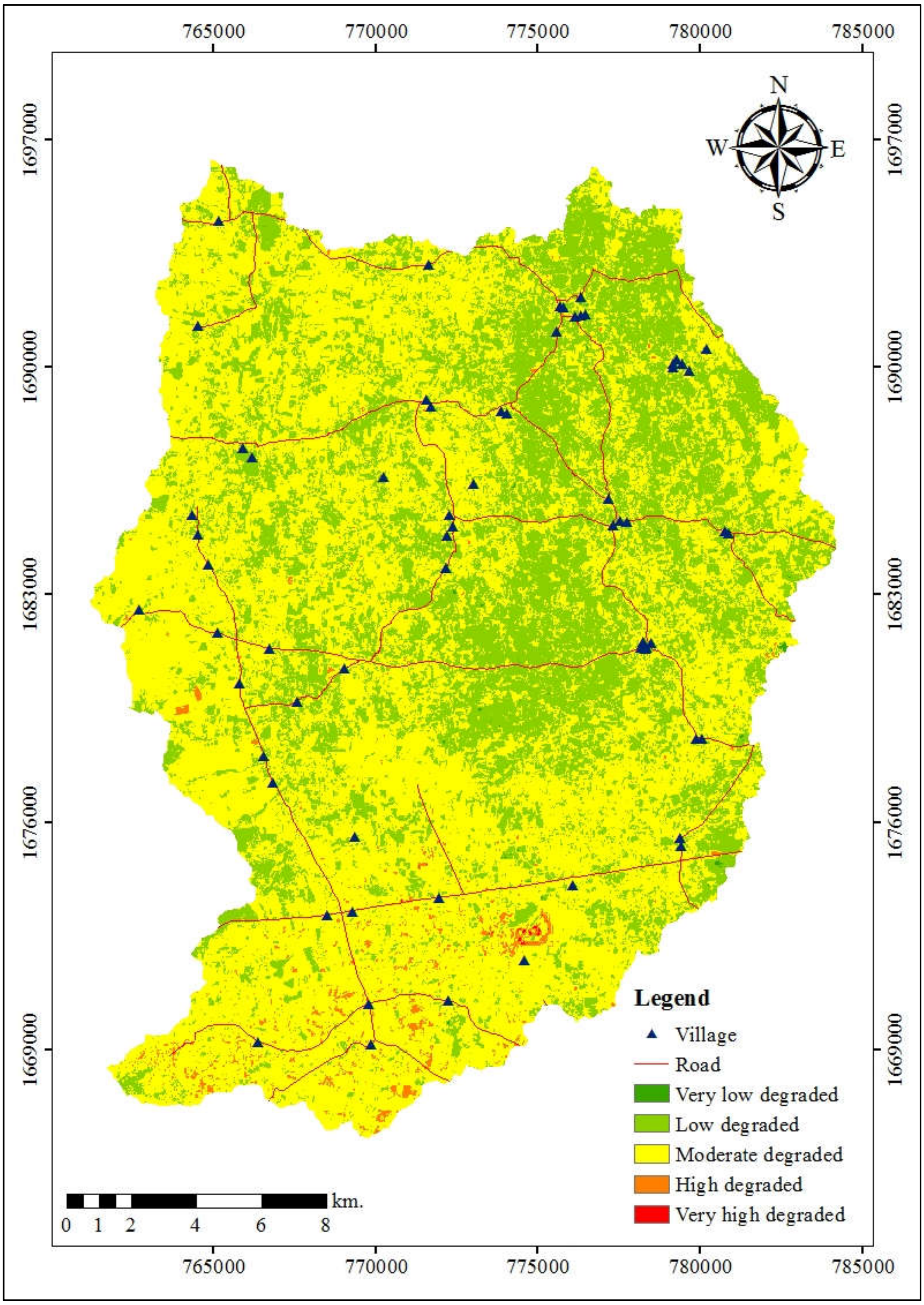

Figure 7.23 Distribution of soil biological degradation classification in the study area.

Table 7.10 Biological degradation index and soil biological degradation classification.

No.	Level of soil biological degradation	BDI (Unit less)	Area in sq. km	Percentage
1	Very low	≤ 0.0125	0.28	0.06
2	Low	0.0125 - 0.0167	163.43	35.15
3	Moderate	0.0167 - 0.0250	296.05	63.67
4	High	0.0250 - 0.0500	5.12	1.10
5	Very High	> 0.0500	0.08	0.02
	Total		**464.96**	**100.00**

The result shows that the most dominant soil biological degradation class in the study area is moderate degradation which covers area of 296.05 sq. km or 63.67% of the total study area. This finding reflects an intensive use of soil for agricultural activities in Upper Lamchiengkrai watershed, particularly cassava cultivation (Table 7.10).

In addition, according to overlay analysis between soil biological degradation classification and LULC data as summary in Table 7.11, the most dominant crop effects soil biological degradation is cassava that situates in moderate soil degradation class about 214 sq. km or 46.025% of the total study area. This phenomena also presents in moderate and very high soil biological degradation classes.

Table 7.11 Soil biological degradation classification and LULC classes.

Land use and land cover classes	Soil biological degradation classification									
	Very Low		Low		Moderate		High		Very High	
	Sq.km.	%	Sq.km.	%	Sq.km.	%	Sq.km.	%	Sq.km.	%
Urban and built-up area	0.00	0.000	4.19	0.900	2.37	0.510	0.08	0.018	0.00	0.000
Paddy field	0.00	0.000	7.92	1.704	13.32	2.864	0.01	0.001	0.00	0.000
Maize	0.00	0.001	17.82	3.832	13.74	2.955	0.00	0.000	0.00	0.000
Sugarcane	0.00	0.001	3.92	0.842	2.82	0.606	0.03	0.006	0.00	0.000
Cassava	0.09	0.019	104.48	22.471	214.00	46.025	3.92	0.843	0.06	0.012
Perennial tree and orchard	0.00	0.001	7.96	1.711	11.88	2.554	0.01	0.002	0.00	0.000
Dense deciduous forest	0.00	0.000	0.65	0.140	3.16	0.679	0.30	0.065	0.00	0.000
Disturbed deciduous forest	0.01	0.002	6.14	1.321	2.89	0.623	0.00	0.000	0.00	0.000
Forest plantation	0.02	0.005	4.02	0.865	7.53	1.619	0.36	0.078	0.02	0.004
Water body	0.09	0.019	2.60	0.559	2.35	0.506	0.04	0.009	0.00	0.000
Scrub	0.06	0.014	0.53	0.114	0.54	0.117	0.03	0.007	0.00	0.000
Miscellaneous land	0.00	0.001	3.21	0.691	21.45	4.614	0.33	0.071	0.00	0.000
Total	**0.28**	**0.061**	**163.43**	**35.149**	**296.05**	**63.673**	**5.12**	**1.101**	**0.08**	**0.016**

CHAPTER VIII

SOIL DEGRADATION EVALUATION

Main result of the fifth objective on evaluation of soil degradation and its severity in 2015 is reported under this chapter. In this study, multiplicative method without and with severity classification among soil loss, soil salinity, and soil biological degradation are examined. Details of each result is separately described and discussed in following sections.

8.1 Soil degradation evaluation using multiplicative method without severity classification

Under this method, the derived soil loss, soil salinity, and soil biological degradation indices in 2015 were firstly separately normalized and combined using multiplicative method for soil degradation evaluation.

Since the values of soil loss, soil salinity, and soil biological degradation indices have different ranges and units among them (Table 8.1). Consequently, it is necessary to normalize these values before data integration for soil degradation evaluation. In this study, the derived three soil indices were normalized using standardization method (Eq. 3.14). The result of normalized value of soil loss, soil salinity, and soil biological degradation indices is displayed in Figures 8.1 to 8.3, respectively and the basic statistics of the normalized values of factors for soil degradation evaluation is presented in Table 8.2. The evaluation of soil degradation using multiplicative without severity classification is displayed in Figure 8.4 while classification of soil degradation with 5 severity classes: very low, low, moderate, high and very high class using Natural break method is presented in Figure 8.5. Area and percentage of soil degradation using multiplicative method without severity classification is summarized in Table 8.3.

Table 8.1 Basic statistics of the values of factors for soil degradation evaluation

Factors for soil degradation evaluation	Basic statistical value (dS m^{-1})				
	Min.	**Max.**	**Mean**	**S.D.**	**Variance**
Soil erosion index	0.000	278.196	3.369	13.247	175.48779
Soil salinity index	-1.602	0.785	0.074	0.082	0.00671
Biological degradation index	0.010	0.363	0.018	0.003	0.00001

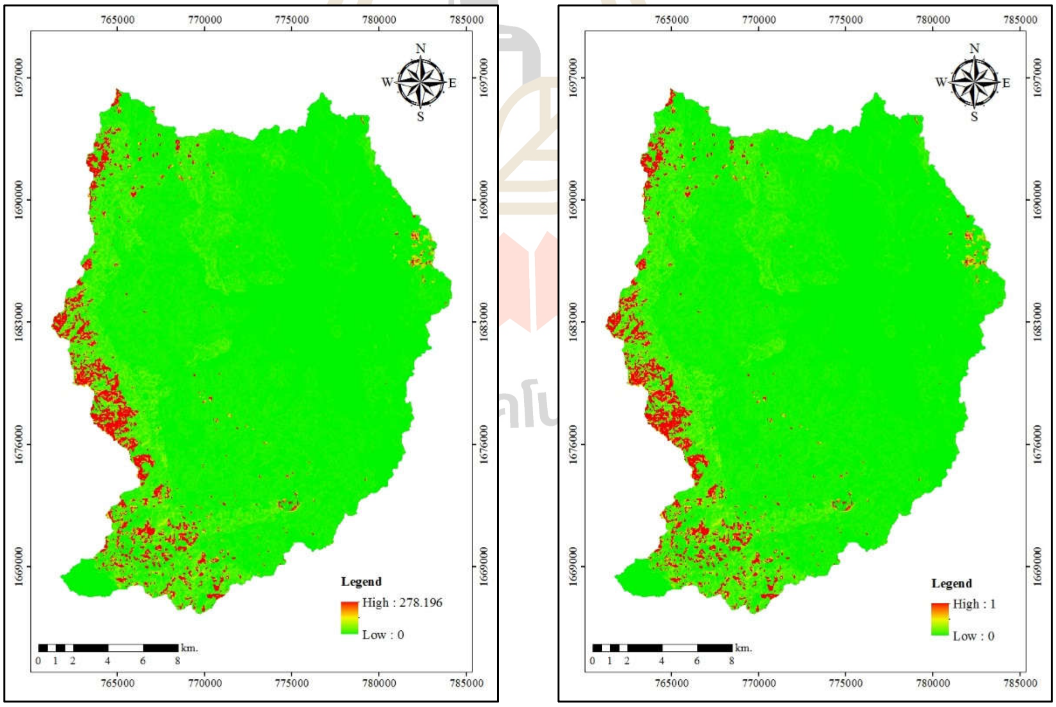

Actual soil loss index

Normalized soil loss index

Figure 8.1 Actual and normalized soil loss index.

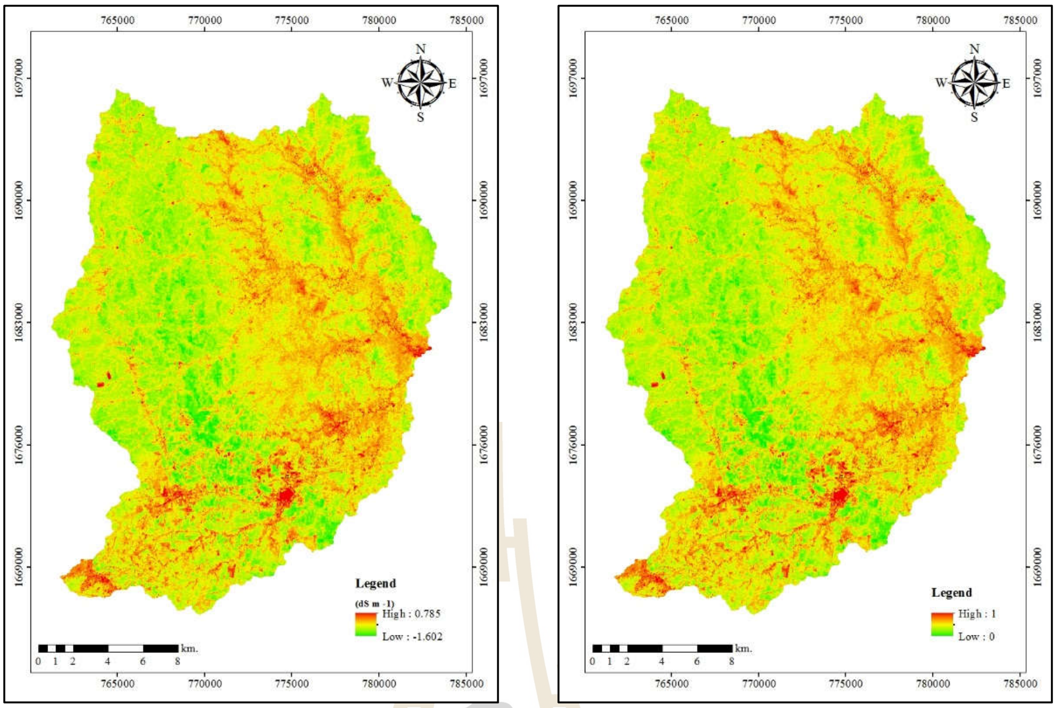

Actual soil salinity index — Normalized soil salinity index

Figure 8.2 Actual and normalized soil salinity index.

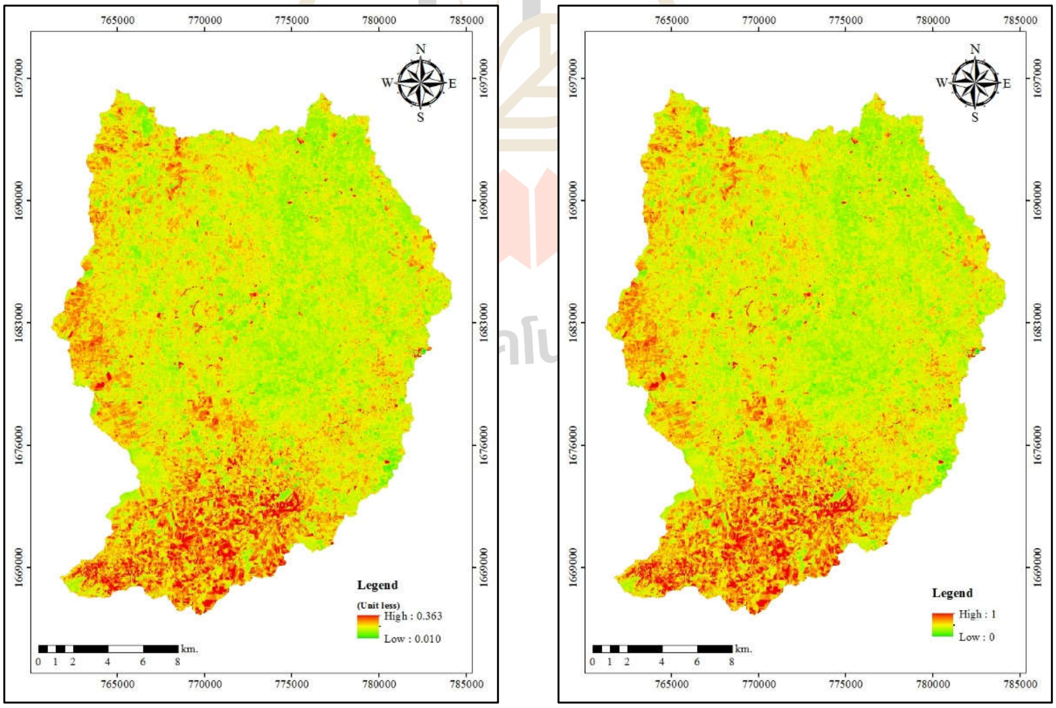

Actual BDI — Normalized BDI

Figure 8.3 Actual and normalized biological degradation index.

Table 8.2 Basic statistics of the normalized values of three factors for soil degradation evaluation.

Factors for soil degradation evaluation	**Basic statistical value (dS m^{-1})**				
	Min.	**Max.**	**Mean**	**S.D.**	**Variance**
Soil erosion index	0	1	0.012	0.048	0.0023
Soil salinity index	0	1	0.702	0.034	0.0012
Biological degradation index	0	1	0.022	0.007	0.0001

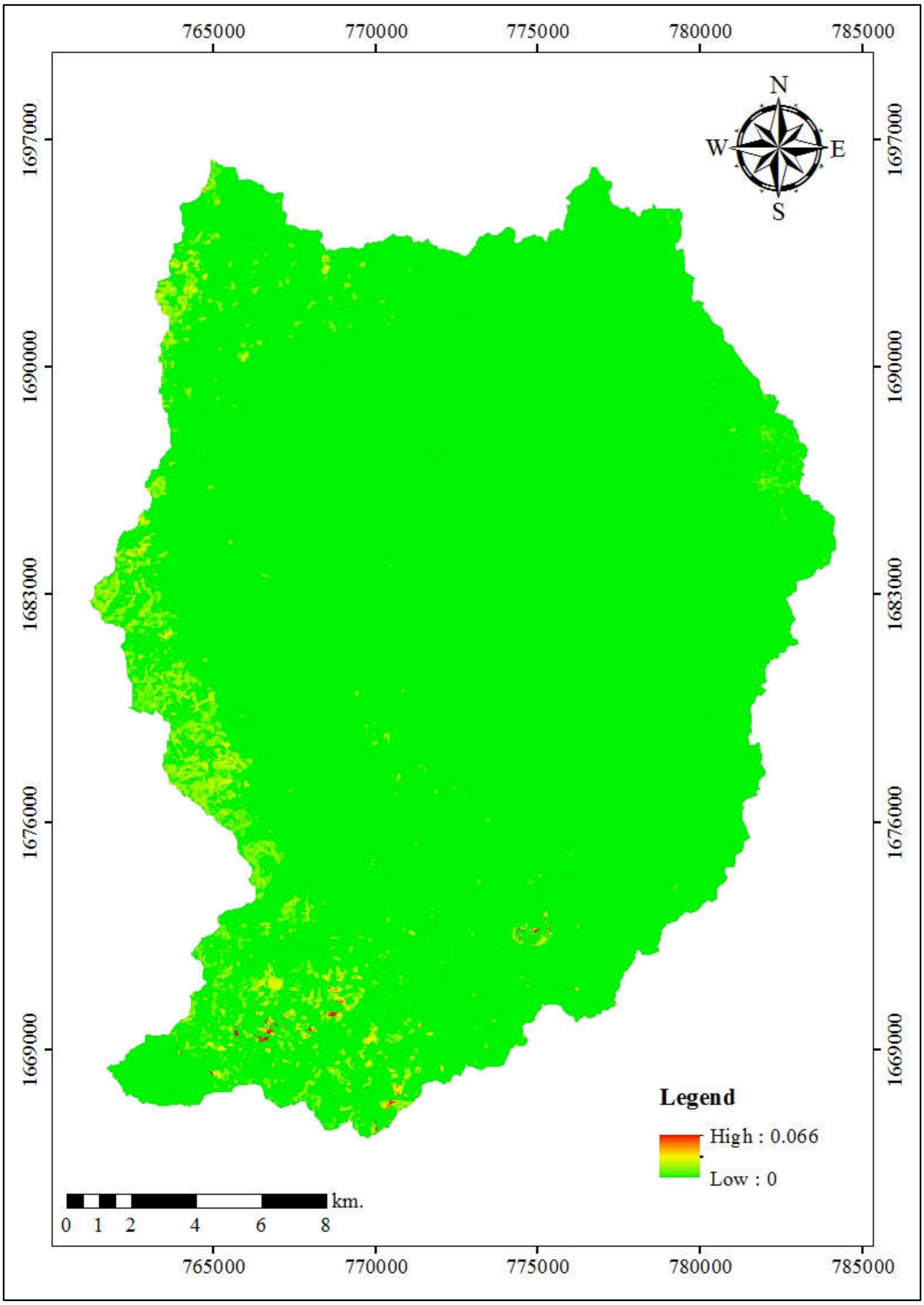

Figure 8.4 Soil degradation evaluation using multiplicative method without severity classification.

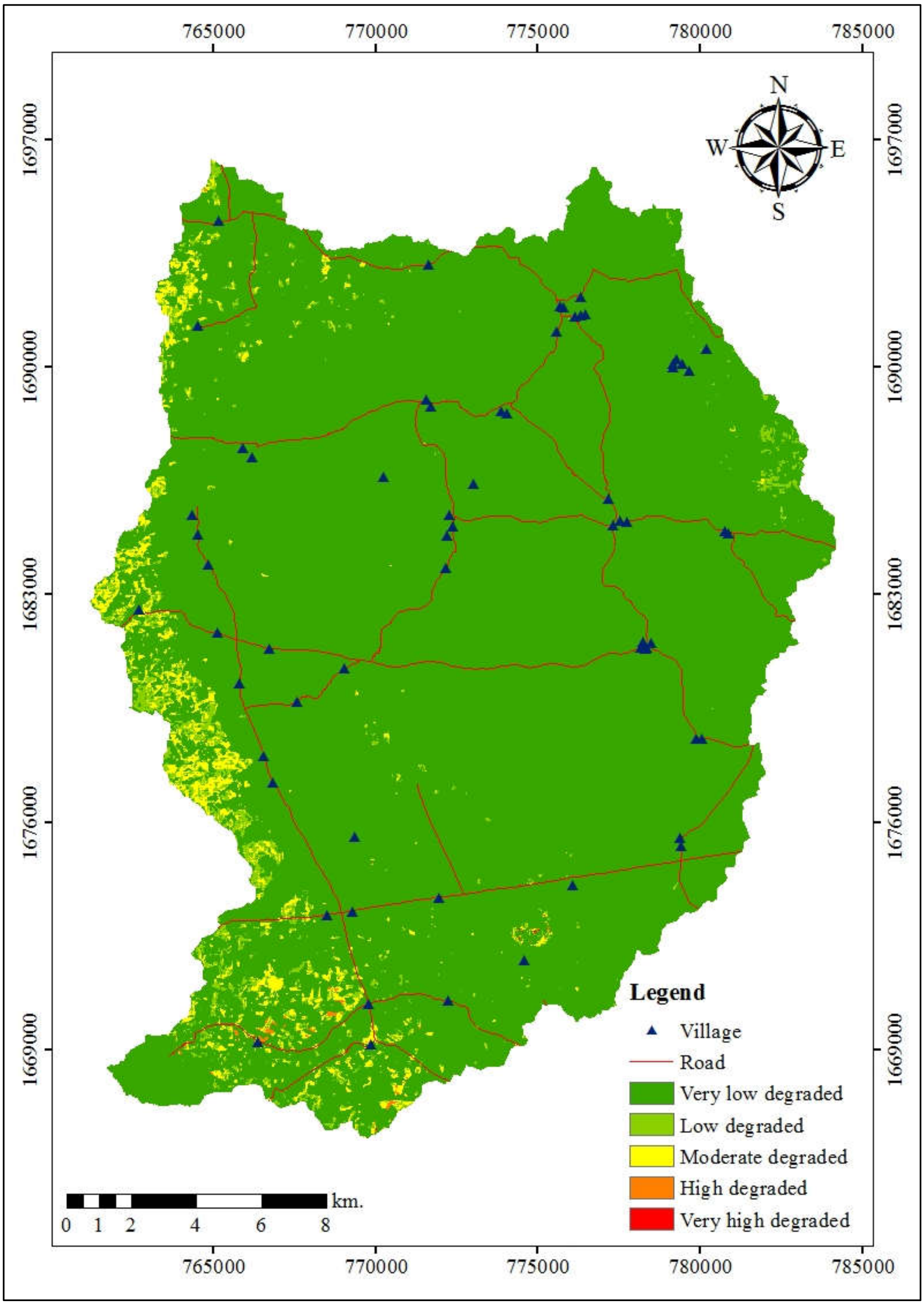

Figure 8.5 Severity class of soil degradation using multiplication without severity classification.

Table 8.3 Severity class of soil degradation using multiplication without severity classification.

No.	Severity class of soil degradation	Area in sq. km	Percentage
1	Very low	443.00	95.278
2	Low	11.67	2.510
3	Moderate	9.83	2.114
4	High	0.45	0.096
5	Very High	0.01	0.003
	Total	**464.96**	**100.000**

As a result it reveals that the most dominant soil degradation class using multiplicative method without severity classification in the study area is very low class that covers area of 443.00 sq. km or 95.278% of the total study area. On contrary, high and very high soil degradation classes only cover area of 0.45 sq. km and 0.01 sq. km or about 0.096% and 0.003% of the total study area.

In addition, according to overlay analysis between soil degradation classes using multiplicative method without severity classification and LULC data as summary in Table 8.4, top three dominant crops in very low soil degradation severity class are cassava, maize, and paddy field. Meanwhile, high and very high soil degradation severity classes are mostly found in miscellaneous land (soil pit, sand pit, and land fill). This finding is true because soil of miscellaneous land, in general is very poor.

Table 8.4 Soil degradation severity classes using multiplication without classify and LULC classes

Land use and land cover classes	Soil degradation severity classes									
	Very Low		Low		Moderate		High		Very High	
	Sq.km.	%	Sq.km.	%	Sq.km.	%	Sq.km.	%	Sq.km.	%
Urban and built-up area	6.640	1.428	0.000	0.000	0.000	0.000	0.000	0.000	0.000	0.000
Paddy field	21.247	4.570	0.000	0.000	0.000	0.000	0.000	0.000	0.000	0.000
Maize	31.560	6.788	0.000	0.000	0.001	0.000	0.000	0.000	0.000	0.000
Sugarcane	6.765	1.455	0.000	0.000	0.001	0.000	0.000	0.000	0.000	0.000
Cassava	319.163	68.643	1.670	0.359	1.579	0.340	0.122	0.026	0.005	0.001
Perennial tree and orchard	19.214	4.132	0.428	0.092	0.196	0.042	0.007	0.002	0.000	0.000
Dense deciduous forest	4.108	0.883	0.002	0.000	0.000	0.000	0.002	0.000	0.000	0.000
Disturbed deciduous forest	9.041	1.944	0.000	0.000	0.002	0.000	0.000	0.000	0.000	0.000
Forest plantation	11.934	2.567	0.008	0.002	0.006	0.001	0.005	0.001	0.001	0.000
Water body	5.082	1.093	0.000	0.000	0.000	0.000	0.000	0.000	0.000	0.000
Scrub	1.170	0.252	0.000	0.000	0.000	0.000	0.000	0.000	0.000	0.000
Miscellaneous land	7.078	1.522	9.563	2.057	8.044	1.730	0.310	0.067	0.005	0.001
Total	**443.002**	**95.278**	**11.670**	**2.510**	**9.829**	**2.114**	**0.446**	**0.096**	**0.012**	**0.003**

8.2 Soil degradation evaluation using multiplicative method with severity classification

Under this method, severity classification of soil erosion, soil salinity and soil biological degradation were combined using multiplicative method for soil degradation evaluation. Herein, ordinal integer values of soil severity indices, which were classified into 5 classes: very low, low, moderate, high, and very high, have value of 1, 2, 3, 4, and 5, respectively were applied multiplication operation. Input data of three soil severity indices for soil degradation are presented in Figures 8.6 to 8.8.

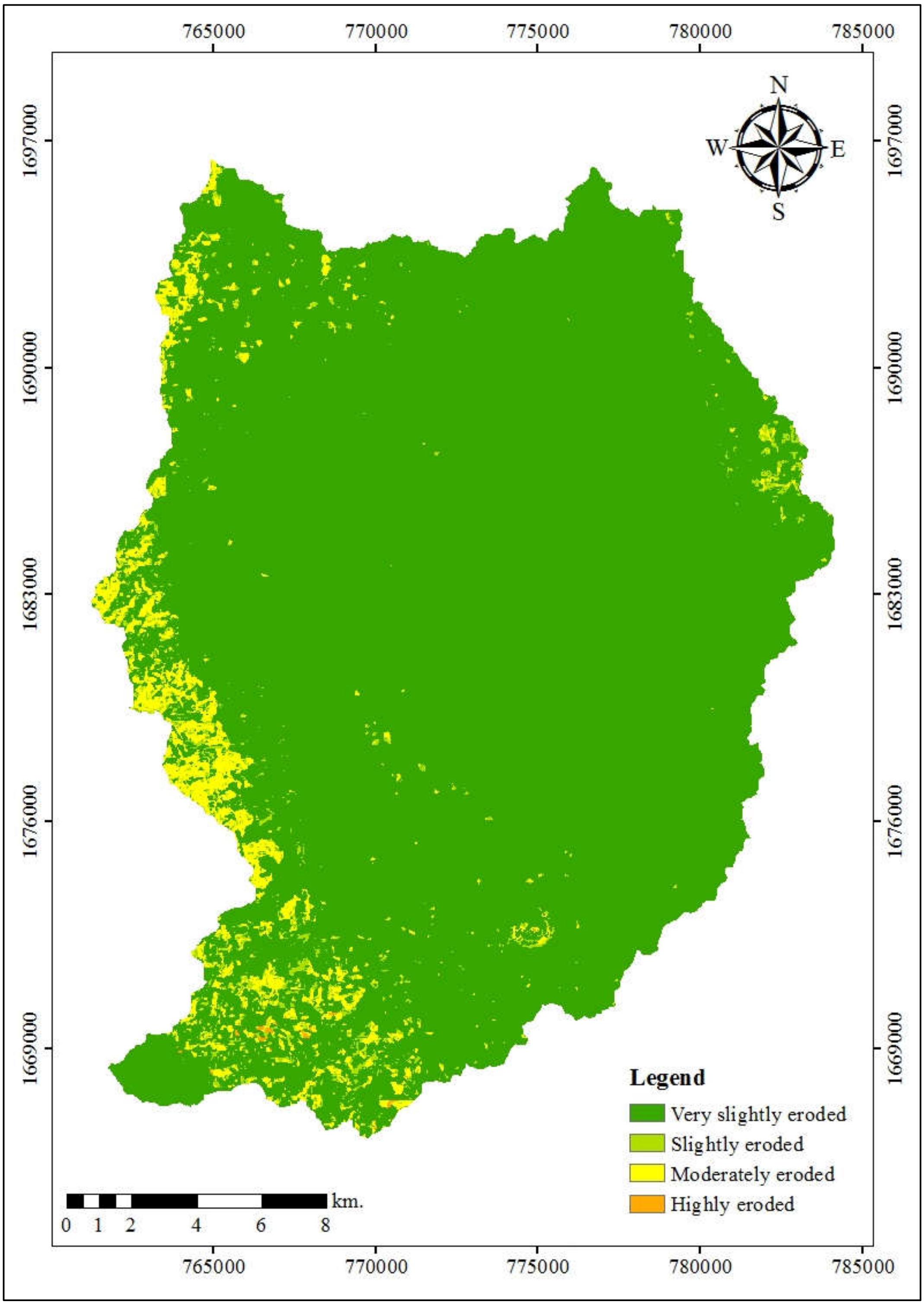

Figure 8.6 Soil erosion severity classification.

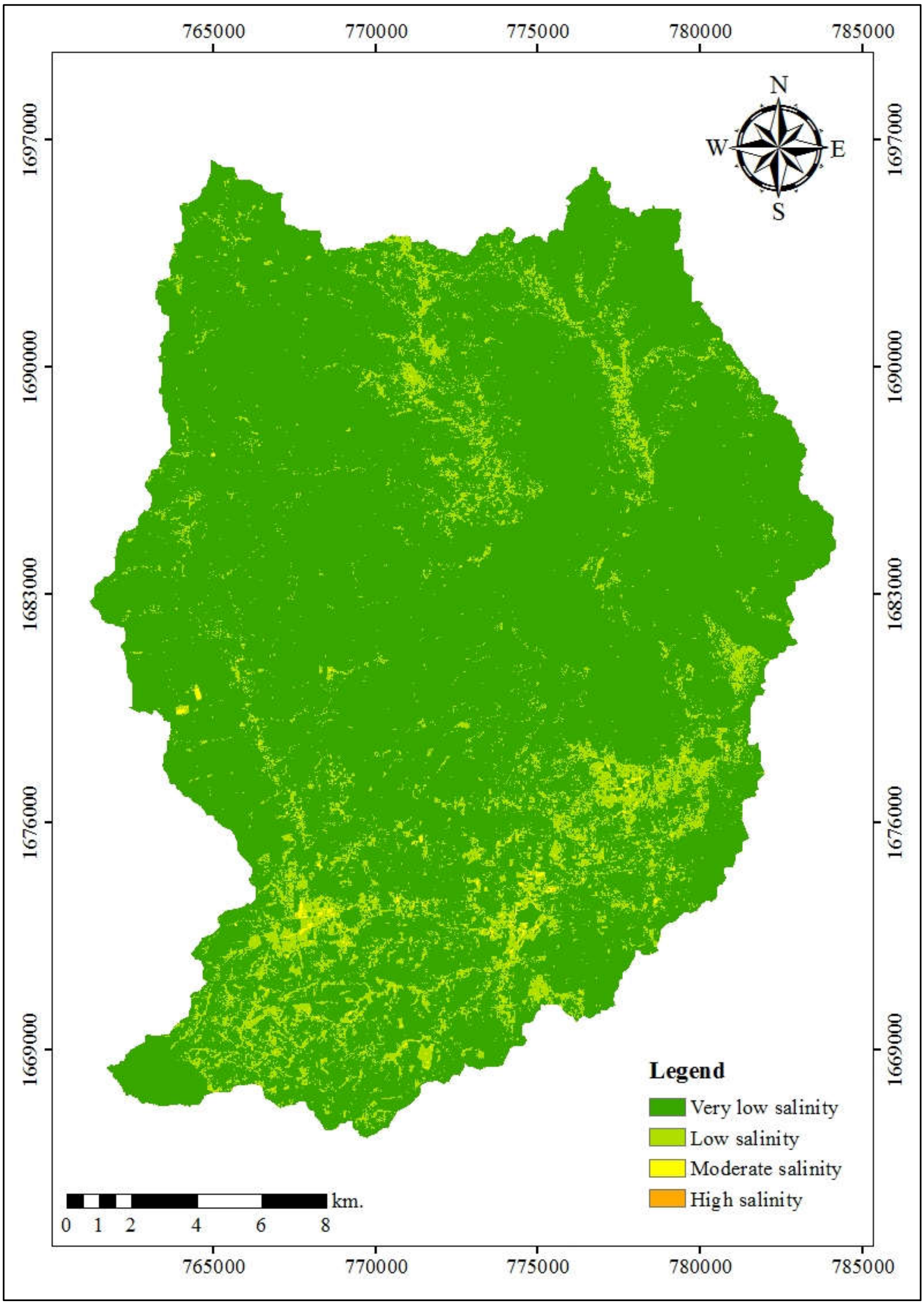

Figure 8.7 Soil salinity severity classification.

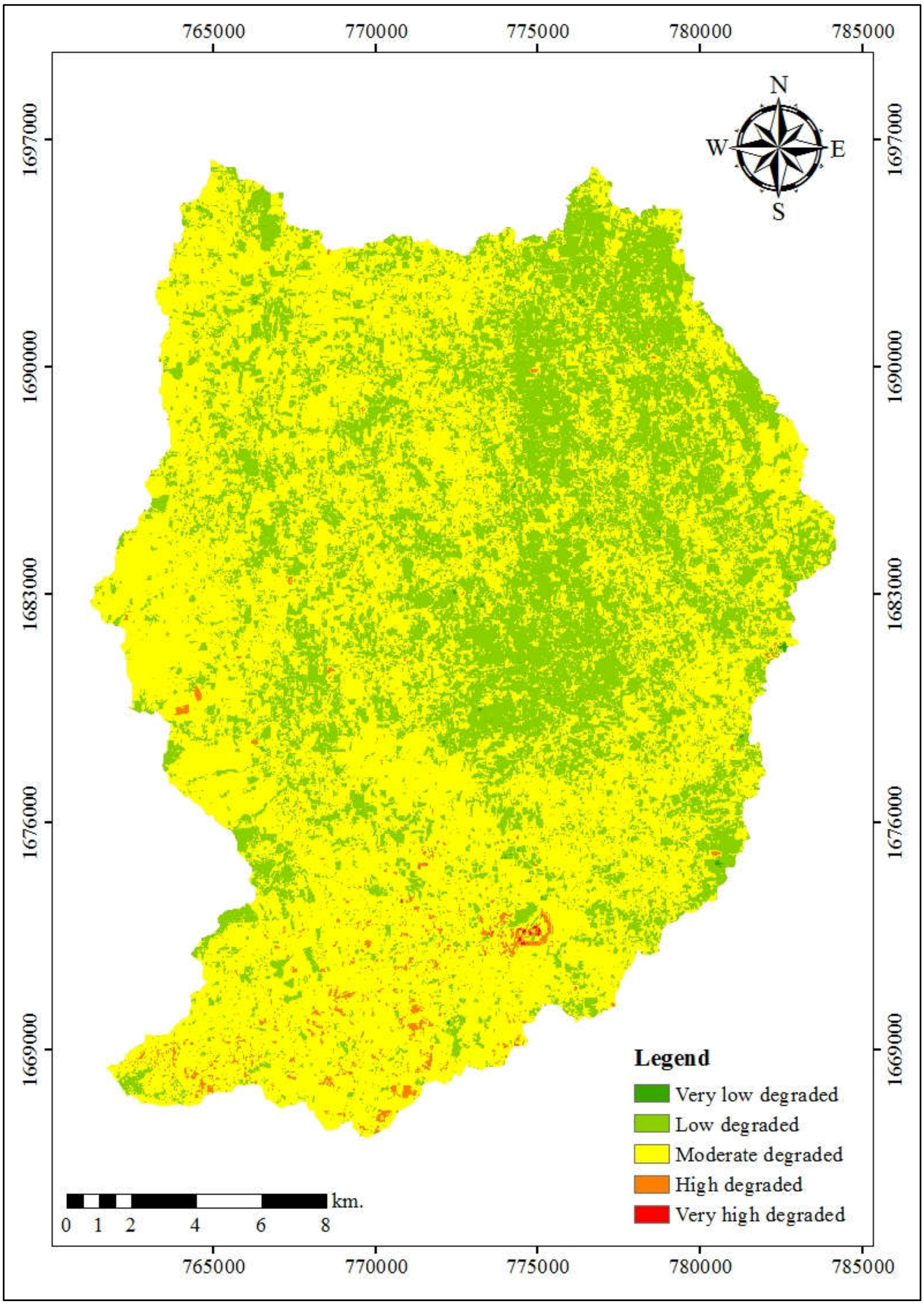

Figure 8.8 Soil biological degradation classification.

The result of soil degradation evaluation using multiplicative method with severity classification is shown in Figure 8.9 while classification of soil degradation with 5 classes: very low, low, moderate, high and very high class using Equal interval method (see Table 3.9) is presented in Figure 8.10. Area and percentage of soil degradation classification using multiplicative method with severity classification is summarized in Table 8.5.

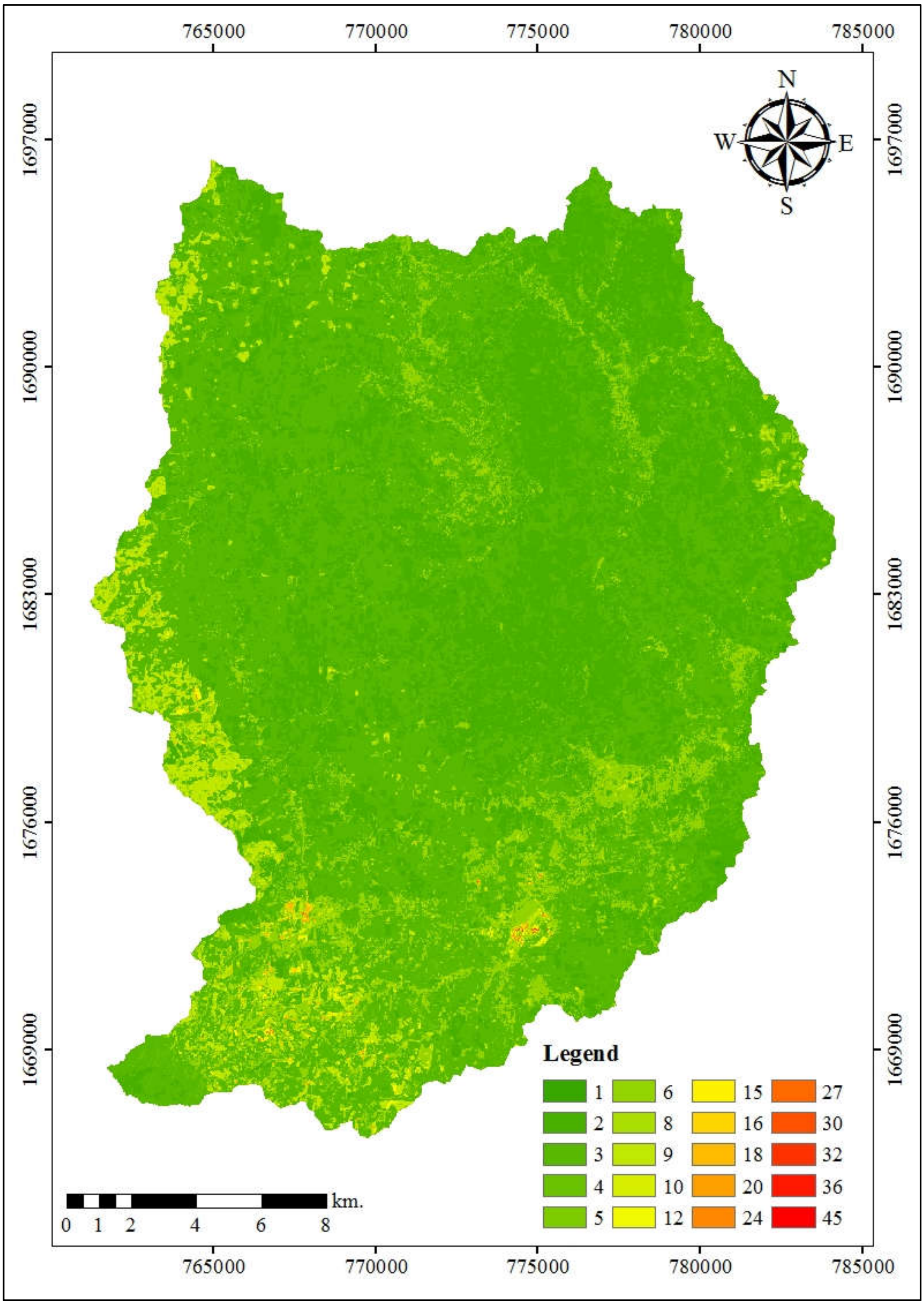

Figure 8.9 Soil degradation evaluation using multiplicative method with severity classification.

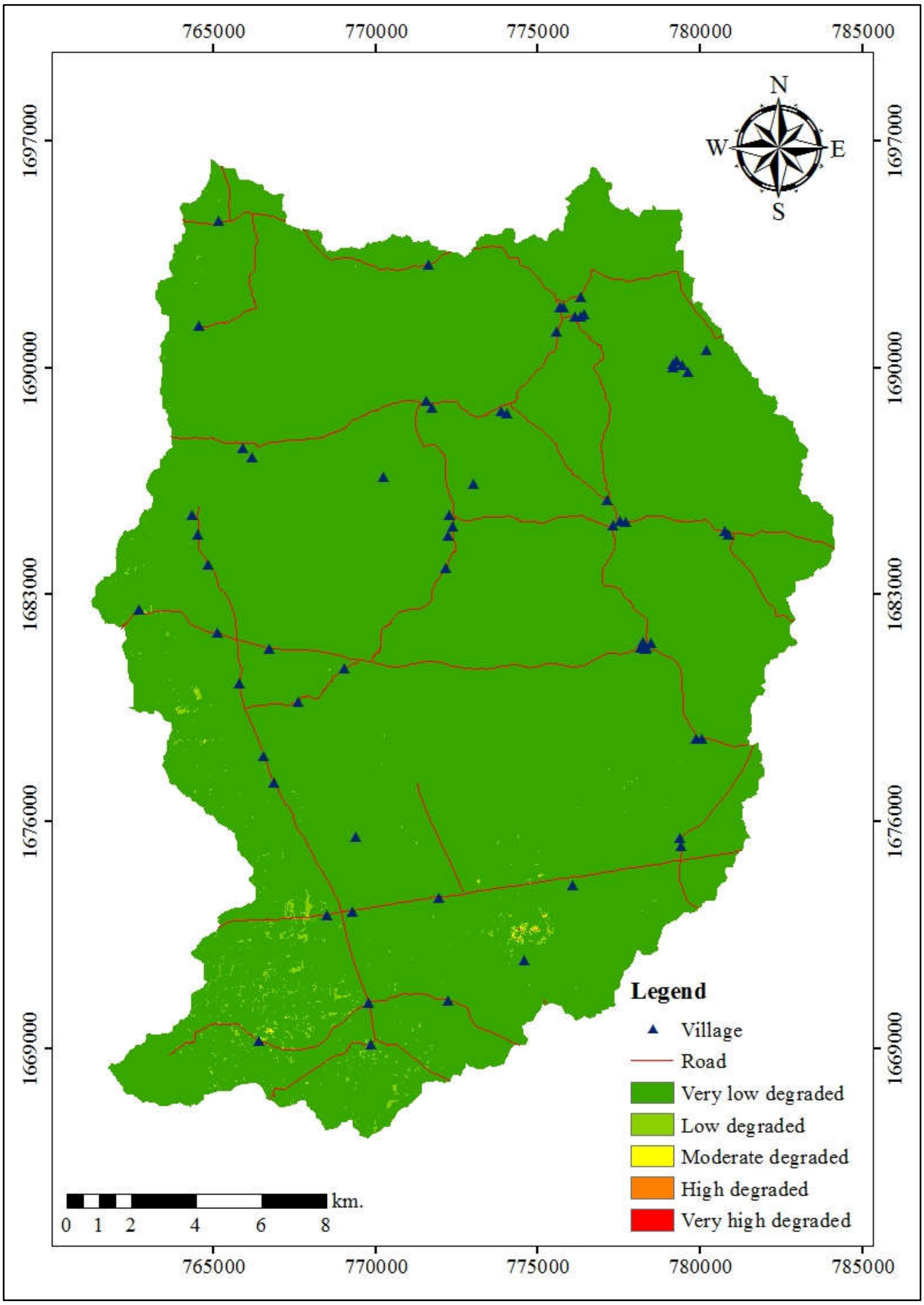

Figure 8.10 Severity class of soil degradation using multiplicative method with severity classification.

Table 8.5 Severity class of soil degradation using multiplication with severity classification.

No.	Severity class of soil degradation	Area in sq. km	Percentage
1	Very low	462.526	99.477
2	Low	2.273	0.489
3	Moderate	0.142	0.031
4	High	0.014	0.003
5	Very High	0.003	0.001
	Total	**464.96**	**100.000**

As a result it reveals that the most dominate soil degradation classes in the study area is very low that covered area of 462.526 sq. km or 99.477% of the total study area. On contrary, high and very high soil degradation only covers area of 0.014 sq. km or about 0.003% and 0.003 sq. km or about 0.001% of the total study area.

In addition, according to overlay analysis between soil degradation classes using multiplicative method with severity classification and LULC data as summary in Table 8.6, top three dominant crops in very low class are cassava, maize, and paddy field. Meanwhile, high and very high classes are mostly found in cassava.

Table 8.6 Soil degradation severity classes using multiplication with severity classification and LULC classes.

Land use and land cover classes	Soil degradation severity classes									
	Very Low		Low		Moderate		High		Very High	
	Sq.km.	%	Sq.km.	%	Sq.km.	%	Sq.km.	%	Sq.km.	%
Urban and built-up area	6.629	1.426	0.011	0.002	0.000	0.000	0.000	0.000	0.000	0.000
Paddy field	21.247	4.570	0.000	0.000	0.000	0.000	0.000	0.000	0.000	0.000
Maize	31.561	6.788	0.000	0.000	0.000	0.000	0.000	0.000	0.000	0.000
Sugarcane	6.766	1.455	0.000	0.000	0.000	0.000	0.000	0.000	0.000	0.000
Cassava	321.418	69.128	1.020	0.219	0.088	0.019	0.010	0.002	0.003	0.001
Perennial tree and orchard	19.635	4.223	0.203	0.044	0.006	0.001	0.000	0.000	0.000	0.000
Dense deciduous forest	4.106	0.883	0.005	0.001	0.001	0.000	0.000	0.000	0.000	0.000
Disturbed deciduous forest	9.039	1.944	0.004	0.001	0.000	0.000	0.000	0.000	0.000	0.000
Forest plantation	11.858	2.550	0.092	0.020	0.004	0.001	0.002	0.000	0.000	0.000
Water body	5.078	1.092	0.005	0.001	0.000	0.000	0.000	0.000	0.000	0.000
Scrub	1.167	0.251	0.003	0.001	0.000	0.000	0.000	0.000	0.000	0.000
Miscellaneous land	24.022	5.166	0.932	0.201	0.043	0.009	0.002	0.000	0.000	0.000
Total	**462.526**	**99.477**	**2.273**	**0.489**	**0.142**	**0.031**	**0.014**	**0.003**	**0.003**	**0.001**

Furthermore, according to overlay analysis between soil degradation classes using multiplicative without and with severity classification as summary in Table 8.7, it founds that soil degradation severity classes of both multiplication methods are in the same classes about 442.82 sq. km or 95.24% of the total study area. This finding reflects that soil degradation severity classification using multiplication without and with severity classification can provide similar result.

Finally, it can be here concluded that soil degradation problem do not exist in the study area since severity of soil erosion and salinity are very low while soil biological degradation is moderately level.

Table 8.7 Overlay analysis between soil degradation severity classes using multiplication without and with severity classification.

Soil degradation severity classes without classification	Soil degradation severity classes using multiplication with classification					Total area (sq.km.)
	Very low	Low	Moderate	High	Very High	
Very low	442.211	11.086	9.132	0.097	0.000	**462.526**
Low	0.790	0.554	0.643	0.281	0.005	**2.273**
Moderate	0.000	0.030	0.050	0.059	0.003	**0.142**
High	0.001	0.000	0.004	0.007	0.002	**0.014**
Very High	0.000	0.000	0.000	0.001	0.002	**0.003**
Total column (sq.km.)	**443.002**	**11.670**	**9.829**	**0.446**	**0.012**	**464.96**

CHAPTER IX

CONCLUSION AND RECOMMENDATION

Under this chapter, major results according to objectives of the study, which were reported in Chapters IV to VIII, are here separately concluded and recommendations for future research and development are suggested.

9.1 Conclusion

9.1.1 Optimum CART model for LULC classification

An optimum CART model for LULC classification using SPSS statistics software, which applied Blue, Green, Red, NIR, SWIR-1, SWIR-2, Wetness, and Elevation to construct a decision tree for LULC classification, provided an overall accuracy of model-based inference statistic at 87.60%. Meanwhile, thematic accuracy assessment of the classified LULC map based on an optimum CART model were 87.50% and 80.10% for an overall accuracy and Kappa hat coefficient, respectively.

9.1.2 Soil erosion assessment and its severity

The result of soil erosion analysis using RMMF model provided an average soil loss of 3.368 ton/ha/year with minimum value of 0 ton/ha/year over urban and built-up area and water bodies and with maximum value of 278.196 ton/ha/year over miscellaneous land. According to soil severity classification, the most dominant soil loss severity class was very slightly eroded (≤ 6.25 ton/ha/year) and it covered area of 437.70 sq. km or about 94.14% of the total study area. On contrary, moderately and highly eroded classes covered area of 17.98 sq. km and 0.31 sq. km or 3.87% and 0.06% of the total study area, respectively.

9.1.3 Soil salinity assessment and its severity

The optimum EC estimation model from multiple linear equation (Y = -5.270 - 0.000008*SI2 + 1.531523*S1 + 0.047627*S3 - 0.002451*S4 + 0.043484*S5 + 0.013310*S6) was here applied to assess soil salinity data and it was then used to classify its severity. As a result, the most dominant soil salinity severity class was very low and it covered area of 415.55 sq. km or about 89.374% of the total study area. In contrast, high soil salinity class covered area of 0.01 sq. km or about 0.002% of the total study area.

9.1.4 Soil organic matter assessment and its depletion

The optimum soil organic matter estimation model from multiple linear equation (Y = 1.058 - 0.607 * Band2 + 0.777 * Band3 - 0.147 * Band4 - 0.032 * Band5 + 0.008 * Band6 - 0.011 * Slope + 73.963 * CI - 61.988 * SI) was here applied to create soil organic matter data and it was then used to classify its severity. As a result, the dominant biological degradation classes in the study area were moderate and low that covered area of 296.05 sq. km or 63.67% and 163.43 sq. km or 35.15% of the total study area, respectively. In contrast, very high biological degradation class covered area of 0.08 sq. km or 0.02% of the total study area.

9.1.5 Soil degradation evaluation

For soil degradation evaluation using multiplicative method without severity classification, it revealed that the most dominant soil degradation class was very low class that covered area of 443.00 sq. km or 95.278% of the total study area. On contrary, high and very high soil degradation classes only covered area of 0.45 sq.

km and 0.01 sq. km or about 0.096% and 0.003% of the total study area. Meanwhile, for soil degradation evaluation using multiplicative method with severity classification, it was found that the most dominant soil degradation class in the study area was also very low that covered area of 462.526 sq. km or 99.477% of the total study area. On contrary, high and very high soil degradation only covered area of 0.014 sq. km or about 0.003% and 0.003 sq. km or about 0.001% of the total study area. Soil degradation severity classification using multiplication without and with severity classification provided similar result with common severities classes about 442.82 sq. km or 95.24% of the total study area. In addition, it can be here concluded that soil degradation problem do not exist in the study area since severity of soil erosion and salinity were very low while soil biological degradation was moderate.

In conclusion, it appears that geoinformatics technology, particularly remote sensing and GIS can be efficiently used as tools to assess soil loss, soil salinity, soil organic matter and their severities for soil degradation evaluation.

9.2 Recommendation

Many objectives were here investigated and implemented, the possibly expected recommendations could be made for further studies as following.

(1) For RMMF model, the input parameters of RMMF model were acquired from literature reviews. Therefore, more field measurement is recommended for the input parameters in order to achieve the realistic model results and it should validate model from data collection of field, for example, plant height and bulk density.

(2) Soil degradation evaluation should be tested in other area which exists actual soil degradation problems include severe soil loss, soil salinity and depletion of soil organic matter for validation of the research framework.

(3) The procedure of soil degradation assessment was here successful implemented by integration of three indicators: soil erosion, soil salinity, and soil biological degradation using geoinformatics technology, particularly remote sensing, GIS and GPS. The developed procedure can be used as a guideline for soil scientist under government offices, e.g. Land Development Department, Department of Agriculture, Department of Agricultural Extension and Department of Mineral Resources, to assess soil degradation in the future.

REFERENCES

REFERENCES

Abbas, A. and Khan, S. (1999). Using remote sensing techniques for appraisal of irrigated soil salinity. **Commonwealth Scientific and Industrial Research Organization (CSIRO).** 2632-2638.

Al-Khaier, F. (2003). **Soil salinity detection using satellite remote sensing.** M.S. thesis, ITC, Netherlands.

Arunin, S. (1989). Reforestation as preventive measure for salinization in Northeast. **J. Agric. Sci.** 22: 141-153. Quoted in Katawatin, R. and Sukchan, S. (2012). Mapping soil salinity and soil erosion in Thailand with emphasis on computer-assisted techniques. **Pedologist.** 343-354.

Bai, Z. G., Dent, D. L., Olsson, L., and Schaepman, M. E. (2008). Review article: Proxy global assessment of land degradation. **Soil Use and Management**. 23-234.

Basayigit, L. and Dinc, U. (2010). Prediction of soil loss in Lake watershed using GIS: a case study of Egirdir lake, Turkey. **Natural & Environmental Sciences.** 1-11.

Bhattacharyya, R., Ghosh, B. N., and Mishra, P. K. (2015). Soil degradation in India: Challenges and potential solutions. **Sustainability 2015.** 7: 3528-3570.

Bowden, P. (2007). **Create carbon sinks by increasing soil organic matter.** [On-line]. Available: http://www.dpi.nsw.gov.au/archive/agriculture-today-stories/ag-today-archives/june-2007/carbon-sinks. (Edition of Agriculture Today in June 2007.

Coleman T. and Montgomery O. (1987). Soil moisture, organic matter and iron content effect on spectral characteristics of selected Vertisols and Alfisols in Alabama. **Photogrammetric Engineering and Remote Sensing**. 53: 1659-1663. In **An official journal of the Italian Society of Remote Sensing. European Journal of Remote Sensing.** 47: 557-573.

De Paz, J. M, Sa´nchez, J. and Visconti, F. (2006). Combined use of GIS and environmental indicators for assessment of chemical, physical and biological soil degradation in a Spanish Mediterranean region. **J. Environ. Manage**. 79: 150-162.

Douaoui, A. E. K., Nicolas, H. and Walter, C. (2006). Detecting salinity hazards within a semiarid context by means of combining soil and remote sensing data. **Geoderma**, 134: 217-230.

Dwivedi R. S. (2001). Soil resource mapping: a remote sensing perspective. **Remote Sensing Reviews.** 20: 89-122.

Eaton, D. (1996). **The economics of soil erosion: a model of farm decision-making.** IIED's Environmental Economics Programme. UK. (Unpublished menuscript).

El-Swaify, S. A. (1997). Factors affecting soil erosion hazards and conservation needs for tropical steeplands. **Soil Technol.** 11: 3-6. Quoted in Katawatin, R. and Sukchan, S. (2012). Mapping soil salinity and soil erosion in Thailand with emphasis on computer-assisted techniques. **Pedologist.** 343-354.

Fadhil, M. A. (2009). Land degradation detection using Geo-Information technology for some sites in Iraq. **Journal of Al-Nahrain University**. 12(3): 94-108.

FAO. (2005). **The importance of soil organic matter key to drought-resistant soil and sustained food production.** FAO Soils Bulletin 80. Publishing Management Service.

FAO. (2011). **Land degradation assessment in drylands: Manual for local level assessment of land degradation and sustainable land management.** Food and agriculture organization of the United Nations, Rome, Italy.

Fitzpatrick-Lins, K. (1981). Comparison of sampling procedures and data analysis for a land-use and land cover map. **Photogramm. Eng. Remote. Sens.** 47(3): 343-351.

Greenfield geography. (2014). Causes of soil degradation. [On-line]. Available: http://greenfieldgeography.wikispaces.com/Soil+and+change.

Hagos, D. W. (1998). **Assessment of the effect of present land use on soil degradation, a case study in Lom Kao Area, Central of Thailand.** M.S. thesis, ITC, Netherlands. Quoted in Yazidhi, B. (2003). **A comparative study of soil erosion modeling in Lom Kao-Phetchabun, Thailand.** MS. Thesis, ITC, Netherlands.

Harmsen, K. (1996). Assessment of current erosion damage land druck, Liebefeld. Quoted in Yazidhi, B. (2003). **A comparative study of soil erosion modeling in Lom Kao-Phetchabun, Thailand.** MS. Thesis, ITC, Netherlands.

Hudson, N. (1995). Soil conservation B T Batsford, London. Quoted in Yazidhi, B. (2003). **A comparative study of soil erosion modeling in Lom Kao-Phetchabun, Thailand.** MS. Thesis, ITC, Netherlands.

Huete, A. (2004). (2004, May 3). Remote sensing of terrestrial ecosystems. **Remote Sensing for Natural Resource Management and Environmental Monitoring.** 1-52.

Ines, R. L. (2013). Soil erosion modeling for a micro watershed. The Canadian society for Bioengineering. **The Canadian society for engineering.** 1-13.

Iqbal, S. and Mastorakis, N. (2015). Soil salinity detection using RS data. **Advances in Environmental Science and Energy Planning.** 277-281.

Ishaq, S., Begum, F., Ali, K., Ahmed, S., Ali, S., Ali, H., Baig, S. S., Khan, M. Z. and Ali, S. (2015). Soil quality assessment using selected physico-chemical indicators in Altit Hunza, Gilgit-Baltistan. **Journal of Biodiversity and Environmental Sciences (JBES).** 6(1): 454-459.

Japakasetr, T. and Workman, D. R. (1981). Evaporite deposits of Northeast Thailand. **American Assoc. of Petroleum Geologists**. 179-187. Quoted in Montoroi, J. P., Grünberger, O., Sukchan, S., and Kungklang, N. (2006). Self-potential method applied to salt-affected soils of Thailand [Abstract no. 607-7962/gra/EGU06-A-10193] **Geophysical Research Abstracts**. 1-2.

Jessica, A. T. (2002). **Land degradation detection, mapping and monitoring in the lake Naivasha Basin, Kenya.** M.S. Thesis, ITC, the Netherlands.

Jha, M. K. and Paudel, R. C. (2010). Erosion predictions by empirical models in a mountainous watershed in Nepal. **Journal of Spatial Hydrology.** 10(1): 89-102.

Jumpa, K. (2012). **Developing a spatial model for soil degradation assessment in Nakhon Ratchasima province, Thailand.** Land Development Department.

Ministry of Agriculture and Cooperatives, Thailand. (Unpublished menuscript).

Kamonrat, T. (2011). **The application of Geo-information technology and mathematic model for soil erosion assessment in the Upper Lam Phra Phloeng watershed, Nakhon Ratchasima province, Thailand.** MS. Thesis, Thammasat University.

Kamonrat, T. and Jirakajohnkool, S. (2012). The application of Geo-information technology and mathematic model for soil erosion assessment in the Upper Lam Phra Phloeng watershed, Nakhon Ratchasima province, Thailand. **Thammasat International Journal of Science and Technology.** 20(2): 167-177.

Kapalanga, T. S. (2008). A review of land degradation assessment methods. **Land Restoration Training Programme.** 17-68.

Katawatin, R. and Sukchan, S. (2012). Mapping soil salinity and soil erosion in Thailand with emphasis on computer-assisted techniques. **Pedologist.** 343-354.

Keller, S. (2010). **Soil degradation.** [On-line]. Available: http://www.sswm.info/category/step-university/module-8-water-and-sanitation-futurechallenges/module-8-water-and-sanita-6.

Khan, N. M., Rastoskuev, V. V., Sato, Y. and Shiozawa, S. (2005). Assessment of hydrosaline land degradation by using a simple approach of remote sensing indicators. **Agric. Water Manage.** 77: 96–109.

Kheoruenromne, I. (2005). **Soil Survey.** Department of soil science, Faculty of Agriculture, Kasetsart University. Bangkok.

Kiekebusch, E. (2009). A review of land degradation assessment & monitoring methods. In **Proceedings of the 13th Namibian rangeland forum conference: The role of biodiversity in rangeland management and policy biodiversity in rangeland management and policy** (pp 1-30), Neudamm Agricultural College, Windhoek.

Lal, R. (1998). Soil Quality and Sustainability, In R. Lal., W. H. Blum., C. Valentine., and B. A. Stewart (eds.). **Methods for assessment of soil degradation, Advances in Soil.** CRC Press LLC. Florida, United States.

Lanyon, D. M., Cass, A. and Hansen, D. (2004). **The Effect of Soil Properties on Vine Performance.** CSIRO land and water technical. Langhorne Creek, South Australia.

Lawrence, R. L. and Wright, A. (2001), Rule-Based Classification Systems Using Classification and Regression Tree (CART) Analysis. **Photogrammetric Engineering & Remote Sensing.** 67(10): 1137-1142.

LDD and ITC. (2002). **Land degradation project approach.** [On-line]. Available: http://www.ldd.go.th/Efiles_project/ldd_plannig/welcome/index.html.

LDD. (2000). **Soil loss map of Thailand. LDD.** Land Development Department (LDD), Ministry of agriculture and cooperatives. Bangkok, Thailand.

LDD. (2001). **Manual on saline soils for government services, saline soil improvement group**. Land Development Department, Bangkok, Thailand. Quoted in Katawatin, R. and Sukchan, S. (2012). Mapping soil salinity and soil erosion in Thailand with emphasis on computer-assisted techniques. **Pedologist**. 343-354.

LDD. (2011). **Manual of Data Analysis and Land Use Classification Using Land Cover Classification System of the Food and Agriculture Organization (FAO).** Office of soil resources survey and research. Bangkok, Thailand

LDD. (2015). **State of soil and land resources of Thailand.** LDD, Ministry of Agriculture and Cooperatives, Bangkok, Thailand: The agricultural co-operative federation of Thailand.

Lickacz, J. and Penny, D. (2001). **Soil organic matter**. [On-line]. Available: http://www1.agric.gov.ab.ca/%24department/deptdocs.nsf/all/agdex890.

Lillesand, T. M., Kiefer, R. W. and Chipman, J. W. (2004). **Remote Sensing and Image Interpretation.** Wiley, New York.

Lohachart, S. (2015). **Soil erosion and guideline for soil and water conservation.** BMA Training and Development Institute.

Mainguet, M. (1994). Desertification: Natural background and human mismanagement. 2. Quoted in Denti, G. D. (2004). **Developing a desertification indicator system for a small mediterranean catchment: a case study from the Serra De Rodes, Alt Emporda, Catalunya, and Ne Spain.** Ph.D. Dissertation, University of Girona.

Martínez-Murillo, J. F., López-Vicente, M., Poesen, J. and Ruiz-Sinoga, J. (2011). Modelling the effects of land use changes on runoff and soil erosion in two Mediterranean catchments with active gullies, South of Spain. **Landform Analysis.** 17: 99–104.

Mathieu, R. and Pouget, M. (1998). Relationships between satellite-based radiometric indices simulated using laboratory reflectance data and typic soil color of an arid environment. **Remote Sens. Environ.** 66: 17-28.

Matinfar, H. R. and Roodposhti, M. S. (2012). Decision tree land use/ land cover change detection of Khoram Abad city using Landsat imagery and ancillary SRTM data. **Annals of Biological Research.** 3(8): 4045-4053.

Mbagwu, J. S. C. (2003). **Aggregate stability and soil degradation in the tropics.** Department of Soil Science, University of Nigeria, Nsukka, Nigeria.

Mhangara, P. (2011). **Land use/cover change modeling and land degradation assessment in the Keiskamma Catchment using remote sensing and GIS.** Ph.D. Dissertation, Nelson Mandela Metropolitan University.

Mkhonta, M. M. (2000). **Use of remote sensing and geographic information system (GIS) in the assessment of soil erosion in the Gwayimane and Mahhuku catchment areas with special attention on soil erodibility (K-factor).** M.S. Thesis, ITC, Netherlands. Quoted in Yazidhi, B. (2003). **A comparative study of soil erosion modeling in Lom Kao-Phetchabun, Thailand.** MS. Thesis, ITC, Netherlands.

Morgan, R. P. C. (1995). **Soil erosion and conservation (2nd Ed).** Longman Group, Cranfield. Quoted in Yazidhi, B. (2003). **A comparative study of soil erosion modeling in Lom Kao-Phetchabun, Thailand.** MS. Thesis, ITC, Netherlands.

Morgan, R. P. C. (2001). A simple approach to soil loss prediction: a revised Morgan–Morgan–Finney model. **Catena.** 44: 305-322.

Morgan, R. P. C. and Duzant, J. H. (2008). Modification of the revised Morgan–Morgan–Finney model for estimating sediment yield in large river basins. **EGU General Assembly 2012.** 14: 12572.

MSU. (2011). (2011, February). Advanced Soil Organic Matter Management. **Extension Bulletin:** 1-6.

Nagle, G. (2006). (2006, January). Soil degradation – A Creeping Concern?. **GeoFact sheets:** 1351-5136.

Nanna, S. (1996). **A Geo-Information theoretical approach to inductive erosion modelling based on terrain mapping units.** Ph.D. Dissertation, Wageningen Agricultural University, Wageningen. Quoted in Yazidhi, B. (2003). **A comparative study of soil erosion modeling in Lom Kao-Phetchabun, Thailand.** MS. Thesis, ITC, Netherlands.

NSO. (2015). **Statistics of Rainfall at Meteorology Station, Nakhon Ratchasima Province: 2003 – 2015.** [On-line]. Available: http://service.nso.go.th/nso/ web/ statseries/statseries 27.html.

Oldeman, L. R. (1994). The global extent of soil degradation. In: D. J. Greenland. and I. Szabolcs (eds.). **Soil resilience and sustainable land use.** (115 p), CAB International, Oxon. Quoted in Katawatin, R. and Sukchan, S. (2012). Mapping soil salinity and soil erosion in Thailand with emphasis on computer-assisted techniques. **Pedologist.** 343-354.

Patterson, R. A. (2006). Consideration of soil salinity when assessing land application of effluent or greywater. **Septic safe: protect your health and environment, Environment & health protection guidelines on-site sewage management for single households.** Department of local government. 1-6.

Petter, P. (1992). **GIS and remote sensing for soil erosion studies in semi-arid environments.** Ph.D. Dissertation, University of Lund, Lund. Quoted in

Yazidhi, B. (2003). **A comparative study of soil erosion modeling in Lom Kao-Phetchabun, Thailand.** MS. Thesis, ITC, Netherlands.

Prince, S. D. (2002). Spatial and temporal scales for identification of desertification. In J. F. Reynolds and D. M. Stafford Smith (eds.). **Global desertification: Do humans cause deserts?** (pp 24-37). Dahlem Workshop Report 88, Dahlem University Press, Berlin. Quoted in Mambo, J. and Archer, E. (2006). An assessment of land degradation in the Save catchment of Zimbabwe. Journal compilation area. 39(3): 380-391.

Richards, L. A. (1954). **Diagnosis and improvement of saline and alkaline soils.** USDA Handbook No. 60, Washington, DC.

Roo, A. P. J. (1993). **Modelling Surface Runoff and Soil Erosion in Catchments Using Geograpgical Information Systems.** Ph.D. Dissertation, Utrecht University, Utrecht. Quoted in Yazidhi, B. (2003). **A comparative study of soil erosion modeling in Lom Kao-Phetchabun, Thailand.** M.S. Thesis, ITC, the Netherlands.

Sapkota, R. (2008). **Modelling runoff and erosion in Namchun Watershed, Thailand.** M. S. Thesis, ITC, the Netherlands.

Saravisutra, A. (2010). **Urban growth pattern modeling and quality of life prediction in Mueang Nakhon Ratchasima district.** Ph.D. Dissertation, Suranaree University of Technology.

Sethabut, P. (2008). **Green mirror desertification.** [On-line]. Available: http://library.cmu.ac.th/ntic/knowledge_show.php?docid=20.

Singh, B. K., Verma, K. and Thoke, A. S. (2015). Investigations on impact of feature normalization techniques on classifier's performance in breast tumor classification. **Int. J. Comput. Appl. Technol**. 116(19): 11-15.

Singh, R. P. and Sirohi, A. (1994). Spectral Reflectance Proper-Ties of Different Types of Soil Surfaces. **ISPRS Journal of Photogrammetry and Remote Sensing.** 49(4): 34-40.

Sobprasonk, N. (2009). **Soil degradation status in Khun Wang Area, Mae Wang district, Chiang Mai province.** M.S. Thesis, Kasetsart University.

SOCO (2009). (2009, May). Organic matter decline. **Sustainable Agriculture and Soil Conservation:** 1-4.

Srisomkiew, S. (2014). Soil degradation assessment using FAO guideline in Kaset Wisai district of Roi Et province in Thailand. **International Symposium on Geoinformatics for Spatial Infrastructure Development in Earth and Allied Sciences 2014**. 1-8.

Suriyaprasit, M. (2008). **Digital terrain analysis and image processing for assessing erosion prone areas: A case study of Nam Chun Watershed, Phetchabun, Thailand.** M.S. Thesis, ITC, the Netherlands.

Thinley, U. (2008). **Spatial modeling for soil erosion assessment in Upper Lam Phra Phloeng Watershed, Nakhon Ratchasima, Thailand.** M.S. Thesis, Suranaree University of Technology.

Tingting, L., Xiaoyu, S., Dandan, Z., Zhenshan, X. and Jianminga, G. (2008). Assessment of soil erosion risk in Northern Thailand. **The International Archives of the Photogrammetry, Remote Sensing and Spatial Information Sciences.** 37: 703-708.

Toparkngarm, B. (2006). **Saline soils in Northeast Thailand**. (pp 177-223). Quoted in Katawatin, R. and Sukchan, S. (2012). Mapping soil salinity and soil erosion in Thailand with emphasis on computer-assisted techniques. **Pedologist.** 343-354.

Torahi, A. A. (2012). Rangeland dynamics monitoring using remotely sensed data, in Dehdez Area, Iran. In **proceedings of the International Conference on Applied Life Sciences (ICALS2012)** (pp 10-12). Turkey.

Tully, K., Sullivan, C., Weil, R. and Sanchez, P. (2015). The state of soil degradation in Sub-Saharan Africa: Baselines, trajectories, and solutions. **Sustainability 2015**. 7: 6523-6552.

Udomsri, S., Huntrakoon, K. and Wattana, S. (2004). **Characterization of established soil series in the Central plain region of Thailand reclassified according to soil taxonomy 2003.** LDD. Thailand.

UNEP. (2006). **Africa environment outlook 2: our environment**, Our Wealth. UNEP/Earthprint, United Nations Environment Programme.

USDA. (2012). **Soil sheet, rill and wind erosion.** [On-line]. Available: www.nrcs.usda.gov.

USGS. (2015). **Frequently asked questions about the Landsat missions.** [On-line]. Available: http://landsat.usgs.gov/best_spectral_bands_to_use.php.

Warren, A. (2002). Land degradation is contextual**. Land degradation & development**. 13: 449-459.

Weil, R. R. and Brady, N. (2015). **Nature and properties of soils (15th Edition)**. Pearson. United States of America. Quoted in Tully, K., Sullivan, C., Weil, R.

and Sanchez, P. (2015). The state of soil degradation in Sub-Saharan Africa: Baselines, trajectories, and solutions. **Sustainability 2015**. 7: 6523-6552.

Williamson, D. R., Peck, A. J., Turner, J. V. and Arunin, S. (1989). Groundwater hydrology and salinity in a valley in Northeast Thailand. In **Groundwater contamination.** 185: 147-154. Quoted in Montoroi, J. P., Grünberger, O., Sukchan, S. and Kungklang, N. (2006). Self-potential method applied to salt-affected soils of Thailand [Abstract no. 607-7962/gra/EGU06-A-10193] **Geophysical Research Abstracts**. 1-2.

Wim, G. and El Hadji, M. (2002). Causes, general extent and physical consequence of land degradation in arid, semi-arid and dry sub humid areas. **Forest Conservation and natural resources, Forest Dept.** FAO, Rome, Italy. Quoted in Kavvadias, V. A. (n.d.). Soil degradation. **Soil science institute of Athens-national agricultural research foundation.** 1-17.

Xiaodong, N., Shuqing, Z., Huaiqing, A., Xiaofeng, L., Huan, Y. and Chunyue, L. (2009). Integrating TM and ancillary geographical data with classification trees for land cover classification of Marsh area. **Chin. Geogra. Sci.** 19(2): 177-185.

Yazidhi, B. (2003). **A comparative study of soil erosion modeling in Lom Kao-Phetchabun, Thailand.** MS. Thesis, ITC, Netherlands.

APPENDICES

APPENDIX A

COMBINATION BETWEEN SOIL SERIES AND LULC DATA FOR SAMPLE POINT ALLOCATION

Table A.1 Combination between soil series and LULC data for sample point allocation.

No.	Soil and LULC combination	LULC	Soil series
1	5	Urban and built-up area (URBAN)	Ban Mi (Bm-A)
2	15	Urban and built-up area (URBAN)	Ban Mi (Bm-A)
3	29	Urban and built-up area (URBAN)	Ban Mi (Bm-A)
4	55	Urban and built-up area (URBAN)	Ban Mi (Bm-A)
5	82	Urban and built-up area (URBAN)	Ban Mi (Bm-A)
6	84	Urban and built-up area (URBAN)	Ban Mi (Bm-A)
7	88	Urban and built-up area (URBAN)	Ban Mi (Bm-A)
8	95	Urban and built-up area (URBAN)	Ban Mi (Bm-A)
9	97	Urban and built-up area (URBAN)	Ban Mi (Bm-A)
10	100	Urban and built-up area (URBAN)	Kula Ronghai (Ki-A)
11	106	Urban and built-up area (URBAN)	Kula Ronghai (Ki-A)
12	121	Urban and built-up area (URBAN)	Kula Ronghai (Ki-A)
13	123	Urban and built-up area (URBAN)	Kula Ronghai (Ki-A)
14	126	Urban and built-up area (URBAN)	Kula Ronghai (Ki-A)
15	131	Urban and built-up area (URBAN)	Kula Ronghai (Ki-A)
16	135	Urban and built-up area (URBAN)	Kula Ronghai (Ki-A)
17	136	Urban and built-up area (URBAN)	Kula Ronghai (Ki-A)
18	176	Urban and built-up area (URBAN)	Kula Ronghai (Ki-A)
19	181	Paddy field (PF)	Kula Ronghai (Ki-A)
20	191	Paddy field (PF)	Nong Bunnak (Nbn-A)
21	205	Paddy field (PF)	Nong Bunnak (Nbn-A)
22	218	Paddy field (PF)	Nong Bunnak (Nbn-A)
23	231	Paddy field (PF)	Nong Bunnak (Nbn-A)
24	258	Paddy field (PF)	Nong Bunnak (Nbn-A)
25	271	Paddy field (PF)	Nong Bunnak (Nbn-A)
26	273	Paddy field (PF)	Nong Bunnak (Nbn-A)
27	276	Paddy field (PF)	Nong Bunnak (Nbn-A)
28	282	Paddy field (PF)	Nong Bunnak (Nbn-A)
29	297	Paddy field (PF)	Nong Bunnak (Nbn-A)
30	299	Paddy field (PF)	Ratchaburi (Rb-A)
31	307	Paddy field (PF)	Ratchaburi (Rb-A)
32	311	Paddy field (PF)	Ratchaburi (Rb-A)
33	312	Paddy field (PF)	Urban and built-up area (URBAN)
34	352	Paddy field (PF)	Urban and built-up area (URBAN)
35	357	Maize (MAIZE)	Urban and built-up area (URBAN)
36	367	Maize (MAIZE)	Urban and built-up area (URBAN)
37	381	Maize (MAIZE)	Urban and built-up area (URBAN)
38	407	Maize (MAIZE)	Urban and built-up area (URBAN)

Table A.1 (Continued).

No.	Soil and LULC combination	LULC	Soil series
39	434	Maize (MAIZE)	Urban and built-up area (URBAN)
40	436	Maize (MAIZE)	Urban and built-up area (URBAN)
41	440	Maize (MAIZE)	Urban and built-up area (URBAN)
42	447	Maize (MAIZE)	Urban and built-up area (URBAN)
43	449	Maize (MAIZE)	Urban and built-up area (URBAN)
44	450	Maize (MAIZE)	Wang Nam Khieo (Wk-D)
45	452	Maize (MAIZE)	Wang Nam Khieo (Wk-D)
46	453	Maize (MAIZE)	Wang Nam Khieo (Wk-D)
47	458	Maize (MAIZE)	Wang Nam Khieo (Wk-B)
48	473	Maize (MAIZE)	Wang Nam Khieo (Wk-B)
49	475	Maize (MAIZE)	Wang Nam Khieo (Wk-B)
50	476	Maize (MAIZE)	Wang Nam Khieo (Wk-B)
51	478	Maize (MAIZE)	Wang Nam Khieo (Wk-B)
52	483	Maize (MAIZE)	Wang Nam Khieo (Wk-B)
53	487	Maize (MAIZE)	Wang Nam Khieo (Wk-B)
54	528	Maize (MAIZE)	Wang Nam Khieo (Wk-B)
55	533	Sugarcane (SGC)	Wang Nam Khieo (Wk-B)
56	543	Sugarcane (SGC)	Wang Nam Khieo (Wk-B)
57	557	Sugarcane (SGC)	Wang Nam Khieo (Wk-B)
58	583	Sugarcane (SGC)	Wang Nam Khieo (Wk-B)
59	610	Sugarcane (SGC)	Bo Thai (Bo-B)
60	616	Sugarcane (SGC)	Bo Thai (Bo-B)
61	619	Sugarcane (SGC)	Bo Thai (Bo-B)
62	623	Sugarcane (SGC)	Bo Thai (Bo-B)
63	624	Sugarcane (SGC)	Bo Thai (Bo-B)
64	625	Sugarcane (SGC)	Bo Thai (Bo-B)
65	626	Sugarcane (SGC)	Ban Phi (Bpi-B)
66	627	Sugarcane (SGC)	Ban Phi (Bpi-B)
67	628	Sugarcane (SGC)	Ban Phi (Bpi-B)
68	629	Sugarcane (SGC)	Ban Phi (Bpi-B)
69	635	Sugarcane (SGC)	Ban Phi (Bpi-B)
70	636	Sugarcane (SGC)	Ban Phi (Bpi-B)
71	638	Sugarcane (SGC)	Ban Phi (Bpi-B)
72	647	Sugarcane (SGC)	Ban Phi (Bpi-B)
73	649	Sugarcane (SGC)	Ban Phi (Bpi-B)
74	651	Sugarcane (SGC)	Ban Phi&Chom Phra (Bpi/Cpr-B)
75	652	Sugarcane (SGC)	Ban Phi&Chom Phra (Bpi/Cpr-B)
76	654	Sugarcane (SGC)	Ban Phi&Chom Phra (Bpi/Cpr-B)

Table A.1 (Continued).

No.	Soil and LULC combination	LULC	Soil series
77	657	Sugarcane (SGC)	Ban Phi&Nam Phong (Bpi/Ng-B)
78	663	Sugarcane (SGC)	Ban Phi&Nam Phong (Bpi/Ng-B)
79	690	Sugarcane (SGC)	Ban Phi&Nam Phong (Bpi/Ng-B)
80	709	Cassava (CAS)	Ban Phi&Nam Phong (Bpi/Ng-B)
81	719	Cassava (CAS)	Ban Phi&Nam Phong (Bpi/Ng-B)
82	733	Cassava (CAS)	Ban Phi&Nam Phong (Bpi/Ng-B)
83	746	Cassava (CAS)	Ban Phi&Nam Phong (Bpi/Ng-B)
84	759	Cassava (CAS)	Chum Puang (Cpg-B)
85	777	Cassava (CAS)	Chum Puang (Cpg-B)
86	786	Cassava (CAS)	Chum Puang (Cpg-B)
87	788	Cassava (CAS)	Chum Puang (Cpg-B)
88	792	Cassava (CAS)	Chum Puang (Cpg-B)
89	794	Cassava (CAS)	Chum Puang (Cpg-B)
90	795	Cassava (CAS)	Chum Puang (Cpg-B)
91	799	Cassava (CAS)	Chum Puang (Cpg-B)
92	800	Cassava (CAS)	Chum Puang (Cpg-B)
93	801	Cassava (CAS)	Chum Puang (Cpg-B)
94	802	Cassava (CAS)	Chum Puang (Cpg-B)
95	803	Cassava (CAS)	Chum Puang (Cpg-B)
96	804	Cassava (CAS)	Chum Puang (Cpg-B)
97	805	Cassava (CAS)	Chum Puang (Cpg-B)
98	810	Cassava (CAS)	Chum Puang (Cpg-B)
99	811	Cassava (CAS)	Chum Puang (Cpg-B)
100	812	Cassava (CAS)	Chum Puang (Cpg-B)
101	814	Cassava (CAS)	Chatturat (Ct-B)
102	823	Cassava (CAS)	Chatturat (Ct-B)
103	825	Cassava (CAS)	Chatturat (Ct-B)
104	827	Cassava (CAS)	Chatturat (Ct-B)
105	828	Cassava (CAS)	Chatturat (Ct-B)
106	830	Cassava (CAS)	Chatturat (Ct-B)
107	833	Cassava (CAS)	Chatturat (Ct-B)
108	835	Cassava (CAS)	Chatturat (Ct-B)
109	839	Cassava (CAS)	Chatturat (Ct-B)
110	840	Cassava (CAS)	Chatturat (Ct-B)
111	845	Cassava (CAS)	Chatturat&Sung Noen (Ct/Sn-B)
112	863	Cassava (CAS)	Chatturat&Sung Noen (Ct/Sn-B)
113	866	Cassava (CAS)	Chatturat&Sung Noen (Ct/Sn-B)
114	872	Cassava (CAS)	Chatturat&Sung Noen (Ct/Sn-B)

Table A.1 (Continued).

No.	Soil and LULC combination	LULC	Soil series
115	876	Cassava (CAS)	Chatturat&Sung Noen (Ct/Sn-B)
116	880	Cassava (CAS)	Chatturat&Sung Noen (Ct/Sn-B)
117	935	Perennial tree and orchard (TREE)	Dan Khun Thot (Dk-B)
118	953	Perennial tree and orchard (TREE)	Dan Khun Thot (Dk-B)
119	962	Perennial tree and orchard (TREE)	Dan Khun Thot (Dk-B)
120	968	Perennial tree and orchard (TREE)	Dan Khun Thot (Dk-B)
121	970	Perennial tree and orchard (TREE)	Dan Khun Thot (Dk-B)
122	971	Perennial tree and orchard (TREE)	Dan Khun Thot (Dk-B)
123	975	Perennial tree and orchard (TREE)	Dan Khun Thot (Dk-md-B)
124	976	Perennial tree and orchard (TREE)	Dan Khun Thot (Dk-md-B)
125	979	Perennial tree and orchard (TREE)	Dan Khun Thot (Dk-md-B)
126	981	Perennial tree and orchard (TREE)	Dan Khun Thot (Dk-md-B)
127	988	Perennial tree and orchard (TREE)	Dan Khun Thot (Dk-md-B)
128	999	Perennial tree and orchard (TREE)	Dan Khun Thot (Dk-md-B)
129	1004	Perennial tree and orchard (TREE)	Dan Khun Thot (Dk-md-B)
130	1006	Perennial tree and orchard (TREE)	Dan Khun Thot (Dk-md-B)
131	1009	Perennial tree and orchard (TREE)	Dan Khun Thot (Dk-md-B)
132	1021	Perennial tree and orchard (TREE)	Dan Khun Thot (Dk-md-B)
133	1039	Perennial tree and orchard (TREE)	Dan Sai (Ds-B)
134	1042	Perennial tree and orchard (TREE)	Dan Sai (Ds-B)
135	1048	Perennial tree and orchard (TREE)	Dan Sai (Ds-B)
136	1052	Perennial tree and orchard (TREE)	Dan Sai (Ds-B)
137	1061	Dense deciduous forest (DDF)	Dan Sai (Ds-B)
138	1071	Dense deciduous forest (DDF)	Dan Sai (Ds-B)
139	1085	Dense deciduous forest (DDF)	Dan Sai (Ds-B)
140	1111	Dense deciduous forest (DDF)	Dan Sai (Ds-B)
141	1138	Dense deciduous forest (DDF)	Kong (Kng-B)
142	1140	Dense deciduous forest (DDF)	Kong (Kng-B)
143	1144	Dense deciduous forest (DDF)	Kong (Kng-B)
144	1147	Dense deciduous forest (DDF)	Kong (Kng-B)
145	1151	Dense deciduous forest (DDF)	Kong (Kng-B)
146	1152	Dense deciduous forest (DDF)	Kong (Kng-B)
147	1153	Dense deciduous forest (DDF)	Kong (Kng-B)
148	1154	Dense deciduous forest (DDF)	Kong (Kng-B)
149	1155	Dense deciduous forest (DDF)	Kra Nuan (Knu-B)
150	1156	Dense deciduous forest (DDF)	Kra Nuan (Knu-B)
151	1157	Dense deciduous forest (DDF)	Kra Nuan (Knu-B)

Table A.1 (Continued).

No.	Soil and LULC combination	LULC	Soil series
152	1162	Dense deciduous forest (DDF)	Kra Nuan (Knu-B)
153	1163	Dense deciduous forest (DDF)	Kra Nuan (Knu-B)
154	1164	Dense deciduous forest (DDF)	Khao Suan Kwang (Ksk-B)
155	1166	Dense deciduous forest (DDF)	Khao Suan Kwang (Ksk-B)
156	1175	Dense deciduous forest (DDF)	Khao Suan Kwang (Ksk-B)
157	1177	Dense deciduous forest (DDF)	Khao Suan Kwang (Ksk-B)
158	1179	Dense deciduous forest (DDF)	Khao Suan Kwang (Ksk-B)
159	1180	Dense deciduous forest (DDF)	Khao Suan Kwang (Ksk-B)
160	1182	Dense deciduous forest (DDF)	Khao Suan Kwang (Ksk-B)
161	1185	Dense deciduous forest (DDF)	Korat (Kt-B)
162	1187	Dense deciduous forest (DDF)	Korat (Kt-B)
163	1191	Dense deciduous forest (DDF)	Korat (Kt-B)
164	1215	Dense deciduous forest (DDF)	Korat (Kt-B)
165	1218	Dense deciduous forest (DDF)	Korat (Kt-B)
166	1224	Dense deciduous forest (DDF)	Nam Phong (Ng-B)
167	1232	Dense deciduous forest (DDF)	Nam Phong (Ng-B)
168	1237	Disturbed deciduous forest (DIDF)	Nam Phong (Ng-B)
169	1247	Disturbed deciduous forest (DIDF)	Nam Phong (Ng-B)
170	1261	Disturbed deciduous forest (DIDF)	Nam Phong (Ng-B)
171	1274	Disturbed deciduous forest (DIDF)	Nam Phong (Ng-B)
172	1287	Disturbed deciduous forest (DIDF)	Nam Phong (Ng-B)
173	1314	Disturbed deciduous forest (DIDF)	Nam Phong (Ng-B)
174	1320	Disturbed deciduous forest (DIDF)	Non sung (Nsu-B)
175	1323	Disturbed deciduous forest (DIDF)	Non sung (Nsu-B)
176	1327	Disturbed deciduous forest (DIDF)	Non sung (Nsu-B)
177	1328	Disturbed deciduous forest (DIDF)	Non sung (Nsu-B)
178	1329	Disturbed deciduous forest (DIDF)	Non sung (Nsu-B)
179	1330	Disturbed deciduous forest (DIDF)	Non sung (Nsu-B)
180	1331	Disturbed deciduous forest (DIDF)	Non sung (Nsu-B)
181	1332	Disturbed deciduous forest (DIDF)	Non sung (Nsu-B)
182	1333	Disturbed deciduous forest (DIDF)	Phon Ngarm (Png-B)
183	1338	Disturbed deciduous forest (DIDF)	Phon Ngarm (Png-B)
184	1339	Disturbed deciduous forest (DIDF)	Phon Ngarm (Png-B)
185	1340	Disturbed deciduous forest (DIDF)	Phon Ngarm (Png-B)
186	1342	Disturbed deciduous forest (DIDF)	Phon Ngarm (Png-B)
187	1351	Disturbed deciduous forest (DIDF)	Phon Ngarm (Png-B)
188	1353	Disturbed deciduous forest (DIDF)	Phon Ngarm (Png-B)

Table A.1 (Continued).

No.	Soil and LULC combination	LULC	Soil series
189	1355	Disturbed deciduous forest (DIDF)	Phon Ngarm (Png-B)
190	1356	Disturbed deciduous forest (DIDF)	Phon Ngarm (Png-B)
191	1358	Disturbed deciduous forest (DIDF)	Phon Ngarm (Png-B)
192	1361	Disturbed deciduous forest (DIDF)	Puk Thong Chai (Ptc-B)
193	1367	Disturbed deciduous forest (DIDF)	Puk Thong Chai (Ptc-B)
194	1368	Disturbed deciduous forest (DIDF)	Puk Thong Chai (Ptc-B)
195	1394	Disturbed deciduous forest (DIDF)	Puk Thong Chai (Ptc-B)
196	1408	Disturbed deciduous forest (DIDF)	Puk Thong Chai (Ptc-B)
197	1413	Forest plantation (FP)	Puk Thong Chai (Ptc-B)
198	1423	Forest plantation (FP)	Puk Thong Chai (Ptc-B)
199	1437	Forest plantation (FP)	Puk Thong Chai (Ptc-B)
200	1463	Forest plantation (FP)	Puk Thong Chai (Ptc-B)
201	1490	Forest plantation (FP)	Si Khiew (Si-B)
202	1492	Forest plantation (FP)	Si Khiew (Si-B)
203	1496	Forest plantation (FP)	Si Khiew (Si-B)
204	1499	Forest plantation (FP)	Si Khiew (Si-B)
205	1503	Forest plantation (FP)	Si Khiew (Si-B)
206	1504	Forest plantation (FP)	Si Khiew (Si-B)
207	1505	Forest plantation (FP)	Si Khiew (Si-B)
208	1506	Forest plantation (FP)	Si Khiew (Si-B)
209	1508	Forest plantation (FP)	Si Khiew (Si-B)
210	1509	Forest plantation (FP)	Si Khiew (Si-B)
211	1514	Forest plantation (FP)	Satuk (Suk-B)
212	1515	Forest plantation (FP)	Satuk (Suk-B)
213	1516	Forest plantation (FP)	Satuk (Suk-B)
214	1518	Forest plantation (FP)	Satuk (Suk-B)
215	1527	Forest plantation (FP)	Satuk (Suk-B)
216	1529	Forest plantation (FP)	Satuk (Suk-B)
217	1531	Forest plantation (FP)	Satuk (Suk-B)
218	1532	Forest plantation (FP)	Thepharak (Tpr-B)
219	1534	Forest plantation (FP)	Thepharak (Tpr-B)
220	1537	Forest plantation (FP)	Thepharak (Tpr-B)
221	1539	Forest plantation (FP)	Thepharak (Tpr-B)
222	1543	Forest plantation (FP)	Thepharak (Tpr-B)
223	1567	Forest plantation (FP)	Thepharak (Tpr-B)
224	1576	Forest plantation (FP)	Thepharak (Tpr-B)
225	1584	Forest plantation (FP)	Wang Nam Khieo& Phon Ngarm (Wk/Png-B)

Table A.1 (Continued).

No.	Soil and LULC combination	LULC	Soil series
226	1589	Water body (WATER)	Wang Nam Khieo& Phon Ngarm (Wk/Png-B)
227	1599	Water body (WATER)	Wang Nam Khieo& Phon Ngarm (Wk/Png-B)
228	1613	Water body (WATER)	Wang Nam Khieo& Phon Ngarm (Wk/Png-B)
229	1639	Water body (WATER)	Wang Nam Khieo& Phon Ngarm (Wk/Png-B)
230	1666	Water body (WATER)	Wang Nam Khieo& Phon Ngarm (Wk/Png-B)
231	1681	Water body (WATER)	Wang Nam Khieo& Phon Ngarm (Wk/Png-B)
232	1684	Water body (WATER)	Wang Nam Khieo& Phon Ngarm (Wk/Png-B)
233	1690	Water body (WATER)	Wang Nam Khieo& Phon Ngarm (Wk/Png-B)
234	1707	Water body (WATER)	Wang Nam Khieo& Phon Ngarm (Wk/Png-B)
235	1708	Water body (WATER)	Warin (Wn-B)
236	1710	Water body (WATER)	Warin (Wn-B)
237	1719	Water body (WATER)	Warin (Wn-B)
238	1720	Water body (WATER)	Warin (Wn-B)
239	1760	Water body (WATER)	Warin (Wn-B)
240	1842	Scrub (SCRUB)	Warin (Wn-B)
241	1879	Scrub (SCRUB)	Bo Thai&Wang Nam Khieo (Bo/Wk-C)
242	1901	Scrub (SCRUB)	Bo Thai&Wang Nam Khieo (Bo/Wk-C)
243	1932	Scrub (SCRUB)	Bo Thai&Wang Nam Khieo (Bo/Wk-C)
244	1951	Miscellaneous land (MISC)	Bo Thai&Wang Nam Khieo (Bo/Wk-C)
245	1965	Miscellaneous land (MISC)	Nam Phong (Ng-C)
246	1991	Miscellaneous land (MISC)	Nam Phong (Ng-C)
247	2009	Miscellaneous land (MISC)	Nam Phong (Ng-C)
248	2018	Miscellaneous land (MISC)	Nam Phong (Ng-C)
249	2020	Miscellaneous land (MISC)	Nam Phong (Ng-C)
250	2024	Miscellaneous land (MISC)	Phon Ngarm (Png-C)
251	2026	Miscellaneous land (MISC)	Phon Ngarm (Png-C)
252	2027	Miscellaneous land (MISC)	Phon Ngarm (Png-C)
253	2031	Miscellaneous land (MISC)	Phon Ngarm (Png-C)
254	2032	Miscellaneous land (MISC)	Phon Ngarm (Png-C)
255	2033	Miscellaneous land (MISC)	Phon Ngarm (Png-C)
256	2035	Miscellaneous land (MISC)	Wang Nam Khieo (Wk-C)
257	2036	Miscellaneous land (MISC)	Wang Nam Khieo (Wk-C)
258	2037	Miscellaneous land (MISC)	Wang Nam Khieo (Wk-C)
259	2044	Miscellaneous land (MISC)	Wang Nam Khieo (Wk-C)
260	2055	Miscellaneous land (MISC)	Wang Nam Khieo (Wk-C)
261	2059	Miscellaneous land (MISC)	Slope complex (SC)
262	2060	Miscellaneous land (MISC)	Slope complex (SC)

Table A.1 (Continued).

No.	Soil and LULC combination	LULC	Soil series
263	2062	Miscellaneous land (MISC)	Slope complex (SC)
264	2065	Miscellaneous land (MISC)	Water body (WATER)
265	2067	Miscellaneous land (MISC)	Water body (WATER)
266	2071	Miscellaneous land (MISC)	Water body (WATER)
267	2072	Miscellaneous land (MISC)	Water body (WATER)
268	2077	Miscellaneous land (MISC)	Water body (WATER)
269	2095	Miscellaneous land (MISC)	Water body (WATER)
270	2098	Miscellaneous land (MISC)	Water body (WATER)
271	2104	Miscellaneous land (MISC)	Water body (WATER)
272	2112	Miscellaneous land (MISC)	Water body (WATER)

APPENDIX B

COMBINATION BETWEEN SOIL EROSION SEVERITY CLASSES, SOIL SALINITY SEVERITY CLASSES, AND SOIL BIOLOGICAL DEGRADATION CLASSES FOR SOIL DEGRADATION EVALUATION USING MULTIPLICATIVE METHOD

Table B.1 Combination between soil erosion severity classes, soil salinity severity classes, and soil biological degradation classes for soil degradation evaluation using multiplicative method.

No.	Soil erosion severity class	Soil salinity severity class	Soil biological degradation class	Multiplicative total score	Soil degradation severity class
1	1	1	1	1	1
2	1	1	2	2	1
3	1	1	3	3	1
4	1	1	4	4	1
5	1	1	5	5	1
6	1	2	1	2	1
7	1	2	2	4	1
8	1	2	3	6	1
9	1	2	4	8	1
10	1	2	5	10	1
11	1	3	1	3	1
12	1	3	2	6	1
13	1	3	3	9	1
14	1	3	4	12	1
15	1	3	5	15	1
16	1	4	1	4	1
17	1	4	2	8	1
18	1	4	3	12	1
19	1	4	4	16	1
20	1	4	5	20	1
21	1	5	1	5	1
22	1	5	2	10	1
23	1	5	3	15	1
24	1	5	4	20	1
25	1	5	5	25	1
26	2	1	1	2	1
27	2	1	2	4	1
28	2	1	3	6	1
29	2	1	4	8	1
30	2	1	5	10	1
31	2	2	1	4	1
32	2	2	2	8	1
33	2	2	3	12	1
34	2	2	4	16	1
35	2	2	5	20	1
36	2	3	1	6	1
37	2	3	2	12	1
38	2	3	3	18	1
39	2	3	4	24	1
40	2	3	5	30	2
41	2	4	1	8	1
42	2	4	2	16	1
43	2	4	3	24	1
44	2	4	4	32	2
45	2	4	5	40	2
46	2	5	1	10	1
47	2	5	2	20	1
48	2	5	3	30	2
49	2	5	4	40	2
50	2	5	5	50	2
51	3	1	1	3	1
52	3	1	2	6	1
53	3	1	3	9	1
54	3	1	4	12	1
55	3	1	5	15	1
56	3	2	1	6	1
57	3	2	2	12	1
58	3	2	3	18	1
59	3	2	4	24	1
60	3	2	5	30	2

Table B.1 (Continued).

No.	Soil erosion severity class	Soil salinity severity class	Soil biological degradation class	Multiplicative total score	Soil degradation severity class
61	3	3	1	9	1
62	3	3	2	18	1
63	3	3	3	27	2
64	3	3	4	36	2
65	3	3	5	45	2
66	3	4	1	12	1
67	3	4	2	24	1
68	3	4	3	36	2
69	3	4	4	48	2
70	3	4	5	60	3
71	3	5	1	15	1
72	3	5	2	30	2
73	3	5	3	45	2
74	3	5	4	60	3
75	3	5	5	75	3
76	4	1	1	4	1
77	4	1	2	8	1
78	4	1	3	12	1
79	4	1	4	16	1
80	4	1	5	20	1
81	4	2	1	8	1
82	4	2	2	16	1
83	4	2	3	24	1
84	4	2	4	32	2
85	4	2	5	40	2
86	4	3	1	12	1
87	4	3	2	24	1
88	4	3	3	36	2
89	4	3	4	48	2
90	4	3	5	60	3
91	4	4	1	16	1
92	4	4	2	32	2
93	4	4	3	48	2
94	4	4	4	64	3
95	4	4	5	80	4
96	4	5	1	20	1
97	4	5	2	40	2
98	4	5	3	60	3
99	4	5	4	80	4
100	4	5	5	100	4
101	5	1	1	5	1
102	5	1	2	10	1
103	5	1	3	15	1
104	5	1	4	20	1
105	5	1	5	25	1
106	5	2	1	10	1
107	5	2	2	20	1
108	5	2	3	30	2
109	5	2	4	40	2
110	5	2	5	50	2
111	5	3	1	15	1
112	5	3	2	30	2
113	5	3	3	45	2
114	5	3	4	60	3
115	5	3	5	75	3
116	5	4	1	20	4
117	5	4	2	40	2
118	5	4	3	60	3
119	5	4	4	80	4
120	5	4	5	100	4
121	5	5	1	25	1
122	5	5	2	50	2
123	5	5	3	75	3
124	5	5	4	100	4
125	5	5	5	125	5

CURRICULUM VITAE

Name Miss Sasikarn Plaiklang

Date of Birth 10 August 1985

Education Background:

2004-2007: Bachelor Degree in Information Technology (Management Information System) Institute of Social Technology, Suranaree University of Technology (SUT)

2008-2011: Master Degree in Geoinformatics, School of Remote Sensing, Institute of Science, SUT

Work Experiences:

2009 - 2015: Research Assistant in Information Technology System Development for Administration Project (ITSDA), SUT

2015: Teacher Assistant in School of Information Technology

2012 - 2015: Special Instructor in Nakhon Ratchasima Rajabhat University

2016 - Present: Instructor in Plookpanya School, Nakhon Ratchasima

Article published: Sasikarn Plaiklang, Yaowaret Jantakat, and Suwit Ongsomwang (2012). Classification of Land Use and Land Cover from THEOS Data using Texture Analysis with Maximum Likelihood Classifier and Artificial Neural Network. In Proceedings of the 33rd Asian Conference on Remote Sensing, Pattaya, Thailand.